Rockefeller University
Digital Commons @ RU

Student Theses and Dissertations

1992

Molecular Approaches to the Genetics of Obesity: Mapping and Characterization of the Murine Diabetes (db) Gene

Nathan Bahary

Follow this and additional works at: http://digitalcommons.rockefeller.edu/student_theses_and_dissertations

Part of the Life Sciences Commons

Recommended Citation

Bahary, Nathan, "Molecular Approaches to the Genetics of Obesity: Mapping and Characterization of the Murine Diabetes (db) Gene" (1992). *Student Theses and Dissertations*. 351.
http://digitalcommons.rockefeller.edu/student_theses_and_dissertations/351

This Thesis is brought to you for free and open access by Digital Commons @ RU. It has been accepted for inclusion in Student Theses and Dissertations by an authorized administrator of Digital Commons @ RU. For more information, please contact mcsweej@mail.rockefeller.edu.

Molecular Approaches to the Genetics of Obesity: Mapping and Characterization of the Murine diabetes (*db*) Gene

A Thesis Submitted to the Trustees of the Rockefeller University in Partial Fulfillment of the Requirements for the Degree of Doctor of Philosophy

by Nathan Bahary M. D.

February 1992
New York, N.Y. 10021

© Copyright by Nathan Bahary, 1992

In remembrance and honor of my Father;

whose love of his family, friends, and learning

is my inspiration

May his example continue to guide my life

Acknowledgements

I am grateful to a number of individuals for their assistance in completing this body of work. I am extremely thankful to Jeffrey Friedman and Rudolph Leibel for giving me the chance to carry out this work, in providing the atmosphere to do so effectively, and for the intellectual support through all my various endeavors. I am grateful for the guidance, and helpful suggestions provided me by Jules Hirsch. Although many people in both Jeff's and Rudy's laboratories worked extremely hard on various aspects of this project, I am especially appreciative of the expert technical assistance afforded by Lisa Joseph, Georgia Zorich, Donna McGraw and Rebecca Shilling. I am indebted to a group of wonderful people for the trust, comraderie, and intellectual stimulation they provided me, and with whom it was my pleasure and honor to work with; Robert Blank, Joel Sohn, Rainer Kern and Streamson Chua. Although all the above applies as well, a special thanks to Donald Siegel — for all our wonderful breakfasts, as well as the friendship and guidance which I look to share in the future. All the above again, this time to Gary Truett, for the pizza, beer, and good times we shared, and for carrying out most of the *fa/fa* rat experiments. Glad you made it out of New York, and back to the South buddy.

I would like to thank Kevin Albright and Scott Cram for carrying out the flow-sorting of the Rb(4:6)Bnr2 translocation, Andrew Greenfield and S. D. M. Brown for teaching me the microdissection/microcloning

techniques, and to Qian Liu for assistance with the preparation of the metaphase spreads. I would also like to thank Doug Coleman for many helpful discussions, and for the generous gift of the C57BL/6J *db/db* animals, D. Corow for performing the ovarian transplants, and Steven Cancellieri for assistance in animal handling. I am grateful to X-P. Sunyer and Y. Dam for performance of the assays for plasma glucose and insulin. My deepest appreciation to Lois Cousseau, for her constant attention to and assistance around, the hurdles of bureaucracy as well in the preparation of my manuscripts.

On a more personal note, I wish to thank Janice for her love and support through all the challenges that confronted me. To my Mother, Judy, Orna and Robert, as well as to all my friends whose support and faith helped me through the rougher times, and who shared my excitement and joy in the better times; this thesis reflects your care for me as much as it does my effort into the work itself.

Table of Contents

Dedication iii

Acknowledgements iv

List of Figures xii

List of Tables xvii

Abbreviations xviii

Abstract 1

Chapter 1: Introduction 3
- Familial segregation of obesity 11
- Mapping and cloning in the mammalian genome 15
- Approaches to map and clone mammalian genes influencing obesity and diabetes 19
  - Mapping and cloning genes affecting obesity/diabetes in humans 19
  - Rodent models of obesity and diabetes 23
    - The obese (*ob*) mutation 26
    - The diabetes (*db*) mutation 27
    - The fat (*fat*) mutation 28
    - The tubby (*tub*) mutation 29
  - Use of the *ob* and *db* mutants to model human obesity and diabetes 30

Chapter 2: Materials and Methods 38
- Materials 39
  - Chemicals 39
  - Disposable plasticware 39
  - Enzymes 39
  - Bacteriological media and reagents 40
  - Tissue culture media and reagents 40
  - Lambda DNA 41
  - Lambda DNA in-vitro packaging extracts 41
  - Plasmid DNA 41
  - Bacteriological Strains 41
  - Nucleic acid radiolabeling materials 42
  - Spectroscopy 43

Electrophoresis, Southern blotting, and hybridization materials 43
Pulse-Field Gel Electrophoresis equipment 43
Polymerase chain reaction (PCR) materials 44
Sequencing materials 44
DNA extractor 45
Microdissection equipment 45
Glassware 45
Non-glassware 45
Bacterial electroporation materials 46
Photography and autoradiography 46
Computer software and hardware 46
Mouse stocks 47
General Methodology 48
Transformation of cloned loci: 48
Calcium mediated transformation: 48
Transformation of Plasmids Using Competent Bacteria: 49
Preparation of *E-Coli* for electroporation: 49
Electroporation of plasmid DNA: 50
Isolation of DNA: 51
Large-scale ('maxi-prep') purification of plasmid DNA 51
Small scale ('miniprep') purification of plasmids: 53
Isolation of high quality lambda phage DNA: 54
Rapid isolation of lambda phage DNA: 56
Isolation of high molecular weight genomic DNA: 56
Isolation of subclone inserts 59
Restriction digestion and electrophoresis of genomic DNA: 59
'Random–priming' radiolabeling of nucleic acids ... 61
Oligoprimer kinasing 61
Hybridization of radiolabelled DNA to a Southern blot 62
Polymerase chain reaction (PCR) amplification of specific DNA sequences: 63
Denaturing gradient gel electrophoresis 63
Genomic clone screening 64
Bacteriophage lambda propagation 66
Autoradiography 67

Creation of a medium density genetic map of mouse chromosomes 4 and 6 using known loci 68
Description of the interspecific C57BL/6J X *M. spretus* backcross 68
Loci typed 69
Mapping of Mouse Chromosomes 4 and 6 using a Flow-Sorted Robertsonian Chromosome 75
Preparation of the cell line carrying the Rb(4:6)Bnr2 translocation 75
Flow sorting of the 4:6 Robertsonian chromosome: 79
Library construction and analysis of clones 80
Somatic cell hybrids 81
Creation and Analysis of Intraspecific, Interspecific, and Intersubspecific Mouse Crosses Segregating the *db* and *ob* Mutations 82
Summary of the intraspecific backcross 82
Summary of the intraspecific intercross 84
Summary of the interspecific intercross 85
Summary of the intersubspecific intercross 86
Progeny Analysis 87
Segregation of the fatty (*fa*) locus in rats 88
Microdissection and microcloning 89
Isolation of a cell line harboring the 4:15 Robertsonian translocation 89
Acquisition of the cell line harboring a 6:16 Robertsonian translocation 92
Preparation of the microinstruments 92
Microneedle preparation 92
Micropipette preparation: 95
Oil chambers and coverslips: 98
Siliconization of glassware 98
Preparation of the λgt10 cloning vector 99
Background 99
Isolation, growth, and testing of the vector ... 100
Preparation and testing of the phenol/chloroform microcloning reagents 101
Description of the microcloning procedure 101
Restriction endonuclease digestion: 101
Phenol-chloroform extraction 102

Ligation of the endonuclease restricted microdissected DNA to the vector 104
In-vitro packaging of the microcloned DNA .. 105
Localization of the *b* locus by in-situ hybridization .. 105
Microdissection of mid/distal mouse chromosome 4 106
Microdissection of proximal mouse 6 108
Manipulation of the microclones 109
Isolation of microcloned inserts from the λgt10 phage 109
Exclusion of highly repetitive microclones ... 109
Subcloning of microclones 110
Sequencing of the microclones 111
Radiolabeling of the microclones 111
Physical Mapping Methods 112
Pulsed-field electrophoresis 112
Preparation of DNA in agarose blocks 112
Digestion of agarose blocks 113
Pulsed field electrophoresis and Southern blotting 113
Isolation and growth of yeast artificial chromosomes (YACS) 114
Hybridization screening of a YAC library 114
PCR based screening of a YAC library 114
Isolation of YAC DNA 116
Isolation of YAC specific probes by inter-B2 repeat PCR 118

Chapter 3: Results 119
Genetic Maps of Mouse Chromosomes 4 and 6 120
Genetic Cross and Probes Utilized 120
Map of Chromosome 4 121
Distribution of chromosome 4 recombination events 134
Segregation distortion testing on chromosome 4 136
Map of Chromosome 6 137
Distribution of chromosome 6 recombination events 142
Segregation distortion testing on chromosome 6 142
Robertsonian (Rb(4:6)Bnr2) flow-sorting 144
Isolation of a cell line harboring the 4:6 Robertsonian chromosome 144
Flow sorting of the 4.6 Robertsonian chromosome 145
Library construction and characterization 150
Genetic mapping of the flow sort clones 150

Microsatellite sequences in the library 153
Intraspecific, Interspecific, and Intersubspecific Mouse Crosses ... 163
Phenotypic Characterization of the (C57BL/6J *db/db* x DBA/2J) F1 x C57BL/6J *db/db* (N2) animals 163
RFLP mapping in the Intraspecific (C57BL/6J *db/db* x DBA/2J) F1 x C57BL/6J *db/db* (N2) cross 170
Phenotypic characterization of the interspecific (C57BL/6J x *M. spretus*)'F2 - *dbspretus*' animals 174
RFLP mapping in the interspecific (C57BL/6J x *M. spretus*) intercross 175
Phenotypic and RFLP characterization of the intraspecific (C57BL/6J *db/db* x DBA/2J) F1 intercross offspring .. 179
Phenotypic characterization of the intersubspecific (C57BL/6J *db/db* x *M. castaneus*) F2 offspring 181
Pedigree analysis of the intersubspecific (C57BL/6J *db/db* x *M. castaneus*) F1 intercrossed offspring 182
Inheritance of glucose tolerance: glucose and insulin levels in the (C57BL/6J *db/db* X DBA/2J) F1 X C57BL/6J *db/db* (N2) animals 184
Genotyping and Phenotyping the *fa/fa* Rat Offspring 187
Identification of *fa/fa* rats (Genotyping at the *fa* locus) 187
Genotyping of the *fa/fa* rats with *Ifa* and *Glut-1* 193
Microdissection and microcloning of mid/distal mouse chromosome 4 197
Analysis and microdissection of the 4:15 cell line 197
Microcloning and analysis of the chromosome 4 microclones 202
Genetic resolution of the chromosome 4 microclones 204
Cloning and analysis of the mouse *Pgm-2* gene 212
Cloning of the *Pgm-2* gene by PCR 212
RFLP mapping of the *Pgm-2* locus in the interspecific laboratorius X spretus crosses 217
Isolation of YACS containing the *C8B* and *D4Rck69* probes 223
Hybridization screen for a *C8B* containing YAC 223
PCR screening for YACs containing the *Pgm-2*, *D4Rck22* and *D4Rck69* locus 230
Pulse-field analysis of the *Pgm–2*, *D4Rck22*, and *D4Rck69* loci 231

Chapter 4: Discussion 232
Physiological determinants of obesity 233
Parabiosis 241
Parabiosis utilizing the *Ay* (Yellow) mouse 241
Parabiosis of *db/db* and +/+ mice 243
Parabiosis of *ob/ob* with *db/db* or +/+ mice 245

Analysis of the *ob* and *db* parabiosis experiments 246
Alteration of the obesity/diabetes phenotype in genetically obese animals by steroids 251
Discussion of experimental results 254
Generation of a moderate resolution genetic map of chromosomes 4 and 6 254
Use of a flow-sorted 4:6 library to increase saturation of the genetic maps 259
Segregation of the *db* gene in interspecific and intraspecific crosses 263
Microdissection and Microcloning of mid/distal chromosome 4 268
Physical mapping and Summary 275

References 283

List of Figures

Figure 2.1. Schematic of the (C57BL/6J X *M. spretus*) F1 X C57BL/6J backcross. 70

Figure 2.2. Karyotype of the cell line harboring the Rb(4:6)Bnr2 translocation 77

Figure 2.3. Schematic representation of the(C57BL/6J *db/db* x DBA/2J) F1 X C57BL/6J *db/db* intraspecific backcross 83

Figure 2.4. Schematic representation of the (C57BL/6J *db/db* x DBA/2J +/+) F1 intercross 84

Figure 2.5. Schematic representation of the (C57BL/6J *db/db* x DBA/2J +/+) F1 X (C57BL/6J *db/db* x *M. spretus*) F1 interspecific intercross 85

Figure 2.6. Schematic representation of the (C57BL/6J *db/db* x *M. castaneus*)F1 intersubspecific intercross 86

Figure 2.7. Photomicrograph of a partial karyotype of the L3ST cell line which harbors the 4:15 Robertsonian translocation 90

Figure 2.8. Diagram of the preparation of the microneedles 94

Figure 2.9. Diagram of the preparation of the micropipettes 97

Figure 3.1. Use of denaturing gradient gel electrophoresis to map the *UROD* locus 126

Figure 3.2. Pedigree analysis of the 19 chromosome 4 loci in 83 (C57BL/6J x *M. spretus*) F1 x C57BL/6J (N2) offspring which demonstrated either no crossover, or a single crossover event and in the 15 N2 offspring that demonstrated double recombination events 128

Figure 3.3. The derived genetic linkage map of mouse chromosome 4 using 98 offspring of the (C57BL/6J X *M.spretus*) F1 x C57BL/6J backcross 130

Figure 3.4. A detailed comparison of the synteny between human chromosomes 1 and 9, and mouse chromosomes 3 and 4 132

Figure 3.5. Pedigree analysis of the 10 chromosome 6 loci in 110 (C57BL/6J x *M. spretus*) F1 x C57BL/6J (N2) offspring 139

Figure 3.6. The derived genetic linkage map of 10 chromosome 6 loci in 110 (C57BL/6J x *M. spretus*) F1 x C57BL/6J (N2) offspring 140

Figure 3.7. Partial karyotype of the transformed 4:6 Robertsonian cell line, 4:6 1500, as photographed by fluorescent microscopy 146

Figure 3.8. Flow sorting of the 4:6 Robertsonian chromosome 148

Figure 3.9. Southern blots of somatic cell hybrids 157

Figure 3.10. Pedigree analysis of subsets of the (C57BL/6J x *M. spretus*) F1 X C57BL/6J (N2) offspring for the chromosome 4 flow-sorted probes 159

Figure 3.11. Pedigree analysis of subsets of the (C57BL/6J x *M. spretus*) F1 X C57BL/6J (N2) offspring for the chromosome 6 flow-sorted probes 160

Figure 3.12. Genetic maps of the chromosome 4 and chromosome 6 flow sorted 4:6 clones 161

Figure 3.13. Photograph of *db/db* and *db/+* animals; 5 month old male littermates derived from the backcross. 165

Figure 3.14. Analysis of individual N2 animals by [insulin], [glucose], weight and BMI (wt. in grams/length in cm^2.). 167

Figure 3.15. Plot of glucose concentration vs. BMI, with separation of the N2 animals into 'high' and 'low' BMI groups. 169

Figure 3.16. C57BL/6J X DBA/2J RFLPs for *PλMm3₂, Ifa, MMTV (Mtv-13)* and *Lck* 171

Figure 3.17. Pedigree analysis of the (C57BL/6J *db/db* x DBA/2J) F1 X C57BL/6J *db/db* intraspecific backcross 173

Figure 3.18. Pedigree analysis of the (C57BL/6J *db/db* x DBA/2J +/+) F1 x (C57BL/6J *db/db* x *M. spretus*) F1 interspecific intercross 176

Figure 3.19. Genetic maps of the region surrounding *db* on mouse chromosome 4 using the offspring of the intraspecific N2 and interspecific C57BL/6J X *M. spretus* crosses segregating the *db* mutation 178

Figure 3.20. Pedigree analysis for the 216 F2 offspring of the (C57BL/6J *db/db* X DBA/2J) F1 intercross 181

Figure 3.21. Pedigree analysis of the 396 obese F2 offspring of the (C57BL/6J *db/db* X *M. castaneus*) F1 intersubspecific intercross 183

Figure 3.22. Graphic representation of the (C57BL/6J *db/db* x DBA/2J) F1 x C57BL/6J *db/db* intraspecific backcross [glucose] and [insulin] divided into three non-overlapping age groups 185

Figure 3.23. Analysis of variance by age and sex (Dixon, 1981) amongst the progeny of the intraspecific backcross segregating *db* 186

Figure 3.24. Photo of an 88 day old *fa/fa* rat compared with its lean littermate 189

Figure 3.25. Scatter plot of the adiposity indices of 13M/BN F2 rats segregating *fa* 191

Figure 3.26. Linkage data for the the three loci (*Ifa, fa, Glut-1*) mapped in the 50 13M/BN F2 rats 194

Figure 3.27. DNA polymorphisms at the *Ifa* and *Glut*–1 loci linked to *fa* 195

Figure 3.28. A photograph of an in-situ hybridization in the 4:15 Robertsonian cell line, with a probe which detects the *b* locus in mouse. 198

Figure 3.29. Photomicrograph of a metaphase spread of the 4:15 Robertsonian cell line demonstrating the dissected area of chromosome 4 200

Figure 3.30. Pedigree analysis of the 41 microclones, 8 previously mapped loci, the anonymous markers *D4Mit205* and *D1S85*, and *db* 208

Figure 3.31. The derived genetic linkage map of mouse chromosome 4 including the mid/distal chromosome 4 microdissection clones 210

Figure 3.32. The 780 bp of DNA sequence obtained from the mouse *Pgm–2* clone as determined by sequencing of the subcloned PCR fragments 215

Figure 3.33. The protein sequence of the mouse *Pgm-2* derived by translation of the cloned cDNA compared to the sequence of rabbit skeletal muscle *Pgm* 216

Figure 3.34. Sequence of intron/exon boundaries of a 1300 bp chromosome 4 specific *Pgm-2* probe generated by PCR. 220

Figure 3.35. Southern hybridization of the Pgm-2 780 bp partial cDNA clone demonstrating C57BL/6J X *M. spretus* RFLPs 221

Figure 3.36. Demonstration of *C8B* RFLPs between inbred mice using inter-B2 repeat PCR of a 1.2 Mb *C8B* YAC 228

Figure 4.1. Relationship of energy expenditure to body weight, among different mammals, when expressed proportionally to (body weight)$^{.75}$, a relationship termed the "Kleiber function" 239

Figure 4.2. Summary map of the *Odc-4*, *Pgm-2*, *D4Rck22*, and *D4Rck69* loci flanking db 281

List of Tables

Table 1.1. Obesity/diabetes syndromes in rodents 25

Table 2.1. Listing of the cloned probes mapped on chromosomes 4 and 6 73

Table 2.2. Listing of the PCR conditions employed in amplifying the *ACADM*, *C8B*, *Fuca*, and *UROD* loci 74

Table 3.1. Data for the typing of the 26 BxD RI lines for the probe which detects the mouse *ACADM* locus 125

Table 3.2. Results of the G-test for segregation distortion on mouse chromosomes 4 and 6 143

Table 3.3. Characteristics of the genetically mapped chromosome 4 and chromosome 6 markers, derived from the cloning of the flow-sorted Robertsonian 4:6 hybrid cell line DNA 155

Table 3.4. Chromosome content of somatic cell hybrids. The percentage of the cells which carry a particular chromosome are shown for each cell line 156

Table 3.5. Characteristics of the mid-4 chromosome microdissection. ... 204

Table 3.6. B X D RI line data for the inter-B2 repeat PCR *C8B* YAC probe 227

Abbreviations

symbol	definition
µl	microliter
µCi	microcuries
µg	microgram
µM	micromolar
A_{260}	absorbance at 260nm
A_{280}	absorbance at 280nm
A_{600}	absorbance at 600nm
Ay	yellow
B6	C57BL/6J
bp	base pairs
BSA	bovine serum albumin
castaneus	*Mus castaneus*
CIP	calf intestinal phosphatase
cM	centimorgan
cm	centimeter
dpm	disintegrations per minute
D2	DBA/2J
dATP	deoxyadenosine triphosphate
db	diabetes
dCTP	deoxycytosine triphosphate
dGTP	deoxyguanosine triphosphate
DNA	deoxyribonucleic acid
dNTP	deoxyribonucleotide triphosphate
DTT	dithiothreitol
dTTP	deoxythymidine triphosphate
fa	fatty (rat)
fat	fat (mouse)
I.D.	inside diameter
IPTG	Isopropyl-β-D-thiogalactopyranoside
kb	kilobase pairs
kd	kilodalton
l	liter
LB	L-broth
LMP	low melting point
M	molar
M.	Mus
Mb	megabase
mg	milligram
MHz	Megahertz
min	minutes
ml	milliliter
mM	millimolar
mm	millimeter
ng	nanogram
nl	nanoliter
nM	nanomolar
nm	nanometers
OD	optical density
O.D.	outside diameter
ob	obese
PCR	polymerase chain reaction
PFGE	Pulse-field gel electrophoresis
pfu	plaque forming units
RFLP	restriction fragment length polymorphism
RNA	ribonucleic acid
rpm	revolutions per minute
spretus	*Mus spretus*
SSR	simple sequence repeat
STS	sequence tagged site

TE	Tris/EDTA
tub	tubby
U	units
v/v	volume/volume
V	volts
X-gal	5-Bromo-4-chloro-3-inodyl-β-D-galactopyranoside

Abstract

Studies of twins, adopted children, and some human populations indicate that there is a substantial genetic influence on body composition in both children and adults. However, in no single instance in either man or animals is the precise etiology of obesity known at the molecular level. Attempts to identify the molecular basis responsible for obesity in humans have been hampered by difficulties in measuring food intake and energy expenditure to sufficient accuracy, as well as the apparent polygenic control of body composition in man. These constraints have stimulated interest in the simpler models available in certain inbred animal strains, and particularly mice.

The murine diabetes, *db*, mutation is an autosomal recessive mutation located on mouse chromosome 4 which demonstrates a metabolic/behavioral phenotype similar to that observed in human obesity and Type II diabetes. Homozygous *db* animals manifest profound obesity with hyperphagia, increased metabolic efficiency, and insulin resistance. In an effort to clone this gene (and the related obese (*ob*) mutant on mouse chromosome 6) by the technique of "positional cloning", several studies were undertaken.

A moderate resolution genetic map of mouse chromosomes 4 and 6 utilizing an interspecific *laboratorius* X *spretus* backcross was first created using RFLPs for 29 known chromosome 4 and 6 markers. These maps

extended over most of the chromosomes' length and detailed large areas of mouse — human homology. Intraspecific crosses segregating the *db* mutation were then established, and markers from the chromosome 4 map were positioned relative to *db*. Several of the markers which are linked to *db* — (*Jun, Glut-1, Lmyc-1,* and *C8B,*) map to human chromosome 1p31–p32, suggesting that *db* may be part of a syntenic group between human 1p and the distal portion of mouse chromosome 4. Additionally, distributions of age-controlled plasma [glucose] and [insulin] among the intraspecific cross obese progeny were not bimodal, suggesting a role for polygenic differences between the progenitor strains (C57BL/6J and DBA/2J) in the development of overt diabetes.

In order to increase the density of probes in the region of *db*, flow-sorting of a 4:6 Robertsonian chromosome was accomplished, establishing a library ~72% pure for chromosomes 4 and 6. In addition, microdissection and microcloning of the mid/distal chromosome 4 region containing *db* produced two clones, *D4Rck22* and *D4Rck69*, located < 0.13 cM distal to *db*. Cloning and mapping of the mouse phosphoglucomutase gene established that *Pgm–2* is located approximately 1.5 cM proximal of *db*. Utilizing these flanking markers and genetic resources, pulse-field electrophoresis mapping, and YAC cloning of the region has begun. These studies should facilitate the eventual cloning and characterization of the *db* gene.

Chapter 1: Introduction

Obesity is, in its simplest form, an excess deposition of energy in the form of triglyceride in adipose tissue. It is indicative of a metabolic state created by the imbalance of energy input and expenditure, leaving excess energy to be stored in fat cells. However, the meaning of the word 'excess' holds the key to a useful definition of obesity. The separation of normal vs. excess adipose tissue deposition is a difficult concept to define. Although everyone states they "know obesity when they see it", attempting to define obesity by social considerations is impractical; different generations and cultures differ as to what the ideal weight and physique should be, and a definition based solely on aesthetics is certainly not scientifically rigorous. The ideal definition should then incorporate a concept, such as morbidity and mortality, which can be applied in a reproducible manner, and whose environmental and biological influences can potentially be understood.

As noted by Bray (Bray, 1990b), it is evident from statues depicting obese figures, that obesity was present >25,000 years ago. Recognition of obesity as being an abnormal state with serious health sequela can be traced back to the time of Hippocrates. Writings of Hippocrates state "sudden death is more common in those who are naturally fat than lean". Infertility and dysmenorrhea were noted by Hippocrates among obese woman, although he attributed the former to a closing of the uterus to semen due to the accumulation of fat surrounding it. Numerous other references to obesity can be found dating from the 15th century - present, and are reviewed

elsewhere (Bray, 1990b). However, all these works, even when noting a possible familial cause to the obesity, could offer no definition or practical solutions. With the development of the cell theory by Schwann and Schleiden, numerous investigators began attempting to understand the physiological basis of the human body, and modern concepts of pathophysiology were born. This in turn allowed the investigation of obesity as a pathophysiological event. Around the same time that the cell theory was published some of the first modern investigations into obesity were published by Quetelet (Quetelet, 1836). Among other contributions, while studying populations in Belgium for a number of physical characteristics, he developed the concept of correcting the weight for height by use of the formula weight/(height)^2 , which we now call the body-mass index or BMI.

The health risks of severe obesity have been documented. An American Cancer Society study demonstrated that people more than 40 per cent overweight suffer increased mortality from diabetes, coronary heart disease and cancer (Lew and Garfinkel, 1979). Numerous published studies have shown that obesity is the most important risk factor for the development of noninsulin-dependent diabetes mellitus (NIDDM) (West, 1978; Bjorntorp, 1990; Daly and Landsberg, 1991; Knowler, et al., 1991; Bray, 1990a; Morris, et al., 1989). Studies have also found that obesity promotes the development of the cardiovascular risk factors (Pi-Sunyer, 1991) of hypertension (Heyden and Schneider, 1990; Dustan, 1991), lipids (Newman, et

al., 1990; Laakso and Pyorala, 1990), and diabetes. Although obesity has been shown to increase the risk of cardiovascular disease (Manson, et al., 1990; Bjorntorp, 1990), it is unclear whether the relationship of obesity to cardiovascular disease (CVD) results from the elevation of these risk factors or is an independent risk factor (Hubert, et al., 1983; Kannel, et al., 1991). Obesity also has a demonstrated impact on left-ventricular function, increasing the myocardial thickness (Lauer, et al., 1991), and reducing left ventricular ejection fraction (Licata, et al., 1991), which could contribute to the morbidity/mortality of cardiac diseases such as heart failure.

A number of investigations have shown that certain cancers have an increased incidence in the obese population. Persons 40 per cent or more overweight have a demonstrated increased risk of colorectal cancer (Lew and Garfinkel, 1979), while one prospective study showed that a BMI > 25 was associated with an increased risk of colon cancer in older men (Nomura, et al., 1985). Adenomatous polyps, a known precursor lesion for most cases of colorectal cancer, increased in frequency in relation to BMI in one study (Neuget, et al., 1991). Woman more than 40 per cent overweight, exhibit a nearly 4-fold increase in endometrial cancer (Lew and Garfinkel, 1979), and a variety of other studies have confirmed and further developed these findings (Henderson, et al., 1983; LaVecchia, et al., 1984; Schapira, et al., 1991; Pi-Sunyer, 1991; Elliot, et al., 1990). Breast cancer has also been linked to obesity (Pi-Sunyer, 1991; Schapira, 1991; De Waard, et al., 1977), with studies

demonstrating that breast cancer incidence rises with small increases in overweight (Lew and Garfinkel, 1979).

The morbidity of obesity is not confined to diabetes, cardiovascular disease and cancer. Studies have demonstrated an important contribution of obesity to osteoarthritis of the knee (Felson, 1990) and other joints (Prikazska and Beno, 1991). In addition, gallstones (La Vecchia, et al., 1991), cerebral vascular accidents (CVA or strokes) (Shinton, et al., 1991), and sleep apnea (Remmers, 1990) have all been associated with obesity.

An important consideration in attempting to measure the health risks of obesity, is defining the level of adipose tissue which constitutes the point where morbidity and mortality is increased over some 'normal' level. Inherent in any such definition are two complicating factors. First, several methods exist for measuring adiposity. In general, the more accurate measures are more difficult and more expensive to employ. These techniques are used mostly in the laboratory setting , clinically useful measures of obesity which are simpler and inexpensive to use, are generally less accurate and more subject to operator bias. And second, the pattern of adipose tissue distribution affects morbidity and mortality as well as does the total adipose tissue content.

The laboratory methods available for assessment of adiposity include underwater weighing, ^{40}K counting, determination of total body water using doubly labeled (deuterium or tritium) water, the tobec, computerized

tomography (CAT scanning) and nuclear magnetic resonance (NMR) imaging. Both CAT scanning and NMR imaging suffer from being able to provide only regional as opposed to total body composition. All these methods, described in detail elsewhere (Lukaski, 1987; Gray, 1989) are difficult and expensive to accomplish, and therefore ill-suited for general clinical and field use.

The most common anthropometric measures utilized in clinical obesity studies as well as in the medical clinic are height and weight, and the derived value of body-mass index or BMI [weight/(length)^2], and skinfold thickness measurements. Skinfold thickness measurements, as reviewed by Lohman (Lohman, 1981), have been compared with underwater measurements yielding standardized regression equations which can predict percent body fat. These equations, provide good correlation between skinfold measurements and body fat within the populations the equations were derived from, however, they are less accurate when applied to other populations. Interobserver errors also limit the utility of skinfold measurements for defining obesity. In addition, a large autopsy study conducted to investigate the correlation of skin-fold thicknesses to body composition found several areas where incorrect assumptions could influence data reliability. Skinfold thickness measurements assume that 1) skinfolds are equally compressible at different sites, which they found to vary from 34 to 64% by site, 2) that adipose tissue is deposited relatively constantly

throughout the body, which it is not, 3) that skin thickness is constant from site to site, which varied in the study from 8.2% in the medial thigh area to 28.1% in the subscapular region, and 4) that internal fat, which is not measured by skinfold thickness, is either relatively small or is relatively constant when compared to subcutaneous fat. Internal fat mass may vary from 10% of total body fat in lean subjects, to as much as 65% in morbidly obese subjects (Allen, et al., 1956).

The BMI, is slightly more difficult to use than weight or height measurements in describing obesity. However, the calculation of BMI (weight/(length)^2) is relatively straightforward, and normograms have also been produced which obviate the need for calculations. The use of BMI is preferred to either height or weight alone since the latter are closely correlated with body frame size. This is an especially important consideration when attempting to define obesity to predict any possible genetic inheritance of the trait, as frame size is strongly hereditable. Most studies have shown that BMI is closely correlated to body fat while being relatively independent of height and frame size (Gray, 1989). With judicious application, BMI can be utilized, with or without concomitant use of skinfold thicknesses, in studies helping to define both the risk of obesity as well as possible hereditable qualities.

The distribution of adipose tissue is, along with total fat, a major influence on the complications of obesity. In general, abdominal (male pattern or "androidal"), obesity is contrasted to femoral-gluteal (female

pattern or "gynecoid") obesity. The former is associated with hypertension and has demonstrated consistent correlation with NIDDM (Ducimetiere, et al., 1986). The ratio of the circumference of waist-to-hip (WHR or waist-to-hip girth ratio) has been demonstrated to be predictive of (and of greater predictive value than BMI) diabetes in men (Ohlson, et al., 1985), and of cardiovascular disease in both men and women (Larsson, et al., 1984; Lapidus, et al., 1984). Baseline WHR were higher in women who subsequently developed endometrial cancer (Lapidus, 1992), although BMI was more weakly correlated with the incidence of endometrial cancer.

Regional differences in adipose tissue metabolism have also been demonstrated. The number of $beta_1$ and $alpha_2$ receptors has been shown to vary by the site of adipose tissue sampling (Leibel and Hirsch, 1987). Premenopausal women have a higher lipoprotein lipase (LPL) activity in their gluteal and femoral regions as compared to men, which is not seen in post-menopausal women (Fried and Kral, 1987; Taskinen and Nikkila, 1981; Rebuffe-Scrive, et al., 1986). Premenopausal women enjoy a relatively low risk of cardiovascular disease, which rises after menopause. In addition, aromatization of androstenedione (an androgen) to estrone has been demonstrated in human adipose tissue (Perel and Killinger, 1979). As noted, certain endocrine sensitive neoplasias in women, such as endometrial and certain breast cancers, are correlated with obesity. The relationship(s) between these metabolic differences and the morbidity and mortality of certain sequela

of obesity, is uncertain. However, they provide the basis for an understanding of certain genetically controlled determinants of obesity, which may have important medical consequences.

Taking these data together, obesity has been defined as a body fat content of greater than 25 per cent of total weight in men, and greater than 30 per cent in women (Bray, 1989b). Since the morbidity and mortality attributable to obesity appears to increase at BMI's > 25 kg/m^2 (Lew and Garfinkel, 1979), most definitions of obesity define overweight by this measurement. The National Center for Health Statistics definition of overweight is a BMI greater than the 85th percentile of 20–29 year olds (~ 27-28 kg/m^2) and severe overweight as greater than the 95th percentile (~ 32 kg/m^2). As a result, the most generally accepted definition of obesity is a BMI greater than the average (30 kg/m^2.) of these two figures (Gray, 1989; Keesey, 1989).

Familial segregation of obesity

Obesity tends to cluster within families (Heller, et al., 1984; Province and Rao, 1985; Laskarzewski, et al., 1982; Longini, et al., 1984; Davenport, 1923; Angel, 1939; Garn and Clark, 1976; Garn, et al., 1989). Measures of body composition (fatness) are more closely correlated in mono than dizygotic twins (Stunkard, et al., 1986; Stunkard, et al., 1990; Selby, et al., 1989; Arlen Price and Stunkard, 1989). Such studies of twins, as well as correlations of

fatness between adoptees and biological vs. adopted family members, suggest that as much as 80% of the risk of obesity is conveyed by genetic factors (Bouchard, et al., 1985; Stunkard, et al., 1986; Sorensen, et al., 1989; Arlen Price, et al., 1987).

In rare instances, human obesity is attributable to differences at a single genetic locus. The Prader-Willi syndrome (PWS) has been localized to the chromosomal segment 15q11-q13 (Buiting, et al., 1990; Kirkilionis, et al., 1991). The syndrome is frequently inherited with deletions of the paternal chromosome in the region, or with maternal disomy of the region, suggesting that the responsible gene(s) are imprinted (Greenstein, 1990; Hall and Smith, 1972). Conversely , inheritance of the 15q11-q13 region of the same paternal chromosome 15 region is seen in in Angelman's syndrome. With an estimated frequency of ~1/25,000, PWS may be the most common genetic syndrome associated with obesity (Butler, 1990).

Two X-linked obesity/mental retardation syndromes have also been described, (Wilson, et al., 1991; Chudley, et al., 1988) as well as a familial t(2;5) (p23;q31) translocation associated with obesity (Kiss and Osztovics, 1990). Other genetic syndromes associated with obesity, the Bardet—Biedl syndrome (Bardet, 1920; Biedl, 1922; Green, et al., 1989), Alstrom syndrome (Alstrom, et al., 1959; Charles, et al., 1990), Cohen syndrome (Cohen Jr., et al., 1973; Carey and Hall, 1978; Fryns, et al., 1990), psudohyperparathyroidism (Spiegel, 1989), and short stature–obesity syndrome (Schinzel and Bernasconi, 1990), have

been phenotypically characterized, but without certain localization of the genetic lesions.

Despite the understanding that genetic defects underlie these rare instances of obesity, no genetic locus has been identified that might account for the majority of human obesity. Three studies attempting to define the mode of inheritance of such obesity gene(s) suggested either a recessive mode of inheritance of a relative–fat–pattern–index (RFPI = ratio of subscapular skinfold thickness to the sum of subscapular and suprailiac skinfold thicknesses) (Hasstedt, et al., 1989), a mixture of both moderate polygenic inheritance (34% of inter-individual variance in BMI caused by many genes with small effects) and common (21% frequency) major recessive genes (Arlen Price, et al., 1990), or a model including a single recessive loci (35% of adjusted variance in BMI), polygenic loci (42% of the variation), and 23% of the variance not explained by genetic factors (Moll, et al., 1991).

Efforts to precisely quantify, and genetically localize, the heritable elements of obesity in man are confounded by problems which derive from 1) lack of knowledge about the number of genes which may contribute to obesity; 2) the potentially powerful impact of developmental (e.g. early nutritional experience), environmental circumstance (Arlen Price and Gottesman, 1991) (e.g. availability of food, amount of physical activity), and cognitive/affective factors (Schlundt, et al., 1990) on the impact of whatever gene(s) may be involved, and on 3) difficulties in measuring, with sufficient

accuracy over extended periods, those characteristics affected by genes (e.g. energy expenditure and food intake) which are the likely pathways to obesity, and which probably define subsets of etiology.

The observation that humans maintain a relatively constant body weight over extended periods of time, despite fluctuating levels of food intake and physical activity (Hirsch and Leibel, 1988) has suggested the existence of regulatory processes which balance food intake and energy expenditure around a "set-point" for body weight. Very small imbalances of energy intake vs. expenditure operating over a prolonged period of time can result in large changes in body weight (Mrosovsky and Powley, 1977; Harris, 1990; Leibel, 1990). Attempts to unravel the complex physiologic systems which must then operate to maintain this relative constancy of body composition, have not yet led to the identification of discrete biochemical mechanisms(s) involved in producing human obesity. The inability to identify lean individuals destined to develop obesity, and the profound effects of obesity on the various metabolic processes which might be involved in its pathogenesis, have made it difficult to distinguish the secondary effects of obesity from possible primary physiological abnormalities (Leibel, et al., 1990). However, access to the molecular basis, or a component of this apparent control loop, would probably enable the elucidation in detail of the molecular physiology of the entire system. These considerations indicate the importance of access to animal models in which the genetics are simplified and in which the

techniques of molecular genetics may be applied to isolate genes which contribute to the control of body composition.

Mapping and cloning in the mammalian genome

Before the advent of modern molecular biological techniques, the ability to map mammalian genes was limited to those genes which encoded a recognizable physical or biochemical phenotype which could be used to discriminate one individual's genotype from another's. By analyzing suitable genetic crosses, cosegregating phenotypes were assigned to a 'linkage group'. By creating an overlapping set of such linkage groups, maps were created which, with occasional exception, contained few physical landmarks. Such landmarks were obtained primarily by: (1) analysis of those phenotypes associated with a chromosomal deletion and (2) hamster/human hybrids which contained a limited amount of stably propagated human DNA encoding an expressed protein which could be distinguished from its hamster analogue. Using these techniques, occasional genes (and their linkage groups) could be localized to a specific chromosome. These procedures, however, did not allow the positioning of many 'markers' on the genome, since most genes do not have an associated phenotype that can be tracked.

Diesseroth et al. (Diesseroth, et al., 1977) first used a DNA marker to assign a gene to a specific mammalian chromosome. A cDNA sequence for the alpha-globin gene was localized to human chromosome 16 by

hybridization to somatic cell hybrids containing known human chromosomes. The technique of somatic cell hybridization, however, does not usually position probes with sufficient accuracy to generate detailed maps of a mammalian genome.

In 1980, Botstein et al. (Botstein, et al., 1980) proposed a method whereby RFLPs could be used as genetic markers. Since only a small portion of the genome codes for protein, the vast majority of DNA is contained in non-coding sequences, where differences among individuals occur as often as every 50-100 base pairs (Botstein, et al., 1980). This high degree of variability can be detected by Southern blotting of enzyme-cleaved, size-fractionated genomic DNA using labeled cloned DNA as a probe. Historically, such probes have been nucleotide sequences coding for part or all of a known gene. However, any unique sequence for which a polymorphism is demonstrable can be used. In fact, some of the most valuable sequences in this context are so called 'variable number of tandem repeats' (VNTRs) (Nakamura, et al., 1987) and 'simple-sequence repeats or dinucleotide repeats (SSRs) (Cornall, et al., 1991; Dietrich, et al., 1991). The size variability of these loci results from their constitution as sets of tandem repeats of either short oligonucleotide sequences (11-60 bp) in the case of VNTRs, or more simple dinucleotide repetitive elements, such as repeating guanodine-thymidine (GT) elements in certain SSRs.

To date, more than 2000 loci have been positioned on the mouse genome, and over 6,000 in man. Using both RFLPs and SSRs, complete genetic maps of the mouse genome have been characterized using between 350-800 probes in a single set of mice (Neil Copeland and Nancy Jenkins, personal communication), (Michael Seldin, personal communication), (Dietrich, et al., 1991). Similar efforts are underway for the human (Donis-Keller, et al., 1987) and rat genomes. Because the markers utilized are both genetic and physical markers, the availability of a dense genetic map of RFLPs greatly accelerates efforts to clone mutant genes by providing information regarding the precise position of the mutant gene on the chromosome.

The earliest successes of molecular genetics were in the cloning of genes for known proteins (e. g. the genes for the normal and mutant hemoglobins). With the availability of dense genetic maps, the location and cloning of genes without prior knowledge of their protein product ('positional cloning') has been greatly simplified. The recent cloning of the genes for Duchenne's muscular dystrophy (Monaco, et al., 1985), cystic fibrosis (Riordan, et al., 1989), and neurofibromatosis I (Wallace, et al., 1990) are examples of this approach.

Since hundreds of genetic markers can be scored in a single genetic cross it is easy to undertake high resolution genetic mapping of single gene traits, and it is feasible to carry out genetic dissection of polygenic traits into discrete Mendelian factors. For example, in an interspecific backcross of

tomato, 6 quantitative trait loci (QTLs) controlling fruit weight, 4 QTLs for the concentration of soluble solids, and 5 QTLs for fruit pH, were described at a resolution of 20-30cM (Paterson, et al., 1988; Lander and Botstein, 1989). Such a paradigm has also proven useful in the localization of loci which affect diabetes in NOD (non-obese diabetic) mice (Cornwall, et al., 1991), which modify tumor development in the MIN (multiple intestinal neoplasia) mouse (Lander et al., personal communication), and which influence the development of hypertension in the rat (Jacob, et al., 1991).

In the mouse, mapping has been carried out using inbred strains (*Mus laboratorius*) of the common house mouse, *Mus musculus domesticus*. Inbred mice are created by sequential brother-sister matings of wild mice which removes significant genetic heterogeneity between individual animals after a sufficient number of generations (usually 20 or more). Heterogeneity *between* inbred strains depends upon the timing of their evolutionary divergence as wild strains.

The genetic or molecular mapping of mouse chromosomes has been greatly facilitated by the use of interspecific *Mus laboratorius/ Mus spretus* and intersubspecific *M. laboratorius/Mus castaneus* crosses. The greater evolutionary distance between the two strains (e.g. ~1 million years between *laboratorius* and *spretus*) as compared to pairs of *M. laboratorius* inbred strains, greatly increases the likelihood of heterozygosity at any genetic locus (Avner, et al., 1988). The progeny of such interspecific and intersubspecific

crosses can therefore be more easily typed for the inheritance of many RFLPs to generate detailed genetic maps.

Approaches to map and clone mammalian genes influencing obesity and diabetes

Mapping and cloning genes affecting obesity/diabetes in humans

Unlike cystic fibrosis, or neurofibromatosis (both of which have been cloned by positional genetic techniques), obesity is a continuous quantitative trait which is difficult to define and to which a number of genes undoubtedly contribute. These genes probably have effects on ingestive behaviors, metabolic energy efficiency, pancreatic beta cell activity, and peripheral insulin metabolism. In addition, it is quite possible that different genes contribute to the risk of obesity at different ages, and that the expression of genetic predisposition to obesity is highly dependent on a "permissive " environment in which sufficient food calories are available. Thus, the various genes which apparently play a role in the development of obesity may or may not be detected by genetic analysis, depending upon the anthropometric definitions used, the ages of ascertainment, and the particular population studied. Several approaches have been taken to this problem. Geographically stable populations in which individual members of families

have been monitored with regard to aspects of phenotype relevant to the diagnosis of obesity and its complications - height, weight, body circumferences, blood pressure, blood glucose and insulin - can be examined for evidence of familial patterns of obesity which are consistent with major effects by one or at most a few genes (Moll, et al., 1991; Arlen Price, et al., 1990; Hasstedt, et al., 1989). Populations such as the Pima Indians (Arizona), the families enrolled in the Muscatine (Iowa) Study, the Amish of Pennsylvania, and the Mormons of Utah are examples of such groups. The somewhat inbred character of some of these populations is an advantage in this instance, since the heterogeneity at a given recessive genetic locus is reduced. The fact that such individuals have been followed for many years permits the investigator to define obesity in several ways which incorporate the effects of age on likelihood of phenotype. One can select for further analysis, individuals with defining aspects of phenotype at various ages, and can analyze linkage data using groups selected for onset/severity which is age dependent.

More generally, specific aspects of phenotype used to define the obese state are selected to produce the most unambiguous distinction between individuals in a population or family. Computer modeling of the segregation of these aspects of phenotype within large pedigrees (several generations "deep") permits conclusions to be drawn concerning the pattern of heritability (single or polygenic, recessive or dominant), and an estimate to be made

regarding the portion of phenotypic variance which is attributable to heritable as opposed to environmental or developmental factors (Moll, et al., 1991; Hasstedt, et al., 1989; Arlen Price, et al., 1990. Such information may be helpful in designing strategies for localizing the responsible genes in the genome).

In one approach, DNA from individuals in families segregating an obese phenotype is examined with molecular markers which, at regular intervals, span the entire genome. Such markers are not restricted to expressed sequences, indeed the vast non-coding region of the genome is usually more polymorphic between individuals. Such diversity increases the likelihood that any meiotic event will be informative. The feasibility of this approach depends upon the number of genes responsible for the phenotype in an affected individual, and the total number of relevant genes in the population. With a disorder whose genetics clearly indicate a single gene with high penetrance, this approach is a reasonable means of identifying the region of the genome in which the responsible gene is located. This approach has been used to locate a variety of human diseases: Huntingtons's Disease to chromosome 4p (Dogget, et al., 1989), Wilm's tumor to 11p13-p15 (Gessler, et al., 1990; Compton, et al., 1988), Friedrich's Ataxia to 9q13-q21 (Wallis, et al., 1990; Hanauer, et al., 1990), and was the initial step in the cloning of the cystic fibrosis gene (Collins, et al., 1987; Riordan, et al., 1989). However, obesity demonstrates an apparently polygenic mode of inheritance with strong

environmental influences on expression. In such a case, scanning the genome at regular intervals for areas linked to the phenotype would be a very laborious, and an inefficient means of looking for genes which influence obesity.

An alternative approach is to identify "candidate genes" whose biochemical or physiological effects are consistent with possible mechanisms for the phenotype being examined. Examples of such genes for obesity would include: lipoprotein lipase, insulin receptor, insulin-like growth factors, various neuropeptides or other neurotransmitters which affect food intake, signal regulation pathways (G-proteins, kinases, phosphorylases), glycolytic enzymes, and genomic promoter and suppressor sequences for these genes. Molecular markers (e.g. RFLPs, simple sequence repeats (SSRs), VNTR's, etc) for such genes could be examined for linkage to the selected aspect of phenotype in families segregating for obesity. An additional source of "candidate genes" is from rodent models of obesity, in which single gene mutations result in phenotypes resembling the disease being studied in humans.

Rodent models of obesity and diabetes

The mouse has a number of distinct advantages over other mammals as a model for studying human disease: (1) a fast breeding rate (1 litter every 6-8 weeks); (2) large average litter size (5-7 offspring) and (3) availability of highly inbred strains, ensuring genetic homogeneity within strains.

Many mouse mutant models of human disease are available, spanning the range of physiological abnormalities from obesity and diabetes to neurological and immunological disturbances. Cloning genes whose phenotype is known, but whose protein product is unidentified (termed 'positional cloning'), is simpler in mice than in humans. Mutant alleles in mice can be 'fixed' on a homogeneous genetic background and large genetic crosses can be generated to permit fine mapping of the gene relative to other genetic markers such as restriction fragment length polymorphisms (RFLPs), known genes or proteins, or simple sequence repeats (SSRs) (Love, et al., 1990). Additionally, mice with defects in specific genes can be created by homologous recombination techniques into embryonic stem cells (ES) (Robertson, 1986; Jackson, 1987), which direct insertions into a specific targeted sequence. Thus, mouse models of human diseases for which a portion of the relevant human genomic sequence is available may be created and studied.

Although there has been an ongoing debate concerning the respective relative contributions of genotype and environment to obesity and diabetes in

humans, clear examples exist in animals of obesity transmitted by single autosomal recessive genes (*ob, db, fat, tub* in mice, *fa* in rats) (Coleman and Eicher, 1990), single dominant alleles (*Ay*, *Aiy*, and *Aiy* in mice), and by 'polygenes', such as the NZO, KK, and 'Wellesley' strains in mice (Coleman, 1982) (Table 1.1), in certain strains of pigs (Large White and Berkshire) and rats (Osborne-Mendel) (Festing, 1979). In no instance is the specific biochemical 'lesion' underlying any of these genetic obesities known.

Single gene mutations

Mice::	*Gene Name*	*Inheritance*	*Chromosome*
	Yellow (A^{y}, A^{vy}, A^{iy})	Autosomal Dominant	2
	Obese (ob)	Autosomal Recessive	6
	Diabetes (db, db^{2J}, db^{3J}, db^{ad}, $db^{pasteur}$)	Autosomal Recessive	4
	Fat (fat)	Autosomal recessive	8
	Tubby (tub)	Autosomal recessive	7
Rats:			
	Fatty (fa)	Autosomal recessive	5
Polygenic Inheritance (mice):			
	NZO	Polygenic	?
	KK	Polygenic	?

Table 1.1. Obesity/diabetes syndromes in rodents. Rodents with obesity/diabetes caused by single recessive genes (mice and rats), a single dominant gene (mice) or polygenes (mice), are available for study. The wide range of obesity/diabetes mutants not only demonstrate different modes of inheritance, but manifest a wide range of severity of their obesity and diabetes as well.

The obese (*ob*) mutation

The *ob* mutation in mouse was originally described in 1950 by Snell and co-workers (Ingalls, et al., 1950) as a recessive mutation that arose spontaneously on a noninbred mouse and which was subsequently transferred to the inbred mouse strain C57BL/6J. Animals homozygous for the mutation are easily distinguishable as obese by several weeks of age, and demonstrate glucose intolerance and diabetes, whose severity depends on the background strain upon which the mutant allele is engrafted (Coleman, 1982; Leiter, et al., 1981; Leiter, 1981; Leiter, 1989). The *ob* gene was localized to proximal mouse chromosome 6 using classical genetic linkage studies. Since then, numerous studies have characterized many of the biochemical, physiological, and behavioral aspects of the *ob/ob* animal (Bray and York, 1979). Among the many defects proposed to be the primary abnormality in *ob/ob* mice are:

1) elevated brain serotonin.
2) diminished cellular K+ ion permeability (Berglund, et al., 1980).
3) low endogenous CCK production (Batt, 1983).
4) altered magnesium and/or manganese metabolism (Welsh, et al., 1985).
5) decreased, or increased production of pancreatic polypeptide (Tomita, et al., 1984).
6) decreased pancreatic dismutase (Asayama, et al., 1985).

Despite this intensive investigation, the primary genetic defect in *ob/ob* mice remains unidentified.

The diabetes (*db*) mutation

Diabetes (*db*) is an autosomal recessive mutation located on chromosome 4 which arose spontaneously in the C57Bl/KsJ strain (Hummel, et al., 1966; Lane, 1968). At least five separate spontaneous mutations allelic to *db* — db^{2J}, db^{ad}, db^{3J} (Leiter, et al., 1980), db^{4J}, and $db^{pasteur}$, all with identical phenotypes, have been described (Coleman, 1982). Homozygous *db/db* mice exhibit a diabetes-obesity syndrome, which like *ob*, varies in severity depending upon the background strain onto which the mutant allele is bred. The *db/db* phenotype, including susceptibility to diabetes, is similar to the phenotype of *ob/ob* mice on every inbred strain of mouse that has been tested (Hummel, et al., 1972). Indeed, *db/db* mice received the name "diabetes", because the mutation originally arose in the C57BL/KsJ mouse strain, on which *db/db* animals are severely diabetic.

The earliest phenotypic evidence of homozygosity for both *ob* and *db* is enhanced fat deposition by 2 weeks, despite a normal energy intake. Hyperphagia and elevated plasma [glucose], [insulin], and triglycerides can be seen at 4 weeks of age accompanying an almost 3-fold increase in the content of carcass fat. *Ob/ob* and *db/db* animals not only consume more calories than their lean littermates, but pair-fed obese animals deposit a higher fraction of ingested calories as fat than do their lean littermates (Coleman, 1978). Homozygous animals also demonstrate an impairment in heat-generating capacity, which causes them to become hypothermic in a cold environment

(Trayhurn and James, 1978). Other metabolic disturbances noted in *db/db* and *ob/ob* animals include infertility, hyperinsulinemia, hyperglycemia, and a diminished metabolic rate. Many of the relevant endocrine and autonomic axes are coordinately controlled in the hypothalamus, leading some investigators to suggest that the primary defect in these mutants is located in the hypothalamus (Bray and York, 1979). Further support for this hypothesis includes the fact that although homozygous *db/db* and *ob/ob* females are infertile, the defect appears to be in hormonal stimulation of the ovaries by the hypothalamus. The ovaries of the homozygous *ob/ob* or *db/db* female function normally when transplanted into a histocompatible host. Whether this phenomenon is due to secondary alteration of the gonadal-hypothalamic/pituitary axis due to the obesity, or is a primary hypothalamic defect is unclear.

The fat (*fat*) mutation

The *fat* mutation was found in an inbred HRS/J mouse colony in 1973, was shown to be inherited in an autosomal recessive fashion, and localized to mouse chromosome 8 near *Es–1* (Coleman and Eicher, 1990). Homozygous *fat/fat* animals develop obesity by 6-8 weeks of age, but the increase is slower than that seen in *ob/ob* or *db/db* mutants. At 24 weeks, weights in excess of 60 g are common (most of the gain is in fat), with a pattern of fat deposition distinct from that seen in either *ob/ob* or *db/db* mutants. Both *fat/fat* and

tub/tub mutants deposit fat primarily throughout the body as opposed to either *ob/ob* or *db/db* animals in which fat deposition occurs primarily in the inguinal and axial regions ('pear-shaped obesity). The homozygous animals are not sterile, however infertility develops after the obesity develops at 5 – 8 weeks of age. On both the original HSR/J background, as well as on the C57BL/KsJ background, females are normoglycemic, whereas males develop only transient hyperglycemia at ~8 weeks, but return to normal thereafter. Similar to C57BL/6J *ob/ob* or *db/db* animals, plasma insulin concentrations remain elevated throughout the life of the *fat/fat* mutant on both the HSR/J and C57BL/KsJ background, without any evidence of β-cell atrophy. However, severe hyperinsulinemia has been noted on either background in *fat/fat* mutants as early as 4 weeks of age, before obesity can be visually detected. This is in contrast to any of the other known mutants which do not develop severe hyperinsulinemia until after the onset on obesity (Coleman and Eicher, 1990).

The tubby (*tub*) mutation

The *tub* mutation arose in a male C57BL/6J (F125) breeder at the Jackson laboratory. Further studies characterized the inheritance of the syndrome as autosomal recessive. Segregation of the *tub* locus in a B6 X *M. castaneus* backcross, localized the gene to chromosome 7, with the order cen — *Gpi-1* — [*tub* , *Hbb*]. Although *tub* appeared to be distal to *Hbb*, the

lack of informative meiosis and the large distance between *Gpi-1* and *tub*, made exact localization of *tub* indeterminable (Coleman and Eicher, 1990). The phenotype is unrecognizable until 9 - 12 weeks of age, depositing fat the slowest of the 4 recessive mouse obesity mutants, and the total weight gain is markedly less in *tub/tub* than in *fat/fat* mutants. As in the case of *fat/fat* animals, the excess body fat in *tub/tub* animals is distributed throughout the body, and infertility develops only after the onset of obesity. Unlike *fat/fat*, *ob/ob*, or *db/db* animals, *tub/tub* mutants of both sexes remain euglycemic or slightly hypoglycemic throughout life. Plasma [insulin] is elevated in the homozygote at 4-8 weeks of age, however the peak [insulin] attained is lower than that seen in C57BL/6J *ob/ob*, *db/db* or C57BL/KsJ *fat/fat* animals. Although the inulin II gene is located on mouse chromosome 7, HPLC analysis revealed no defect in insulin associated with *tub/tub* mutants (unpublished observations in (Coleman and Eicher, 1990))

Use of the *ob* and *db* mutants to model human obesity and diabetes

Since the *db/db* and *ob/ob* phenotypes are indistinguishable in mice of identical genetic background, it is possible that the two genes may code for components/regulators of a single biochemical or regulatory pathway. Parabiosis experiments in which animal pairs exchange blood through a capillary anastomosis (~ 1-2% of cardiac output), suggest that *ob* animals are missing a circulating satiety factor that suppresses appetite, and that *db*

animals are missing the receptor for that factor. When an *ob/ob* animal and a normal animal were parabiosed, the *ob/ob* animal failed to gain weight as typical of *ob/ob* mice. A similar experiment with *db/db* instead of *ob/ob* animals resulted in the death of the normal animal by starvation, although both animals were allowed access to food and water ad libitum. The third parabiosis experiment, between an *ob/ob* animal and a *db/db* animal resulted in the starvation and eventual death of the *ob/ob* animal (Coleman and Hummel, 1969; Coleman, 1973; Coleman, 1978). If these experiments are interpreted as indicating that the *ob/ob* animal is lacking a circulating satiety factor to which the *db/db* animal is lacking the receptor, then *db/db* animals would overproduce this circulating factor, causing cachexia in either *ob/ob* or normal animals whose circulations are artificially connected.

It has been proposed that the harsh environment in which our forbears evolved may have conferred a survival advantage on individuals of high metabolic efficiency ('thrifty genotype') (Neel, 1962). The positive selection pressure on the relevant genes, and their relative overrepresentation in modern populations, may lead to a predisposition to obesity and diabetes in environmental circumstances characterized by ready access to calorically dense foods. Coleman has reported that *ob/+* and *db/+* animals survive a fast 2-3 days longer than their +/+ littermates (Coleman, 1979), and that this advantage may be due to enhanced rates of conversion of ketones (acetone) to gluconeogenic precursors (lactate) (Coleman, 1980).

As noted, the genetic background (strain) onto which the *ob* or *db* mutant alleles have been bred has a potent effect on the phenotype of these mutations. Homozygosity for the *ob* and *db* genes on the C57BL/KsJ background results in hyperphagia, polydipsia, polyuria, hyperinsulinemia, sustained hyperglucagonemia, severe hyperglycemia, and peripheral insulin resistance. The concentration of plasma insulin is elevated by a factor of approximately 10 by 2-3 months of age. Necrosis of beta-cells, insulinopenia, and hyperglycemia occur by 5-8 months of age, resulting in the death of the animal (Coleman, 1978). On the C57BL/6J background, both mutations result in massive obesity, but the severity of the accompanying diabetes mellitus is greatly diminished compared to the mutant phenotype on the C57BL/KsJ background. Homozygous C57BL/6J *db/db* animals demonstrate hyperglycemia with compensating beta-cell hypertrophy and only a mildly reduced lifespan (Hummel, et al., 1972). Because inbred strains differ in their susceptibility to the diabetes-obesity syndrome produced by homozygosity for the *ob* and *db* alleles, examination of the distribution of metabolic phenotypes of offspring from inter-strain crosses permits estimates of the number of background genes influencing the mutant phenotype. Used in conjunction with the complete genetic maps of the mouse genome previously described, such a strategy may permit the assignment to specific chromosomes of the phenotype-influencing genes.

As discussed, a number of recessively inherited rodent models of obesity, *ob, db, tub, fat,* and the Zucker fatty rat *fa* mutations, exhibit striking resemblance to the metabolic/behavioral phenotype observed in obese humans. The coexistence of hyperphagia, enhanced metabolic efficiency and hyperinsulinemic diabetes mellitus in homozygous *ob* and *db* mice makes these animals particularly interesting models relative to human obesity and diabetes.

Diabetes in humans is classified broadly into three categories. Type I diabetes, or insulin dependent diabetes mellitus (IDDM), is characterized by little or no endogenous insulin production necessitating exogenous insulin therapy. The onset of IDDM is usually before age 30, and is not correlated with the patient's weight. Pancreatic islet cell antibodies are frequently present in type I diabetics, and IDDM is HLA associated. Type II diabetes, or non-insulin dependent diabetes mellitus (NIDDM), commonly has its onset after age 40, and from 50 – 90 % of those suffering from NIDDM are overweight. Identical twins are almost 100 % concordant for NIDDM suggesting a genetic component to this disorder. Type II diabetics demonstrate an increase in insulin resistance but usually maintain sufficient insulin production to insure that ketoacidosis does not occur. This state of relative insulin resistance is typically not severe enough to warrant exogenous insulin; oral sulfonylurea based hypoglycemic agents are usually sufficient to maintain relatively normal plasma glucose levels. Weight

reduction by patients suffering from Type II diabetes is often sufficient to normalize glucose homeostasis. The third and last category of human diabetes is "secondary diabetes", that is, diabetes caused by a variety of identifiable agents which destroy the pancreas' insulin producing capacity.

Although rodent models of obesity/diabetes may greatly facilitate our understanding of the metabolic control of body composition and glucose homeostasis in humans, differences between the syndromes produced by these mice and Type II diabetes (which most closely resembles the diabetes seen in genetically obese/diabetic mice) in human exist. Metabolic characteristics of diabetes are manifested in homozygous *db*, *ob*, and *tub* animals only after the onset of obesity. HRS/J *fat/fat* animals and the C57BL/KsJ *fat/fat* mutant however, do manifest hyperinsulinemia before the onset of phenotypically obvious obesity. Despite this difference, the metabolic defect in the *fat* mutant does ultimately give rise to obesity as well as diabetes. Although Type II diabetes in humans is associated with obesity, it is not an absolute requirement for the disease, nor does obesity develop in all Type II diabetics. Therefore differences between these genetically determined mice models of diabetes and Type II diabetes in humans do exist. In addition, since most new rodent mutants are discovered by visual inspection, detection of mutants which demonstrate only Type II diabetes (clinically mild diabetes of later onset) is difficult. The NOD (non-obese diabetic) mouse is an example of

a polygenic mouse model of human Type I diabetes, which due to the severity and early onset of the disease, was detected.

Despite intensive investigation into the pathophysiology of obesity and diabetes, it has been impossible to distinguish the *primary* pathway which gives rise to these diseases from their *secondary* metabolic alterations. Access to molecular markers for obesity, diabetes and their modifiers would accelerate efforts to understand the complex physiological mechanisms which give rise to these diseases. The availability of the murine models of obesity/diabetes, *ob* and *db*, provides a system for modeling the analogous physiological human states while affording a means to clone (via the technique of "positional cloning") and characterize genes which contribute to the obese/diabetic phenotype. For this reason the approach of "positional cloning" was undertaken in order to isolate the *ob* and *db* gene products. This approach requires no knowledge or assumptions concerning the biological nature of the defect, and provides an approach for cloning genes solely on the basis of chromosomal location.

The steps involved in "positional cloning" are to :

1) determine the chromosomal location of the mutant gene.

2) obtain markers and genetically map the chromosomal region surrounding the gene.

3) build a physical map, and a YAC contig of the closest flanking markers to narrow the region of interest making possible the cloning and characterization of the gene itself.

In order to facilitate cloning of the *db* gene (and the *ob* gene by co-workers), experiments were completed which entailed:

1) the creation of a medium resolution genetic map (with offspring of an interspecific *M. laboratorius* X *M. spretus* cross) of chromosomes 4 (*db*) and chromosome 6 (*ob*), using genes previously assigned to these chromosomes.

2) the generation of a chromosome 4 and 6 specific library by cloning of a flow-sorted Robertsonian 4:6 chromosome, and the chromosomal assignment of markers obtained from this library utilizing both the interspecific *spretus* cross and somatic cell hybrids.

3) the development of intra and intersubspecific crosses segregating *db* to position markers relative to *db*.

4) sub-centimorgan "fine-mapping" of the *db* region using a microdissected clone bank and other genomic markers utilizing the offspring of the all the aforementioned crosses. In addition, a proximal

6 microdissection was accomplished to assist isolation of the *ob* gene by co-workers.

and 5) initialization of the physical mapping stage utilizing the closest *db* flanking markers.

Chapter 2: Materials and Methods

Materials

Chemicals

All chemicals were molecular biology grade supplied by Sigma Chemicals (St. Louis, Mo.) with the exception of: ethanol supplied by Quantum (Tusca, Il.), agarose and LMP agarose supplied by Bethesda Research Labs (BRL, Gaithersburg, Md.) , hydrochloric acid [HCl] by Fisher Scientific (Pittsburgh, Pa.), and X-gal and IPTG from New Jersey Glove and Lab Supply, (Livingston, N.J.).

Disposable plasticware

Disposable sterile pipettes were purchased from Fisher Scientific. Pipette tips were acquired from Rainin (Emeryville, Ca), Denville Scientific (Denville, N.J.), or USA/Scientific Plastics (Ocala, Fl.). Eppendorf tubes were purchased from USA/Scientific and Fisher Scientific. Cryostorage tubes were obtained from Sarstedt Corp. (Princeton, N.J.). Centrifuge tubes were purchased from Beckmann Instruments (Palo Alto, Ca.), and conical tubes were obtained from Corning Glass Works (Corning, N.Y.).

Enzymes

Restriction endonucleases for digestion of genomic DNA and plasmids, with two exceptions, were purchased from either New England Biolabs (Beverly, Ma.), Bethesda Research Labs, Stratagene (La Jolla, Ca.), or

Boehringer-Mannheim (Indianapolis, In.) in concentrations which varied from 4-20U/μl. The EcoRI used in the microdissection procedures which was the peak collected fraction of activity (>4000U/μl), purchased from New England Biolabs. The restriction endonucleases used for the digestion of the agarose blocks for pulse-field analysis were purchased either from Boehringer-Mannheim or New England Biolabs. All restriction endonuclease digestions were carried out in the buffer supplied by the manufacturer, at the recommended concentrations.

Klenow (1U/μl), T4 DNA ligase, proteinase K and calf intestinal alkaline phosphatase (CIP) were purchased from Boehringer-Mannheim and buffers prepared to manufacturer's specifications.

Bacteriological media and reagents

Tryptone, yeast extract, agar, and NZ amine were supplied by Difco Labs (Detroit, Mi). Ampicillin and tetracycline were obtained from Sigma. 100mm and 150mm sterile petri dishes were purchased from Fisher Scientific.

Tissue culture media and reagents

DME was purchased from Gibco/BRL as a powder and reconstituted in doubly distilled and deonized water. Both Fetal Calf Serum (FCS) and Bovine Calf Serum (BCS) were also purchased from Gibco Labs and heat inactivated for 45 minutes at 55°C before being added to the DME media. 100 X Penicillin

and streptomycin (Gibco) were added to the DME to a final concentration of 1X. Colchemid was supplied by Gibco as a 1 mg/ml solution. Sterile tissue culture flasks and/or dishes (Nunc) were purchased from Fisher Scientific.

Lambda DNA

The original stock of λgt10 phage DNA (genotype: *LsrIL1* ◦ *b527 srIL3*◦ *imm434 (srI434+) srIL4*◦ *srIL5*◦) was purchased from Stratagene.

Lambda DNA in-vitro packaging extracts

Lambda in-vitro packaging extracts (Gigapack Gold) were purchased from Stratagene.

Plasmid DNA

Bluescript I KS+ and Bluescript II KS+ DNAs were purchased from Stratagene and grown in the hosts DH5 or DH5α-F′ (BRL).

Bacteriological Strains

The strains used to propagate the λgt10 vector were C600 and POP101. The strain used to propagate the bacteriophage λFIXII (Stratagene) was LE392. Plasmids were grown in the hosts XL1-blue, DH5α-F′, DH5, and HB101. The genotypes of the strains are as follows:

C600: *sup*E44, *thi*-1, *thr*-1, *leu*B6, *Lac*Y1, *ton*A21, *mcr*A

POP101: *sup*E44, *thi*-1, *thr*-1, *leu*B6, *Lac*Y1, *ton*A21, *mcr*A, *hflA150*::Tn*10*

HB101: *hsd*S20, *sup*E44, *ara*14, *gal*K2, *lac*Y1, *pro*A2, *rsp*L20, *xyl-5*, *mtl-1*, *rec*A13, *mcr*B, *mcr*A, *mrr*

DH5: F-, *rec*A1, *end*A1, *hsd*R17(r_k^-, m_k^+), *sup*E44, λ-, *thi*-1, *gry*A, *rel*A1

DH5α: F-, φ80d*lac*ZΔM15, Δ(*lac*ZYA-*arg*F)U169, *rec*A1, *end*A1, *hsd*R17, (r_k^-, m_k^+), *sup*E44, λ-, *thi*-1, *gry*A, *rel*A1

DH5α-F': F-, φ80d*lac*ZΔM15, Δ(*lac*ZYA-*arg*F)U169, *rec*A1, *end*A1, *hsd*R17, (r_k^-, m_k^+), *sup*E44, λ-, *thi*-1, *gry*A, *rel*A1, [F' *pro*AB+, *lac*Iq ZΔM15, zzf::Tn5 (Km^r)]

XL1-Blue: *rec*A1, *end*A1, *gry*A96, *thi*-1,*hsd*R17, (r_k^-, m_k^+), *sup*E44, *rel*A1, *lac*, [F' proAB, *lac*Iq ZΔM15, Tn10 (tet^r)]

Nucleic acid radiolabeling materials:

α^{32}P-dCTP, γ^{32}P-dCTP, and α^{35}S-dCTP were acquired from NEN Nuclear Research (Boston, Ma.). The dNTPs, random hexamers, and RNAse/DNAase free BSA were purchased from Pharmacia (Pistcataway, N.J.). Push columns for the removal of unincorporated radionucleotides were obtained from Stratagene.

Spectroscopy

Optical densities were obtained on a model DU30 Beckmann spectrophotometer.

Electrophoresis, Southern blotting, and hybridization materials

Agarose gel electrophoresis equipment (gel boxes and combs) were constructed to the author's specifications by the Rockefeller University Machine Shop or acquired from Ann Arbor Plastics (Ann Arbor, Mi.). High voltage power supplies were manufactured by Blair Craft Scientific (Huntington Station, N.Y.) or EC apparatus (St. Petersburg, Fl.). Acrylamide and sequencing gel apparatus were obtained from BRL.

Nylon membranes (Genescreen Plus) were obtained from NEN Research Products, , Zetabind from AMF-Cuno, and Immobilon–N membranes from Millipore (Bedford, Ma.). Rapid-hybridization solution was purchased from Amersham (Arlington Hts, Il.).

Pulse-Field Gel Electrophoresis equipment

DNA was prepared employing Incert agarose obtained from Biorad Corporation (Melville, N.Y.). Electrophoresis was accomplished using an LKB 2015 Pulsaphor apparatus fitted with an hexagonal electrode array and a model 2015 Pulsaphor plus control unit.

Polymerase chain reaction (PCR) materials

PCR reactions were accomplished with native Taq polymerase purchased from Boehringer-Mannheim and both native and recombinant Taq polymerase obtained from Perkin-Elmer Cetus (Emeryville, Ca). PCR reactions using the Taq polymerase from Boehringer Mannheim were carried out in the buffer supplied by the manufacturer, while PCR reactions using Taq polymerase obtained from Perkin Elmer-Cetus were carried out in buffers made to specifications prescribed by the manufacturer.

A Perkin-Elmer Cetus model 4800 automated thermocycler was used for the PCR reactions. Polypropylene tubes (0.4 ml) used in the machine were purchased from USA/Scientific Products. Non-spectroscopic grade paraffin oil (Sigma) was used in the thermocycler to promote rapid thermal exchange with the PCR reactions, while spectroscopic grade paraffin oil was used to overlay the reactions during cycling.

Sequencing materials

Sequencing reactions were carried out using the Sequenase kit for dideoxy-sequencing purchased from United States Biochemical Corp. (Cleveland, Oh.) or using a model 373A automated sequencer system manufactured by Applied Bio Systems Inc. (*ABI*, Foster City, Ca.)

DNA extractor

Organs and cells whose DNA were not prepared manually were made utilizing an ABI model 340A DNA extractor using chemicals and methods specific for the machine, prepared by the manufacturer.

Microdissection equipment

Glassware: 2 mm O.D. solid pyrex tubing was purchased from Fisher Scientific. 10 mm O.D., 1 mm I.D. capillaries were drawn to ~1 mm O.D. and 0.1 mm I.D. and polished by Vibrodynamics. Coverslips were purchased from AB Termoglas (Göetenberg, Sweden). Spectroscopic grade paraffin oil was acquired from Fisher Scientific.

Non-glassware: The de-Fonbrunne type micromanipulator and Leitz microforge were purchased from Kramer Scientific (Yonkers, N.Y.). The Leitz serial/model # 4287931 microscope was obtained from the Rockefeller University storage facility. The injector was made to specifications by the Rockefeller University machine shop. the system was insulated from outside vibrations by placement on a Vibraplane #1201-02-12 table purchased from Kinetic Systems (Palinsdale, Ma.).

Bacterial electroporation materials

Plasmids were electroporated into appropriately prepared bacteria using the Bio-Rad Gene-Pulser apparatus equipped with a Pulse Controller unit. 0.1 cm electrode gap cuvettes (Bio-Rad) were used for the electroporation.

Photography and autoradiography

Agarose gels were photographed using a Polaroid Land Camera using type 107C film after staining with ethidium bromide and visualization with a UV light box (Fisher Scientific). Acrylamide gels, and autoradiograms were exposed to Kodak XAR-5 film (Eastman-Kodak, Rochester, N.Y.) in Wolf autoradiography cassettes equipped with Lightning Plus intensifying screens (New Jersey Glove and Lab Supply) and developed in a Kodak X-OMAT processor using RGS developer and fixer purchased from RGS X-ray (Freeport, N.Y.).

Chromosome microdissections were videotaped using a Sony videocamera and NEC model 550U videocassette recorder and then electronically transferred to negative film (Rockefeller University Graphics Service, N.Y., N.Y.).

Computer software and hardware

Pedigree analysis's were accomplished using either the program 'Spretus Madness' (Kinglsey, et al., 1989) running on a SIREX IBM compatible

(8/12 MHz) '286' computer or the multipoint linkage analysis program 'MAPMAKER' (Lander, et al., 1987) compiled and running on a SUN SPARCstation employing the Berkeley System 4.3 version of the UNIX operating system. The oligonucleotide design program 'PRIMER' (Lincoln, et al., 1991) was run on either a MacIntosh IIci equipped with a Motorola math co-processor, or a Macintosh LC employing the floating point unit interception INIT 'Software FPU' (shareware, John Neil Inc.), under system version 6.0.7. All statistical calculations were performed with the BMDP statistical package running on a Harris mainframe employing the Berkeley System 4.3 distribution of the UNIX operating system.

Mouse stocks

Mice were purchased from The Jackson Laboratories (Bar Harbor, Ma.), housed in N.I.H. approved facilities (The Rockefeller University) and provided food (Pico laboratory mouse breeding chow #5058 (Purina) containing 9% fat) and water *ad libitum*. Ovarian transplants were performed by D. Corow at The Jackson Laboratories.

General Methodology

Transformation of cloned loci:

DNAs cloned in plasmid vectors were transformed by either calcium mediated transformation into competent bacteria or by electroporation into appropriately prepared bacteria.

Calcium mediated transformation: To 50 ml of N broth (10 g Bactotryptone, 1g yeast extract, 8 g NaCl, 1 g glucose, and 0.3 g $CaCl_2$ per liter), a single colony of an appropriate *Escherichia coli* strain was added and the broth incubated at 37° C in an orbital shaker at >200 rpm. Aliqouts were withdrawn after a few hours and the culture allowed to grow until the bacteria reached a density of OD_{650}= 0.6 - 0.7. The culture was then fractionated into 4 equal 12.5 ml aliquots, chilled on ice for 30 minutes and spun at 4000 rpm at 0° C for 5 minutes. The aqueous top was decanted and the brown pellet resuspended in 25 ml of 50 mM $CaCl_2$ at 0° C. The resuspended bacteria were left at 0° C for 60 minutes and then spun at 0° C at 3000 rpm for five minutes. The supernatants were decanted and each bacterial pellet was resuspended in 5 ml of a 50 mM $CaCl_2$/20% glycerol solution at 0° C. The resuspended mixture was frozen at –80° C in 0.5 ml aliquots in eppendorf tubes.

Transformation of Plasmids Using Competent Bacteria: Plasmids were diluted to a concentration of 0.2 ng/ml. Competent bacteria were thawed from –70° C to 0° C on ice. At 0° C, 50ml (10 ng) of DNA, 20 ml of 10X TCM (10X TCM = 100 mM Tris pH7.4, 100 mM $CaCl_2$ and 100 mM $MgCl_2$), and 125 µl of cells were combined and allowed to stand in ice for 20 minutes. The mixture was then heat shocked at 42° C for 90 seconds after which 1 ml of room temperature L broth (10 g Bactotryptone, 10 g NaCl, 5 g yeast extract per liter) was added. After 10 minutes at room temperature, the mixture was shaken at 37° C for 60 minutes at > 200 rpm, and 5, 20 and 200 µl aliquots plated on appropriately prepared antibiotic containing LB plates (L broth + 15g agarose/liter) which were incubated at 37° C after drying. The final concentrations of ampicillin and tetracycline in the LB plates were 100 µg/ml and 15 µg/ml respectively.

Preparation of E-Coli for electroporation: A single colony of an appropriate bacterial strain was inoculated into 10 ml of L-broth, containing antibiotics where appropriate, and shaken overnight at 37° C at >200 rpm The next morning the cultures were inoculated into 1 liter of SOB medium (20 g bacto-tryptone, 5 g bacto-yeast extract, 0.5 g NaCl per liter) containing the appropriate antibiotic and shaken for ~4 hours at 37° C at >200 r.p.m until an OD_{550} = ~0.7. The culture was then transferred to two 500 ml autoclaved plastic centrifugation bottles and centrifuged at 0° C at 3000g X 30 min. The

pellet was then resuspended in a half volume of ice-cold 10% v/v molecular biology grade glycerol/H_2O, and centrifuged as before. The resulting pellet was again resuspended in a half volume of ice-cold 10% v/v molecular biology grade glycerol/H_2O, and recentrifuged. This pellet was resuspended in 20 ml of 10% glycerol/H_2O, recentrifuged and the supernatant decanted. The resultant slurry was quickly pipetted into 220 µl aliquots and frozen in liquid nitrogen.

Electroporation of plasmid DNA: To a 40 µl aliquot of freshly thawed electroporation bacteria, no more than 1µl of plasmid, containing no more than 0.1ng of DNA, was added to a prechilled cuvette. The cuvette containing the plasmid/bacterial mixture was then subjected to a 1700V pulse at 200 Ohms and a 25 micorfarad (µFd) capacitance. If a time-constant of at least 3.9 was not obtained, the DNA solution was diluted by 10X, and the procedure repeated. Within 60 seconds of electroporation, 1.0 ml of SOC (SOB with 20 ml sterile 1M glucose [18 g glucose/100 ml water] and 20 ml of 1 M $MgSO_4$/1 M $MgCl_2$ added per liter) was added, and the cells transferred to a 4.5 ml plastic tube and shaken for 1 hour before plating on an appropriately prepared antibiotic containing LB plate.

Isolation of DNA:

Large-scale ('maxi-prep') purification of plasmid DNA: A single colony pick of a transformed plasmid was inoculated into 10 ml of L broth. After significant growth occurred, the entire 10 ml of broth was added to 1 liter of L broth containing the antibiotic appropriate for the plasmid and the mixture incubated at 37° C overnight with shaking at >200 rpm. The next morning, the broth was transferred to plastic bottles and spun at 3000xg for 30 minutes at 4° C. The supernatant was decanted and the pellets resuspended in 25 ml of ice cold TE (10 mM Tris pH 8.0, 1 mM EDTA pH 8.0) and then spun at 5000 rpm for 15 minutes in a GSA Sorvall rotor. Each pellet was then resuspended in 20 ml of solution I (50 mM Glucose, 25 mM Tris pH 8.0, 10 mM EDTA pH 8.0), after which another 20 ml of the same solution containing 4 mg/ml of lysozyme was added. This mixture was left to stand at room temperature for 10 minutes. When the cells were reasonably in suspension, 60 ml of solution II (0.2 N NaOH, 1% SDS) was added after which the solution became fairly clear and viscous almost immediately. After swirling gently to mix and allowing it to stand at room temperature until clear, 60 ml of solution III (300 ml of 5 M Potassium Acetate, 57.5 ml of glacial acetic acid, and 145.5 ml of H_2O) was added. The resultant mixture was inverted gently to mix (after which a fluffy white precipitate formed) and left to stand at room temperature for 10 minutes. After centrifugation at 5000 rpm for 15 minutes at 4° C, the

pellet was fairly hard and white, and the supernatant was poured off through a small wad of glass wool into another flask. To the supernatant, 80 ml of isopropanol was added, the mixture left at room temperature for 10 minutes, and then spun at 4° C for 30 minutes at 5000 rpm. The resultant pellet was dissolved in 20 ml of TE, pH 8.0 to which 21.5 g CsCl and 1.6 ml of 10 mg/ml ethidium bromide was added. The mixture was loaded into a VTi50 tube, filled with mineral oil and sealed. The tube was then centrifuged at 45K for at least 24 hours at 20° C in a vertical Beckman VTi50 rotor, or at 45K rpm for 48 hours at 20° C in a Ti60 rotor.

The lower supercoiled band was removed using a 10 ml syringe and an 18 gauge needle by inserting the needle through the side of the centrifuge tube under UV illumination/guidance. The ethidium bromide was extracted with an equal volume of 5M NaCl-saturated isopropanol while the extracted band is still within the syringe. The aqueous phase (approximately 4 ml) was ejected into a 30 ml corex tube to which 10 ml of water is added, and then filled with 95% ethanol. The plasmid was then precipitated at -20oC overnight. The plasmid was harvested by spinning at 10K rpm for 30 minutes, resuspending the pellet in 0.3M sodium acetate pH 5.3, and reprecipitating with 3 volumes of ethanol. The recovered pellet was then rinsed twice with cold 70% ethanol/H_20 and vacuum dried. The OD_{260} was established and the plasmid brought to a final concentration of 1 μg/ml with

a 10 mM Tris pH 7.6/1mM EDTA solution (10,1 TE). The yield from this procedure varied from 800 µg - 2 mg of supercoiled plasmid.

Small scale ('miniprep') purification of plasmids: A single bacterial colony was inoculated into 10 ml of LB containing the appropriate antibiotic. After overnight growth at 37° C at >200 rpm, a 1ml aliquot was removed and spun 2 minutes in a microcentrifuge (~11,000 rpm). The supernatant was decanted and any remaining liquid was removed by pipetting. To the pellet, 100 µl of solution I (50 mM Glucose, 25 mM Tris pH 8.0, 10 mM EDTA pH 8.0) was added, the pellet resuspended well and 200 µl of solution II (0.2 N NaOH, 1% SDS) was subsequently added, the mixture vortexed, and left on ice for 5 min. To the mixture, 150 µl of solution III (300 ml of 5 M Potassium Acetate, 57.5 ml of glacial acetic acid, and 145.5 ml of H_2O) was then added and the mixture vortexed and placed on ice for 2 min. After 2 min of centrifugation in a microcentrifuge, the supernatant was carefully removed without disturbing the white precipitate that had formed. To this supernatant an equal volume of phenol/chloroform was added, vortexed, and centrifuged for 2 minutes. The top aqueous layer was then transferred to a clean eppendorf tube, two volumes of 100% ethanol were added, the mixture incubated for 5 minutes at room temperature and then centrifuged for 5 minutes. The supernatant was discarded, the pellet washed twice with 70% ethanol, and the remaining ethanol removed by rotary evaporation. The pellet was resuspended in 25 µl

of a 10 mM Tris pH 7.6 /1 mM EDTA pH 8.0 solution containing 20 μg/ml RNAse A. A 2.5 μl aliquot was usually sufficient for most restriction digests.

Isolation of high quality lambda phage DNA: An overnight culture of the bacterial strain appropriate for the bacteriophage was incubated overnight at 37° C. The culture was centrifuged at 3000xg for 10 minutes and the supernatant was decanted. The bacterial pellet was resuspended in a half volume of phage dilution media (10 mM Tris pH 7.6, 10 mM MgSO4) and aerated at 37° C for 1 hour. A 300 μl aliquot of bacteria was incubated for 20 minutes at 37° C with 10^5 pfu of bacteriophage and then plated on 150 mm^2 LB plates containing 10 mM $MgSO_4$. The plates were incubated upright in a closed container lined with wet paper towels, to promote confluency.

After confluent lysis, the plates were cooled in a cold room, and overlaid with 12 ml of cold phage dilution media. The overlaid solution was harvested after 6 hours of rotation in the cold room, and 50 ml of $CHCl_3$ was added. Bacterial debris were removed by centrifugation at 10,000 rpm for 10 minutes in a Beckman JA-20 rotor and the phage were sedimented by centrifugation at 20,000 rpm for 3 hours. The phage pellets were serially resuspended in 1/2 ml of phage diluent.

In order to remove contaminating proteins (r ~ 1.3), the phage were sedimented into CsCl from the top of a tube. In a Beckman SW-65 polyamor tube, 1 ml of a 5.0M CsCl solution [r ~ 1.6] in 10 mM $MgSO_4$, 10 mM Tris pH

8.0, 1 mM EDTA pH 8.0 was placed. This was overlaid with 3 ml of 3 M CsCl [r ~ 1.5] in 10 mM $MgSO_4$, 10 mM Tris pH 8.0, 1 mM EDTA pH 8.0. The phage was placed on top of this second layer and centrifuged in a Beckman SW-65 rotor at 30,000 rpm for 1 hour with the brake disengaged. A 1/2 ml volume of CsCl including the light blue phage band, was removed from the side of the tube using a 1 ml syringe and a 26 gauge needle.

To remove contaminating DNA and RNA , the phage removed from the first gradient were floated up into CsCl from the bottom of a tube. The phage was suspended in buoyant [r ~ 1.5] CsCl (3 M CsCl, 10 mM $MgSO_4$, 10 mM Tris pH 8.0, 1 mM EDTA pH 8.0) in the bottom of a Beckman SW-65 polyamor tube. An equal volume (0.5 ml) of saturated (25° C) CsCl (7.2 M CsCl, 10 mM $MgSO_4$, 10 mM Tris pH 8.0, 1 mM EDTA pH 8.0) was added and mixed well. The mixture was overlaid with 3 ml of 5.0 M CsCl [r ~ 1.6] in 10 mM $MgSO_4$, 10 mM Tris pH 8.0, 1 mM EDTA pH 8.0. Subsequently, 1 ml of 3.0 M CsCl [r ~ 1.3] in 10 mM $MgSO_4$, 10 mM Tris pH 8.0, 1 mM EDTA pH 8.0 was overlaid. The phage were centrifuged in a Beckman SW-65 rotor at 30,000 rpm for 1 hour with the brake disengaged. The blue phage band was extracted from the interface of the 3 M and 5 M CsCl layers using a 1 ml syringe and 26 gauge needle.

The eluted phage were mixed with 1/10th volume unit 0.2 M Na_2EDTA and dialyzed against 50% deionized formamide, 0.2 M Tris pH 8.0,

and 0.02 M Na_2EDTA for 24 hours at room temperature. The resulting solution was then dialyzed against 0.1 M NaCl, 0.05 M Tris pH 7.6, and 0.001 M Na_2EDTA, with 4 buffer changes at 200 fold dilution.

Rapid isolation of lambda phage DNA: As with the preparation of high quality phage just described, 10 LB plates were inoculated with the appropriate bacteria and phage, harvested and the bacterial debris removed. After isolation of the phage particles and resuspension in 2.5 ml of phage storage media, the phage particles were extracted on the ABI DNA extractor with a Proteinase K digestion time of 90 minutes. The resultant DNA was resuspended in ~500 µl of a 10 mM Tris pH 7.6/1 mM EDTA pH 8.0 /20 µM RNAse A solution.

Isolation of high molecular weight genomic DNA: Frozen organs were thawed on ice and then added to 8 ml of 10,10 TE (10 mM Tris pH7.6, 10 mM EDTA pH 8.0). The organ was then fragmented between the frosted ends of standard microscope slides and pipetted into a 15 ml conical tube. Fresh organs were placed in a 1.5 ml eppendorf tube and homogenized using a miniature homogenizer (Kontes). The homogenate was then added to 8 ml of 10,10 TE in a 15 ml conical tube. The procedure for fresh and frozen organ DNA preparation was similar from then on.

The conical tubes were vigorously vortexed and then spun at 2000 rpm for 5 minutes at 4° C. The supernatant was aspirated, and the pellet resuspended in 8 ml of 10,10 TE. After vigorous vortexing 1 ml of 10% NP40 nonanionic detergent was added to each tube and the tubes gently vortexed. After centrifugation as before, the supernatant was aspirated and 5 ml of 10,10 TE was added, breaking up the now fluffy white/brown pellet by pipetting the mixture several times. To this suspension 500 µl of a 20% SDS (Sodium Dodecyl Sulfate), and 200 µl of a 10 mg/ml Proteinase K solution was added. The mixture was then incubated overnight at 65° C in a rotating water bath.

The following morning, 200 µl of the Proteinase K solution was again added and the incubation continued for 6 hours. The volume of the DNA dilution was brought up to 6 ml with 10,10 TE and an equal volume of TE (10 mM Tris pH 8.0, 1 mM EDTA pH 8.0) equilibrated phenol was then added. This mixture was nutated for approximately 3 minutes after which the solutions were centrifuged at 3000 rpm for 15 minutes at 4° C. The bottom phenol layer and as much of the white interface as possible, was discarded. An equal volume of 50% $CHCl_3$ / 50% equilibrated phenol was then added, the tubes nutated for 3 minutes and centrifuged at 3000 rpm for 15 minutes. The lower organic phase and the interface were removed and 6 ml of $CHCl_3$ added. After nutation and centrifugation, the aqueous layer was carefully removed avoiding removal of any of the interface. A half volume of 7.5 N NH_4Acetate and an equal volume of isopropanol were added and the ensuing

mixture inverted by hand until the precipitation of DNA strands were visible. The DNA was spooled and removed, using a 200 µl Rainen pipette tip, to a suitable container. Approximately 300 µl of 10,1 TE was added, the mixture incubated at 65° C for 5 hours and then nutated until homogeneity. A 5 µl aliquot was electrophoresed overnight to ensure no degradation occurred. Another 5 µl aliquot was subjected to UV spectroscopy at A_{260} and A_{280}, and then the stock solution was diluted to a concentration of approximately 1 µg/µl using 10,1 TE. Yields varied from 300 µg from a single kidney, to over 2 mg for an entire liver. If degradation of the DNA had occurred, as shown by electrophoresis, or significant RNA/protein contamination was suspected because of an abnormally high A_{260}/A_{280} ratio, another organ's DNA was isolated.

Alternatively, both fresh and previously thawed organs were homogenized in a Kontes LC 7 ml dounce using the 'A' pestle. After homogenization, the DNA was extracted from the organs utilizing the ABI DNA extractor with Proteinase K digestions ranging from 6 - 18 hours. Yields of DNA from these tissues were typically ~3 µg/mg tissue. Resuspension, quantification, and degradation checking were unchanged from that just described.

Isolation of subclone inserts:

The plasmid or bacteriophage bearing the insert of interest was restriction digested with the appropriate enzymes to excise the insert. Restriction digests were carried out in the restriction endonucleases manufacturer's buffers under the recommended conditions. The digested mixture was electrophoresed on a 0.6% -1.0% LMP agarose gel, and the DNA fragment of interest was excised from the gel. The excised band was weighed and 3 µl of water was added per mg of agarose weight. The diluted DNA fragment was heated to 65° C for 15 minutes and then stored at 4° C.

Restriction digestion and electrophoresis of genomic DNA:

Approximately 10 µg of DNA (as determined by UV absorption) was digested with the appropriate restriction endonucleases using the recommended manufacturer protocol and reaction buffers. The DNA was electrophoresed through 1X TBE (5X = 54 g Tris base, 27.5 g boric acid, 20 ml 0.5 M EDTA pH 8.0) or 1X TAE (50X = 242 g Tris base, 57.1 ml glacial acetic acid, and 100 ml 0.5 M EDTA pH 8.0) employing agarose gels of concentrations between 0.5% and 1.2% depending upon the expected size range of the DNA fragments of interest. Loading of the restriction digested DNA and monitoring of gel progress was accomplished by the addition of 10% v/v xylene cylanol/bromophenol blue loading dye. Electrophoresis was carried out in buffer identical to the gel buffer, containing 100 µl 0.1% ethidium

bromide/1 liter of buffer, at ~2.5 - 5.0 V/cm At completion, the gel was then photographed and the DNA nicked using UV irradiation (5 minutes) from the transilluminator. The conditions for transfer of the electrophoresed DNA to a solid support, depended upon the membrane utilized. For Genescreen Plus nylon membranes, following a 20 minute denaturation of the gel with agitation in 0.6 N NaOH/0.4 N NaCl, the gel was transferred, "Southern blotted" by the procedure of Southern (Southern, 1975) using the denaturation solution as transfer buffer. After 12 hours the membrane was briefly washed in the transfer buffer and then neutralized in 0.5 N TrisHCl pH 7.6/ 0.5 N NaOH. For Zetabind membranes, the gel was denatured in 0.5 M NaOH/1.5 M NaCl for 30 minutes, neutralized in 1.0 M Tris pH 7.6/1.5 M NaCl for 30 minutes and then transferred for 4-24 hours using 10X SSC (20X = 175.3 g NaCl and 88.2 g of sodium citrate per liter). The gels transferred to Immobilon-N were prepared identically to those transferred to Zetabind membranes, however the Immobilon-N membrane was first rinsed in 100% methanol for 10 seconds, distilled water for ~30 seconds, and then equilibrated in 10X SSC before being used for the transfer. Transfer of the DNA from the gel to the membrane was established by examination with a hand held long wave UV lamp. After examination, the blots were briefly rinsed in 6X SSC and baked at 80° C for 1 hour.

'Random-priming' radiolabeling of nucleic acids:

Inserts to be labeled were incubated at 65° C for 15 minutes to liquefy the LMP agarose, after which a 20 µl aliquot was removed, combined with 13 µl of water, 10 µl of oligolabeling buffer (OLB) (Feinberg and Vogelstein, 1983; Feinberg and Vogelstein, 1984) [50 OD units random hexamers in 1.85 ml of a 250 mM Tris pH 8.0, 25 mM $MgCl_2$, 0.5M Hepes, and 7.2 ml β-mercaptoethanol solution], 5 µl of α-^{32}P dCTP, and 1 µl of a 125 µM mixture of dGTP, dATP, and dTTP. The mixture was denatured in a 105° C heating block for 10 minutes after which the probe was placed in a 37° C water bath for 15 minutes. 2 µl of a 3 mg/ml BSA solution and one unit of Klenow enzyme (1 µl) was added and the mixture incubated at 37° C for one hour. The unincorporated nucleotides were subsequently removed by passage of the reaction through a push column.

Oligoprimer kinasing:

Approximately 1 µg of an oligo was added to a mixture of 1 µl 10X kinase buffer (10 X = 0.5M Tris pH 7.6, 100 mM $MgCl_2$, 50 mM dithiotreitol, 1 mM spermidine HCl, 1 mM EDTA pH 8.0), 5 µl of γ^{32}P-ATP (50 µCi), 1 µl of 10 U/µl polynucleotide kinase (PNK), and 3 µl H_2O. The mixture was incubated at 37° C for 30 minutes, a second 1 µl aliquot of PNK added and the mixture reincubated for an additional 30 minutes. The unincorporated nucleotides

were subsequently removed by passage of the reaction through a push column if the primer was to be used for hybridization (such as in the case of screening a digested clone for dinucleotide repeats with a labeled GT multimer), or was not further purified if the oligo was intended for use in a PCR reaction.

Hybridization of radiolabelled DNA to a Southern blot :

GeneScreen Plus and Zetabind filters were prehybridized in 5X Denhardt's solution (50X Denhardt's is 10 g/l Ficoll 400, 10 g/l polyvinyl-pyrrolidone, and 10 g/l BSA pentax fraction V), 6X SSC, 0.2% (w/v) sodium pyrophosphate, 0.5% SDS, and 10 mM EDTA pH 8.0 overnight at 65° C in a rotisserie hybridization oven rotating at ~6 revolutions/min. The filters were subsequently hybridized in a total volume of 10 ml of fresh prehybridization solution with 10% w/v dextran sulfate added at 65° C with ~10^6 dpm/ml of radiolabelled probe added. Immobilon-N filters were pre-wetted for 10 seconds in 100% methanol, rinsed in distilled water for 30 seconds and then prehybridized for 1 hour in 10 ml Rapid-Hyb hybridization solution at 65° C. Hybridization of the filter was accomplished in a total volume of 10 ml of fresh solution containing 10^6 dpm/ml over a total of 2 hours - overnight. GeneScreen Plus filters were washed in 2X SSC/0.1% SDS at room temperature for 15 minutes X 2, and then to a final stringency of 2X (or 1X) SSC/1.0% SDS for 30 minutes at 65° C. Zetabind membranes were washed to a

final stringency of 1X SSPC, 0.1% SDS at 65° C, and Immobilon-N membranes in two washes of 0.1X SSC/0.1% SDS at 65° C for 30 minutes.

Polymerase chain reaction (PCR) amplification of specific DNA sequences:

Locus specific oligonucleotides (20 - 36 bp in length) were obtained from The Rockefeller University Sequencing facility or were synthesized on an ABI model 392 DNA/RNA synthesizer. Some of the primer sequences were derived with the aid of the computer program 'PRIMER' (Lincoln, et al., 1991). PCR reactions were carried out in a 100 µl. (50 µl as noted) total reaction volume (1X buffer= 50 mM KCl, 10 mM Tris pH 8.3, 1.5 mM $MgCl_2$, and 0.01% gelatin), with the addition of 250 ng of each specific primer, 16 µl of a 1.25 mM dNTP solution, 250 ng of genomic target DNA or 10 µl of an appropriate phage stock stored in phage storage media (5.8 g NaCl, 2 g $MgSO_4 \cdot 7 H_2O$, 50 ml 1 M Tris pH 7.6, 5 ml 2% gelatin per liter), and 0.1 µl (0.5 U) Taq Polymerase.

Denaturing gradient gel electrophoresis

For optimal separation of fragments in the 250-750 bp range, a 6.5% polyacrylamide gel was employed (40% acrylamide stock = 37.5:1 acrylamide:bisacrylamide) with a 20% - 80% denaturant gradient (100% denaturant = 6.5% acrylamide, 40% formamide, and 7 M urea) in 1X TAE buffer (Myers, et al., 1985; Noll and Collins, 1987). The gels were poured to a

thickness of 0.75 mm with ~20 mm wide wells. The entire apparatus was then completely immersed in a 1X TAE buffer chamber which was maintained at 60° C with circulation between the chambers effected with a peristaltic pump. Electrophoresis was carried out at ~60V for 18 hours after which the gels were stained with ethidium bromide and photographed.

Genomic clone screening:

LE392 cells were grown overnight in a 10ml culture and then spun at 3000xg X 10 minutes, and the pellet resuspended in 5ml of phage dilution buffer (10 mM Tris pH 8.0, 10 mM $MgSO_4$). To each of 10 X 300 µl aliquots of an O/N growth of LE392 cells, 40,000 pfu of a Stratagene custom genomic mouse library (mouse strain is privileged information) in the bacteriophage λFIXII, was mixed and incubated for 20 minutes at 37° C. To each mixture, 8ml of 55° C top agar was quickly added, swirled, and then plated on 150mm^2 plates that had been thoroughly dried at 37° C. The plates were then incubated for ~8 hours, agar side up, to minimize interplaque contamination. After growing, the plates were chilled for 2 hours at 4° C, and lifted in duplicate using nitrocellulose membranes that had previously been autoclaved for 90 seconds under steam bypass conditions. The pre-autoclaving helped ensure that the membrane did not shrink during the binding of the phage, which would make realignment of positive clones more difficult. The first filter was lifted for 30 seconds while the duplicate

filters remained on the plates for 2 minutes. The filters were dried at room temperature for ~15 minutes and then placed in the autoclave between 2 sheets of Whatmann 3mm paper for 90 seconds under steam bypass, 15 second fast exhaust, and 5 seconds drying.

The autoclaved filters were washed at 65° C in 500 ml 2X SSC, 0.1% SDS 4X for 30 minutes each. Using light strokes with a kimwipe tissue, small pieces of top agar that remained affixed to the filters were removed after the washes were complete. The filters were prehybridized in 6X SSC, 5X Denhardt's, 0.1% SDS, 200 μg/ml sonicated/denatured salmon sperm DNA, and 200 μg/ml tRNA in a total volume of 50ml for 2 hours at 65° C. Approximately 20 X 10^6 dpm of α-^{32}P labeled probe was then added to 50 ml of fresh prehybridization / hybridization solution in plastic tupperware and the mixture hybridized to the filters at 65° C overnight. The filters were washed twice in 2X SSC 0.1% SDS for 30 minutes each, and if few disintegrations were noted, the films exposed to XAR-5 film overnight. Further washes, when necessary, were accomplished in 0.5X SSC/0.1% SDS at 65° C for 30 minutes and then 0.1X SSC/0.1% SDS at 65° C for 30 minutes.

Positive plaques were aligned to the original plates by use of small holes punched through both the filters and the plates and were picked with either the wide end of a pasteur pipette, or the wide end of a standard 200 μl Rainin yellow tip and ejected into 1 ml of phage storage media. The phage

plugs were vortexed and then left to stand at room temperature for 4 hours to allow diffusion of the phage from the agarose.

Second round purification of the phage was accomplished by plating both 5 µl and 25 µl aliquots of a 10^{-4} dilution of the picked phage and processing as above. In only one case was a third round screen necessary, and it was accomplished in a fashion identical to the second round screen.

Bacteriophage lambda propagation:

Bacteriophage were propagated and isolated by plating on agar plates. LB plates were made by adding 15 g bacto-agar per liter of L-broth (15 g bacto-tryptone, 10 g yeast extract, 10 g NaCl per liter) with 10 mM $MgSO_4$ added and autoclaving the mixture. Top agar was similarly made but with the addition of 7.5 g of bacto-agar per liter and 10 mM $MgSO_4$.

Bacteria grown for use in bacteriophage platings were grown in LB with both 10 mM $MgSO_4$ added before autoclaving and 0.2% filter-sterilized maltose after autoclaving. A single bacterial culture was inoculated into 10 ml of LB with maltose and $MgSO_4$, grown with >200 rpm shaking overnight and then centrifuged at 3000xg for 10 minutes. The bacteria were then resuspended in 5 ml (1/2 volume) of phage dilution buffer (10 mM Tris pH 7.6, 10 mM $MgSO_4$) and stored at 4° C for a maximum of two days before plating. One hour before plating, the bacteria were removed from the cold room and shaken at >200 rpm at 37° C.

Autoradiography:

Filters were exposed to XAR-5 film at -70° C for 1-14 days with intensifying screens.

Creation of a medium density genetic map of mouse chromosomes 4 and 6 using known loci

Description of the interspecific C57BL/6J X *M. spretus* backcross

The female offspring (males are infertile) of a cross between C57BL/6J females and *M. spretus* males were mated to male C57BL/6J animals to generate N2 offspring (see Figure 2.1). At approximately 3 months of age, the N2 animals were sacrificed by CO_2 asphyxiation, and the kidney, liver, spleen, tail and thorax were removed and immediately frozen for subsequent isolation of DNA. Forty-three similarly bred N2 animals were the kind gift of Neil Copeland and Nancy Jenkins (Frederickson Cancer Research Center), and were sacrificed in a similar manner at approximately 4 months of age.. This group of forty-three N2 progeny were used exclusively in the mapping studies described herein. The two groups of N2 offspring were typed for the RFLPs described to generate the genetic map, the assignment of genotype at the *UROD* locus was then confirmed by application of PCR and denaturing gradient gel electrophoresis. A total of 98 animals were typed for the chromosome 4 loci, and 110 animals for the chromosome 6 loci. The progenitor animals were obtained from The Jackson Labs for both groups of N2 animals and the data did not differ substantially when the two groups were considered separately.

Loci typed

Nineteen loci on chromosome 4, and 10 loci on chromosome 6 were typed by either RFLP or DGG analysis, for their inheritance of the *M. spretus* allele amongst the backcrossed animals (Figure 2.1). These loci were either acquired from outside sources (Table 2.1), or by using the polymerase chain reaction (PCR) to amplify segments of the gene of interest using either the available human or rat sequences (Table 2.2).

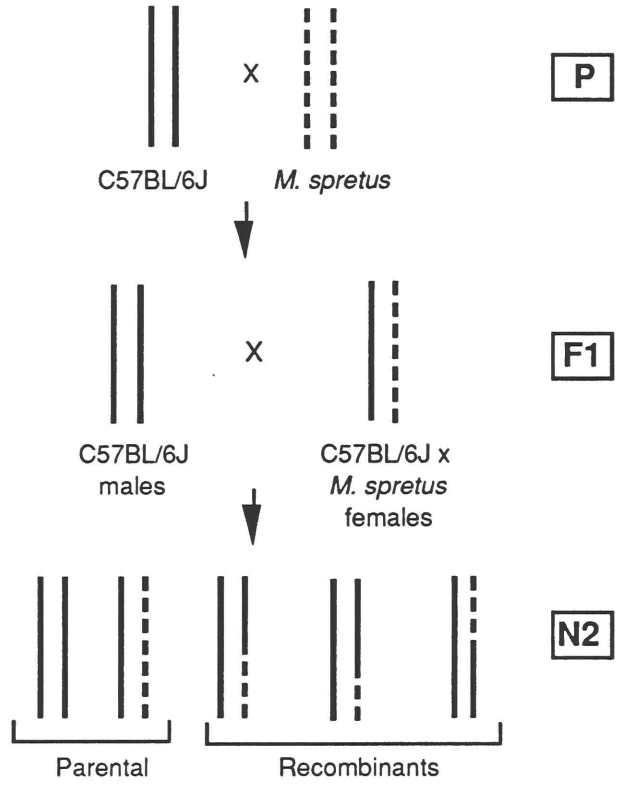

Figure 2.1. Schematic of the (C57BL/6J X *M. spretus*) F1 X C57BL/6J backcross. The solid lines represent genetic contribution from the C57BL/6J inbred strain and the dashed line the contribution from the *M. spretus* strain. Five possible genotypes of the N2 animals are shown, three of which demonstrate recombinational events.

Mouse	Human	Locus detected	C	RE	B6 allele	spretus allele	Reference
-	*ACADM*	Medium-chain acyl-CoA dehydrogenase	8	Eco RI	~4	~3 (DBA/2J allele size = *M. spretus*)	(Kelley, et al., 1987; Kidd, et al., 1990), Table 2.2
Akp1	*ALPL*	alkaline phosphatase-2, liver	4	Pst I	4.0, 2.9	4.5, 4.0, 2.9	(Terao and Mintz, 1987)
b	-	brown	4	Taq I	12.8, 6.6, 3.7, 3.3, 2.7, 1.2	6.6, 3.7, 2.4, 0.9	(Jackson, 1988; Shibahara, et al., 1986)
Cpa	*CPA1*	carboxypeptidase A1	6	Taq I	2.1, 1.8, 0.5	3.0, 2.1, 1.8	(Honey, et al., 1986)
Cola-2	*COL1A2*	α2(I) collagen procollagen type I, alpha 2	6	Taq I	6.6	6.0	(Irving, et al., 1989; Liau, et al., 1985)
-	*C8B*	complement 8b subunit	4	Pst I	2, 4	6	(Howard, et al., 1987), Table 2.2
D4Rp1	-	DNA segment Roswell Park 1	4	Taq I	9.0, 5.0	4.3, 4.2, 3.8	(Berger, et al., 1984; Huppi, et al., 1988)
-	*EL1*	elliptocytosis-1 (protein 4.1)	4	Pst I	0.9, 1.3, 1.8	0.9, 1.2,1.6	Gift of Dr. G. Pasternack (unpublished)
Fuca	*FUCA1*	alpha-L-fucosidase	4	Bgl II	3	6	(Darby, et al., 1988; Fukushima, et al., 1985)
Ggtb	*GGTB2*	4-beta-galactosyltransferase	4	TaqI	4.5	4.5, 3.5	(Shaper, et al., 1986; Shaper, et al., 1986; Shaper, et al., 1987; Shaper, et al., 1990)
Glut-1	*GLUT1*	facilitated glucose transporter	4	Taq I	~15, 8.5, 4.7, 3.5, 1.4, 1.1, 0.7	~9, 2.5, 1.5, 1.4	(Birnbaum, et al., 1986)
Fabph-1	*FABP1*	fatty acid binding protein heart -1	4	Taq I	~9, 2.1	~7, 1.8[a]	(Heuckeroth, et al., 1987)
Igk	*IGK*	immunoglobulin variable kappa chain complex	6	Taq I	4.2, 1.7	6.7, 1.7	(D'Hoostelaere and Gibson, 1986)

Ifa	*IFNA*	interferon alpha gene family (leukocyte)	4	Eco RI	~15, 9.2, 7.5, 5.5, 3.8, 3.0	~15, 7.1, 5.0, 3.8, 3.0	(Kelley and Pitha, 1985; Nadeau, et al., 1986)
Jun	*JUN*	avian sarcoma virus 17 (v-jun) oncogene homolgoue	4	Pst I	4.6	4.1	(Haluska, et al., 1988; Hattori, et al., 1988; Ryder and Nathans, 1988)
Kras-2	*KRAS2*	Kirsten rat sarcoma oncogene - 2, expressed	6	Hind III	~15	~9, 5.5	(Huppi, et al., 1988; Ryan, et al., 1986)
Lck	*LCK*	lymphocyte specific protein tyrosine kinase	4	BgIII	triplet ~10 kb	~10, 6.0, 4.8, 3.2	(Marth, et al., 1985; Marth, et al., 1986)
Lmyc-1	*MYCL1*	avian myeloctomatosis viral (v-myc) oncogene homolgoue, lung carcinoma derived	4	Taq I	0.7	0.4	(Legoury, et al., 1987; Nau, et al., 1985; Zelinski, et al., 1988)
Met	*MET*	met proto-oncogne	6	Bgl II	8.0, 7.1	7.8, 6.1	(Dean, et al., 1987)
Mos	*MOS*	Moloney murine sarcoma viral (v-mos) oncogene homologue	4	Hind III	~12	~9	(Propst, et al., 1987; Wood, et al., 1983)
Mup-1	-	major urinary protein-1	4	Eco RI	1.7, 3.0, 6.0, ~9	1.7, 3.0, 6.0, ~7	(Derman, et al., 1981)
Npy	*NPY*	neuropeptide Y	6	Taq I	6.0, 3.7	6.6, 2.1	(Allen, et al., 1987)
Orm-2	*ORM2*	orsomucoid-2	4	Taq I	2.5, 1.2	7.0, 4.1, 3.9, 3.0, 2.5, 1.2	(Baumann, et al., 1984; Baumann and Berger, 1985; Nadeau, et al., 1986)
-	*NKNA*	neurokinin A (substance P)	6	Bgl II	2.7, 1.7, 1.4, 0.4	4.1, 1.7, 0.4	(Krause, et al., 1987)
Pnd	*PND*	pronatriodilantin	4	Taq I	9.0, 4.4	~12, 4.8	(Yang-Feng, et al., 1985)
Prp	*PRP*	proline rich protein	6	Bgl II	7.1, 6.6, 6.0, 1.7	7.1, 6.2[a], 1.4	(Ann, et al., 1988; Azen, et al., 1989)
Rpl32	-	mouse ribosomal protein L32	6	Taq I	~10, 1.5, 1.2, 0.5	~12, 1.5, 1.2, 0.5	(Dudov and Perry, 1984)
Tcrb	*TCRB*	Watson -Star CTB1 T cell receptor b region	6	Taq I	~20	5.5 -- (5.0, 0.5)[b]	(Caccia, et al., 1984)
Tsha	*CGA*	thyroid stimulating hormone-a subunit	4	Taq I	1.7, 1.3	2.5, 1.3	(Kourides, et al., 1984)
-	*UROD*	Uroporphyrinogen decarboxylase	4	TaqI	1.1, 1.5, 2.0	3.5	(Mattei, et al., 1985; Romano, et al., 1987)

Table 2.1. Listing of the cloned probes mapped on chromosomes 4 and 6, the restriction enzyme used to detect an RFLP between the C57BL/6J and *M. spretus* strains, and the sizes of each strain's alleles. The approximate size(s) (in kb) of the informative *M. spretus* allele(s) is/are underlined. Those probes without assigned mouse names as of the February 1991 Jackson Labs computerized genome database (GBASE; Doolittle, et al., 1991), are referred to by their proper human nomenclature, obtained from GDB, The Johns Hopkins University, The William H. Welch Medical Library/The Howard Hughes Medical Institute's human genome database.(GDB, 1990) This pertains specifically to the probes which detect the *ACADM*, *C8B*, *EL1*, *NKNA*, and *UROD* loci, which did not have assigned locus names in GBASE.

Locus Name (mouse)	Oligonucleotide sequence	Ref	fragment size (bp)	annealing (ºC)
ACADM	a) 5'-GAG CCT GGG AAC TTG G(T/G)T TGA T(C/G)A ACA CAC b) 5'-GAA TTT GTG (C/A)AG TAC CTT C(A/G)T AAA TCT GAT	(Kelley, et al., 1987)	1000	30 sec. @ 63ºC
C8B	a) 5'-CAG TCA AGT GTT TCT GAA GCA GGG CCT GAA CAG GGG b) 5'-GGG GCA AGT GAG CAC ATC ACA CCT GGC ATA CCA GGA	(Howard, et al., 1987)	450	1 min. @ 50ºC
Fuca	a) 5'-CGC GAC AAC TAC CCG CCC GGC TTC AGC TAC GCC GAC b) 5'- TTG GAA GAT GGG AAC AAT CAG TCC ATC TTT AGT TGG	(Fukushima, et al., 1985)	750	2 min. @ 50ºC
UROD	a) 5'- TCA ATT CTG TCG AAG CAG GCG TGA GTG b) 5'-CTG GAA GAG CTG GCC CAG GCT GGC TAT GAG	(Romano, et al., 1987)	1300	30 sec. @ 63ºC

Table 2.2. Listing of the PCR conditions employed in amplifying the *ACADM*, *C8B*, *Fuca*, and *UROD* loci. Locus specific oligonucleotides were synthesized using available human (*C8B* and *Fuca*), rat (*UROD*), or both human and rat (*ACADM*) cDNA sequences. 250 ng of each primer was added to a 100 µl reaction (50 mM KCl, 10 mM Tris pH 8.3, 1.5 mM $MgCl_2$, and 0.01% gelatin) containing either 1) for *C8B* and *Fuca*, 10 µl of a 10^7 pfu/ml Balb/C mouse liver cDNA library 2) for *ACADM*, 10 µl of a 10^7 pfu/ml Sprague Dawley rat liver cDNA library (Stratagene, La Jolla, Ca.) and 3) for *UROD*, 125 ng of C57BL/6J genomic DNA. Each reaction was subjected to 30 cycles of denaturation at 94º C for 1 minute, annealing at the temperature and time indicated, and extension for 2 minutes at 72º C with 3 seconds of autoextension per cycle in an automated thermocycler (Perkin-Elmer Cetus). The expected band sizes are provided for reference.

Mapping of Mouse Chromosomes 4 and 6 using a Flow-Sorted Robertsonian Chromosome

Preparation of the cell line carrying the Rb(4:6)Bnr2 translocation

Eighteen day old fetal offspring of an intercross between mice heterozygous for a 4:6 Robertsonian translocation, Rb(4.6)2BNR (stock designation #CD-Rb4Rma, The Jackson Laboratory, Bar Harbor, Me.) were collected, euthanized by CO_2 asphyxiation, and the lung tissue was dissected. After mincing the tissue between two frosted glass coverslips in 5 mL of 0.05% trypsin/0.53 mM EDTA, the homogenate was added to an additional 5 ml of trypsin/EDTA at 37° C and the mixture gently swirled for 30 minutes at 37° C. Non-digestible material was allowed to settle for 10 minutes, and the viscous supernatant removed and added to 5 ml of trypsin EDTA and again swirled for 30 minutes at 37° C. The pellet was collected by spinning at 1000xg for 5 minutes and was then resuspended in a 100 mm^2 culture plate containing DME with 10% fetal calf serum. After approximately 5 passages the cells were infected with 10 PFU/cell of adenovirus 2. The cells were grown in low calcium media and after 4 weeks two independent transformed foci were picked and further characterized. Metaphase spreads were made using standard cytological procedures, with fixations for 15 minutes using a mixture of 3:1 methanol/acetic acid, and spread on 50 mm x 30 mm glass coverslips.

Spreads were Giemsa stained according to standard procedures. One tetraploid cell line, designated 4:6 1500, contained four copies of a cytologically intact, by Giemsa banding, 4:6 Robertsonian chromosome (see Figures 2.2 and 3.7).

Figure 2.2. Karyotype of the cell line harboring the Rb(4:6)Bnr2 translocation. The fused 4:6 metacentric is clearly visible, and is the largest chromosome as well. No gross abnormalities of either chromosomes 4 or 6 are evident.

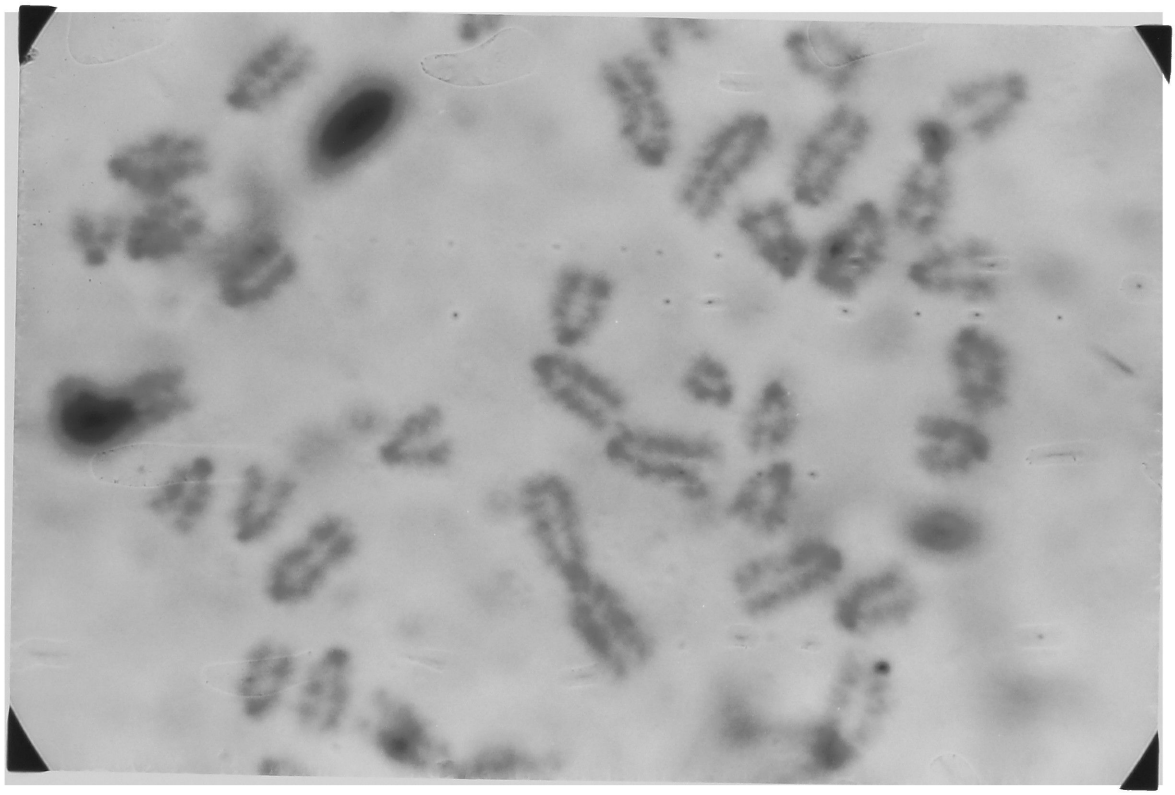

Flow sorting of the 4:6 Robertsonian chromosome:

4:6.1500 cells were cultured in DME media containing 10% fetal calf serum (plus penicillin and streptomycin) in a 5% CO_2 environment at 37° C. Cell cultures were subcultured on a regular basis to maintain exponential cell growth. The number of successive cell passages was limited in order to avoid karyotype instability resulting in loss or rearrangements involving the Robertsonian chromosome. Chromosomes were only isolated from cell cultures having undergone fewer than about ten passages post transformation. Old cultures were discarded and a new aliquot of cells frozen following transformation were thawed and placed in culture.

For each chromosome preparation, 20 to 30 T-150 tissue culture flasks of 4:6.1500 were blocked with .01 mg/ml of colchemid for 12 to 14 hours. Mitotic cells were selectively detached from the surface of the tissue culture flasks by standard mitotic shakeoff procedures. Approximately 10^7 mitotic cells were recovered, nuclear membranes swollen and mitotic chromosomes released into a polyamine buffer designed to stabilize the structure and molecular weight of the chromosome. Isolated suspensions of chromosomes were maintained at 4° C until sufficient quantities were obtained to warrant sorting. Prior to sorting the fluorochromes chromomycin A3 and Hoechst 33258 were added as described in the standard protocol (Cram, et al., 1990).

Following chromosome isolation and staining the 4:6 Robertsonian chromosome was sorted using either a commercial flow sorter (EPICS V,

Coulter Corp.) or a high speed chromosome sorter using standard chromosome sorting conditions as described elsewhere (Bartholdi, et al., 1987; Gray and Cram, 1990). Typical sorting rates were about 40-60 chromosomes per second when using the EPICS V flow cytometer and five times that rate when the high speed sorter was used. Two to four million chromosomes were sorted for each sample, frozen and saved for library construction. DNA was prepared from the sorted chromosomes as described (McCormick, et al., 1989; Disteche, et al., 1981; Gray and Cram, 1990).

Library construction and analysis of clones

Flow sorted DNA at a concentration of 1 ng/μl was restriction endonuclease digested with EcoRI, cloned into the λgt10 bacteriophage and packaged using Gigapack Gold packaging extracts (Stratagene). Recombinant clones were selected by plating on the selective *E. coli* strain POP101, a high frequency of lysogeny (hfl) strain, which induces λgt10 bacteriophage to choose the lysogenic pathway and not cell lysis. As a result, only recombinant bacteriophage form plaques.

Individual plaques were picked, placed into 1 ml of phage storage media and vortexed lightly. After 4 hours, a 10 μl sample was withdrawn and used to inoculate 150mm^2 plates. DNA was prepared from the resulting phage stocks as described (see page 56). Phage were restriction endonuclease digested with EcoRI, the inserts Southern blotted and probed with

radiolabelled total mouse genomic DNA. Those inserts which contained highly repetitive sequences, hybridized to the radiolabeled total mouse DNA, and were discarded. The remaining inserts were characterized further. The insert was excised from a 1.0% LMP agarose after digestion of the phage DNA with EcoRI and either radiolabeled and used to probe a Southern blot, or subcloned into the unique EcoRI site of a phosphatased EcoRI digested bluescript II +KS plasmid. The subcloned inserts were then propagated and isolated as plasmids. Alternatively, in order to block out repetitive sequences in the insert, an insert was radiolabelled and preannealed to 200 μg of sonicated total mouse genomic DNA at 65° C x 4 hours in 5X SSC to block the repetitive sequences. The preannealed probe was then hybridized directly to Southern blots.

Somatic cell hybrids

The somatic cell hybrids Bem1-4, Bl, C2, H3, Ecm4e and R22-4 (Ruddle, et al., 1978; Fournier and Ruddle, 1977; Goff, et al., 1982) were grown according to published procedures and were kindly provided by Peter D'Eustachio and Frank Ruddle. DNA was prepared from each line by harvesting five confluent 150mm^2 tissue culture dishes by gently scraping the cells with a rubber policeman and extracting their DNA using the ABI DNA extractor. Southern blotting was performed as described (see page 62).

Creation and Analysis of Intraspecific, Interspecific, and Intersubspecific Mouse Crosses Segregating the *db* and *ob* Mutations

Summary of the intraspecific backcross

The intraspecific cross segregating the *db* mutation were performed as shown in Figure 2.3. In this cross, as well as the other crosses which segregate the *db* mutation, the segregation of *db* can be compared to that of RFLPs or simple sequence repeats which differ between the progenitor strains, thus generating information regarding the relative orders and genetic distances between the detected loci and *db*. Homozygous *db/db* animals are infertile, necessitating the use of ovarian transplantation for breeding of homozygotes (Coleman, 1982). Agouti females bearing the transplanted ovaries of C57BL/6J *db/db* mice (generously provided by Dr. Douglas Coleman of the Jackson Labs, who has maintained *db* congenic stocks on C57BL/6J for 7 generations) were mated to DBA/2J +/+ males. After weaning at approximately 4 weeks of age, F1 black (indicating their origin from transplanted ovarian tissue) male progeny were backcrossed to the female transplants. A total of 170 N2 progeny were born, of which 134 were black. Agouti offspring, whose coat color indicated their origin from host (non-transplanted) ovarian tissue, were excluded from further analysis.

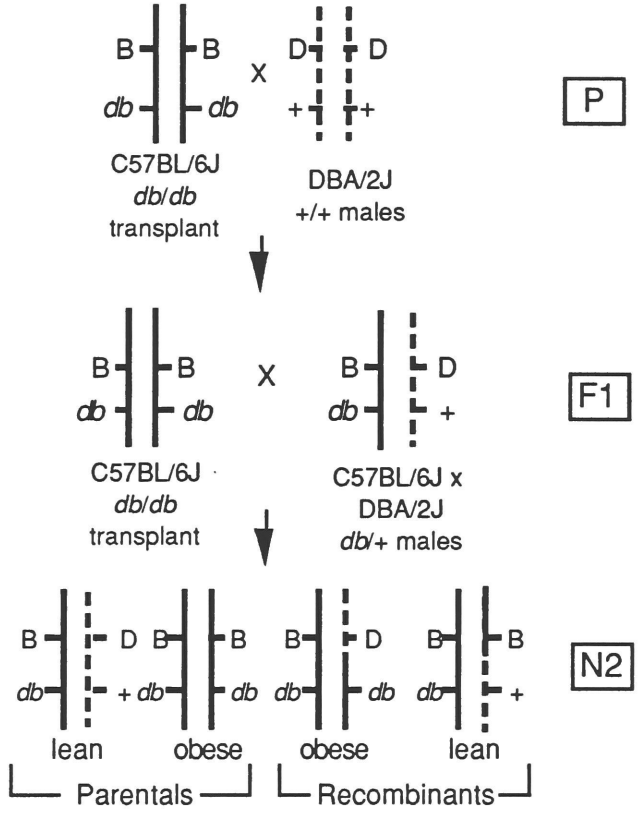

Figure 2.3. Schematic representation of the(C57BL/6J *db/db* x DBA/2J) F1 X C57BL/6J *db/db* intraspecific backcross. The four possible genotypes (2 lean, 2 obese) for the offspring are shown. Recombination between *db* and a particular locus is demonstrated when an obese N2 offspring is shown to have both the C57BL/6J and the DBA/2J alleles for a particular locus, or a lean animal has only the C57BL/6J allele.

Summary of the intraspecific intercross

Black F1 offspring of a (C57BL/6J *db/db* X DBA/2J) cross were mated to one another (see Figure 2.4). A total of 216 offspring which appeared obese at approximately 4 months of age were harvested from a total of ~900 offspring born.

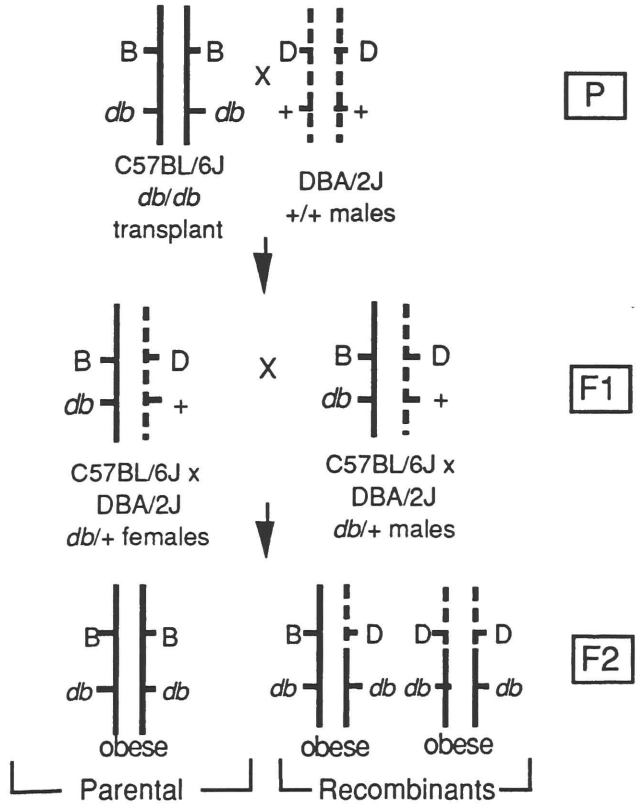

Figure 2.4. Schematic representation of the (C57BL/6J *db/db* x DBA/2J +/+) F1 intercross. Since each F2 animal is the offspring of two possibly recombinogenic parents, each animal can score two separate potential recombination events. The RFLP haplotypes for the three possible genotypically distinct obese F2 animals are shown.

Summary of the interspecific intercross

Black (C57BL/6J *db/db* X DBA/2J) F1 [B6D2 F1] males were subsequently mated to F1 black females of a C57BL/6J x *M. spretus* cross (see figure 2.5). A total of 228 offspring were born, of which 51 were obese.

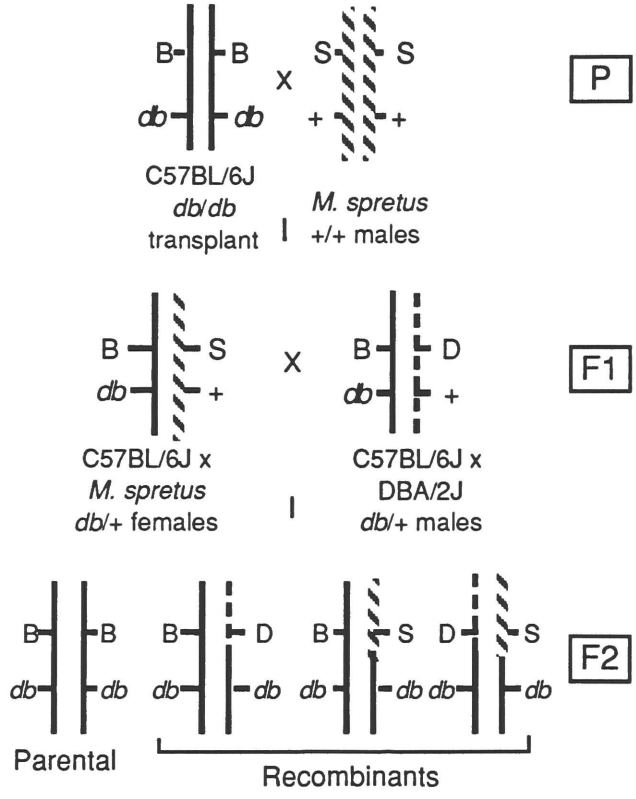

Figure 2.5. Schematic representation of the (C57BL/6J *db/db* x DBA/2J +/+) F1 X (C57BL/6J *db/db* x *M. spretus*) F1 interspecific intercross. If an obese F2 animals demonstrates any combination of DBA/2J and *M. spretus* alleles for a particular locus, then a recombination event between *db* and that locus occurred. The three possible recombinant, and the non-recombinant obese F2 genotype, are shown.

Summary of the intersubspecific intercross

The F1 progeny of a C57BL/6J *db/db* x *M. castaneus* cross were mated and the F2 progeny sacrificed at ~ 3 months of age (Figure 2.6). A total of 1957 progeny were born of which 497 were obese.

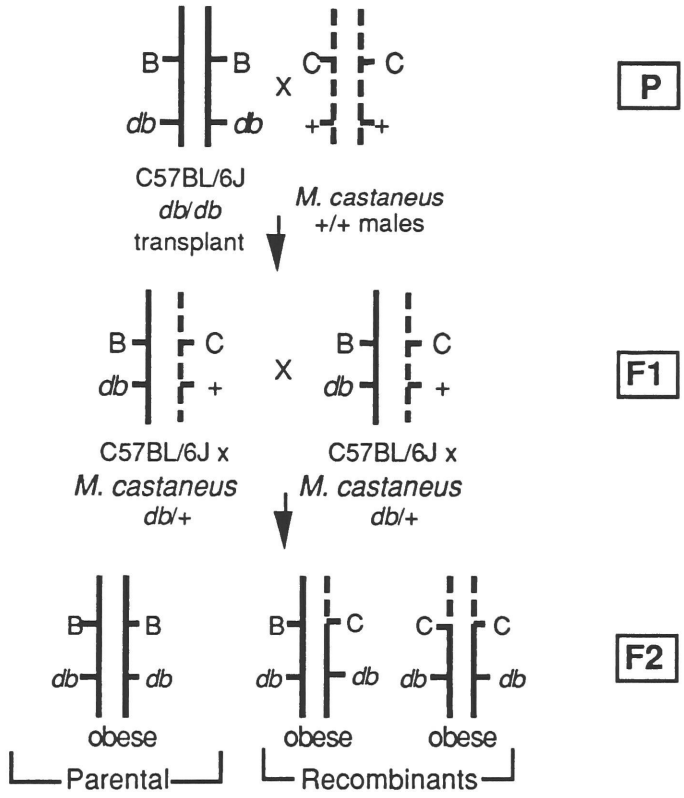

Figure 2.6. Schematic representation of the (C57BL/6J *db/db* x *M. castaneus*)F1 intersubspecific intercross. Since each F2 animal is the offspring of two possibly recombinogenic parents, each progeny can score two separate potential recombination events. The genotypes of the two possible obese recombinants, and the nonrecombinant offspring, are shown.

Progeny Analysis

One hundred and thirty four N2 progeny (57 males, 77 females) were sacrificed by CO_2 asphyxiation between 87 and 186 days of age (Figure 2.3). Two hundred and sixteen obese F2 progeny (92 males and 124 females),and their lean littermates, of the intraspecific (C57BL/6J *db/db* X DBA/2J) F1 intercross (Figure 2.4) were sacrificed between 51 and 140 days of age. Forty-nine obese (23 males, 26 females -- two obese animals died before sacrifice) F2 progeny of the B6D2 F1 x B6*spretus* F1 intercross (Figure 2.5), and their lean littermates, were sacrificed between 75 and 176 days of age. Three hundred and ninety six obese F2 offspring (182 males and 214 females) of the (B6*castaneus db*/+) F1 intercross (Figure 2.6), and their lean littermates, were sacrificed at about 3 months of age. All animals were fasted for 15 hours prior to sacrifice. Each mouse had approximately 1.0 ml of whole blood withdrawn by cardiac puncture into an eppendorf tube containing 50 µl of 82µM EDTA solution as anticoagulant. The plasma was decanted and frozen at –80°C for subsequent assay of [insulin] (Herbert, et al., 1965) and [glucose] (Kadish, et al., 1968). All progeny were scored for sex, weight, and length (nose to anus). Kidney, liver, spleen, tail and thoracic contents were immediately frozen at -80°C for subsequent isolation of DNA.

Segregation of the fatty (*fa*) locus in rats

A cross segregating the fatty (*fa*) mutation was constructed as an intercross between random (13M/Vc x (BN)/Crl) fa/+ offspring. Briefly, Male 13M/Vc fa/+ rats were bred to female (BN)/Crl +/+ animals. The use of the Brown Norway females as the counter strain was made upon the available historical record (Zucker, 1960; Lindsey, 1979) which suggested that these two inbred rat strains would be sufficiently genetically distant for RFLPs to be readily found. Since only half of the F1 animals should carry the *fa* gene, and the phenotype of fa/+ animals is indistinguishable from their +/+ siblings, random brother-sister matings were carried out as test crosses. Those crosses not demonstrating obese offspring by ~6 weeks of age were excluded.

The F2 progeny of the intercross were weaned at 3 weeks of age. At 50-73 days of age the offspring were fasted overnight, sacrificed by CO_2 asphyxiation, and their body weight recorded. Both inguinal adipose pads were dissected and weighed to the nearest milligram. Liver, spleen, thorax and tail were dissected and immediately frozen in liquid nitrogen and stored at -70°C for subsequent high molecular weight genomic DNA isolation.

Microdissection and microcloning

Isolation of a cell line harboring the 4:15 Robertsonian translocation

The neonatal offspring of an intercross between mice heterozygous for a 4:15 Robertsonian translocation, Rb(4.15)4Rma (stock designation #CD–Rb4Rma, The Jackson Laboratory, Bar Harbor, Ma.) were collected, euthanized by CO_2 asphyxiation, and the lung tissue dissected. After mincing the tissue between two frosted glass coverslips in 5ml of 0.05% trypsin/0.53 mM EDTA, the homogenate was added to an additional 5 ml of trypsin/EDTA at 37°C and the mixture gently nutated for 30 minutes at 37°C. Non digestible material was allowed to settle for 10 minutes, and the viscous supernatant removed and added to 5 ml of trypsin/EDTA and again nutated for 30 minutes at 37°C. The pellet was collected by spinning at 1000g for 5 minutes and was then resuspended in a 100mm^2 plate containing DME with 10% Fetal Calf Serum. After approximately 5 subsequent passages of the cell line 2 foci were generated, one of which, designated L3ST, was found to harbor the 4:15 translocation and appeared immortalized. Metaphase spreads were made using standard cytological methods, with fixations for 15 minutes using a mixture of 3:1 methanol/acetic acid, and spread on 50 mm x 30 mm glass coverslips. The 4:15 chromosome appeared cytologically intact by giemsa banding.

Figure 2.7. Photomicrograph of a partial karyotype of the L3ST cell line which harbors the 4:15 Robertsonian translocation. No gross cytological aberration of mouse chromosome 4 is apparent in the karyotype.

Acquisition of the cell line harboring a 6:16 Robertsonian translocation

A fibroblast cell line, harboring the Rb(6.16)24Lub Robertsonian translocation was the kind gift of Dr. Kristine Kozak. The cell line was grown in DME containing 10% Fetal calf serum in a 5% CO_2 incubator at 37° C. Karyotyping of the cell line was performed by Dr. Kozak, who did not detect any gross cytological abnormalities in the cell line.

Preparation of the microinstruments

Microneedle preparation: The preparation of the microneedles is schematically diagrammed in Figure 2.8. Five foot long glass rods were scored using a triangular metal file and broken into approximately 10 inch segments. Each ten inch segment was heated over a standard bunsen burner, until just red and then quickly removed from the heat and stretched until an ~0.5mm diameter was reached. The thinned glass was snapped between two fingernails halfway between the two thick ends. More thinned glass was removed in a similar fashion until brushing the thinned tip end across a hard object did not cause it to break. The needle tip was cleared of any uneven fragments and placed adjacent to the microforge filament at an angle of 45° with respect to an imaginary line drawn out horizontally from the tip the filament. The filament was heated until red hot, placed on the glass rod, and a small cone shaped piece of glass was drawn out. As the cone shaped glass

was drawn the heat applied to the filament was reduced, allowing for a gradual tapering of the glass cone. As near as possible to the point where the tapering cone shaped glass would disconnect from the filament, with the filament still sufficiently hot to prevent a long thin piece of glass to be drawn instead of a cone, the filament was removed from the vicinity of the glass cone while simultaneously reducing the filament heat. The proper microneedle tip had a cone shape that demonstrated a minimum of concavity and tapered to a sharp point.

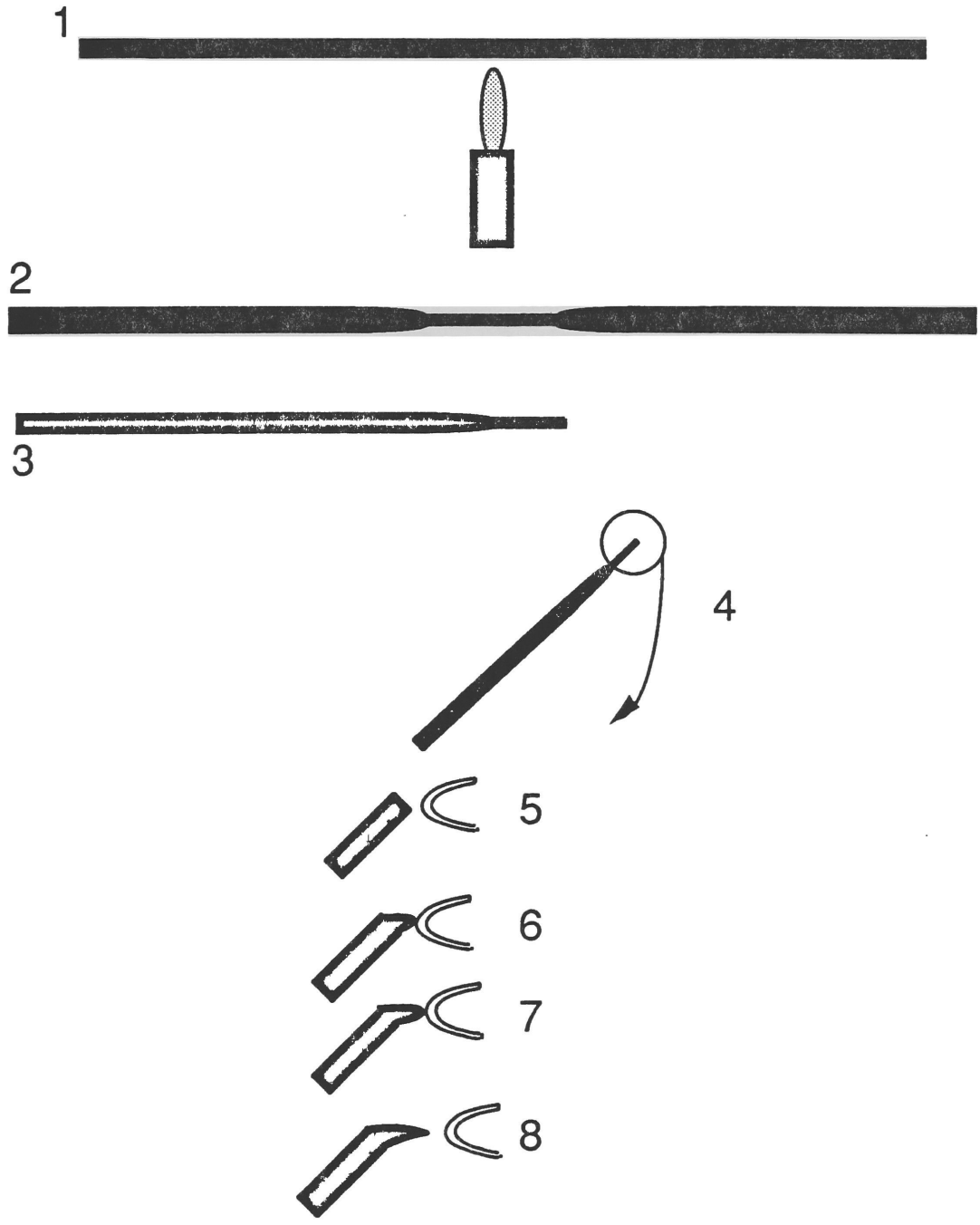

Figure 2.8. Diagram of the preparation of the microneedles.

Micropipette preparation: The procedure for preparing the micropipettes is diagrammed in Figure 2.9. To make a micropipette, 15cm long Pyrex glass 1mm capillaries, were first drawn over a over a low-temperature flame, using either an alcohol lamp, or a small fashioning gas burner, until just red and then quickly removed from the heat and stretched until an ~0.25mm -0.5mm O.D. diameter was reached. One end was placed into a micropipette holder, a 4mm O.D. soda glass tubing bent at a 90° angle with arms of ~10cm and 4cm lengths. Solid paraffin wax was heated in an erlenmeyer flask until liquid and was then quickly added to the end of the micropipette holder with the inserted drawn capillary tube. Once the wax solidified, a hook of approximately 75°, bending in the same direction as the bend in the pipette holder, was created on the wide end of the drawn capillary most distal to the micropipette holder by heating over the low temperature flame. This assembly was inserted into the microforge at an approximately 135° angle with respect to an imaginary line drawn horizontally from the filament edge. The micropipette was placed such that the bent edges of both the capillary tube and pipette holder were facing up. The capillary was heated in the thinned region, by positioning the filament adjacent to the capillary. The micropipette was placed such that the bent edges of both the capillary tube and pipette holder were facing up. The capillary was heated in the thinned region, by positioning the filament adjacent to the capillary, until the V shaped bend was positioned vertically. A weight was attached to this V

shaped region of the pipette, and heated applied to the pipette until the pipette constricted to about 10% of its original diameter. The micropipette was repositioned slightly higher and then reheated. As the capillary tubing narrowed, the heat applied to the filament was lowered so as not to melt the narrowing tubing. These cycles of heating/narrowing and then reducing the filament temperature were repeated until the capillary broke due to the applied weight.

The width of the pipette opening could be altered by altering the weight added to the hooked region. In general the lower the weight applied was, the narrower was the opening of the micropipette. Micropipettes drawn with 2g weights were utilized for fine control of added aqueous solutions during the microcloning procedures, while micropipettes drawn with 4 or 5g weights were used for both the chloroform extraction and for removal of the microdrop from the oil chamber for in-vitro packaging of the ligated microclones.

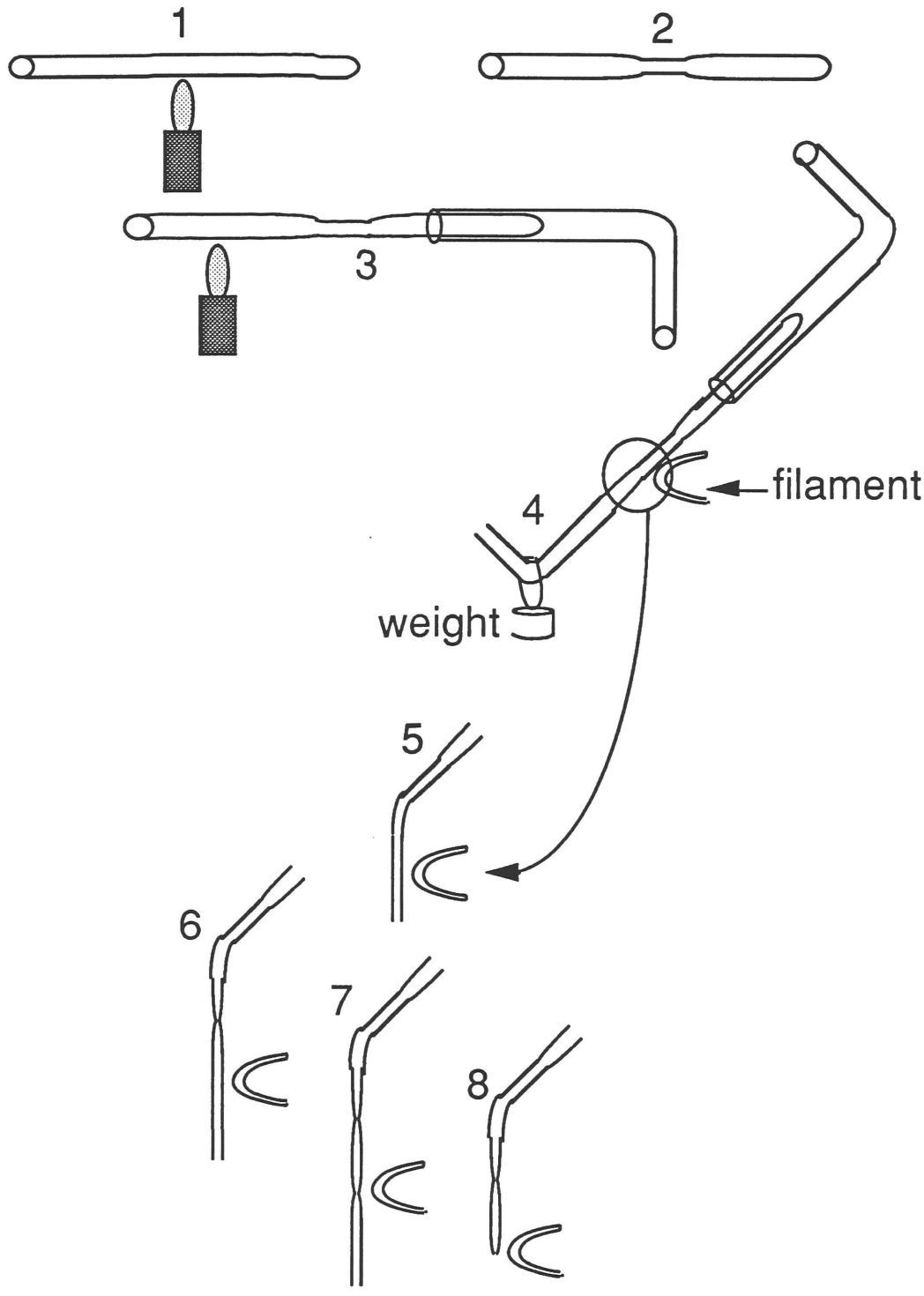

Figure 2.9. Diagram of the preparation of the micropipettes.

Oil chambers and coverslips: The oil chambers were fashioned from three separate glass pieces melted together by heat. Their dimensions were 70 X 30 X 6 mm with a central trough of 24 X 30 X 3 mm. The coverslips were 6 x 50 x 0.17mm is size. To prepare the chambers and coverslips for use, they were acid washed in 0.2M HCl overnight and rinsed in 100% ethanol a minimum of 15 times before two final rinses in autoclaved water. Both coverslips and the oil chambers were stored in 100% ethanol until use.

Siliconization of glassware: The microneedles, and glass coverslips were placed in a vacuum desiccator containing 5 ml dichlorodimethylsilane. The chamber was evacuated and quickly repressurized twice . The chamber was then reevacuated for 5 minutes, repressurized and reevacuated one final time and left overnight. The micropipettes were immersed in a 5% dichlorodimethylsilane/$CHCl_3$ mixture with a 60 ml syringe attached to the micropipette holder. While the tip was left immersed in the solution for five minutes, the solution was drawn into the pipette. The micropipettes were then air dried for one week, and a similar procedure carried out using 1mM EDTA pH 8.0 to wash away any residual dichlorodimethylsilane.

Preparation of the lambda gt10 cloning vector

Background: The insertion lambda phage vector λgt10, which can accept inserts of up to 7.2kb in size, is uniquely suited for use in microcloning. The unique EcoRI site is situated in the CII repressor gene, allowing for selection of recombinant phage based on the plaque morphology (Huynh, et al., 1985). Because cloning into the vector causes an insertion into the CII gene, recombinant phage can be only lytic with respect to the host's life-cycle and therefore manifest a clear plaque morphology. Non-recombinant phage particles can be either lytic or lysogenic, and therefore exhibit a turbid plaque morphology with most hosts (such as the permissive C600 strain). Additionally, by plating the phage with a restrictive host containing an *hfl* mutation, a so-called 'high frequency of lysogeny' mutation such as found in the POP101 strain, nonrecombinant phage are completely lysogenic, and display an exceedingly low rate of plaque forming units. This provides an ability to isolate recombinant phage despite the presence of large numbers of non-recombinant phage in a ligation. Because the amount of DNA recovered during microdissection is only ~2pg of DNA, successful microcloning requires use of a vector that has i) a low plaque forming background when digested and religated to itself and ii) a high in-vitro packaging efficiency.

Isolation, growth, and testing of the vector: Approximately 200ng of λgt10 vector was packaged and plated on the permissive C600 host. Five plaques with a turbid morphology were isolated with a pasteur pipette and grown using the high-quality phage DNA preparation procedure (see page #54). Exactly 500ng of purified DNA was restricted with 1U EcoRI for 1 hour at 37° C. The restriction digest was heated at 70° C for 30 minutes and subjected to several cycles of freeze/thawing to inactivate the EcoRI. Equal aliquots of the five digests were religated in Stratagene phage ligation buffer with 1mM ATP at 4° C overnight. Equivalent aliquots of digested and religated bacteriophage were packaged in-vitro and plated with both the C600 and POP101 bacterial strains. The λgt10 phage prep which demonstrated the highest efficiency of packaging, and the lowest background of clear plaques when plated with the restrictive POP101 host, was utilized for the microcloning. The λgt10 phage prep which was utilized had an efficiency of packaging of ~1.2 x 10^8 pfu/μg of EcoRI digested/religated phage, and close to a 10^4 decrease in packaging efficiency of the digested vector in comparison to the digested and religated vector. The remaining digested material of this particular preparation was used for all subsequent microcloning steps involving the λgt10 vector.

Preparation and testing of the phenol/chloroform microcloning reagents

A <0.2µl drop of 1.2 µg/µl C57Bl/6J genomic DNA in 10,1 TE was placed on a siliconized coverslip and then positioned inverted on a paraffin oil containing oil chamber. Equivalent drops of 5 separate batches of phenol/chloroform were spotted surrounding slightly smaller drops of 1X EcoRI endonuclease buffer, on a separate cover slip and then added to the oil chamber. Five approximately 1nl volumes of genomic DNA (~1ng of DNA each) were aliquoted, phenol/chloroform extracted and then chloroformed extracted. The drops were restriction digested with EcoRI as described and then reextracted using fresh phenol/chloroform and chloroform. The drops were then ligated into the prepared λgt10 vector in a total volume of approximately 8 - 12 nl, overnight at 4°C. The ligated vectors were packaged and plated as described. Two of the five batches of phenol/chloroform used to extract the digested genomic DNA gave equivalent packaging efficiencies that varied from 2 - 3 fold higher than the other three batches. One of these batches was used for all subsequent phenol/chloroform extractions.

Description of the microcloning procedure

Restriction endonuclease digestion: A siliconized coverslip containing the microdissected DNA was positioned near the front of an oil chamber containing water saturated paraffin oil. Another coverslip containing a

<0.2µl supply drop of an equal volume of EcoRI (4000U/µl) and 4X EcoRI digestion buffer was then placed directly behind this first coverslip. An aliquot of this mix, equal in diameter to the size of the microdrop containing the DNA, was then placed alongside the DNA drop. The tip of the micropipette was placed alongside either of these two drops, raised to the plane of the drop and used to push the two drops together until they coalesced.

The oil chamber was removed from the microscope stage and a piece of 1mm Whatmann paper soaked in autoclaved water was then positioned in the well of the oil chamber underneath the siliconized slips. The oil chamber was then placed inside a 100mm^2 petri dish lined with water saturated 3mm Whatmann paper. This petri dish/oil chamber assembly was then placed inside a 150mm^2 tissue culture dish lined with water saturated 3mm Whatmann paper. This entire assembly was then placed in a humidified 37°C incubator for 2 hours.

Phenol-chloroform extraction: After incubation, the oil chamber was removed from its containment dishes and the lining Whatmann paper was removed, being careful not to disturb the microdrops. A siliconized coverslip with a supply drop of phenol/chloroform surrounding a <.1µl drop of 1X ligation buffer (to ensure aqueous saturation of the phenol/chloroform) was placed directly behind the first coverslip. A new thin-bore micropipette was

used to transfer the phenol/chloroform mixture from the supply drop to the collection drop containing the restriction endonuclease digested DNA. The phenol was slowly ejected from the pipette, which was placed directly alongside the collection drop, until the diameter of the phenol surrounding the collection drop was approximately 3X that of the original drop. Under phase microscopy, the phenol mixture was tinged blue. To remove the phenol/chloroform, the pipette end was placed in the surrounding phenol layer and with gentle suction on the injector, the phenol was removed.

Because chloroform is both soluble in paraffin oil, and has a low vapor pressure, a chloroform supply drop could not be formed. Chloroform extractions were done by immersing a large-bore micropipette into a large aliquot of chloroform in a beaker and suctioning as much chloroform as possible into the pipette. The pipette was then positioned in front of the phenol extracted collection drop, and chloroform gently blown over the drop. As the chloroform passed over the collection drop, the thick rim normally seen surrounding the drop reappeared. This is presumably due to the removal of small amounts of phenol that could not be pipetted off. The tip of the chloroform pipette was also placed in the collection drop and chloroform bubbled through the aqueous collection drop. Care must be exercised to have sufficient chloroform in the pipette, insuring no air is accidently pushed into the oil chamber through the pipette.

Because molecular biological enzymes are sensitive to phenol/chloroform inactivation, the final step in a phenol extraction—chloroform extraction cycle is to provide a phenol/chloroform-free oil environment for the collection drop. This is done by placing a new oil chamber with fresh water-saturated oil directly in front of the one containing the collection and phenol drops. The collection drop containing coverslip is then pushed from the old oil chamber to the new one. This cycle is repeated twice more allowing 5 minutes in each new oil chamber for equilibration of any phenol/chloroform remaining in the collection drop with the fresh oil. A standard phenol/chloroform extraction cycle thus consists of three phenol extractions, followed by two chloroform extractions, followed by transfer of the collection drop through three fresh oil chambers.

Ligation of the endonuclease restricted microdissected DNA to the vector:

After phenol/chloroform extraction, a new siliconized coverslip with two supply drops consisting of i) an equal mixture of 4X ligation buffer and 4 mM ATP, and ii) an equal mixture of 500 ng/µl λgt10 and 1U/µl T4 DNA ligase was placed directly behind the coverslip containing the collection drop. Using a new narrow-bore micropipette, a volume of either supply drop equal in diameter to the collection drop was placed alongside the collection drop and then manipulated to combine the two drops. A volume of the other supply drop equal in diameter to the combined drop was then placed alongside the

combined drop and the two drops forced together. This new large drop was placed in a double dish assembly as described for the endonuclease digestion step, and incubated overnight at 4°C.

In-vitro packaging of the microcloned DNA: The ligated DNA was removed from the oil chamber in a micropipette with an oil buffer flanking it. This pipette was carefully removed from the vicinity of the microdissection microscope and then placed inside a siliconized 1.4 ml eppendorf containing a 2 µl hanging drop of phage dilution buffer (10mM Tris pH8.0 and 10mM $MgSO_4$). This drop was packaged according to the manufacturer's instructions except that both the freeze/thaw and the sonic extracts were added to the eppendorf containing the microcloned material.

Localization of the *b* locus by in-situ hybridization

In order to more precisely define the physical area of mouse chromosome 4 wherein the *db* locus resides, an in-situ hybridization of the 4:15 Robertsonian cell line used for the microdissection was performed with a probe which detects the *b* locus, by Dr. Ian Jackson. The *b* locus is located between 5 and 10cM proximal to the *db* locus (Figure 3.19) (Doolittle, et al., 1991) and localization of the *b* locus in the cell line would provide a reference for which area of chromosome 4 should be microdissected.

Microdissection of mid/distal mouse chromosome 4

The 4:15 Robertsonian cell line was thawed and plated on 50mm^2 plates. Once confluent, the plate was harvested and split into two 150mm^2 plates. As they became nearly confluent, metaphase spreads were prepared from the cell line on non-siliconized 60mm X 24 mm ethanol washed coverslips. The metaphase spreads were allowed to dry at room temperature overnight. A dried metaphase preparation was placed inverted on a dry oil chamber, and a supply drop consisting of 10mM Tris pH7.6, 10mM NaCl, 0.1% (v/v) SDS, and 0.5mg/ml (20U/mg) proteinase K was placed on a siliconized coverslip which was then positioned inverted on a second oil chamber with water-saturated paraffin oil added. This second chamber was positioned on the microscope and a micropipette was used to place a number of ~1nl. drops of this mixture on a separate proximal coverslip. The dry chamber containing the metaphase spreads was then placed on the microscope. The larger metacentric chromosome was clearly visible among the background of acrocentric chromosomes, as was the distinction between the smaller chromosome 15 and the larger chromosome 4 which made up the metacentric. Because a microneedle attached to the deFonbrunne micromanipulator is limited to motion directly parallel to the X, Y and Z axis, only those metacentric chromosomes whose long axis parallels the two horizontal X and Y axis could be dissected. Once a suitable chromosome was apparent, the microneedle was lined up with the mid/distal area of mouse

chromosome 4 and then pushed through the chromosomal material. Usually, the dissected chromosomal area remained affixed to the microneedle. In cases where the dissected material did not remain on the needle, it was always clearly visible in the metaphase spread and could be regained in a second attempt. If it appeared as if too large an area had been dissected, or an incorrect chromosome had been taken, the material was discarded.

After collection, the microneedle was withdrawn from the chamber containing the metaphase spreads and placed in the oil bearing chamber that had the collection drop. The microneedle, with a small black dot of chromosomal dissection material still visible in the microscope on its tip, was placed inside the collection drop where the material immediately came unbound from the needle. If the microneedle was not siliconized properly, the collection drop would stick to the needle, and the needle would have to be replaced. With repeated collections, small masses of black material appeared in the collection drop that persisted throughout the collection steps until the phenol/chloroform extraction.

A total of 73 mid/distal mouse chromosome 4 fragments were dissected over a two day period from the metaphase spreads and placed in a single collection drop. After the collection of dissection fragments was complete, an equal volume of fresh SDS/proteinase K solution was placed alongside the collection drop, combined with it, and the mixture incubated in

the assembly described for the restriction digestion for 2 hours at 55°C. A standard set of phenol/chloroform extractions was carried out on the collection drop (see page #102) after which it was restriction digested, ligated and packaged in-vitro as described above.

Control drops were added to the microdissection protocol at the following steps: 1) a drop consisting of 1 ng of C57BL/6J genomic DNA before the restriction enzyme digestion, 2) a drop consisting of ~0.2ng of EcoRI digested C57BL/6J DNA at the post restriction digestion phenol extraction step, and 3) a mixture of 500ng/μl λgt10 DNA with 1ng/μl EcoRI digested/heat inactivated C57Bl/6J genomic DNA as a control for the ligation reactions. Each of these drops were kept separate from the collection drop in ensure no contamination of the dissection with genomic DNA occurred.

Microdissection of proximal mouse 6

The microdissection of proximal chromosome 6 was carried out in an identical fashion with the chromosome 4 microdissection with a few exceptions. Since the *ob* locus is known to reside extremely close to the centromere, no in-situ hybridization was needed. In addition, the cell line harboring the 6:16 Robertsonian was used in place of the 4:15 Robertsonian cell line, and a total of 93 proximal chromosome 6 fragments were collected over a 2 1/2 day period.

Manipulation of the microclones

Isolation of microcloned inserts from the lambda gt10 phage: Recombinant clones were selected by plating on the selective E-coli strain POP101. Individual plaques were picked, placed into 1 ml of phage storage media and vortexed lightly. After 4 hours, a 10 µl sample was withdrawn, and subjected to 35 cycles of the polymerase chain reaction using oligoprimers 15 base pairs on either side of the unique EcoRI site in the λgt10 vector. The primers (5' and 3' of the insertion site, respectively) were of the sequence 5' ACC TTT TGA GCA AGT TCA GCC TGG and 5'GGC TTA TGA GTA TTT CTT CCA GGG. The conditions employed for the polymerase chain reaction were denaturing at 94° C for 1 minute, annealing/extension at 55° C for 2 minutes using 250 ng of each primer in a 100 ml reaction (50 mM KCl, 10 mM Tris pH 8.3, 1.5 mM $MgCl_2$, 0.01% gelatin, 125 mM of each dNTP). The sizes of the inserts were determined from a 3% agarose gel, taking into account the contribution of phage to the size of the PCR product under analysis.

Exclusion of highly repetitive microclones: The 3% agarose gel used to determine the size of the microclones was transferred to Immobilon-N by Southern blotting (Mann, et al., 1989), and probed using 10^6 dpm/ml of random primed total C57BL/6J genomic DNA (Feinberg and Vogelstein, 1983). Clones which did not hybridize, indicating that they did not contain

any highly repetitive elements within them, were then excised from a 0.6% low melting point gel into an eppendorf containing 250 µl of water.

Subcloning of microclones: A 5µg aliquot of Bluescript II +KS was digested with EcoRI and phosphatased according to the manufacturer's recommendations. The plasmid was then phenol/chloroform extracted, precipitated using 2 1/2 volumes of ethanol and a final sodium acetate pH 5.3 concentration of 0.25M, and resuspended at a concentration of ~100ng/µl. The microclone to be subcloned was amplified using the λgt10 specific oligos and the PCR protocol described above for isolating the microcloned inserts from the λgt10 bacteriophage. To the 50µl reaction was added 5µl of 10X EcoRI buffer and 10U of EcoRI. After incubation at 37°C for 30 minutes, the mixture was heated at 65°C for 30 minutes and repeatedly frozen and thawed to inactivate the EcoRI. A 5µl aliquot was withdrawn, and added to a mixture of 1µl (100ng) EcoRI digested/phosphatased plasmid, 1µl 10mM ATP, 1µl 10X ligation buffer, 1µl of T4 DNA ligase, and 1µl of water. The resultant mixture was incubated at room temperature for two hours and then transformed into bacteria.

Sequencing of the microclones: Plasmids bearing the microclone insert were grown in large-scale cesium chloride preparations. They were subsequently sequenced using a Sequenase kit by electrophoresis through a 6% denaturing acrylamide gel.

Radiolabeling of the microclones: The inserts were radiolabeled by use of the polymerase chain reaction as described above with the exception that dATP, dTTP, and dGTP were added to a final concentration of 200 μM, non radioactive dCTP to 1.25 mM, 5 μl of [α-^{32}P]dCTP (50 μCi) was added as the radioisotope, and only 25 cycles were carried out in the thermocycler.

Physical Mapping Methods

Pulsed-field electrophoresis

Preparation of DNA in agarose blocks: 4:6 1500 cells were grown to confluence and then detached and split in half. Usually 16 150 mm^2 plates were prepared simultaneously. Each plate was quickly washed with 5ml of Hanks buffered saline solution (HBSS) at room temperature, and then with 3 ml of trypsin/EDTA at 37° C. An additional 2 ml of trypsin/EDTA was then added and the plates incubated at 37° C for ~5 minutes until the cells became detached. If necessary this was confirmed by use of a microscope. To each plate was added 3 ml of DME with 10% bovine calf serum (BCS). The eluents were collected and the cells were added to 50 ml conical tubes. The tubes were then centrifuged at 1000 rpm for 5 minutes, and the supernatant aspirated. Following aspiration, the cells were resuspended in 40 ml 1X PBS and counted on a 5 X 5 0.1µl grid, recentrifuged for 5 minutes and then resuspended in 1X PBS at a final concentration of 10^6 cells/40 µl. The resuspended cells were then mixed with an equal volume of liquified 1% incert agarose and pipetted in 80 µl aliquots into the molds. After hardening, the blocks were removed from the molds, and immersed in 1 ml ESP (10 ml = 9 ml 0.5 M EDTA pH 8.0, 1ml 10 mg/ml proteinase K, and 330 µl 30% sarcosyl) per block and shaken for 48 hours at 50° C. After two days, the ESP was

decanted, the blocks washed in 3 volumes of 10 mM Tris pH 7.6/1 mM EDTA pH 8.0 (TE) for 20 minutes each at room temperature. The remaining TE was aspirated and 50 ml of TE containing 50 µl PMSF solution (PMSF solution = 40 µg PMSF + 1 ml isopropanol) was added and the blocks incubated for 4 hours at room temperature. The PMSF solution was removed and the blocks washed in 3 X 50 ml TE for 30 minutes each. The blocks were then stored in 30 - 50 ml of ESP at 4° C until use.

Digestion of agarose blocks: Blocks to be digested were removed from the ESP storage solution and washed in ~25 ml of TE, 4 times for 15 minutes each. Since a single cell contains about 6 pg of DNA, a single block containing 10^6 cells contains approximately 6 µg of DNA. Each block was incubated with ~15U of enzyme (~2.5X overdigestion) in a total volume of 100 µl for 4 hours in the manufacturer's buffer. After digestion, 0.5 ml of 0.5 M EDTA pH 8.0 was added and the blocks stored until use at 4° C.

Pulsed field electrophoresis and Southern blotting: 0.8% agarose gels were cast in the LKB insert molds, and the blocks inserted by manipulation with 24mm X 60mm glass coverslips, and by aspirating the air in a well underneath a block with a 1ml syringe and 25 gauge needle. Standard blocks consisting of *S. cerevisae* and *S. pombe* (BRL – Gibco) chromosomes were also added in a similar manner. Electrophoresis conditions resolving up to ~1-2

million bp of the agarose embedded DNA were 60 second switching for 15 hours followed by 90 second switching for 8 hours.

After electrophoresis, the gels were stained for 1 hour in 100 µl/l 0.1% ethidium bromide with shaking, photographed , and then the DNA was nicked by placement for 4500 x 10^3 µjoules of UV irradiation in a Stratagene UV crosslinker. The gels were then blotted to Immobilon-N over a 24-48 hour period using the standard protocol. After transfer the gel was restained to ensure near complete transfer of the DNA to the membrane.

Isolation and growth of yeast artificial chromosomes (YACS)

Hybridization screening of a YAC library: The mouse YAC library utilized for hybridization screening was made available by Dr. Roger Cox and Dr. Hans Lehrach (Imperial Cancer Research Fund). Probes were supplied to them as twice purified inserts at a concentration of ~3 ng/µl. Screening and isolation of a primary pick was then carried out by Dr, Cox. Because of the manner in which the hybridization is carried out on gridded filters, the recombinant yeast were plated and rescreened to ensure that the recombinant yeast isolated contained a YAC bearing the target sequence.

PCR based screening of a YAC library: The library which was screened by PCR was made available by Dr. Shirley Tilghman (Princeton). The library consists of as a set of 18 'complex pools', each of which is further subdivided into 20

'simple pools', with each 'simple pool' comprised of 96 YAC bearing yeasts. A set of DNA made from each of the 8 'rows' and 12 'columns' of a 96 well microtiter plate (20 'row and column DNAs') are used to isolate a single YAC containing the target. For example a positive in row 'F' DNA and in column '7' DNA means the targeted YAC is located in that microtiter dish at position 'F7'.

A 5µl sample of each of the 18 complex pools was subjected to PCR under conditions that could detect a specific signal using 0.5ng of total mouse genomic DNA as template among 200ng of yeast DNA. To minimize contamination, sterile plugged pipette tips were employed in making each PCR reaction, separate pipetteman were used for setting up and analyzing the reactions, and the water and buffer used in a reaction were UV irradiated for a total of 480000 µjoules.

In standard PCR screening, no signal was apparent on electrophoresis, necessitating Southern transfer of the gel and hybridization with labelled target DNA. Radiographic signals were seen in 1 or 2 complex pools, for which the corresponding simple pools were obtained, and screened by PCR. The 'rows' and 'columns' comprising a 'simple pool' to which a positive signal was seen were then obtained and used as template for PCR. Hybridization of labelled target to the Southern blotted gel provided coordinates for a microtiter dish containing the desired YAC bearing yeast. Alternatively, screening was accomplished using "nested PCR". In nested

PCR, a second set of oligos, non-overlapping with the first, is used in a second-round PCR with an aliquot of the first round PCR as template. This method increases the sensitivity of the assay and precludes the need for Southern blotting. Unfortunately, it also increases the number of false positives, which accounts for the large number of positives obtained in the complex pool screens. To ensure that no contamination by other YAC bearing yeasts occurred, the yeast thought to contain the target were plated and screened by hybridization, and a single positive pick effected.

Isolation of YAC DNA:

Solution DNA:

Cells were grown at 30° C in 40 ml YPD overnight to saturation. The cells were then spun in a desktop centrifuge at 3000 rpm for 5 minutes, the solution decanted and the pellet resuspended in 3 ml of SE (0.9 M sorbitol, 0.1 M EDTA pH 7.5). 75 µl of 10 mg/ml zymolyase 20,000 was then added and the mixture incubated for 2.5 hours. The solution was then centrifuged for 5 minutes at 1200 rpm, and the pellet gently resuspended in 5 ml 50 mM Tris pH 7.4, 20 mM EDTA. 0.5 ml of 10% SDS was added and the mixture incubated at 65° C for 30 minutes, after which 1.5 ml of 5 M potassium acetate was added and the mixture left on ice for 60 minutes. After centrifugation in a Beckman model J6B, rotor 4.2, at 3500 rpm for 10 minutes, the supernatant was transferred to a fresh centrifuge tube and 2 volumes of 100% ethanol was

added. The mixture was then centrifuged at 3500 rpm for 15 minutes. The pellet was dried and then resuspended in 3 ml of 10,1 TE (10 mM Tris pH 7.4, 1 mM EDTA). The solution DNA was then centrifuged at 3500 rpm for 15 minutes, the supernatant transferred to a new tube, and 150 µl of a 1 mg/ml RNase solution added and then incubated at 37° C. After 30 minutes, 1 volume of isopropanol was added, the precipitated DNA spooled and resuspended in ~0.5 ml of 10,1 TE to a final concentration of ~200 ng/µl. If the final solution was milky, the DNA was reprecipitated until clear or recentrifuged at 3500 rpm for 15 minutes as before.

Agarose embedded yeast DNA:

Cell are grown to saturation (24-36 hours at 30° C) in 50 ml of YPD. Once the cells were saturated, 10 ml was pipetted into a 15 ml conical flask, and centrifuged at 3000 rpm for 5 minutes. The supernatant was decanted and the pellet washed in 2 ml of SE, centrifuged at 3000 rpm for minutes, and the supernatant decanted. To the pellet, 400 µl of STEMZ (5.5 ml STEM + 1/1000 volume of β-mercaptoethanol + 0.5 ml zymolyase) was added, the mixture gently vortexed and 500 µl of 2% Incert agarose added (held at 37° - 45° C). The mixture was pipetted into the molds, placed at 4° C for ~30 minutes until hardened and then pushed into 5.5 ml STEMX and incubated at 37° C for 3 hours. The solution was then decanted and 5 ml of yeast lysis buffer (YLB) added, incubated at 37° C for 0.5 - 1 hour, the solution decanted

and fresh YLB added. After overnight digestion, fresh YLB was added, and the blocks stored at room temperature. Before use the blocks were thoroughly washed in 3 X 30 min each in 10,1 TE at 50° C, 3 X 30 minutes at room temperature, and then 2 X 30 minutes in pulse-field gel 0.5X TBE running buffer.

Isolation of YAC specific probes by inter-B2 repeat PCR: To 1 µl of YAC solution DNA (~200 ng/µl), was added a mouse specific B2 oligomer of sequence GAC AGC TAC AGT GTA CTT ACA TAT in a total PCR reaction volume of 100 µl. 35 cycles of PCR were carried out at 55° C annealing for 1 minute and extension at 72° C for 1 minute followed by electrophoresis of a 25 µl aliquot in 1.5% agarose to ensure amplification of a product from the YAC bearing the cloned mouse DNA. If any bands were visualized, a radiolabelled probe was prepared from the product(s) by first removing unincorporated nucleotides from the remaining PCR mixture by passage of the PCR amplified material through the same Stratagene push columns used for purifying radiolabelled probes. A 2 µl aliquot of the eluent was random hexamer labelled and purified. To use the radiolabelled product as a probe, repetitive sequences were first blocked by preannealing the probe to 200 µg of sonicated total mouse DNA for 5 hours at 65° C in 5X SSC. The probe was then used for hybridization without further purification.

Chapter 3: Results

Genetic Maps of Mouse Chromosomes 4 and 6

Genetic Cross and Probes Utilized

In order to map mouse chromosomes 4 and 6, DNA probes were in general selected from two different sources 1) probes previously reported to be on chromosome 4 or 6 by linkage analysis or by use of somatic cell hybrids and 2) probes reported to be on regions of the human genome syntenic with either of these mouse chromosomes. The 29 cloned probes, which were utilized are listed in Table 2.1. The chromosomal assignment of each probe is also shown in Table 2.1. This panel included several genes whose positions are considered to be anchor loci on the June 1990 linkage map of the mouse chromosome 4 compiled by A.L. Hillyard et. al. (personal communication) by virtue of the fact that their positions are well known from three-point crosses and extensive data: *Mup-1*, *b* and *Ifa* on chromosome 4 and *Igk* on mouse chromosome 6. The use of these anchor loci in the present study provides suitable reference points by which the linkage data can be related to those from other mapping studies.

Each probe was first used to define an RFLP between C57BL/6J and *M. spretus*. The enzyme that revealed the RFLP, and informative allele size, for a specific probe is shown in Table 2.1. Additionally, since the *UROD* probe did not hybridize particularly well to Southern blots, a denaturing gradient gel polymorphism between C57BL/6J and *M. spretus* was also characterized to

confirm the Southern blot findings (Figure 3.1). Approximately 100 progeny of the *M. laboratorius* x *M. spretus* interspecific backcross were then typed for the presence of the C57BL/6J or *M. spretus* alleles for each polymorphism. No novel genotypes were observed although for one gene, *Tcrb*, there were two different alleles in the *spretus* strains for the enzyme Taq I. This allelic difference within the *spretus* population was not restricted to either of the two groups of animals which comprised the mapping panel.

Map of Chromosome 4

The pedigree analysis for all loci tested on chromosome 4 is shown in Fig 3.2; gene order was determined by minimizing the number of double crossovers, and confirmed by use of the MAPMAKER program which constructs genetic linkage maps by multi-point linkage analysis (Lander, et al., 1987). In carrying out the MAPMAKER analysis, the order of the *UROD*, *D4Rp1*, and *Glut-1* markers were left undetermined since no crossover events between them were detected in the 97 animals scored for all three loci. The order cen—*Mup-1* — *Orm-2* is approximately 58 times more likely than the order cen — *Orm-2* — *Mup-1*, the order cen — *Ifa* — *Jun* is approximately 1000 times more likely than the order cen — *Jun* — *Ifa*, and the order cen — *Jun* — (*UROD*, *D4Rp1*, *Glut-1*) — *Lmyc-1* — *Lck* is approximately 300 times more likely than any alternate regional order. If the genetic map is reanalyzed using MAPMAKER, with the most likely order of markers in

these three regions determined as described above, the order presented (Fig. 3. 3) is 65,000 times more likely than any other remaining order. The genetic map for chromosome 4 (Fig. 3.3) covers 77 cM. and was anchored around *Ifa*, *Mup* and/or *b* for comparison to the previously published genetic maps. (Ceci, et al., 1989; Fletcher, et al., 1991; T. H. Roderick, personal communication). Three new gene assignments to chromosome 4 were made: *UROD*, *EL1* (protein 4.1) and *C8B*, all of which have been previously mapped to human chromosome 1p. In addition, regional assignments for three other genes: *Glut-1*, *Fuca*, and *Fabph-1*, were made, and refinements in the positions of *Mup-1*, *Orm-2*, and *Jun* were established.

In general, these data agree well with previous reports (Fig. 3.3). One deviation from previous maps was notable compared to the map reported here. *Orm–2* was positioned more proximally than previously reported(Nadeau, et al., 1986; Baumann, et al., 1984; Baumann and Berger, 1985) (see Fig. 3.3). *Orm–2* was recombinant with *Mup-1* in 1/97 animals scored for both loci, and was placed distal to *Mup–1* by minimizing double crossovers. This assignment of *Orm–2* is confirmed by use of the MAPMAKER program; the order cen -- *Mup–1* -- *Orm–2* is 58 times more likely than the order cen -- *Orm–2* -- *Mup–1*.

The map position of the human homologues of the cloned genes are shown left of the line in Fig. 3.3. Of particular note is the 30 cM syntenic group between mid-chromosome 4 and the telomere in mouse, and lp31-pter

in man (Fig. 3.4). In mouse, the breakpoint between this syntenic group and genes syntenic with human 9q likely occurred between *Jun* (*JUN*, 1p31) and *Ifa* (*IFNA*, 9q34). Two recombinants have been identified which position *Jun* ~2 cM distal to *Ifa*.

In order to further explore the synteny relationship between human 1p and mouse 4, the mouse gene for medium chain acyl-coA dehydrogenase (*ACADM*) was mapped. *ACADM* has been genetically mapped in human to chromosome 1p31 and is proximal to *PGM1* (*Pgm-2* in mouse) and *JUN* in human (Kidd et al., 1990). A probe of the predicted size was generated in PCR reactions from a rat liver cDNA library using two oligonucleotides determined from the aligned sequences of the human and rat ACADM cDNAs (Table 2.2). This probe detected an RFLP amongst C57BL/6J, DBA/2J, and *M. spretus* using the restriction enzyme EcoRI (Table 2.1). Linkage was not detected between *ACADM* and any other chromosome 4 marker, as determined by typing the 49 offspring of the (C57BL/6J x DBA/2J) F1 *db*/+ X (C57BL/6J x *M. spretus*) F1 *db*/+ cross which was typed for *Ifa, Jun, db, D4Rp1, Glut-1*, and *Lck* (see intraspecific cross results). The probe was then used to type the 26 BxD RI lines (Table 3.1). Three differences were noted between this probe and Es-1 (Kirchgessner, et al., 1989) on mouse chromosome 8 which strongly suggests linkage. Four differences with *Zfp-4* also on mouse chromosome 8 (Ashworth, et al., 1989), were noted, suggesting the order *Es-1* -- *ACADM* -- *Zfp-4* (Table 3.1). Previous studies have demonstrated the

difficulty of precisely ordering markers using the RI strains, therefore the exact location of *ACADM* on chromosome 8, remains to be determined (Nadeau, et al., 1991; Eicher and Lee, 1990). The assignment of *ACADM* to mouse chromosome 8 suggests that the breakpoint of the 1p syntenic group in human is distal to *ACADM*. Of interest is that most of the other markers from proximal human 1p map to mouse chromosome 3 (Nadeau, 1989). A more detailed comparison of the mouse — human synteny in this region is shown in Figure 3.4.

	1	2	5	6	8	9	11	12	13	14
Es-1	D	B	B	D	D	D	D	B	D	B
			X							
ACADM	D	B	D	D	D	D	D	B	D	B
Zfp-4	D	B	D	D	D	D	D	B	D	B

	15	16	18	19	20	21	22	23	24	25
Es-1	B	D	D	B	D	B	B	B	D	B
ACADM	B	D	D	B	D	B	B	B	D	B
						X				X
Zfp-4	B	D	D	B	D	D	B	B	D	D

	27	28	29	30	31	32
Es-1	D	B	B	B	B	D
		X		X		
ACADM	D	D	B	D	B	D
		X	X			
Zfp-4	D	B	D	D	B	O

Table 3.1. Data for the typing of the 26 BxD RI lines for the probe which detects the mouse *ACADM* locus. Three differences were noted between this probe and *Es-1*, and four differences between this probe and *Zfp-4*, on mouse chromosome 8. These findings strongly suggest linkage, however order cannot not be ascertained with certainty. Since the location of the *ACADM* locus in man is known to be 1p31, proximal to *JUN*, it appears that the breakpoint of the human 1p31-ter to mouse chromosome 4 synteny lies distal to the *ACADM* locus in humans. The letter 'B' denotes inheritance of the C57BL/6J allele, 'D' the DBA/2J allele, and 'O' denotes an RI strain for which the strain distribution pattern (SDP) is unknown for a specific marker.

Figure 3.1. Use of denaturing gradient gel electrophoresis to map the *UROD* locus. DNA from each animal was subjected to PCR as described (Table 2.2). and a 75 µl PCR sample was electrophoresed and photographed under UV illumination. The letter 'B' denotes C57BL/6J control, 'S' the *M. spretus control,* and eight N2 offspring are shown numbered '1' through '8'.

Use of denaturing gradient gel electrophoresis (DGG) to map the *UroD* locus

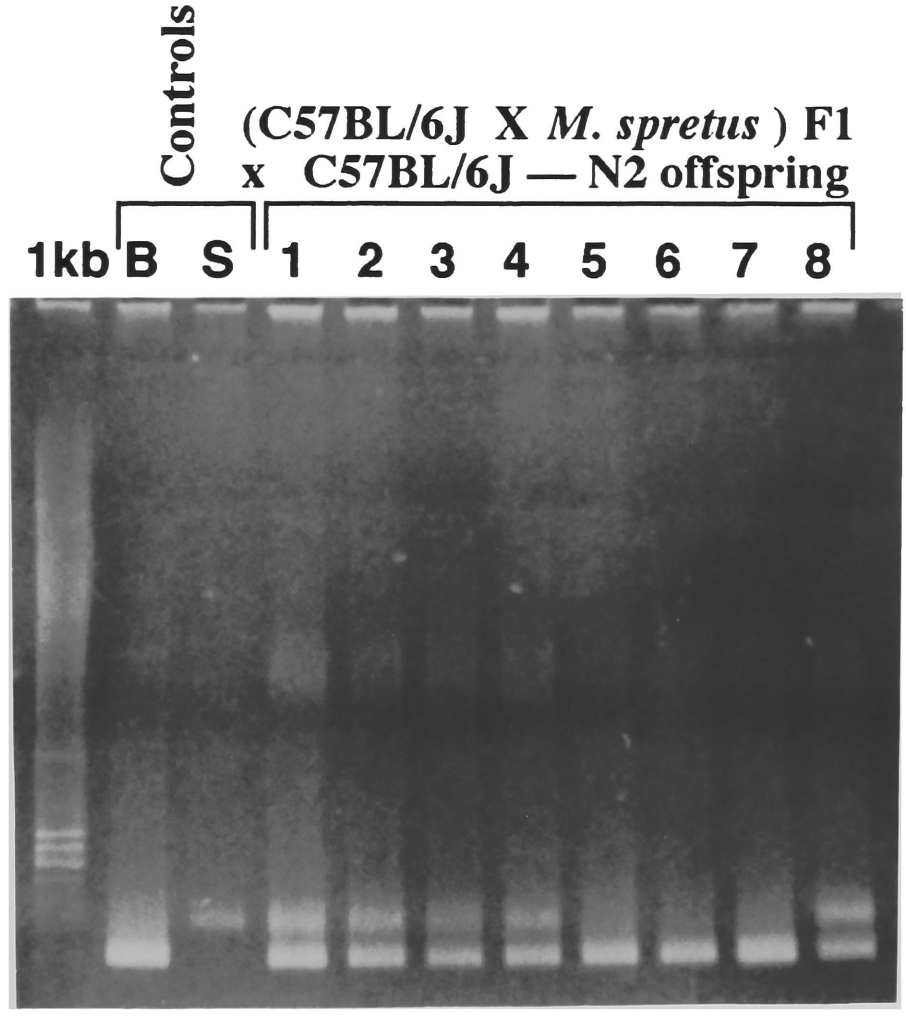

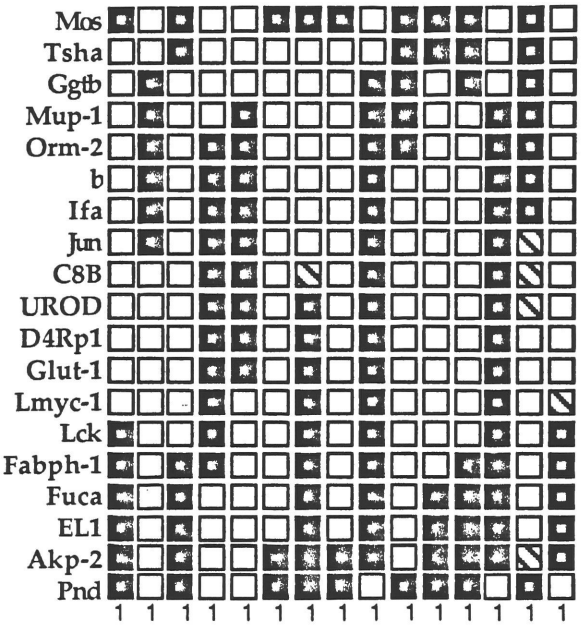

Figure 3.2. Pedigree analysis of the 19 chromosome 4 loci in 83 (C57BL/6J x *M. spretus*) F1 x C57BL/6J (N2) offspring which demonstrated either no crossover, or a single crossover event and in the 15 N2 offspring that demonstrated double recombination events. The mapped loci are listed on the left and/or right. Each column represents N2 progeny whose typing of RFLPs for each locus gave the pattern of C57BL/6J and *M. spretus* alleles shown. The number of N2 offspring with a particular pattern of alleles is shown at the bottom. The blackened boxes represent the *M. spretus* allele, the white boxes the C57BL/6J allele, and the diagonally striped boxes represent instances for which data is not available.

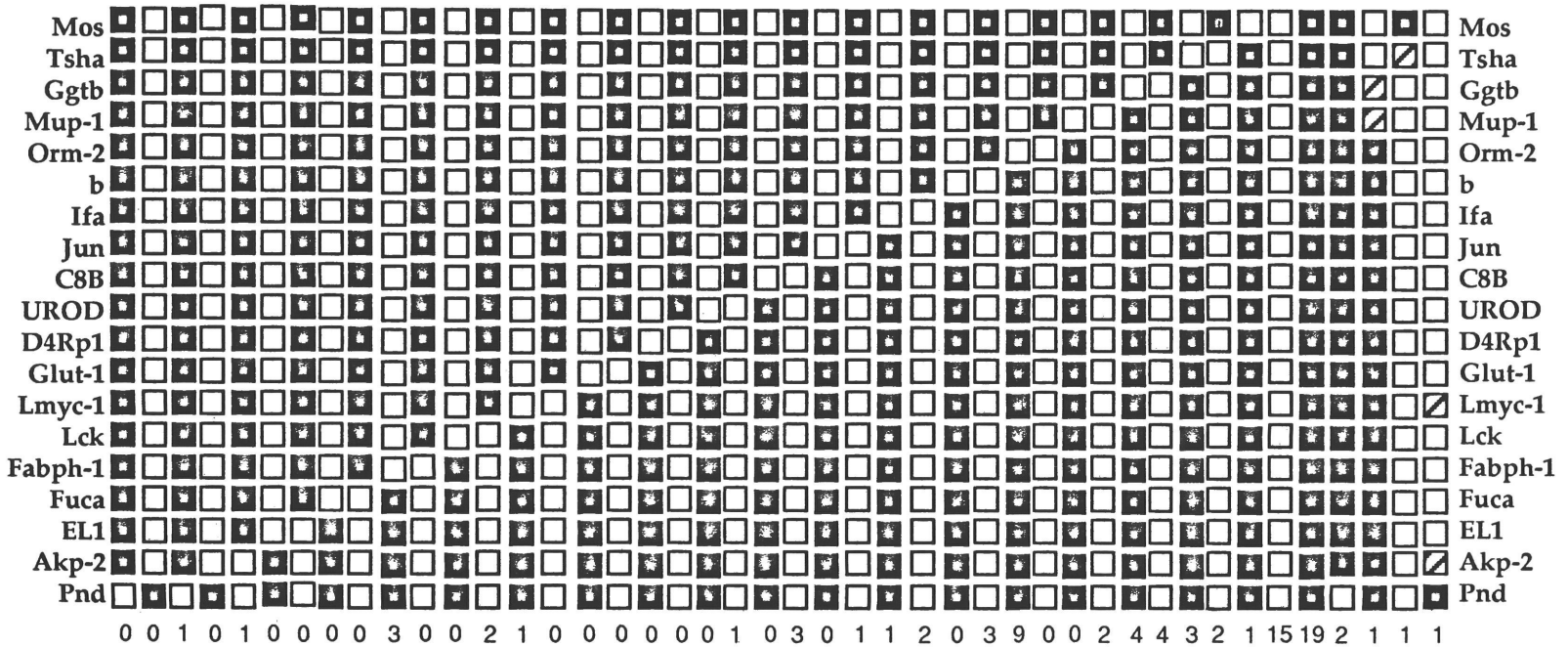
Mos
Tsha
Ggtb
Mup-1
Orm-2
b
Ifa
Jun
C8B
UROD
D4Rp1
Glut-1
Lmyc-1
Lck
Fabph-1
Fuca
EL1
Akp-2
Pnd
0 0 1 0 1 0 0 0 0 3 0 0 2 1 0 0 0 0 0 0 1 0 3 0 1 1 2 0 3 9 0 0 2 4 4 3 2 1 15 19 2 1 1 1

Figure 3.3. The derived genetic linkage map of mouse chromosome 4 using 98 offspring of the (C57BL/6J X *M.spretus*) F1 x C57BL/6J backcross is shown on the left. The positioning of the centromere and telomere is arbitrary, and no inference should be drawn concerning the distance of either the most proximal marker with respect to the centromere, or the most distal marker with respect to the telomere. The twenty markers were positioned by minimizing the number of double crossover events between pairs of markers, and confirmed by use of the MAPMAKER program (Lander, et al., 1987) which uses multipoint linkage analysis to determine order and to compare orders with respect to their likelihood. The order *Mup-1 -- Orm-2* is approximately 58 times more likely than the order *Orm-2 -- Mup-1*, the order *Ifa -- Jun* is approximately 1000 times more likely than the order *Jun -- Ifa*, and the order *Jun -- (UROD, D4Rp1, Glut-1) -- Lmyc-1 -- Lck* is 300 times more likely than any other regional order. The order presented is 65,000 times more likely than any other order, allowing for these three regional orders to be determined in their most likely configuration. The distances between markers (in cM) are the recombination frequencies between successive markers [(# recombinant animals / total number of animals scored)] X 100. The markers span a total distance of approximately 77 cM. To the left of each marker, is shown its homologous position in the human genome, obtained from the human genome database (GDB, 1990). Of note is the ~ 30 cM of synteny between mid-chromosome 4 to the telomere in the mouse, and human chromosome 1p31-pter. The apparent breakpoint in that synteny is located in an ~2cM interval between *Jun* and *Ifa*. The genetic map from these studies is compared to the composite of this chromosome (shown on the right) compiled by T. H. Roderick, M. T. Davisson, A. L. Hillyard, and D. P. Doolittle (personal communication, June 1990). Several new assignments were made including *UROD, EL1, D4RCK128* (see the results of the Rb4:6 flow-sort for more information on this probe), and *C8B* as well as regional assignments of *Ggtb, Glut-1, Fuca,* and *Fabph-1* and refinements in the positions of *Mup-1, Orm-2, b, Jun* and *Ifa*.

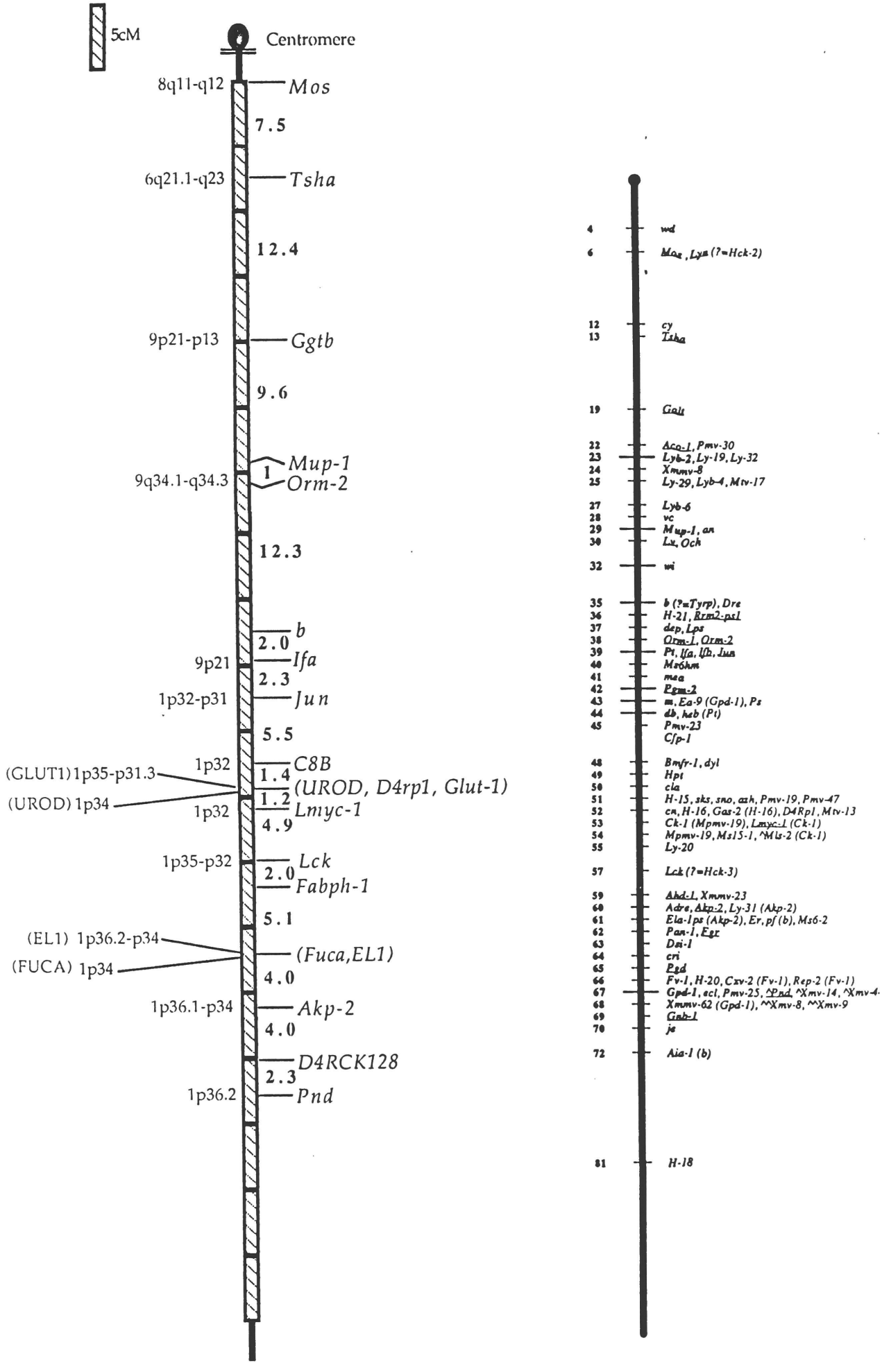
5cM
Centromere
8q11-q12
Mos
7.5
6q21.1-q23
Tsha
12.4
9p21-p13
Ggtb
9.6
1
Mup-1
9q34.1-q34.3
Orm-2
12.3
b
2.0
9p21
Ifa
2.3
1p32-p31
Jun
5.5
1p32
C8B
(GLUT1) 1p35-p31.3
1.4
(UROD, D4rp1, Glut-1)
(UROD) 1p34
1.2
1p32
Lmyc-1
4.9
1p35-p32
Lck
2.0
Fabph-1
5.1
(EL1) 1p36.2-p34
(Fuca,EL1)
(FUCA) 1p34
4.0
1p36.1-p34
Akp-2
4.0
D4RCK128
2.3
1p36.2
Pnd
4
wd
6
Mos, Lyn (?=Hck-2)
12
cy
13
Tsha
19
Galt
22
Aco-1, Pmv-30
23
Lyb-2, Ly-19, Ly-32
24
Xmmv-8
25
Ly-29, Lyb-4, Mtv-17
27
Lyb-6
28
vc
29
Mup-1, an
30
Lv, Och
32
wi
35
b (?=Tyrp), Dre
36
H-21, Rrm2-ps1
37
dep, Lps
38
Orm-1, Orm-2
39
Pt, Ifa, Ifb, Jun
40
Mt6hm
41
mea
42
Pgm-2
43
m, Ea-9 (Gpd-1), Ps
44
db, hab (Pt)
45
Pmv-23
Cfp-1
48
Bmfr-1, dyl
49
Hpt
50
cla
51
H-15, sks, sno, ash, Pmv-19, Pmv-47
52
cn, H-16, Gas-2 (H-16), D4Rp1, Mtv-13
53
Ck-1 (Mpmv-19), Lmyc-1 (Ck-1)
54
Mpmv-19, Ms15-1, ^Mls-2 (Ck-1)
55
Ly-20
57
Lck (?=Hck-3)
59
Abd-1, Xmmv-23
60
Adre, Akp-2, Ly-31 (Akp-2)
61
Ela-1ps (Akp-2), Er, pf (b), Ms6-2
62
Pan-1, Egr
63
Dsi-1
64
cri
65
Pgd
66
Fv-1, H-20, Czv-2 (Fv-1), Rep-2 (Fv-1)
67
Gpd-1, ecl, Pmv-25, ^Pnd, ^Xmv-14, ^Xmv-4
68
Xmmv-62 (Gpd-1), ^^Xmv-8, ^^Xmv-9
69
Gab-1
70
je
72
Aia-1 (b)
81
H-18

Figure 3.4. A detailed comparison of the synteny between human chromosomes 1 and 9, and mouse chromosomes 3 and 4. The genetic maps of human 1p and 9q are shown to left and right respectively of the mouse chromosome 4 map. There is a large region of homology between human 1p31-pter and chromosome 4 (see Figure 3.3) as well as a smaller segment of homology between proximal human 1p and mouse chromosome 3. The mouse chromosome 3 regional assignments (shown in cM distances from the centromere) are obtained from the composite of this chromosome compiled by T. H. Roderick, M. T. Davisson, A. L. Hillyard, and D. P. Doolittle (personal communication, June 1990). The human chromosomal assignments shown were obtained from the human Genome Data Base (GDB, 1990). The gene encoding the mouse medium chain acyl-coA dehydrogenase (*ACADM*) gene was mapped to mouse chromosome 8 by use of the 26 BxD RI lines (Table 3.1). Thus, the breakpoint of the human 1p31-ter to mouse chromosome 4 synteny appears to be distal to *ACADM* on human chromosome 1. The apparent breakpoint in mouse chromosome 4, with regards to its synteny to 1p31-pter, is located in an ~2cM interval between *Jun* and *Ifa*.

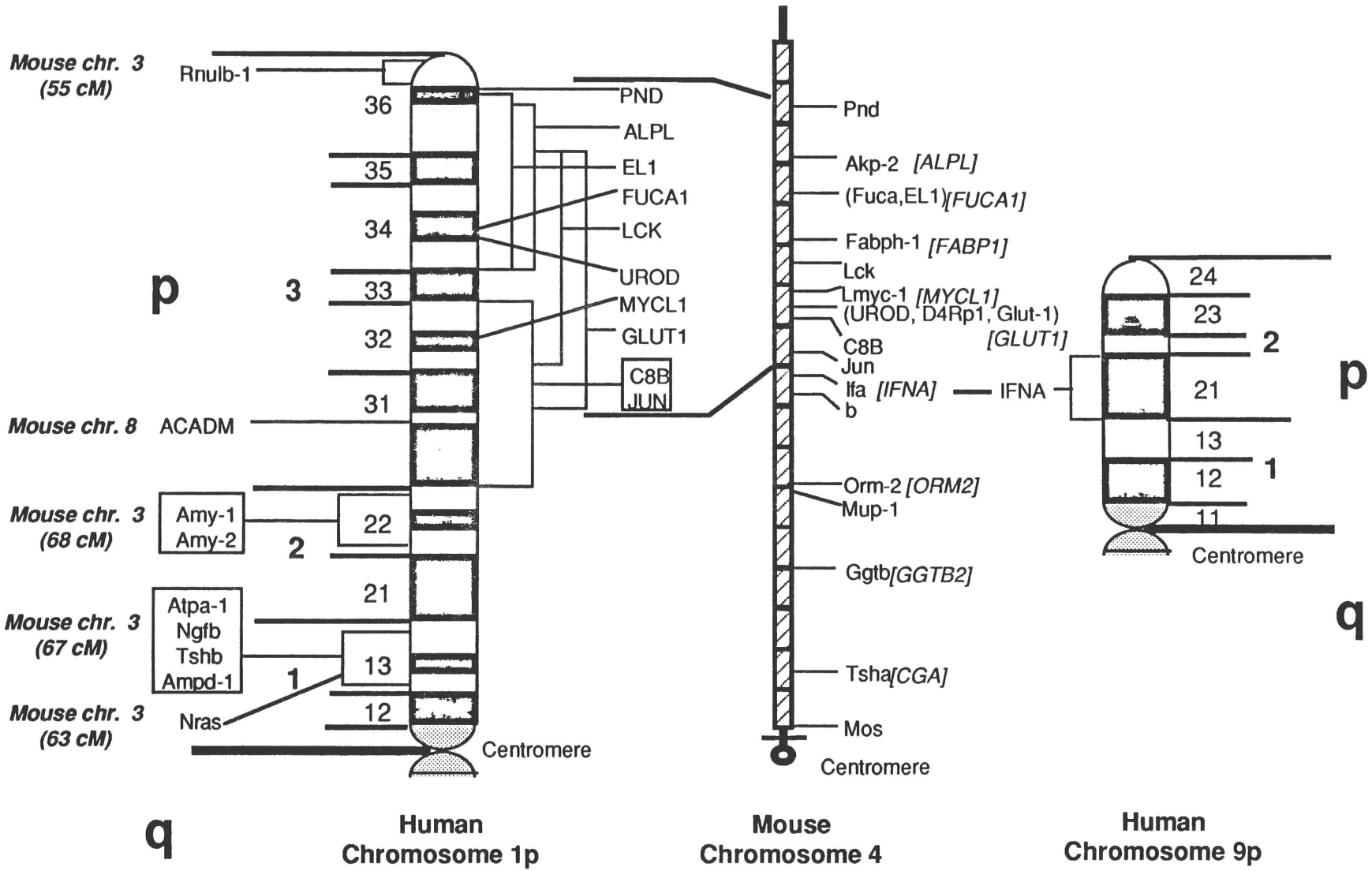
Mouse chr. 3
(55 cM)
Rnulb-1
36
35
34
33
32
31
Mouse chr. 8
ACADM
Mouse chr. 3
(68 cM)
Amy-1
Amy-2
22
2
21
Mouse chr. 3
(67 cM)
Atpa-1
Ngfb
Tshb
Ampd-1
13
1
Mouse chr. 3
(63 cM)
Nras
12
Centromere
p
3
q
PND
ALPL
EL1
FUCA1
LCK
UROD
MYCL1
GLUT1
C8B
JUN
Human
Chromosome 1p
Pnd
Akp-2 [ALPL]
(Fuca,EL1) [FUCA1]
Fabph-1 [FABP1]
Lck
Lmyc-1 [MYCL1]
(UROD, D4Rp1, Glut-1) [GLUT1]
C8B
Jun
Ifa [IFNA]
b
Orm-2 [ORM2]
Mup-1
Ggtb [GGTB2]
Tsha [CGA]
Mos
Centromere
Mouse
Chromosome 4
IFNA
24
23
2
21
13
1
12
11
Centromere
p
q
Human
Chromosome 9p

With the exception of *UROD*, the order of the markers on distal chromosome 4 correlates well with the respective map positions in human (Figure 3.4). In human the map position of *UROD* was determined cytogenetically (Mattei, et al., 1985). The in-situ hybridization performed did not provide any reference to previously mapped clones, and because of the close conservation in the order of the markers in the human 1p31-pter and distal mouse 4 intervals, it is possible that the 1p34 position given for *UROD* in human (GDB, 1990), is incorrect. The data shown in Figure 3.4, suggests that *UROD* is more likely to be located in the 1p32 interval in human.

Distribution of chromosome 4 recombination events

The number of chromosomes containing a single, double, triple or higher order recombination event should be distributed in a Poisson fashion provided there is no mechanism which causes over or under representation of any of the events. If these events are distributed in a Poisson fashion, then the expected number of chromosomes containing **n** recombination events are given by the equation e^{-m} ($m^n/n!$). The terms of the equation are defined as follows:

m = *mean number of recombinations* calculated as the weighted number of recombinations (single crossovers count as 1, double recombinations for 2, triple for 3, etc.) noted over an entire chromosome/total number of chromosomes analyzed)

and $\underline{n}$ = the order of the recombinational event being analyzed (n=1 for single recombinations, 2 for doubles, etc.)

By substituting into the equation above the value of $\underline{m}$ as determined from a particular cross, one can calculate the number of expected singly (n=1), doubly (n=2), and triply (n=3) recombinant chromosomes. Using a chi-square analysis, the predicted Poisson distribution can be compared to the observed distribution, pooling rare event classes if necessary. The number of degrees of freedom (df) for the chi-square analysis is the number of event classes - 1. The chi square statistic is given by the following formula:

$$\chi^2 (df) = \Sigma [(O-E)^2/E]$$

where O = observed number of $\underline{n}$ recombinant chromosomes and

E = expected number of $\underline{n}$ recombinant chromosomes

For the described loci on chromosome 4, a total of 98 animals were scored for their frequency of recombination. If the frequency of recombination events were Poisson distributed, 41 nonrecombinant chromosomes, 35 singly recombinant chromosomes, 15 double recombinants, 4 triply recombinant, and 3 higher order recombinant chromosomes would be expected. A total of 34 chromosomes were observed with no recombination, 49 were singly recombinant, 15 doubly recombinant and no triply

recombinant chromosomes were observed. Analysis of these data show statistically significant deviation from that predicted by the Poisson distribution ($\chi^2 = 11.50$, $.01 < p < .05$) and suggest significant overrepresentation of single crossover recombination events (Blank, et al., 1988).

Segregation distortion testing on chromosome 4

Because the C57BL/6J and *M. spretus* mouse strains are significantly diverged from one another, it is possible that certain allelic segments of their genomes could differ significantly when compared to one another. This divergence could result in preferential inheritance, or selective advantage of inheritance, of allelic C57BL/6J and *M. spretus* segments of a particular chromosome, and is termed segregation distortion. This would appear as an overrepresentation of one strain's allele (as detected by RFLP) as compared to the other strain's allele for a particular locus. By performing a chi-square analysis comparing the observed number of C57BL/6J and *M. spretus* alleles as detected by RFLP analysis for each loci, to the expected number (which is 50% for each), segregation distortion can be detected.

G tests were performed on these data as described (Sokal and Rohlf, 1981) to determine whether segregation of *M. spretus* and C57BL/6J alleles differed significantly from 1:1 at any of these loci. The *b* locus and the loci on distal 4 between *Fuca* and *Akp-2* tended to show deviation from the 50:50

expected ratio, however, the deviation was not statistically significant by chi-square analysis (Table 3.2). This finding is in agreement with a previous report indicating no segregation distortion in this region (Fletcher, et al., 1991), but is in conflict with separate previous reports of segregation distortion on distal (Ceci, et al., 1989) and proximal chromosome 4 (Shaper, et al., 1990).

Map of Chromosome 6

The pedigree analysis of chromosome 6 is shown in Fig. 3.5. The ten probes were ordered by minimizing double crossovers, and confirmed with the MAPMAKER program (Lander, et al., 1987), to yield an order: (*Cola-2, NKNA*), *Met, Cpa, Tcrb, Npy, Igk, Rpl32, Prp, Kras-2* (Fig. 3.6). Using the MAPMAKER program, this order (allowing the position of *Cola-2* and *NKNA* to remain undetermined since no recombination events between them were found) is approximately 30 times more likely than the same order with the *Met* and (*Cola-2, NKNA*) loci reversed. If the order (*Cola-2, NKNA*) -- *Met* is fixed, then the order presented is >100,000 times more likely than any other remaining order. The map is shown in Fig. 3.6 and spans 65 cM. The map includes the new assignment of *NKNA* and *Npy* to chromosome 6, and positions *Rpl32* distal to *IgK*. These data also position *Cola-2* proximal to *Met*. Of note, linkage was not detected between two P450 gene clusters, *Pcn* and *Por*

and any of the RFLPs mapped here, in disagreement with a previous assignment of these loci to chromosome 6 (Simmons, et al., 1985).

As previously reported, many of the RFLPs from proximal chromosome 6 map to chromosome 7 in humans (Bucan et al., 1986). This syntenic group spans ~18 cM in mouse and includes the assignment of two new genes which also map to human 7p: *Npy* to mid mouse 6 and *NKNA* to proximal mouse 6. The other genes in this syntenic group -- *Cola-2*, *Met*, *Cpa* and *Tcrb* -- all map to human 7q with the same approximate order as in mouse (GDB, 1990).

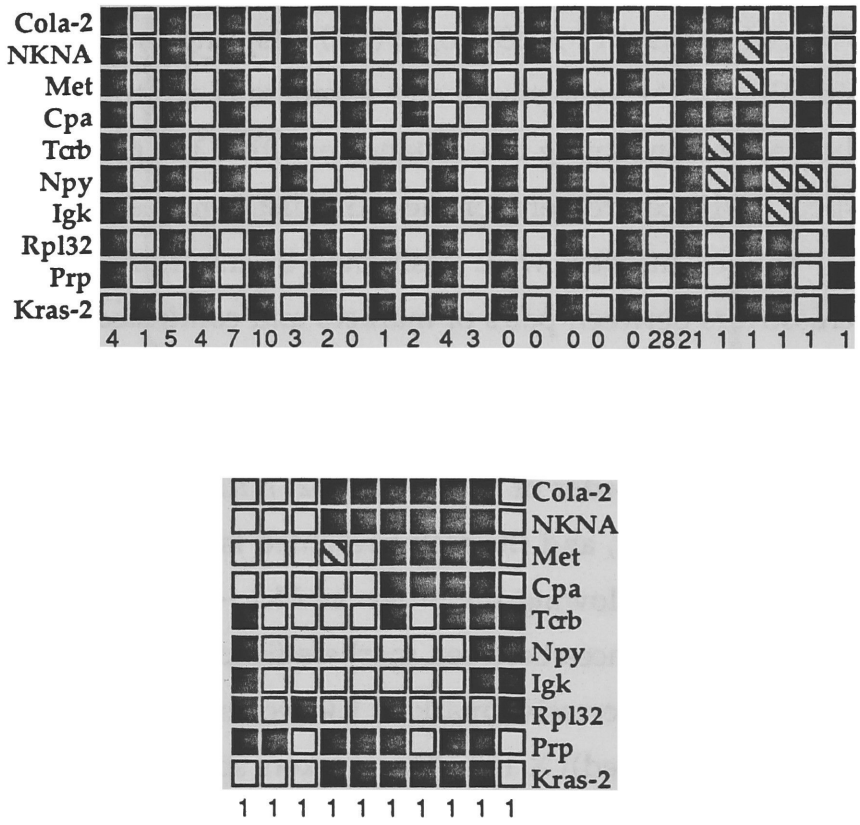

Figure 3.5. Pedigree analysis of the 10 chromosome 6 loci in 110 (C57BL/6J x *M. spretus*) F1 x C57BL/6J (N2) offspring. The mapped loci are listed on the left and right. Each column represents N2 progeny whose typing of RFLPs for each locus gave the pattern of C57BL/6J and *M. spretus* alleles shown. The number of N2 offspring with a particular pattern of alleles is shown at the bottom. The blackened boxes represent the *M. spretus* allele, the white boxes the C57BL/6J allele, and the diagonally striped boxes represent instances for which data is not available.

Figure 3.6. The derived genetic linkage map of 10 chromosome 6 loci in 110 (C57BL/6J x *M. spretus*) F1 x C57BL/6J (N2) offspring as shown on the left. The positioning of the centromere and telomere is arbitrary, and no inference should be drawn concerning the distance of either the most proximal marker with respect to the centromere, or the most distal marker with respect to the telomere. The ten markers were positioned by minimizing the number of double crossovers between pairs of markers and confirmed by use of the MAPMAKER program (Lander, et al., 1987). Allowing the order of *Cola–2* and *NKNA* to remain undetermined because no recombination between them were noted, the order of *Met* -- (*Cola–2, NKNA*) is 30 times more likely than the order reversed, and the map presented is >100,000 times more likely than any other order allowing the order of *Met* -- (*Cola–2, NKNA*) to be determined. The distances between markers (in cM) are the recombination frequencies between successive markers [(# recombinant animals / total number of animals scored)] X 100. The markers span a total distance of approximately 65 cM. To the left of each marker, is shown its homologous human position. Of note is the large area (~18 cM) of synteny between proximal mouse chromosome 6 and human chromosome 7q. The human chromosomal assignments shown were obtained from the Genome Data Base (GDB, 1990). The genetic map from these studies is compared to the composite of this chromosome (shown on the right) compiled by T. H. Roderick, M. T. Davisson, A. L. Hillyard, and D. P. Doolittle (personal communication, June 1990). The derived map on the left includes the new assignment of *NKNA* and *Npy* to chromosome 6 and positions *Rpl32* distal to *Igk*. These data also position *Cola-2* proximal to *Met*. *D6Rck132* is discussed with the flow-sorted Rb4:6 clones.

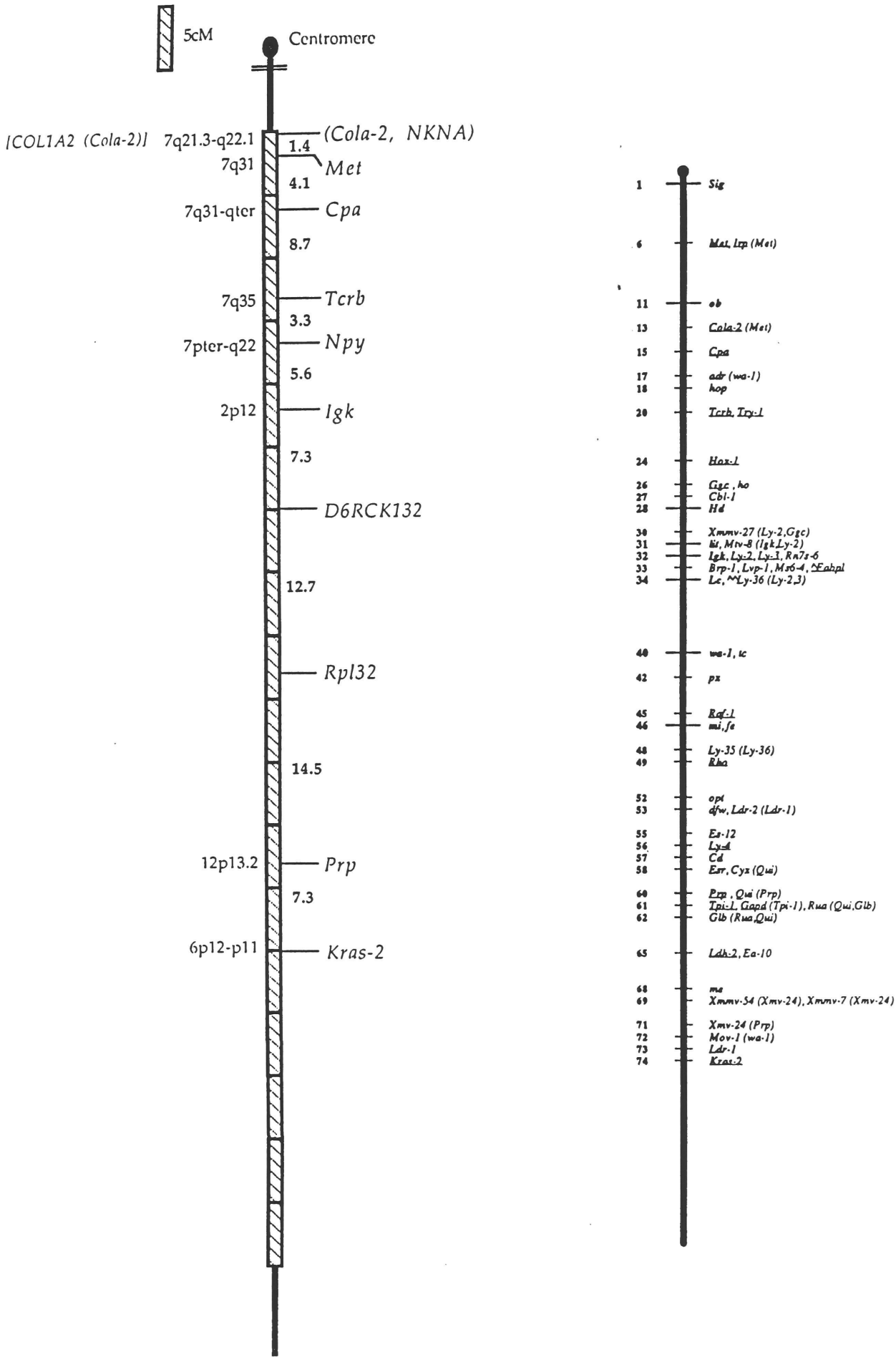
5cM
Centromere
[COL1A2 (Cola-2)]
7q21.3-q22.1
(Cola-2, NKNA)
1.4
7q31
Met
4.1
7q31-qter
Cpa
8.7
7q35
Tcrb
3.3
7pter-q22
Npy
5.6
2p12
Igk
7.3
D6RCK132
12.7
Rpl32
14.5
12p13.2
Prp
7.3
6p12-p11
Kras-2
1 Sig
6 Mat, Lrp (Met)
11 ob
13 Cola-2 (Met)
15 Cpa
17 adr (wa-1)
18 hop
20 Tcrb, Try-1
24 Hox-1
26 Ggc, ho
27 Cbl-1
28 Hd
30 Xmmv-27 (Ly-2,Ggc)
31 lit, Mtv-8 (Igk,Ly-2)
32 Igk, Ly-2, Ly-3, Rn7s-6
33 Brp-1, Lvp-1, Ms6-4, ^Eahpl
34 Lc, ^Ly-36 (Ly-2,3)
40 wa-1, tc
42 px
45 Raf-1
46 mi, fe
48 Ly-35 (Ly-36)
49 Rho
52 opt
53 dfw, Ldr-2 (Ldr-1)
55 Es-12
56 Ly-4
57 Cd
58 Esr, Cyz (Qui)
60 Prp, Qui (Prp)
61 Tpi-1, Gapd (Tpi-1), Rua (Qui,Glb)
62 Glb (Rua,Qui)
65 Ldh-2, Es-10
68 ms
69 Xmmv-54 (Xmv-24), Xmmv-7 (Xmv-24)
71 Xmv-24 (Prp)
72 Mov-1 (wa-1)
73 Ldr-1
74 Kras-2

Distribution of chromosome 6 recombination events

As for chromosome 4, evidence for suppression of nonrecombinants and multiple recombinants on chromosome 6 is suggested by comparing the actual number of nonrecombinant (49), singly (51), doubly (10) and triply (0) recombinant chromosomes to that predicted by a Poisson distribution (56, 38, 12 and 3, respectively) (Blank, et al., 1988). Chi-square analyses of these data show a statistically significant difference ($\chi^2 = 8.65$, $.01 < p < .05$) and offers evidence for significant overrepresentation of single crossover recombination events in this span of chromosome 6.

Segregation distortion testing on chromosome 6

A χ^2 test was performed as described (Sokal and Rohlf, 1981) to determine whether the transmission of C57BL/6J and *M. spretus* alleles deviated from that of the 50:50 ratio expected for Mendelian loci. A tendency toward deviation is seen with *Cpa* ($p >= 0.5$), *Npy* ($p >= 0.38$), and *Igk* ($p >= 0.21$), however none were statistically significant by chi-square analysis (Table 3.2).

	Mos	*Tsha*	*Ggtb*	*Mup-1*	*Orm-2*	*b*	*Ifa*	*Jun*	*C8B*	*UROD*
M. spretus	53	47	48	47	50	56	54	53	49	50
C57BL/6J	45	50	49	50	48	42	44	44	47	47
G value	0.65	0.09	0.10	0.09	0.04	2.0	1.02	0.84	0.04	0.09
(χ^2) P>=	0.42	0.76	0.91	0.76	0.84	0.16	0.31	0.36	0.84	0.76

	D4Rp1	*Glut-1*	*Lmyc-1*	*Lck*	*Fabph-1*	*Fuca*	*EL1*	*Akp-2*	*Pnd*
M. spretus	50	50	48	49	51	54	54	55	52
C57BL/6J	48	48	48	49	47	44	44	41	46
G value	0.04	0.04	0	0	0.16	1.02	1.02	2.0	0.37
(χ^2) P>=	0.84	0.84	1.0	1.0	0.69	0.31	0.31	0.15	0.55

	Cola-2	*NKNA*	*Met*	*Cpa*	*Tcrb*	*Npy*
M. spretus	53	53	51	49	51	49
C57BL/6J	57	56	57	61	58	58
G value	0.15	0.08	0.33	1.30	0.45	0.76
(χ^2) P>=	0.70	0.77	0.56	0.25	0.50	0.38

	Igk	*Rpl32*	*Prp*	*Kras-2*
M. spretus	48	54	54	52
C57BL/6J	61	56	56	58
G value	1.55	0.04	0.04	0.33
(χ^2) P>=	0.21	0.85	0.85	0.57

Table 3.2. Results of the G-test for segregation distortion on mouse chromosomes 4 and 6. The test was performed as described (Sokal and Rohlf, 1981) to determine whether the transmission of C57BL/6J and *M. spretus* alleles deviated from that of the 50:50 ratio expected from Mendelian Loci. On chromosome 4, although the *b* locus and the loci on distal 4 between *Fuca* and *Akp-2* tended to show deviation from the 50:50 expected ratio, the deviation was not statistically significant by chi-square analysis. On chromosome 6, a similar tendency was demonstrated with *Cpa* and with the loci between *Npy* and *Prp*, however it also was not statistically significant by chi-square analysis.

Robertsonian (Rb(4:6)Bnr2) flow-sorting

Isolation of a cell line harboring the 4:6 Robertsonian chromosome

Flow sorting of chromosomes is most easily accomplished when the chromosome of interest is carried in a cell culture line. In order to isolate a cell line harboring a 4.6 Robertsonian chromosome, male and female mice of the Rb (4.6)2Bnr line, which are homozygous for a 4.6 Robertsonian chromosome, were mated. Individual 18-day embryos were harvested from pregnant females, and lung tissue disaggregated with trypsin and plated as described (Todaro and Green, 1963). Since the resulting cell lines grew poorly, individual cell lines were infected with human adenovirus, which is nonlytic for murine cells and has transforming activity, in order to derive a more vigorously growing transformed subline. Transformed cell lines were selected by passage in low calcium media and after four weeks two transformed loci were selected. G-banding of metaphase chromosomes prepared from these two cell lines demonstrated that one of the cell lines, Rb(4.6)Bnr2 (also designated 4:6 1500), was tetraploid and carried four copies of a metacentric chromosome which had a Giemsa banding pattern consistent with that of a 4.6 Robertsonian. The rest of the karyotype appeared normal (Figures 2.2 and 3.7).

Flow sorting of the 4.6 Robertsonian chromosome

Chromosome preparations were made from 20 to 30 T1500 flasks of Rb4:6.1500 cells heated with colchemid. Approximately 2-4 x 10^6 chromosomes were stained with chromomycin A3 and Hoechst 33528 and sorted on a high speed chromosome sorter. The Robertsonian chromosome sorted well ahead of the other mouse chromosomes and it was estimated that this peak was ~80-90% pure (Figure 3.8). DNA was prepared from the sorted chromosomes as described. Approximately 70 ng of high molecular weight DNA was recovered.

Figure 3.7. Partial karyotype of the transformed 4:6 Robertsonian cell line, 4:6 1500, as photographed by fluorescent microscopy. The 4:6 Robertsonian chromosome is substantially larger than the other mouse chromosomes as a result of its fusion of chromosomes 4 and 6 at the centromeres, and is shown by the arrows. It is also the only metacentric chromosome in the field. Giemsa staining of this chromosome was consistent with chromosomes 4 and 6 (Figure 2.2). The metacentric can be physically separated from the remaining acrocentric chromosomes on the basis of its larger size.

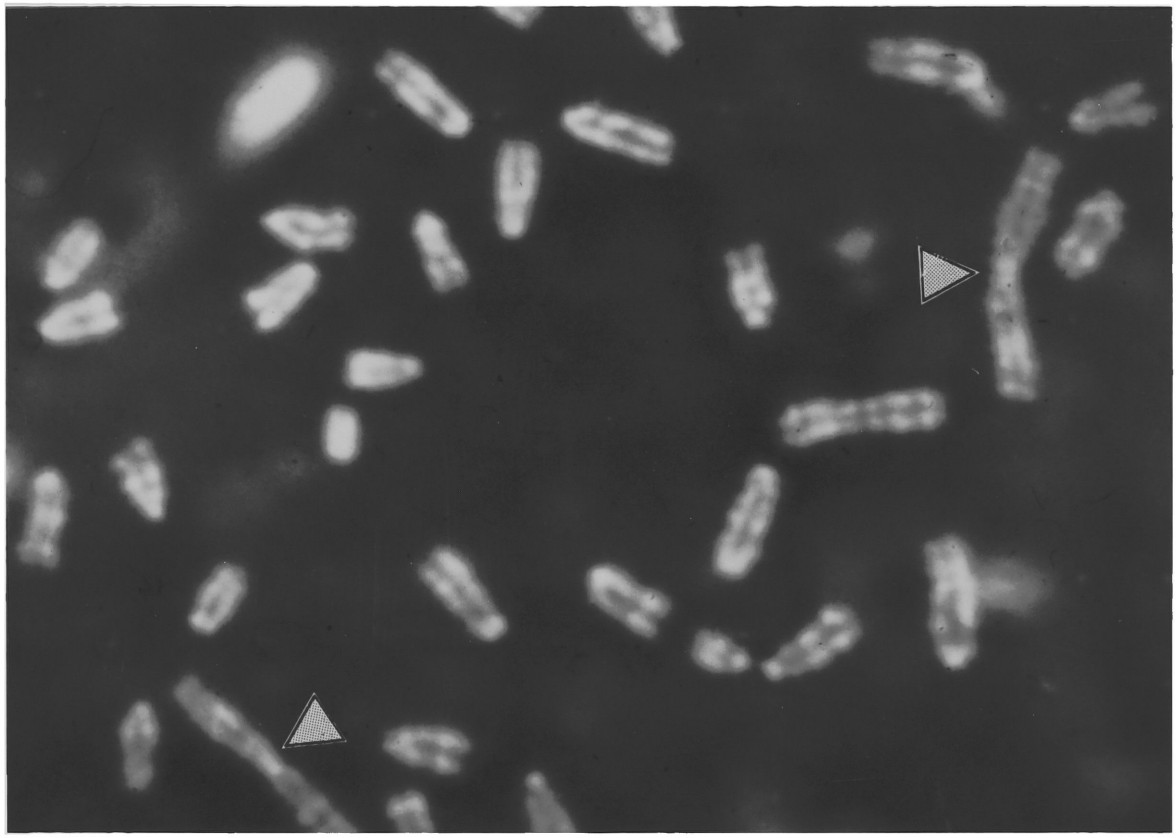

Figure 3.8. Flow sorting of the 4:6 Robertsonian chromosome. Twenty to thirty T-150 tissue culture flasks of 4:6.1500 cells were blocked with .01 μg/ml of colchemid for 12 to 14 hours and mitotic cells were shaken from the surface. Chromosomes from ~10^7 cells were stained with chromomycin A3 (shown on the abscissa) and Hoechst 33258 (shown on the ordinate) and sorted using a high speed chromosome sorter. The intensity of staining with these stains is shown on those axes. The 4:6 Robertsonian chromosome is the high molecular peak which sorts well ahead of the rest of the mouse chromosomes.

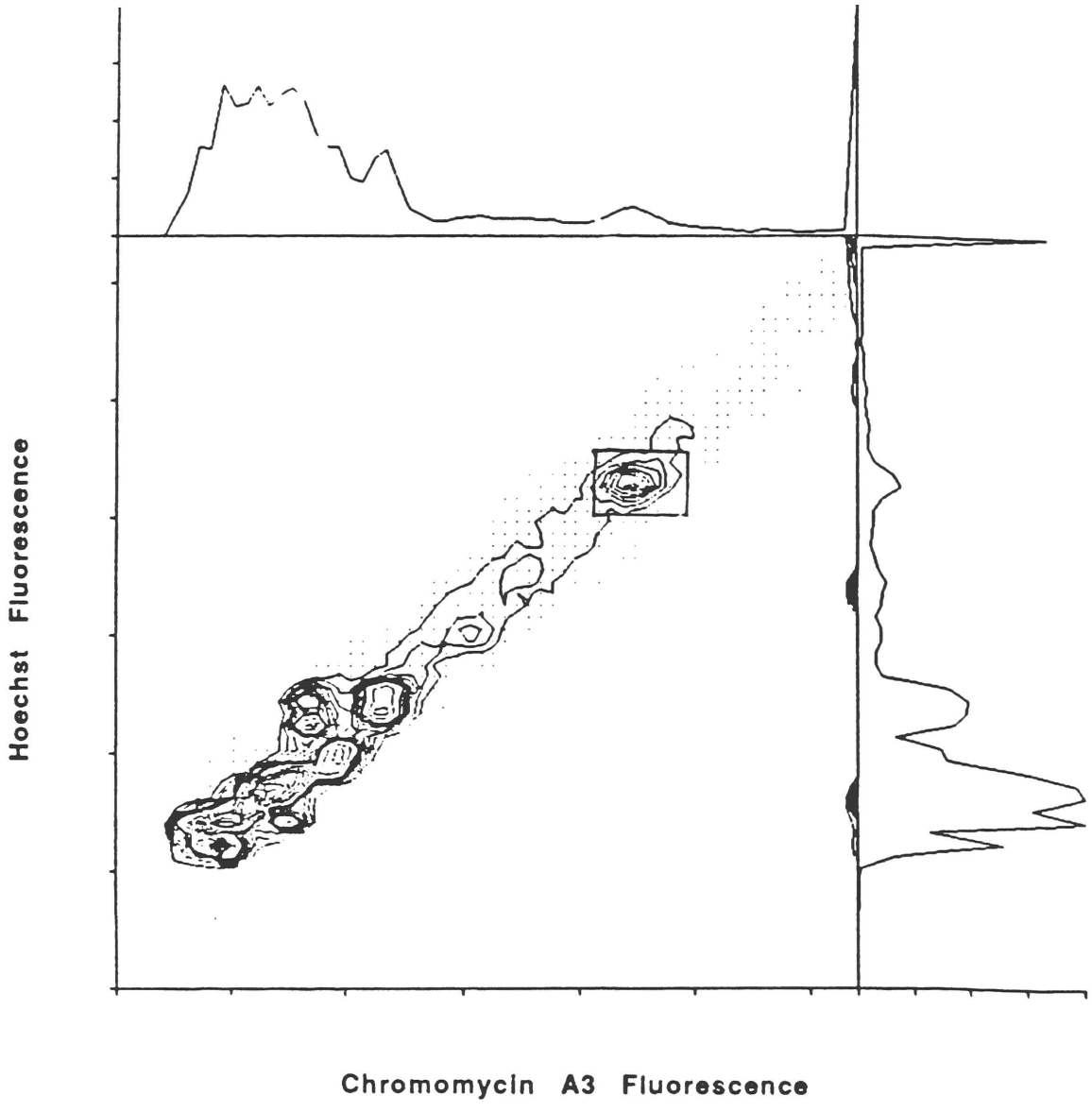
Hoechst Fluorescence
Chromomycin A3 Fluorescence

Library construction and characterization

After a limit digest with EcoRI, the chromosome specific DNA was cloned into λgt10 and plated on the hfl (high frequency of lysogeny) bacterial strain POP101, in which nonrecombinant phage cannot form plaques. A total of 4.6×10^5 individual plaques were recovered. If one assumes that the average EcoRI fragment is ~2500 bp, then the library contains a complexity of 1.15×10^9 base pairs. This corresponds to ~3.5 X coverage of mouse chromosomes 4 and 6 assuming that the 4:6 Robertsonian accounts for ~11% of the ~3×10^9 bp mouse genome. This rough calculation does not consider the possibility that sequences other than those from chromosomes 4 and 6 were cloned, nor does it take into account the fact that EcoRI fragments greater than 7.2 kB cannot be cloned into the λgt10 bacteriophage. Nevertheless, it indicates that a library of sufficient complexity is available for the development of dense genetic maps of these chromosomes.

Genetic mapping of the flow sort clones

Individual phage from the 4.6 flow sort library, or individual EcoRI plasmid subclones, were restriction digested with EcoRI. Southern blots of the restriction digests were probed with total mouse genomic DNA to identify single copy phage clones. The characteristics of the 20 different clones isolated in this fashion are shown in Table 3.3. Each clone was used as a probe on Southern blots to identify polymorphisms between C57BL/6J and *M. spretus*

mice. In all cases the size of the insert matched the size of the EcoRI fragment on the Southern blot of C57BL/6J DNA, indicating that the clone resulted from a single insertion into the vector. Polymorphic probes were subsequently used to type some or all of the 98 progeny of the (C57BL/6J x *M. spretus*) F1 x C57BL/6J backcross (Figure 2.1). After finding a restriction fragment length polymorphism between the two progenitor strains (C57BL/6J and *M. spretus*) for each of the 19 single copy flow sort clones, subsets of the interspecific backcross progeny were scored for their inheritance of the *M. spretus* RFLP for each probe. The resulting strain distribution pattern of each probe (Figures 3.10, and 3.11) was compared to the SDP of the previously typed chromosome 4 and 6 markers (Figure 3.2). Eight of the 19 clones demonstrated linkage to chromosome 6 markers, five to chromosome 4 markers, and six were unlinked to the previously typed chromosome 4 and 6 markers. In order to accelerate the mapping of the flow-sorted probes, probes were mapped on subsets of the backcrossed animals. Once assigned to a defined interval, the mapping effort was extended to include any remaining animals with a demonstrated recombination event in that interval. However, while efforts to extend the pedigree analysis for all of the probes is not complete, in each case a sufficient number of animals were typed to position the locus to a defined interval. The haplotype data used to generate the genetic maps are shown in Figures 3.10, and 3.11) and the position of each of the probes on chromosomes 4 and 6 is shown in Figure 3.12.

In Figures 3.12, the order *Mup-1--Orm-2* is approximately 58 times more likely than the order *Orm-2--Mup-1*, the order *Ifa--Jun* is approximately 1000 times more likely than the order *Jun--Ifa* and the order *Jun--(UROD, D4Rp1, Glut-1)--Lmyc-1--Lck* is 300 times more likely than any other regional order. The five new anonymous markers, *D4Rck128f, D4Rck173f, D4Rck94f, D4Rck723f* and *D4Rck193f* were positioned on this map by minimizing the number of double crossover events between pairs of markers and confirmed by use of the MAPMAKER (Lander, et al., 1987) program. The likelihood of the order of markers presented in comparison to any other order of markers was unchanged by the addition of the four new anonymous markers.

On chromosome 6, the previously mapped genes were positioned by minimizing the number of double crossovers between pairs of markers and confirmed by use of the MAPMAKER program. Allowing the order of *Cola-2* and *NKNA* to remain undetermined because no recombinations between them were noted, the order of *(Cola-2, NKNA)--Met* is 30 times more likely than the reversed order, and the map presented is >100,000 times more likely than any other order allowing the order of *(Cola-2, NKNA)--Met* to be determined. Sufficient numbers of progeny were typed for the *D6Rck132f* (previously designated *D6Rck132, D6Rck179f, D6Rck68f,* and *D6Rck31f* loci to allow the calculation of distances between these loci and the anchor loci (Figure 3.12). However, the loci *D6Rck30f, D6Rck21f* and *D6Rck133f* could

only be assigned to a specific interval because not all the recombinants between the marker and its neighbor were typed.

While many of the clones mapped to the distal ends of chromosomes 4 and 6, several also mapped proximally. Because of the limited number of clones that have been mapped, it is unclear whether the clustering of the typed markers along these two chromosomes is statistically significant.

Microsatellite sequences in the library

The above data suggested that ~70% of the phage inserts mapped to either chromosome 4 or 6. In order to rapidly assign additional probes to either of these chromosomes we made use of a limited somatic cell hybrid panel of seven cell lines that permitted the unambiguous assignment of probes to either of these chromosomes. The characteristics of each of these cell lines is shown in Table 3.4 and Southern blots representative of probes mapping to either chromosome 4 or 6 are shown in Figure 3.9 (Ruddle, et al., 1978; Fournier and Ruddle, 1977; Goff, et al., 1982). All of the probes described above, which had been genetically mapped to either chromosome 4 or 6, gave the expected hybridization pattern on Southern blots of the somatic cell hybrids (data not shown).

Twenty-four additional clones were isolated and used to probe Southern blots of the somatic cell hybrid DNAs. These clones were selected by first probing λgt10 plaque lifts with a ^{32}P labelled poly GT oligonucleotide.

These dinucleotide repeat containing inserts were purified from phage carrying microsatellite sequences, labelled and used to probe Southern blots of the hybrid DNAs after preannealing with mouse DNA to suppress hybridization to repetitive DNA. Of the 24 clones characterized in this fashion, 11 were assigned to chromosome 6 and nine were assigned to chromosome 4.

Since these phage were selected for the presence of microsatellite sequences, this approach should allow the rapid development of a dense genetic map of these chromosomes using PCR-based polymorphisms. The microsatellites were sequenced as subcloned Sau3A restriction digested purified inserts ligated into the BamHI site of M13 phage. Plaque lifts of the M13 subclones were screened with a ^{32}P labelled $(GT)_{20}$ oligonucleotide and the phage harboring a GT dinucleotide repeat were isolated and sequenced. Primers were then made spanning the simple sequence repeat and used to type the progeny of this cross. The first clone characterized in this fashion, D4Rck2f mapped to proximal 4. The haplotype data and map position of this locus are included in Figures 3.10 and 3.12. Cornall et al. (Cornall, et al., 1991) have taken a similar approach using this library and have found that 8 out of 13 clones characterized mapped to either chromosome 4 or 6. If all the data are totalled, 42 out of 57 independent probes (~74%) from the library mapped to one of these two chromosomes. Since ~11% of the probes would map to

these chromosomes by chance this corresponds to a ~6-fold enrichment for sequences from these chromosomes.

Clone	Enzyme	C57BL/6J approximate allele size (kb)	*M. spretus* approximate allele size (kb)	Insert Size (kb)
D4Rck94f	BamHI	3 kb	1.5 kb	1.5 kb
D4Rck128f	PstI	>6	5, >6	0.5
D4Rck173f	TaqI	~8	>8	0.8
D4Rck193f	EcoRI	2	2.5	0.5
D4Rck723f	BglII	1.3	1.7	0.9
D6Rck21f	TaqI	1.4	2	1.6
D6Rck30f	EcoRI	1.5	>6	1.5
D6Rck31f	TaqI	2	>5	0.7
D6Rck68f	BamHI	7	1.5	2.2
D6Rck132f	BglII	6	6.5	1.7
D6Rck133f	BglII	3	4	1.6
D6Rck136f	RsaI	0.5,0.6,0.8,0.9	0.5, 0.7, 0.8	3
D6Rck179f	TaqI	>8	7	1.5

Table 3.3. Characteristics of the genetically mapped chromosome 4 and chromosome 6 markers, derived from the cloning of the flow-sorted Robertsonian 4:6 hybrid cell line DNA. The size of the clone, the restriction endonuclease enzyme used to define the RFLP, and the size(s) of the informative allele(s) are provided.

Chromosome number	BEM1-4	2A2-B1	2A2-C2	2A2-H3	Ecm-4c
1	0.72	0.80	0.50	0.65	–
2	0.83	1.10	0.60	0.00	–
3	0.88	0.75	0.45	0.75	–
4	0.03	0.35	0.10	0.15	–
5	0.20	0.00	0.00	0.00	–
6	0.67	0.60	0.00	0.80	–
7	0.00	0.45	0.55	0.85	–
8	0.32	0.60	0.40	0.90	–
9	0.00	0.80	0.85	0.90	–
10	0.00	0.70	0.50	0.75	–
11	0.00	0.00	0.00	0.00	–
12	1.03	1.00	0.90	1.40	–
13	0.63	0.00	0.45	0.75	–
14	0.83	1.30	0.00	1.15	1.00
15	0.82	0.65	0.35	1.30	1.00
16	0.95	0.45	0.65	0.55	–
17	0.67	0.50	0.85	1.05	–
18	0.78	0.00	0.00	0.60	–
19	0.67	0.00	0.50	0.95	–
X	0.87	0.35	0.60	0.70	–

Table 3.4. Chromosome content of somatic cell hybrids. The percentage of the cells which carry a particular chromosome are shown for each cell line.

Figure 3.9. Southern blots of somatic cell hybrids. In order to assess the utility of a limited somatic cell hybrid panel for identifying genes from mouse chromosomes 4 and 6, DNA from each cell line was restriction digested with EcoRI and Southern blotted. The cell lines utilized are characterized in Table 3.4.

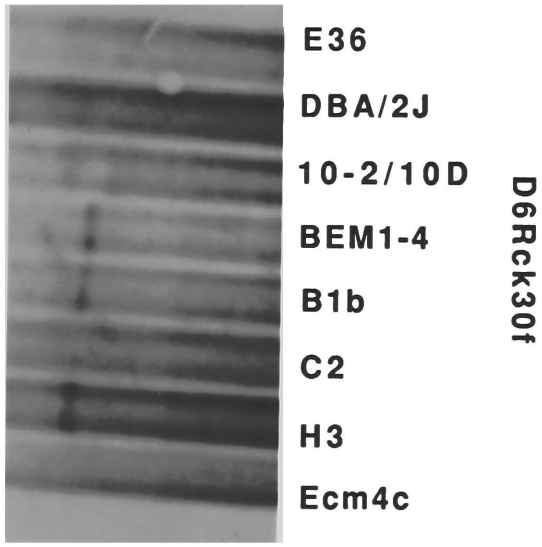
E36
DBA/2J
10-2/10D
BEM1-4
B1b
C2
H3
Ecm4c
D6Rck30f

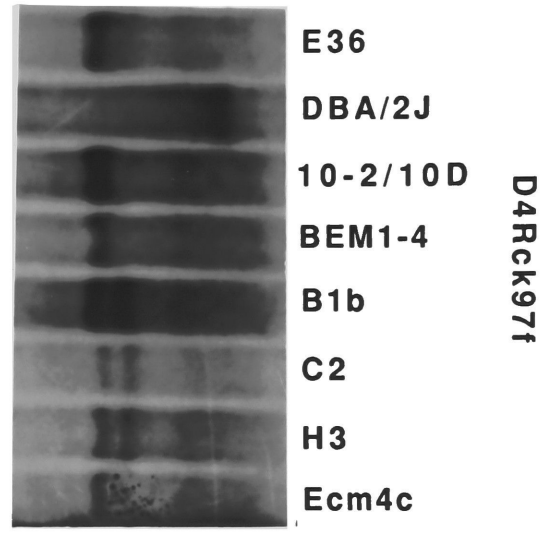
E36
DBA/2J
10-2/10D
BEM1-4
B1b
C2
H3
Ecm4c
D4Rck97f

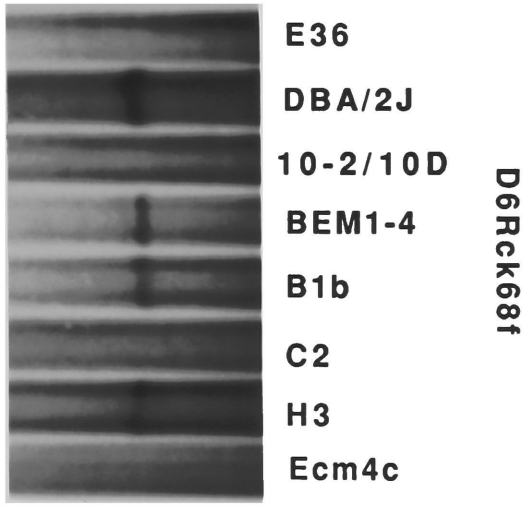
E36
DBA/2J
10-2/10D
BEM1-4
B1b
C2
H3
Ecm4c
D6Rck68f

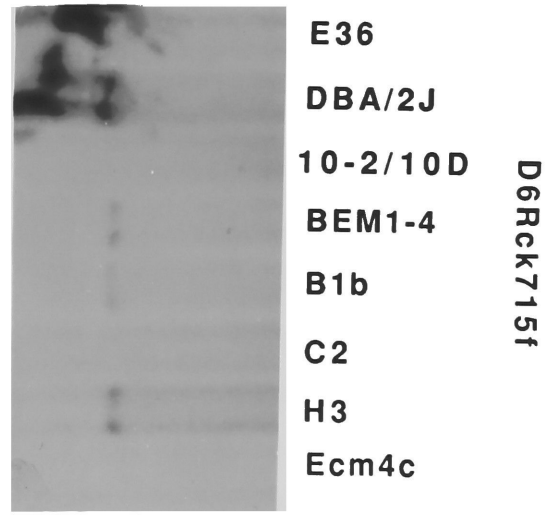
E36
DBA/2J
10-2/10D
BEM1-4
B1b
C2
H3
Ecm4c
D6Rck715f

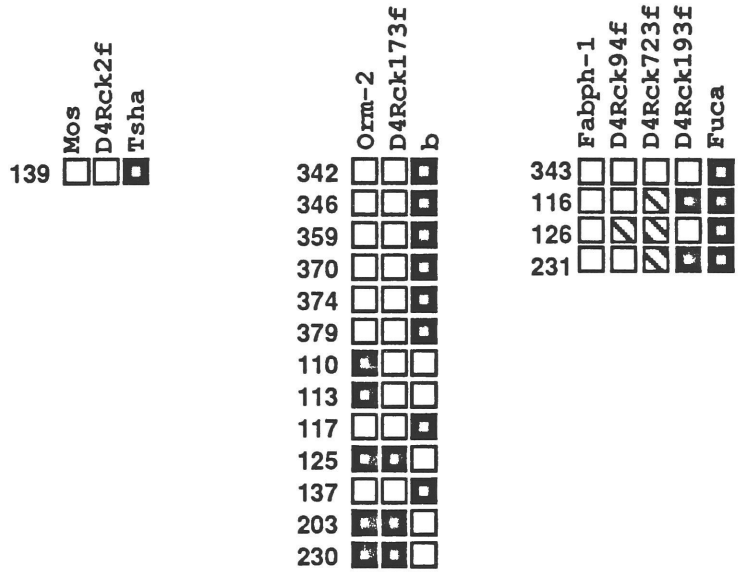

Figure 3.10. Pedigree analysis of subsets of the (C57BL/6J x *M. spretus*) F1 X C57BL/6J (N2) offspring for the chromosome 4 flow-sorted probes with a recombination event between itself and neighboring chromosome 4 loci. Each row represents an N2 progeny whose typing of RFLPs for each locus gave the pattern of C57BL/6J and *M. spretus* alleles shown, while the mapped loci are listed on the top. The blackened boxes represent the *M. spretus* allele, the white boxes represent the C57BL/6J allele, and the diagonally striped boxes represent instances for which data are not available. A total of 87 offspring were typed for their inheritance of the *M. spretus* RFLP for *D4Rck173f* and *D4Rck193f*, 63 progeny for *D4Rck94f*, and 22 progeny for *D4Rck723f*.

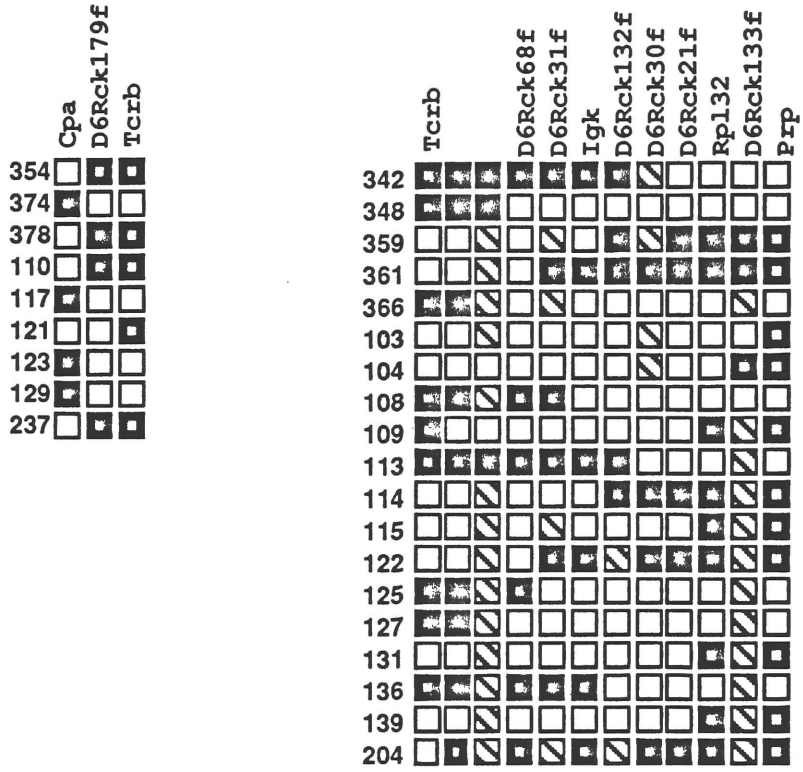

Figure 3.11. Pedigree analysis of subsets of the (C57BL/6J x *M. spretus*) F1 X C57BL/6J (N2) offspring for the chromosome 6 flow-sorted probes with a recombination between itself and neighboring chromosome 6 loci. Each row represents an N2 progeny whose typing of RFLPs for each locus gave the pattern of C57BL/6J and *M. spretus* alleles shown, while the mapped loci are listed on the top. The blackened boxes represent the *M. spretus* allele, the white boxes represent the C57BL/6J allele, and the diagonally striped boxes represent instances for which data are not available. In the *Npy – Igk* interval, the seven previously described potential recombinants between these two loci (Figure 3.5) were scored for *D6Rck68f* and *D4Rk31f*, while only 16 total offspring were typed for *D4Rck136f*. *D6Rck30f* and *D6Rck21f* were not typed for all the recombinants described in the *D6Rck132f – Rpl32* interval, nor was *D6Rck133f* for all the recombinants in the *Rpl32 – Prp* interval.

Figure 3.12. Genetic maps of the chromosome 4 and chromosome 6 flow-sorted 4:6 clones (left and right respectively). The five new anonymous markers, *D4Rck128f, D4Rck173f, D4Rck94f, D4Rck723f* and *D4Rck193f* were positioned on the chromosome 4 map (Figure 3.3) by minimizing the number of double crossover events between pairs of markers and confirmed by use of the MAPMAKER program. The likelihood of the order of markers presented in comparison to any other order of markers was unchanged by the addition of the four new anonymous markers. On chromosome 6, sufficient numbers of progeny were typed for the *D6Rck179f, D6Rck68f,* and *D6Rck31f* loci to allow the calculation of distances between these loci and the previously reported neighboring loci by use of the MAPMAKER program. However, the loci *D6Rck30f, D6Rck21f* and *D6Rck133f* could only be assigned to a specific interval because not all the recombinants between the marker and its neighbor were typed. No information as to the placement of the centromere or telomere is intended.

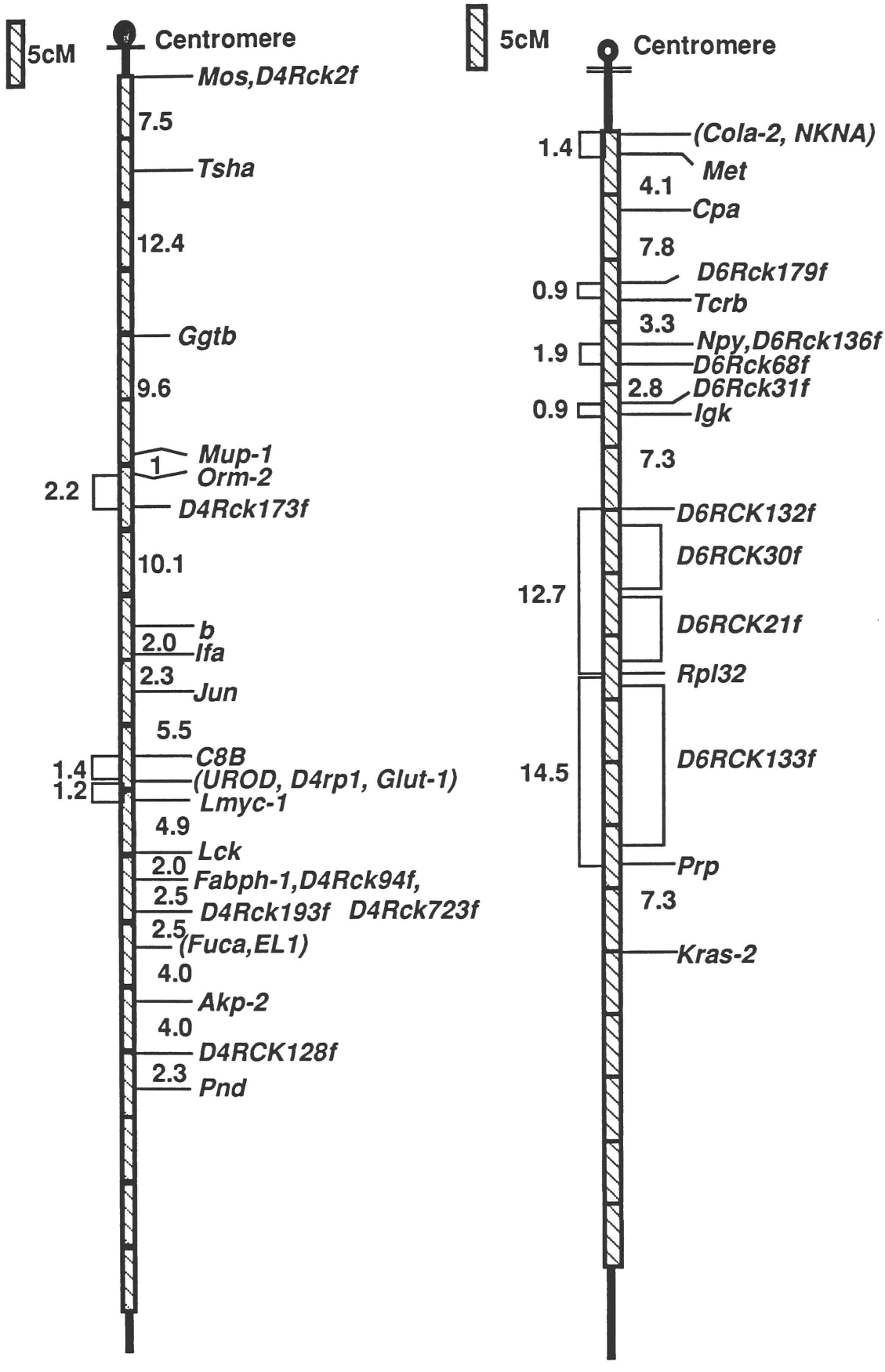
5cM
Centromere
Mos,D4Rck2f
7.5
Tsha
12.4
Ggtb
9.6
1
Mup-1
Orm-2
2.2
D4Rck173f
10.1
b
2.0
Ifa
2.3
Jun
5.5
C8B
1.4
(UROD, D4rp1, Glut-1)
1.2
Lmyc-1
4.9
Lck
2.0
Fabph-1,D4Rck94f,
2.5
D4Rck193f D4Rck723f
2.5
(Fuca,EL1)
4.0
Akp-2
4.0
D4RCK128f
2.3
Pnd
5cM
Centromere
1.4
(Cola-2, NKNA)
Met
4.1
Cpa
7.8
D6Rck179f
0.9
Tcrb
3.3
Npy,D6Rck136f
1.9
D6Rck68f
2.8
D6Rck31f
0.9
Igk
7.3
D6RCK132f
D6RCK30f
12.7
D6RCK21f
Rpl32
D6RCK133f
14.5
Prp
7.3
Kras-2

Intraspecific, Interspecific, and Intersubspecific Mouse Crosses

Phenotypic Characterization of the (C57BL/6J *db/db* x DBA/2J) F1 x C57BL/6J *db/db* (N2) animals.

The progeny of the intraspecific backcross between C57BL/6J *db/db* female ovarian transplants and DBA/2J males (Figure 2.3) are referred to as N2 animals. The offspring of the interspecific intercross (Figure 2.5) between B6D2 F1 *db/+* males X B6*spretus* F1 *db/+* females are referred to as 'F2 - db*spretus*' animals. Mapping of loci relative to *db* requires both the assignment of genotype at the *db* locus and typing the animal for the inheritance of a particular RFLP. Generally, the phenotypic differentiation between *db/db* and *db/+* in the N2 cross, and *db/db* and *db*(or +)/+ in the 'F2 - db*spretus*' cross was obvious on physical inspection of the animal (Figure 3.13). Nevertheless, to ensure the unambiguous assignment of *db* genotype, body weight, BMI [body mass index = weight/(nose-to-anus length)^2], plasma [glucose] and plasma [insulin] were measured in each animal. Of these four parameters, only BMI produced a clear separation of the animals into two distinct groups with values which generally were either greater than 0.450 or less than 0.400 gm/cm^2 (Figure 3.14). The lean N2 animals had a mean BMI of .320 with a SD of .037 (n=76). N2 animals with a BMI > 0.450 were tentatively designated as *db/db*, while those N2 animals with a BMI < 0.400 were considered to be *db/+*. Plasma from the N2 animals was assayed for

[glucose] and [insulin]. The mean [glucose] of the lean animals was 241 mg/dl ± 78 SD (n=76) and the mean [insulin] was 102.1 μu/ml ± 65.1 SD (n=76). All N2 animals with a BMI > 0.450 had either a plasma [glucose] or [insulin] which was more than three standard deviations above the mean of their lean littermates, thus confirming their classification as genotypically *db/db*. For the 58 *db/db* N2 animals, the mean BMI = .582, mean [glucose] = 488 mg/dl and [insulin] = 717.4 μu/ml The *db* genotype of three animals with BMIs between .400 and .450 were assigned on the basis of their plasma [glucose] and [insulin].

Figure 3.13. Photograph of *db/db* and *db/+* animals; 5 month old male littermates derived from the backcross. The animal on the left is *db/+* and weighed 26.7 grams. The animal on the right is *db/db* and weighed 83.7 grams.

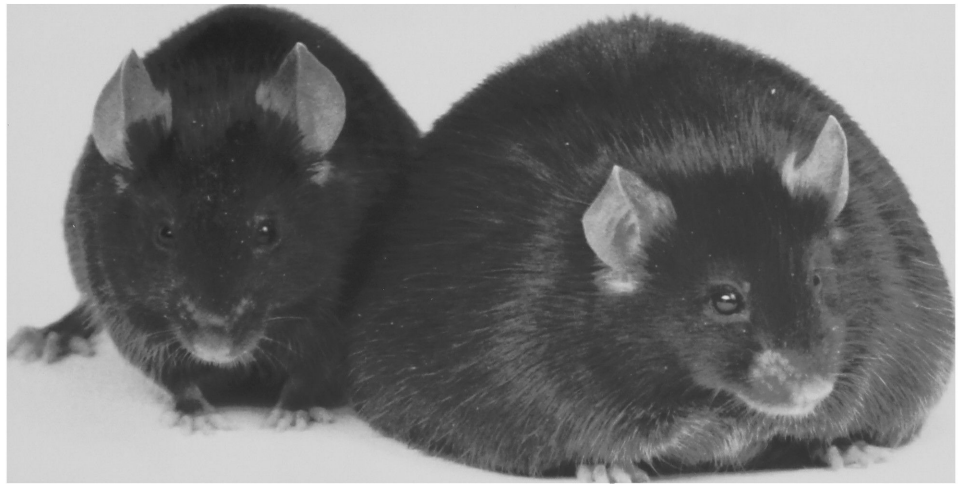

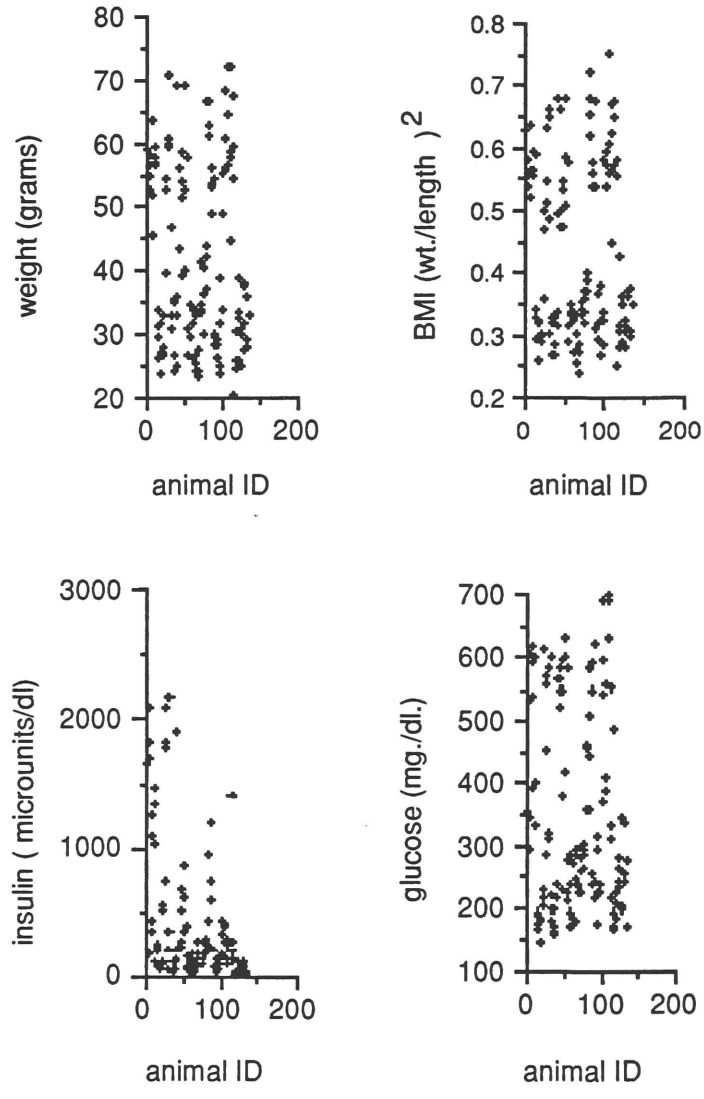

Figure 3.14. Analysis of individual N2 animals by [insulin], [glucose], weight and BMI (wt. in grams/length in cm.^{2}). The BMI is comparable to the body mass index in man, and is used as an indirect measurement of adiposity. Of the parameters tested, the BMI was the only one which clearly separated the animals into two distinct groups.

Of concern in these experiments was the possibility that some of the *db/db* N2 animals might become overtly diabetic, lose weight, and thus be mistakenly classified by BMI (<0.400) as *db/+*. To identify such examples of incomplete phenotypic penetrance of body weight (hence, BMI) amongst the N2 *db/db* animals, the concentrations of glucose and insulin among all the low BMI (<0.400) N2 animals were examined to identify N2 *db/db* animals whose overt diabetes might have resulted in weight loss and misassignment as *db/+*. In fact, two "low BMI" N2 animals had plasma [glucose] more than three standard deviations above the mean of the "low BMI" group (i.e. plasma [glucose] ≥ 475 mg/dl). These two "low BMI" animals had high concentrations of plasma glucose and relatively low concentrations of plasma insulin: animal #123 whose [glucose] was 613 mg/dl and whose [insulin] was 119.8 μu/ml; and animal #191 which had a [glucose] of 623 mg/dl and an [insulin] of 213.4 μu/ml (Figure 3.15). Of note, the haplotype at all loci linked to *db* was homozygous C57BL/6J in both these animals (see below). Thus, these two animals probably represent examples of incomplete penetrance of the *db* mutation with regard to body weight. These animals were not included in the mapping panel. Of all the animals characterized using this protocol, only one animal was doubly recombinant for *db* and other linked loci on chromosome 4, supporting the notion that the N2 animals were correctly genotyped as *db/db* or *db/+* (see below).

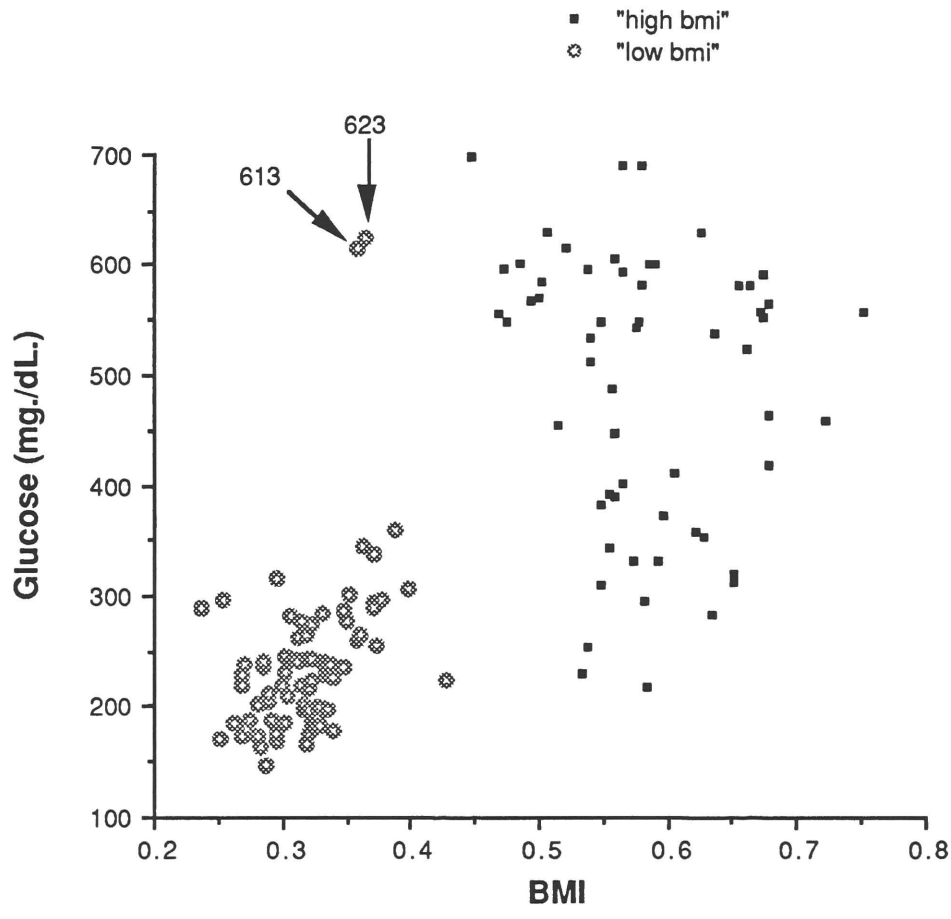

Figure 3.15. Plot of glucose concentration vs. BMI, with separation of the N2 animals into 'high' and 'low' BMI groups.

As a result of these analyses of the N2 progeny, 74 animals were designated *db/+* (36 females and 38 males), and 58 were designated *db/db* (41 females and 17 males). The number of *db/db* N2 males is clearly less than expected (chi-square $p < 0.001$), while there was no statistical difference between the number of males and females in the interspecific intercross described below (chi-square $p > 0.5$). The number of N2 males, according to

our weekly census, did not change substantially after weaning suggesting that the less than expected number of *db/db* N2 males was likely the result of death before 4 weeks of age.

RFLP mapping in the Intraspecific (C57BL/6J *db/db* x DBA/2J) F1 x C57BL/6J *db/db* (N2) cross:

Initially, five genomic probes, known to map to the region of chromosome 4 near *db* by means of the interspecific *M. spretus* backcross mapping (Figure 3.3), were used to type the backcross (N2) progeny for the inheritance of RFLPs between the C57BL/6J and DBA/2J inbred lines. In the case of *Ifa*, $P\lambda Mm3_2$ and *Lck*, a polymorphism was detected with the restriction enzyme BglII. An RFLP for the *Mtv-13* locus detected by the retroviral MMTV probe was scored with EcoRI (Figure 3.16). The brown locus (*b*) was mapped using the the Mt4 probe for which an RFLP between C57BL/6J and DBA/2J animals is detectable using TaqI (Jackson, 1988). The informative DBA/2J alleles for each probe are as follows: *Lck* (3.5 kb, 1.7 kb), *Mtv-13* (9.0 kb), $P\lambda MM3_2$ (6.0 kb), *Ifa* (3.2 kb) and *b* (4.9 kb). The probes were separately hybridized to restriction digests of DNA obtained from both the *db/db* and *db/+* progeny of the *db* backcross, and scored for the presence of the DBA/2J allele. All N2 animals were scored for *b*, $P\lambda Mm3_2$, *Ifa*, and *Lck* (Figure 3.17).

Figure 3.16. C57BL/6J X DBA/2J RFLPs for *Pλ$Mm3_2$*, *Ifa*, *MMTV* (*Mtv-13*) and *Lck*. The letter 'B' denotes the C57BL/6J allele, and 'D' the DBA/2J allele. The arrow(s) point to the polymorphic band(s) used to score the inheritance of the DBA/2J allele, while the enzyme utilized to demonstrate the RFLP is provided below the gene names. The allele sizes were determined by comparison to both the 1kb ladder as well as a HindIII digest of wild-type lambda DNA (Gibco-BRL).

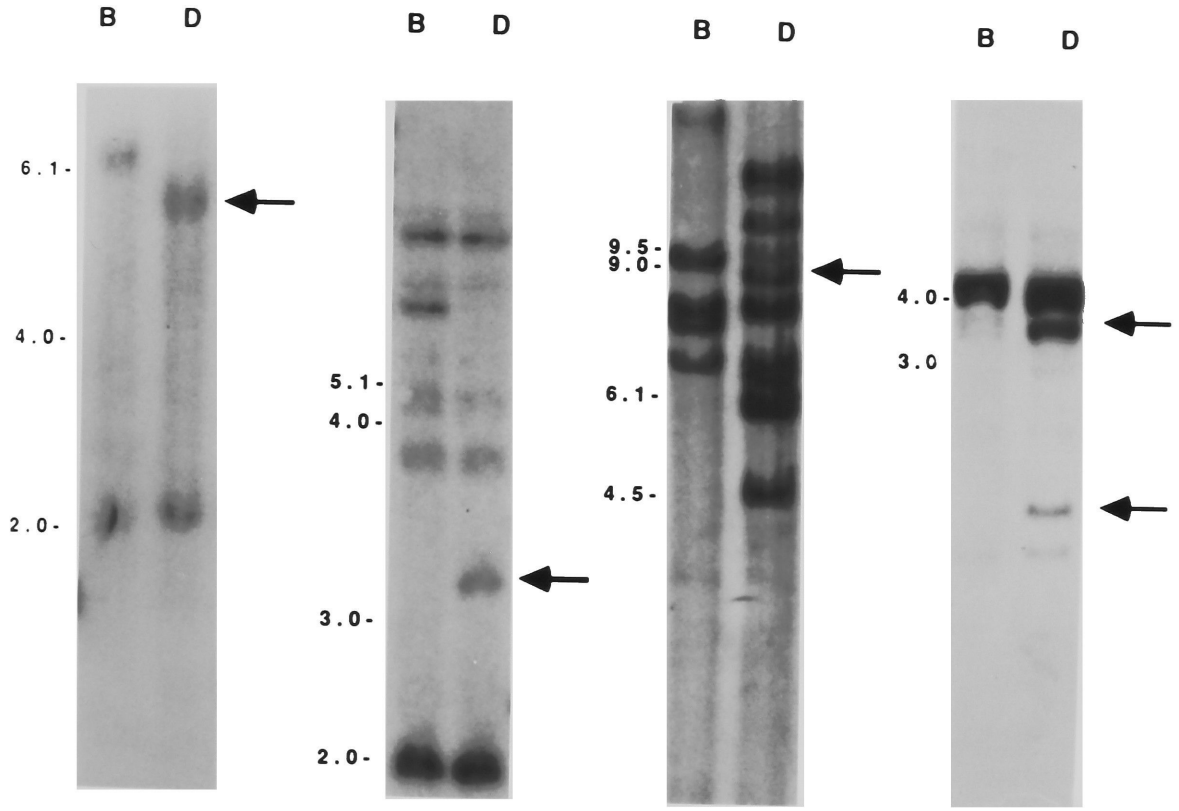
B
D
6.1-
4.0-
2.0-
PλMm3
(Bgl II)
B
D
5.1-
4.0-
3.0-
2.0-
Interferon-α
(Bgl II)
B
D
9.5-
9.0-
6.1-
4.5-
MMTV
(Eco R1)
B
D
4.0-
3.0
LCK
(Bgl II)

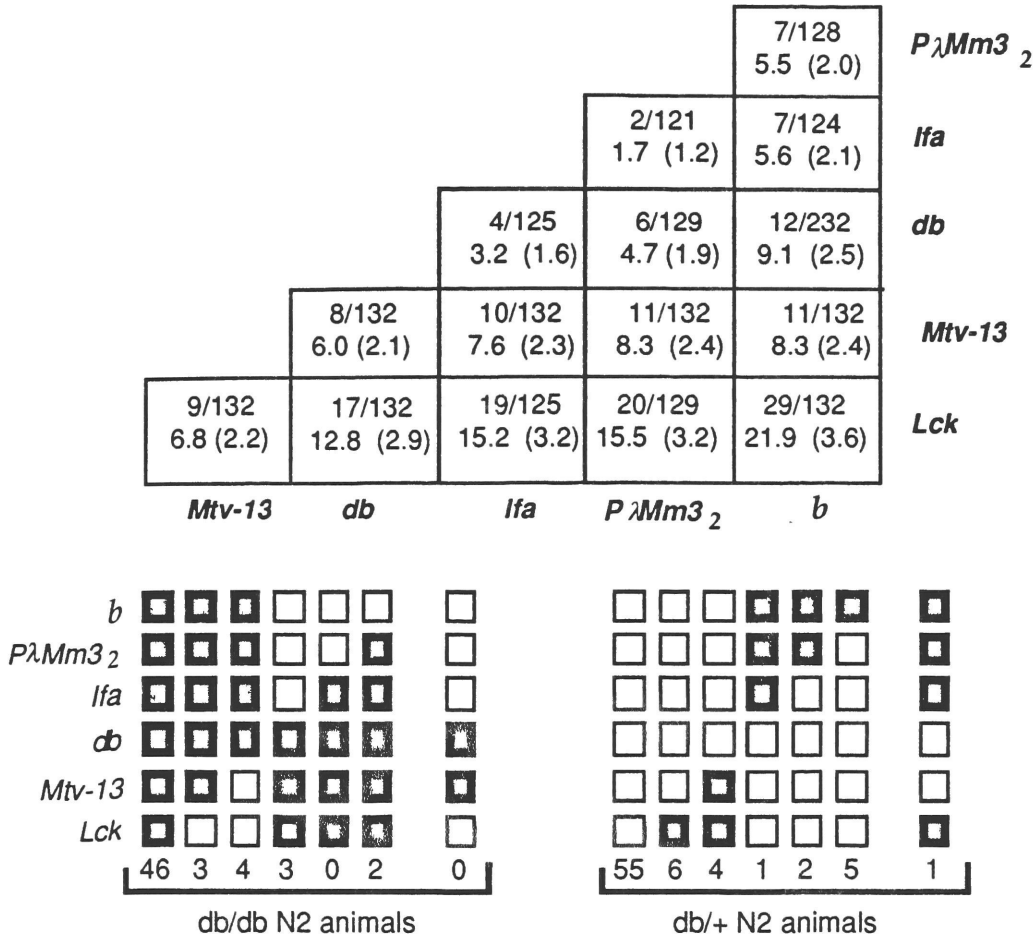

Figure 3.17. Pedigree analysis of the (C57BL/6J *db/db* x DBA/2J) F1 X C57BL/6J *db/db* intraspecific backcross. The approximate map distances in centimorgans (map distance in cM = */100 between probes (+/- S.D) were calculated using the program "Spretus Madness" (Siracusa, et al., 1989). Each of the loci mapped in the crosses is listed on the left of the grid; each column represents a possible configuration of inherited DBA/2J alleles. The number underneath each column is the number of animals that have inherited that particular pattern of alleles. The black boxes represent the C57BL/6J alleles and the open boxes represent the DBA/2J allele.

Phenotypic characterization of the interspecific (C57BL/6J x *M. spretus*)'F2 - dbspretus' animals:

In order to facilitate mapping of probes for which B X D RFLPs were not readily identifiable, an interspecific intercross between C57BL/6J *db/db* and *M. spretus* was developed (Amar, et al., 1985) (Figure 2.5). In this cross, DBA/2J +/+ x C57BL/6J *db/db* F1 males were mated to C57BL/6J *db/db* x *M. spretus* +/+ F1 females, and only obese 'F2 - db*spretus*' animals were scored. Genotype at the *db* locus was tentatively assigned on the basis of BMI, and plasma concentrations of glucose and insulin as described for the N2 cross. For the 85 lean control animals, mean BMI = .319 ±.049 SD; plasma [glucose] = 237 mg/dl ± 93 SD and plasma [insulin] = 28.2 μu/ml ± 33.4 SD. Forty-eight obese-appearing progeny from this cross had a BMI > 0.450, and either a plasma [insulin] or [glucose] that was elevated three standard deviations above the mean of lean 'F2 - db*spretus*' littermates (as defined by BMI, glucose and insulin). For these 48 animals, mean BMI = .577, mean [glucose] = 557 mg/dl and [insulin] = 252.9 μu/ml These 48 progeny were tentatively designated as *db/db* 'F2 - db*spretus*' animals.

One obese 'F2 - db*spretus*' animal rates special attention in this regard. Animal #337, which was originally designated *db/db*, had a BMI of 0.459, and an [insulin] of 199.4 μu/ml This concentration of insulin is elevated more than three standard deviations above the lean 'F2 - db*spretus*' mean of 8.4 ± 10.8 μu/ml Despite these data which suggest that this animal is *db/db*, RFLP

analysis of animal #337 revealed *M. spretus* alleles for all the probes linked to *db* (described previously). Thus, animal #337 is either a wild type animal with an unusually high BMI, or is doubly recombinant between the flanking markers *Jun* and *D4Rp1*. Since the animal carries the *M. spretus* allele at all loci tested, inclusion of this animal in the mapping panel does not affect the order of the loci shown in Figure 3.19 but does slightly alter the relative distances between the loci. Of note, progeny of interspecific crosses do occasionally attain weights of >50 grams (unpublished observation).

RFLP mapping in the interspecific (C57BL/6J x *M. spretus*) intercross:

The 'F2 - db*spretus*' obese mice were typed for the presence of the *M. spretus* allele with the same probes as were used in the intraspecific cross (with the exception of *Mtv-13*) as well as three additional probes: *Jun, Glut–1* and *D4Rp1* (Figure 3.18). *Jun* was scored using PstI; both *D4Rp1* and *Glut–1* were followed using TaqI. In addition, 'F2 - db*spretus*' obese mice were typed for the presence of the DBA/2J alleles for *Ifa* and *Lck*, using the RFLPs described earlier for the typing of the N2 animals.

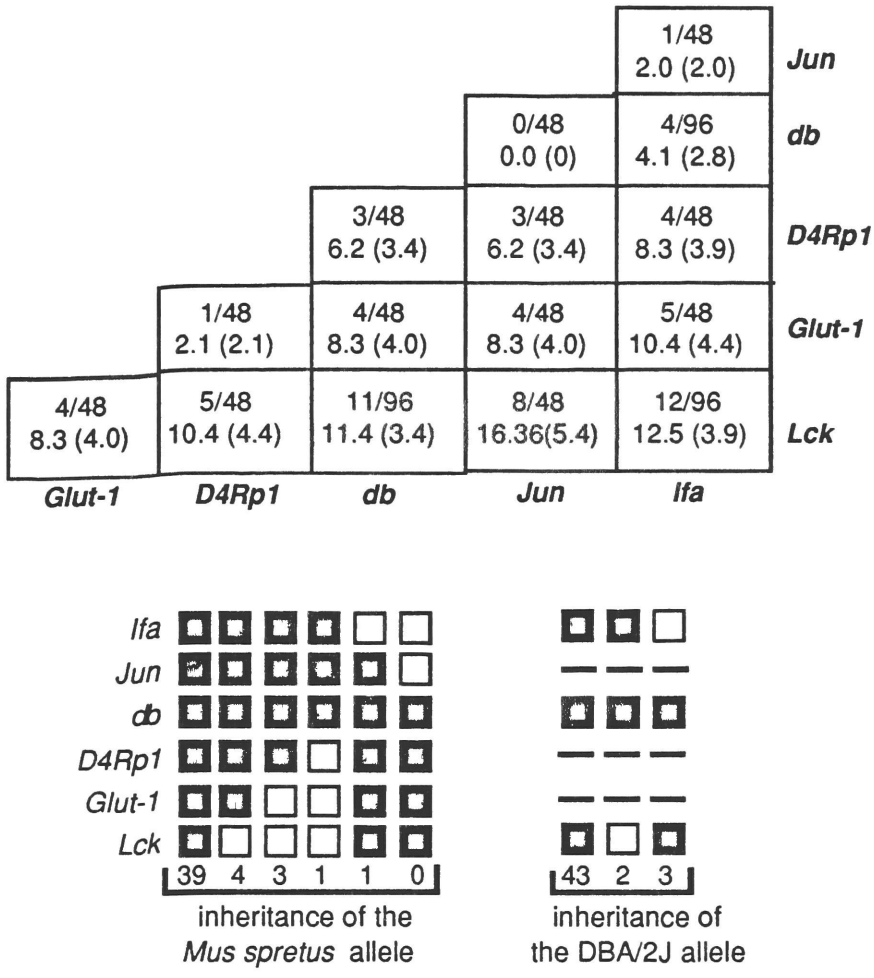

Figure 3.18. Pedigree analysis of the (C57BL/6J *db/db* x DBA/2J +/+) F1 x (C57BL/6J *db/db* x *M. spretus*) F1 interspecific intercross. The approximate map distances in centimorgans (map distance in cM = */100 between probes (+/- S.D) were calculated using the program "Spretus Madness" (Siracusa, et al., 1989). Each of the loci mapped in the crosses is listed on the left of the grid; each column represents a possible configuration of inherited DBA/2J and/or *M. spretus* alleles. The number underneath each column is the number of animals that have inherited that particular pattern of alleles. The black boxes represent the C57BL/6J alleles and the open boxes represent the DBA/2J or *M. spretus* allele.

By counting recombinants, and minimizing double crossovers among the progeny of the intraspecific backcross (Figure 3.17) and the interspecific intercross (Figure 3.18), the genetic map of the region adjacent to the *db* locus was refined (Figure 3.19). The gene order of these loci was: Cen - *b* - *PλMm3*$_2$ - *Ifa* - *Jun* - *db* - *D4Rp1* -*Glut–1*/*Mtv-13* - *Lck*. In Figure 3.19, the location of the loci mapped among progeny of the *intraspecific* cross are shown above the line, while those for the *interspecific* cross are shown below the line. Order was determined between *D4Rp1*, *Ifa* and *Glut–1*. However, definitive order could not be determined between *Mtv-13* and either *Glut–1* or *D4Rp1*, because these probes were not mapped in the same cross. There was only one double crossover across this interval (Figure 3.17), and this order is 10000-fold more likely than any other (allowing the order of *Mtv-13* relative to *Glut–1* and *D4Rp1* to remain undetermined) when the recombination frequencies between all loci are analyzed with the MAPMAKER program (Lander, et al., 1987). Of note, three of the markers which flank *db*: *Jun*, *Glut–1*, and *Lck*, all map to human chromosome 1p31-36 (Davisson, et al., 1988; Nadeau, 1989), suggesting that the human homologue of *db* may reside in this interval.

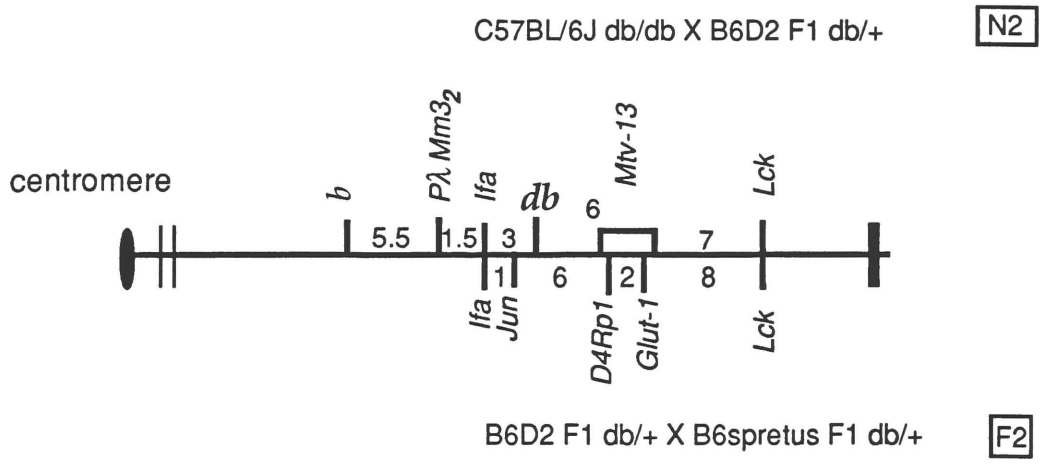

Figure 3.19. Genetic maps of the region surrounding *db* on mouse chromosome 4 using the offspring of the intraspecific N2 and interspecific C57BL/6J X *M. spretus* crosses segregating the *db* mutation. The genetic map shown above the line was derived from the intraspecific N2 backcross animals (see Figure 2.3), the genetic map shown below the line was derived form the interspecific *M. spretus* intercross (see Figure 2.5). For each N2 animal, the genotype at each of the loci typed was analyzed by pedigree analysis to generate a genetic map in the region around *db*. For the F2 animals, the genotype at the *Ifa*, *Jun*, *D4Rp1*, *Glut-1*, and *Lck* loci was determined, and the resulting map aligned to the N2 map at the *Ifa* and *Lck* loci. The actual order of the probes *Mtv-13* and *D4Rp1* — *Glut-1* relative to one another cannot be determined since *Mtv-13* were analyzed in the interspecific (F2) cross, and *Glut-1* and *D4Rp1* were not analyzed on the intraspecific (N2) cross. The loci are shown in their most likely order based upon the pedigree analysis, and this order is 10000-fold more likely than any other (allowing for the order of *Mtv-13* relative to *Glut-1* and *D4Rp1* to remain undetermined) by use of the MAPMAKER program (Lander, et al., 1987). The N2 map is based on 132 meiotic events, the F2 map is based on the 48 *M. spretus* meioses scored for *Jun*, *Glut-1*, and *D4Rp1* and an additional 48 DBA/2J meiotic events (for a total of 96) for the *Ifa* and *Lck* loci.

Phenotypic and RFLP characterization of the intraspecific (C57BL/6J *db/db* X DBA/2J) F1 intercross offspring:

Genotype at the *db* locus was tentatively assigned on the basis of BMI, and plasma concentrations of glucose and insulin as described for the B X D N2 and interspecific C57BL/6J X *M. spretus* crosses. For a total of 151 lean control animals (83 female, 68 male), the mean female [glucose] was 216 ± 51 mg/dl [S. D] and [insulin] was 37.9 ± 54.1, the mean male [glucose] 220 ± 51 mg/dl and [insulin] was 60.30 ± 98.9 μu/μl. Among the 216 obese (124 female, 92 male) offspring, the female progeny had an mean [glucose] of 401 ± 163 mg/dl and a mean [insulin] of 438.5 ± 548 μu/μl, while the male offspring manifested a mean [glucose] of 514 ± 170 mg/dl, and a mean [insulin] of 420 ± 521.7 μu/μl. One male animal, assigned to the obese group on the basis of phenotype (#678), had an insulin (49.72 μu/ml) and glucose (240 mg/ml) consistent with a lean (*db*/+ or +/+) genotype. RFLP analysis of the animal for the flanking markers *Ifa* and *Lck* (see below) manifested DBA/2J alleles at both loci, supporting the hypothesis that it was truly a lean animal. In order to avoid ambiguity, it was not used in the pedigree analysis.

RFLP analysis was carried out using the B X D polymorphisms described for *Ifa* and *Lck* (Figure 3.16) and the results shown in Figure 3.20. A total of 24 recombination events were seen in a total of 192 animals (384 meiosis) scored for the inheritance of the *Ifa* DBA/2J allele (Figure 3.20). The calculated distance of *Ifa* from *db* of 6.3 cM (24/384 X 100) in these F2 animals

is larger than the 3.2 cM calculated in the N2 cross (Figure 3.20). Between *db* and *Lck*, a total of 48 recombination events were noted amongst 182 animals (364 meiosis) scored for the inheritance of the *Lck* DBA/2J allele (Figure 3.20). The calculated distance of 13.4 cM between *db* and *Lck* amongst these F2 animals is close to the 12.8 cM demonstrated between these two loci in the N2 animals (Figure 3.17).

Four of the F2 offspring manifested DBA/2J alleles for both *Ifa* and *Lck*. As was discussed, one of the male progeny (# 678) was probably a lean animal which was mistaken for an obese animal. Offspring #678 had a [glucose] of 240 mg/dl and an [insulin] of 49.72 μu/ml as compared to the means of the lean male control group ([glucose]= 220mg/dl ; [insulin] = 37.9 μu/ml). The difference is not statistically significant, and that animal was not used in any of the analysis. It is unlikely that the remaining three animals with both DBA/2J alleles for both *Ifa* and *Lck*, represent misassignment since their [insulin], [glucose], and BMI's were all consistent with a *db/db* genotype, ([glucose] or [insulin] greater than 3 standard deviations from the mean of the lean control group's). Additionally, since the *Lck* locus is located ~13 cM distal to *db*, and each F2 animal represents two independent meiosis, any animal with a demonstrated recombination event between *Ifa* and *db* would have an ~13% chance of having an additional *db* — *Lck* recombination. Therefore, among the 24 *db* — *Ifa* noted, three (24 X 0.13) would also be

expected to have a *db* — *Lck* recombination, exactly the number that were noted.

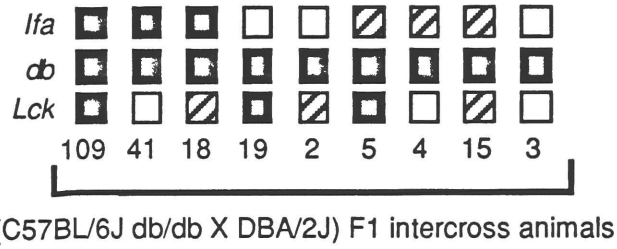

Figure 3.20. Pedigree analysis for the 216 F2 offspring of the (C57BL/6J *db/db* X DBA/2J) F1 intercross. The number below each column of boxes represents the number of animals with that particular set of loci genotypes. The filled box represents inheritance of the C57BL/6J allele, the white box the DBA/2J allele, and the diagonally striped box represents instances for which no data is available.

Phenotypic characterization of the intersubspecific (C57BL/6J x *M. castaneus*) F2 offspring:

Genotype at the *db* locus was tentatively assigned on the basis of BMI, and plasma concentrations of glucose and insulin as described for the B X D N2 and F2 and interspecific *M. laboratorius* X *M. spretus* crosses. A total of 399 F2 offspring, representing 798 meiotic events were analyzed for BMI, [insulin] and [glucose]. Animal numbers 1053, 1244, and 1246 which had BMI's of 0.356, 0.393, and 0.373 respectively, and were recombinant for both *Ifa* and *D4Rck22* (which flank *db*), demonstrated [glucose] and [insulin] which were not significantly different from the lean controls. These animals

probably represent instances in which the incorrect phenotype was assigned by visual inspection. The remaining 396 'obese' appearing animals had a [glucose] and/or [insulin] concentration that was elevated greater than 3 times the mean of the lean control group's and are almost certainly *db/db* animals.

Pedigree analysis of the intersubspecific (C57BL/6J *db/db* x *M. castaneus*) F1 intercrossed offspring:

Genotype at the *Ifa* locus and a microclone locus (*D4Rck22*) described later (see microcloning section), for the offspring of the (C57BL/6J *db/db* x *M. castaneus*) F1 intercross were assigned by use of simple sequence repeats (Figure 3.21). For the *Ifa* locus, oligos of the sequence 1) TCA GTA TGT ACA TCC ATG CC and 2) TAA AAA TGA TAA GTT GTT TTA TGA A were designed which flank a GT repeat in the *Ifa* locus. By screening a digest of a genomic clone containing *D4Rck22* with a $(CA)_{20}$ oligomer, a GT simple sequence repeat was identified, subcloned into bluescript II KS+, and sequenced. Oligos were designed to flank the SSR. To genotype either locus, one of each oligo pair was kinased and then used in a standard PCR assay with tail DNA from each obese mouse as template. A 10 µl total reaction was subjected to 35 cycles of 94° C denaturation for 20 seconds, 53° annealing for 20 seconds, and 20 seconds extension at 72° C in a Perkin-Elmer model 9600 thermocycler. The amplified material was then electrophoresed through a 6% denaturing acrylamide gel, which was dried and then exposed to standard

X-Ray film overnight. The size difference between the C57BL/6J and *M. castaneus* alleles was easily apparent in both cases.

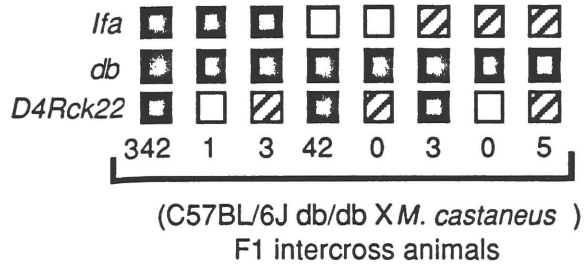

Figure 3.21. Pedigree analysis of the 396 obese F2 offspring of the (C57BL/6J *db/db* X *M. castaneus*) F1 intersubspecific intercross. The number below each column of boxes represents the number of animals with that particular set of loci genotypes. The filled box represents inheritance of the C57BL/6J allele, the white box the *M. castaneus* allele, and the diagonally striped box represents instances for which no data is available.

The *Ifa* — *db* distance of 5.4 cM (42 recombination events / 772 meiosis scored) is quite similar to the 6.3 cM seen among the F2 intraspecific cross progeny (Figure 3.20), although it not unusual that an intraspecific and intersubspecific cross would have differing recombination values between loci. The calculated distance between *db* and *D4Rck22* of 0.13 cM (1/772) is extremely small and within the range (<500 kb) that YAC walking and other physical methods may be employed as a means of cloning the *db* —*D4Rck22* interval.

Inheritance of glucose tolerance: glucose and insulin levels in the (C57BL/6J *db/db* X DBA/2J) F1 X C57BL/6J *db/db* (N2) animals:

Values of plasma [glucose] and [insulin] among the *db/db* N2 animals (Figure 2.3) were examined for possible effects of genetic background — including sex on diabetogenicity, of the *db* mutation. The plasma [glucose] and [insulin] of the *db/db* N2 animals were analyzed in three nonoverlapping age groups,3-4, 4-5, and 5-6 months (Figure 3.22). Analysis of variance by age and sex (Dixon, 1981) demonstrated statistically significant effects of age and sex on [insulin] but not on [glucose] (Figure 3.23). Despite the lower [insulin] in males than females (males often develop a worse diabetic syndrome and earlier pancreatic exhaustion as compared to females (Leiter, et al., 1989)), and the decline of [insulin] with age in both sexes, no age or sex effect on [glucose] was seen. Of note, in all three age groups a wide range of plasma [glucose] and [insulin] was evident; animals with [glucose] varying from nondiabetic to frankly diabetic were apparent with a relatively continuous distribution. Among the *db/db* N2 animals the plasma [glucose] ranged between 218 and 698 mg/dl and the plasma [insulin] ranged between 106.2 and 2160.8 μu/ml. There was no evidence of a bimodal distribution of plasma [glucose] or [insulin] among the *db/db* backcross progeny (Figure 3.14), i.e. numerous animals with intermediate levels of [glucose] and [insulin] were notable.

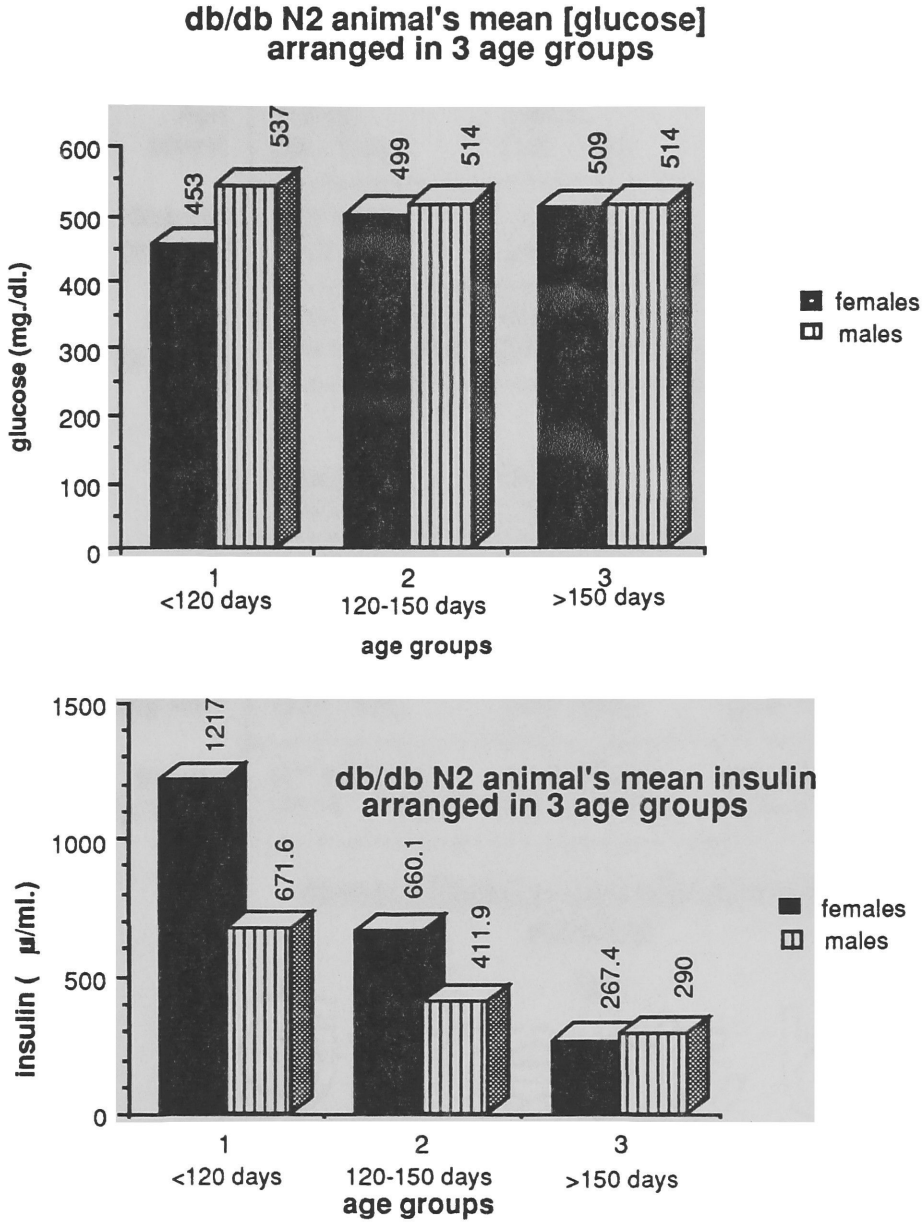

Figure 3.22. Graphic representation of the (C57BL/6J *db/db* x DBA/2J) F1 x C57BL/6J *db/db* intraspecific backcross [glucose] and [insulin] divided into three non-overlapping age groups.

db/db N2 animals arranged in 3 age groups

mean (SEM) [range]

	Group 1 (n=18)	Group 2 (n=12)	Group 3 (n=11)	
Age (days)	107 (2) [86 - 119]	138 (1) [128 - 145]	165 (3) [152 - 176]	N2 Females
Glucose (mg./ml/)	453 (30) [284 - 605]	499 (32) [254 - 629]	508 (40) [312- 698]	
Insulin (μ u/ml.)	1217.0 (165.0) [184.0 - 2160.8]	660.1 (141.9) [233.0 - 1900.0]	267.4 (28.6) [146.4 - 423.4]	

	Group 1 (n=6)	Group 2 (n=4)	Group 3 (n=6)	
Age (days)	103 (5) [91 - 115]	132 (4) [123 - 141]	164(4) [152 - 176]	N2 males
Glucose (mg./ml/)	537(34) [381 - 616]	514(39) [418 - 602]	514 (71) [229 - 691]	
Insulin (μ u/ml.)	671.6 (217.2) [238.4 - 1708.6]	411.9 (158.1) [141.0 - 865.8]	290.4 (65.0)) [106..0-518.4]	

Brown - Forsythe two-way analysis of variance

	Age	Sex	Interaction
glucose	F (2,11) = 0.11; p=0.90	F (1,18) = 1.00; p= 0.33	F (2,21) = 0.56; p=0.58
insulin	F (2,11) = 11.75, p=0.0003	F (1,21) = 9.50; p=0.038	F (2,23) = 2.54; p=0.104

Figure 3.23. Analysis of variance by age and sex (Dixon, 1981) amongst the progeny of the intraspecific backcross segregating *db*. The analysis demonstrates statistically significant effects of age and sex on [insulin] but not on [glucose]

Genotyping and Phenotyping the *fa/fa* Rat Offspring

Identification of *fa/fa* rats (Genotyping at the *fa* locus):

Because the genetically *fa*/+ lean offspring of the (13M/Vc x (BN)/Crl) *fa*/+ intercross cannot be phenotypically distinguished from their +/+ siblings, only the genetically obese (*fa/fa*) rats were to be utilized for the linkage analysis. The obese (*fa/fa*) rat can be visually distinguished from their lean littermates at ~5 weeks of age (Figure 3.24). A total of 172 F2 offspring resulted from the (13M/Vc x (BN)/Crl) *fa*/+ intercross. Eight progeny were not phenotyped due to either early death or missing progenitor data. Of the remaining 164 F2 offspring, 50 appeared obese and 114 appeared lean by visual inspection. Of concern in the experiments was that the phenotype of the *fa/fa* rats on the mixed 13M/BN background might be incompletely penetrant or that some genetically *fa*/+ F2 progeny might mistakenly be considered obese. Since accurate identification of the *fa* genotype is essential for the mapping of the locus, the animals were genotyped by an index of body fatness, the inguinal adiposity index. The adiposity index is calculated as (inguinal adipose tissue weight/body weight) X 100. This index divides the rats into two clear non-overlapping groups (Figure 3.25). The adiposity index values (mean ± SEM) were 0.71 (±0.02) for the visual 'lean' (*fa*/+ or +/+) rats, and 4.44 (±0.11) for the visual obese (*fa/fa*) rats. The statistical difference between these means is highly significant ($t=32.1$; $P < 10^{-6}$). By this criterion, the

genotype of the obese appearing rats was confirmed. The frequency of obese individuals in the population (50/164 = 0.328) was not significantly different from the value of 0.25 that would be expected from a fully penetrant autosomally recessively inherited gene ($\chi^2 = 2.63$; $P > .10$).

Figure 3.24. Photo of an 88 day old *fa/fa* rat compared with its lean littermate. A) Obese animal on the left is significantly more obese than its lean littermate. B) Dissection of inguinal fat pads demonstrates significantly more deposition in the obese animal on the right as compared to its lean littermate on the left.

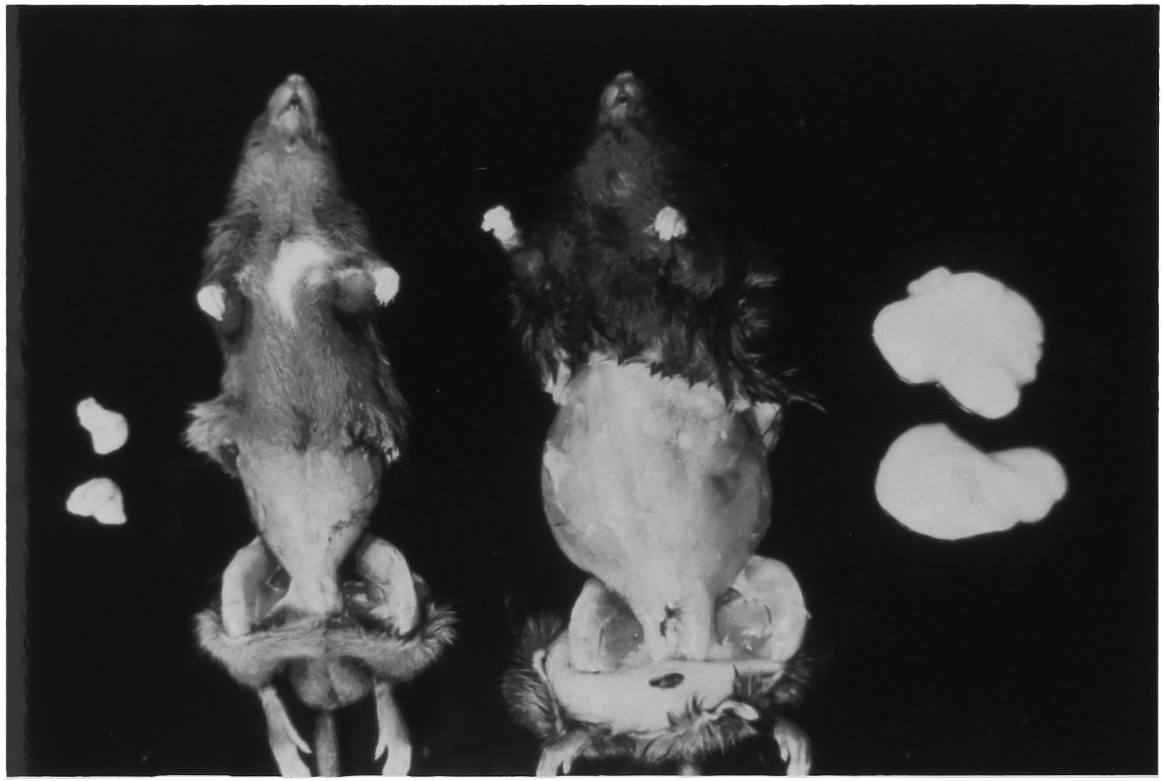

Figure 3.25. Scatter plot of the adiposity indices of 13M/BN F_2 rats segregating *fa*. The adiposity index was calculated as (inguinal adipose tissue weight/body weight) X 100. A total of 164 values are plotted; 50 in the upper cluster, designating obese (*fa*/*fa*) rats, and 114 in the lower cluster, designating lean (*fa*/+ or +/+) rats. Note the complete separation of the two clusters; the lowest adiposity index among the obese rats is >8 standard deviations from the mean of the lean rats.

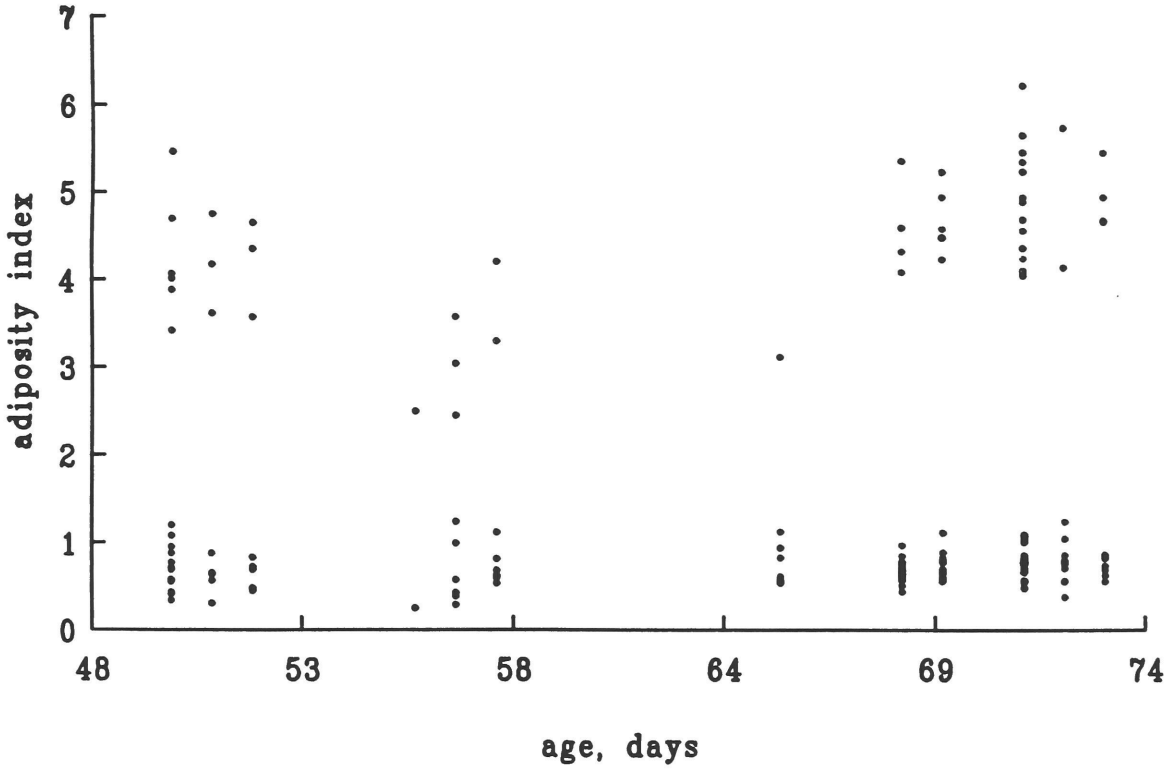
adiposity index
0
1
2
3
4
5
6
7
48
53
58
64
69
74
age, days

Genotyping of the *fa/fa* rats with *Ifa* and *Glut-1*:

The 50 13M/BN F2 *fa/fa* rats were haplotyped for 13M and BN alleles at the *Ifa* locus by RFLP analysis and at the *Glut-1* locus by use of a simple sequence repeat (SSR). The *Ifa* gene probe previously described (Table 2.1) was random-primed radiolabeled with α-^{32}P-dCTP, and hybridized to RsaI digested F2 progeny DNAs that were Southern blotted to Gene-Screen*Plus* membranes. As shown in figure 3.26, 27, an RsaI 13M X BN RFLP is clearly distinguishable.

The 13M/BN F2 *fa/fa* rats were scored for the inheritance of the BN *Glut-1* allele by use of a difference in the dinucleotide repeat number of a $(CA)_x$ repeat in Intron H of *Glut-1* (Williams and Birnbaum, 1988). Oligonucleotides of the sequence 5'-GAA TGA AGC TAA GAA TTG ACC TTA GGT and 5'-GTC CAT GCC TGT CCT TTT AGT GCT CTT G were used to amplify the intervening dinucleotide repeat using 30 cycles of the PCR at an annealing temperature of 50°C for 1 minute. The products were electrophoresed in 6% NuSieve 3:1 and stained and photographed as usual.

In the 100 meiosis, representing the 50 obese (*fa/fa*) F2 offspring, 6 BN alleles were observed in RFLP analysis of the *Ifa* locus, 7 BN alleles were seen for *Glut-1*, and 13 recombination events were noted between *Ifa* and *Glut-1* (Figure 3.26). No individual inherited more than a single BN allele at these loci. By minimizing the number of double crossovers the order of the loci was determined to be *Ifa—fa—Glut-1*. Confirmation of this order by the

MAPMAKER program demonstrated that this order was $>10^5$ times more likely than the two alternate gene orders.

Paired loci	Recombination fraction	Map distance (cM)
Ifa — fa	6/100	6.4 ± 2.4
fa — Glut-1	7/100	7.5 ± 2.7
Ifa — Glut-1	13/100	15.1 ± 3.6

Figure 3.26. Linkage data for the the three loci (*Ifa, fa, Glut-1*) mapped in the 50 13M/BN F_2 rats. The map distance in centimorgans (cM) is the (number of observed recombinations between loci/total number of meiosis scored) X 100. The observed recombination fractions all differed from non-linkage (50 recombinations/100 meiosis scored) at $P<0.00001$ by the χ^2 test. The expressed map distances were adjusted by the Haldane function (Haldane, 1919) to correct for undetected mutiple crossovers.

Figure 3.27. DNA polymorphisms at the *Ifa* and *Glut–1* loci linked to *fa*. (A) An RsaI restriction fragment length polymorphism for *Ifa*. Parental alleles (13M and BN) are shown in the first and last lanes. Arrows designate the bands chosen to define the parental alleles. The middle lane illustrates the combined restriction fragment length polymorphism found in the F_1 generation. (B) An amplified simple sequence (dinucleotide) repeat polymorphism for *Glut-1*. Parental alleles are shown in the outside lanes. The heterozygous genotype of the F_1 rats is shown in the middle lane.

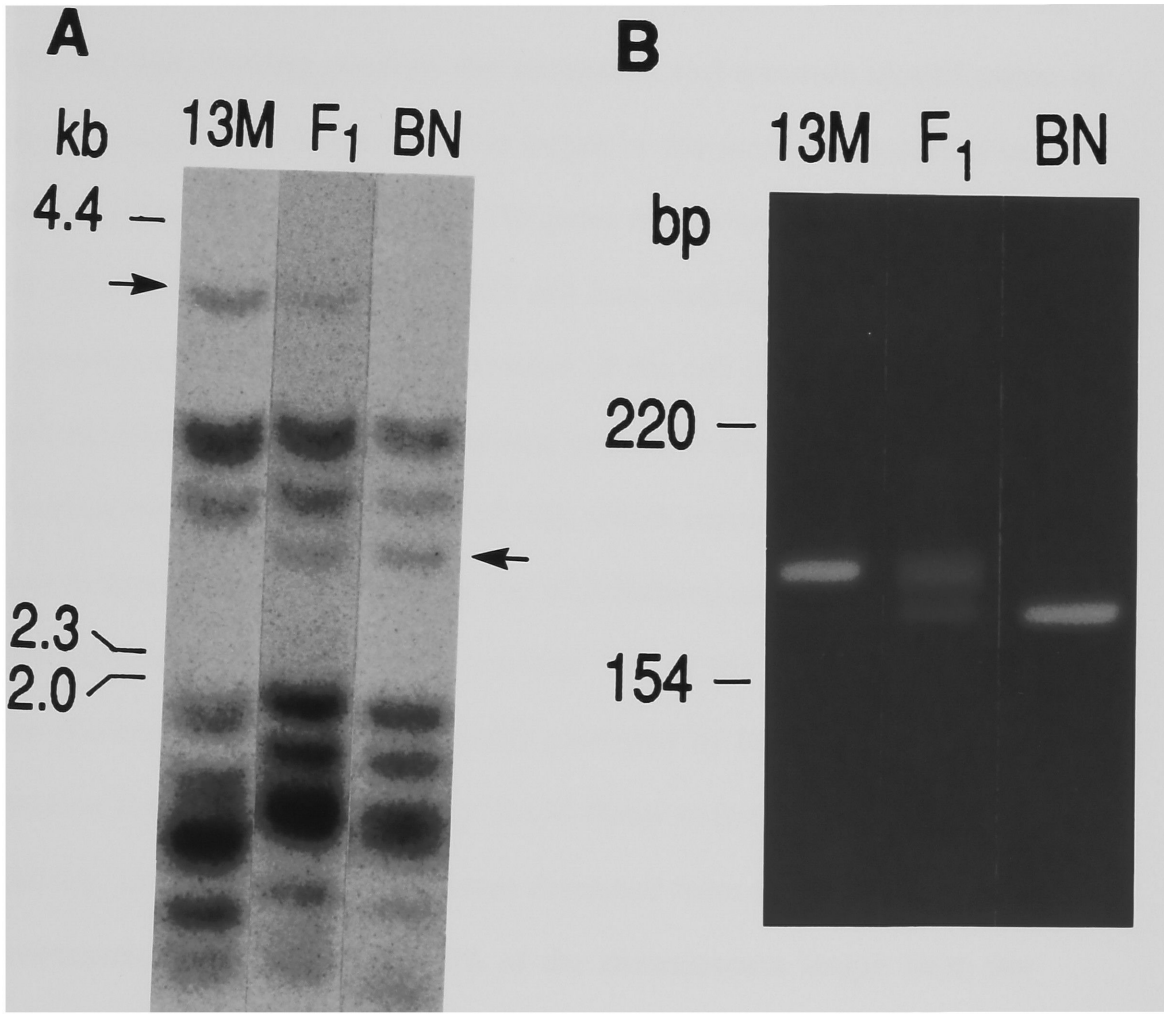
A
kb
13M
F1
BN
4.4
2.3
2.0
B
13M
F1
BN
bp
220
154

Microdissection and microcloning of mid/distal mouse chromosome 4

Analysis and microdissection of the 4:15 cell line:

The 4:15 Robertsonian chromosome appeared significantly larger than the rest of the chromosomes in an unstained metaphase karyotype of the L3ST cell line, making possible the consistent and accurate identification of mouse chromosome 4, which is the larger of the two chromosomes in the Robertsonian fusion (Figure 2.7). No gross aberration in G-banding pattern was observed with the L3ST Rb 4:15 cell line, making any large rearrangement of chromosome 4 due to transformation of the cell line unlikely. However, small deletions and/or rearrangements cannot be excluded. In-situ hybridization of the cloned gene (pMt4), which corresponds to the brown (*b*) locus in mouse (Jackson, 1988), in the 4:15 Robertsonian cell line demonstrated hybridization at a position 40% of the chromosome length from the telomere (Figure 3.28, kindly provided by Ian Jackson). Since the *db* mutation is located approximately 10 cM distal to the *b* locus (Figure 3.19) (Nadeau, 1989), gene fragments were dissected from the area of mouse chromosome 4 approximately 40% of the chromosome length from the telomere (Figure 3.29).

Figure 3.28. A photograph of an in-situ hybridization in the 4:15 Robertsonian cell line, with a probe which detects the *b* locus in mouse. The hybridization spots are located at a distance of approximately 40% of the length of the chromosome from the telomere. Since the *db* locus is located just distal to the *b* locus (Figure 3.19), this approximate area of mouse chromosome 4 in the 4:15 Robertsonian cell line was targeted for dissection. (In-situ hybridization and photo provided by I. Jackson)

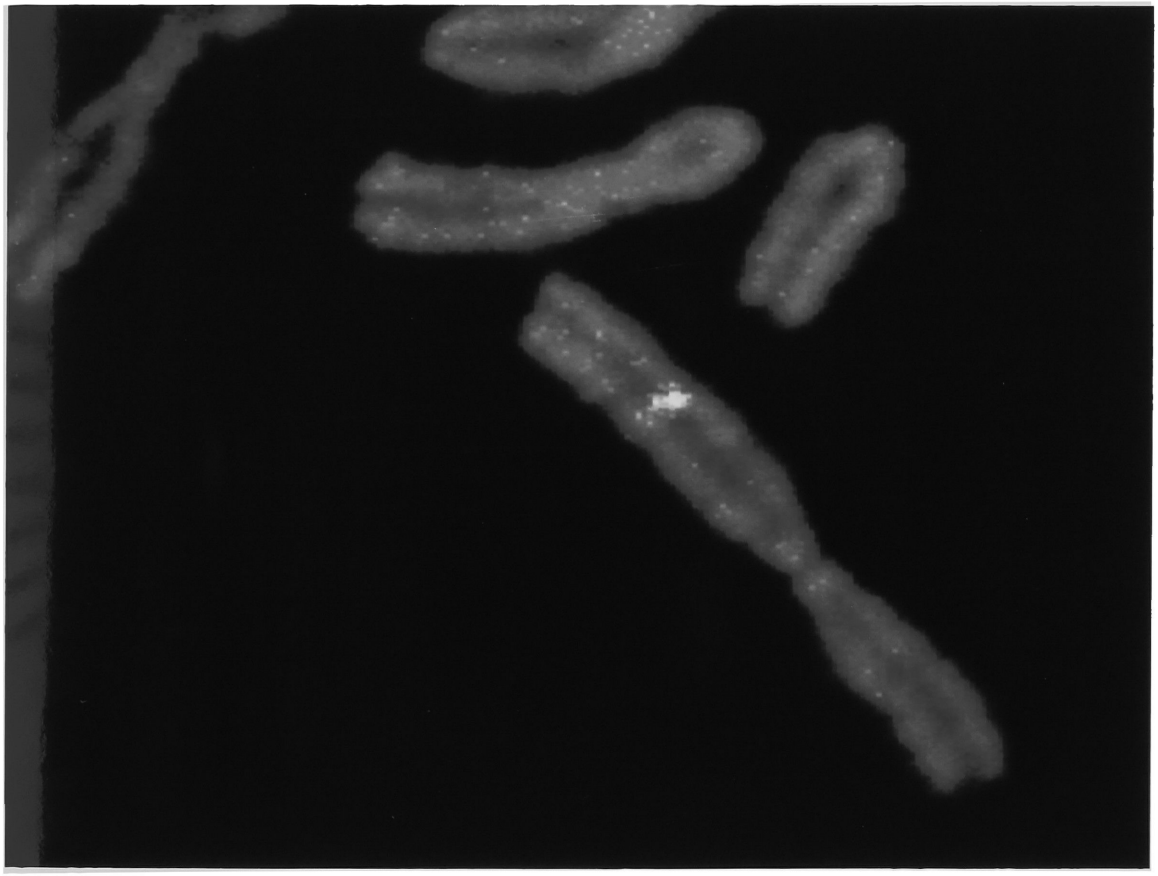

Figure 3.29. Photomicrograph of a metaphase spread of the 4:15 Robertsonian cell line demonstrating the dissected area of chromosome 4. (A) the arrow points to the chromosome 4 segment of a Rb 4:15 fusion. In (B), the arrow points to the area of chromosome 4, nearly 40% of the chromosome length from the telomere, where approximately 20% of the chromosome has been dissected.

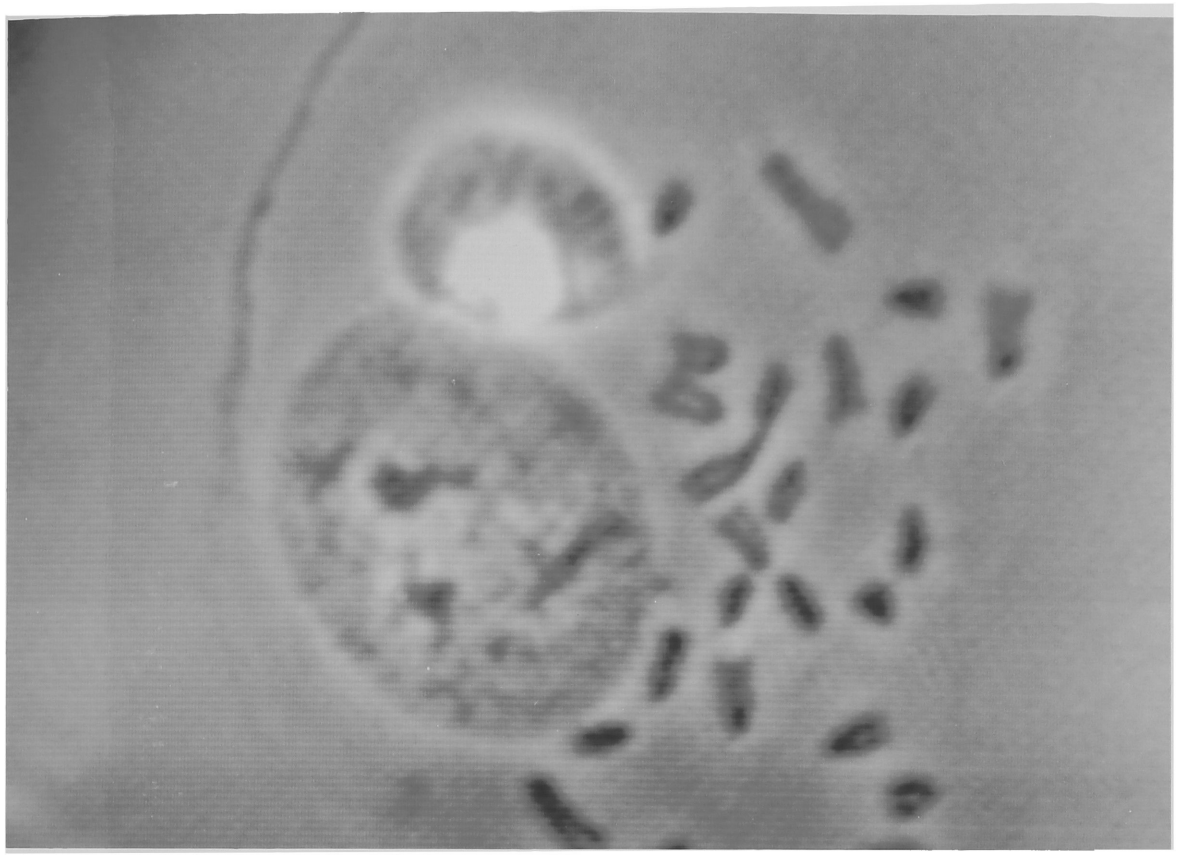

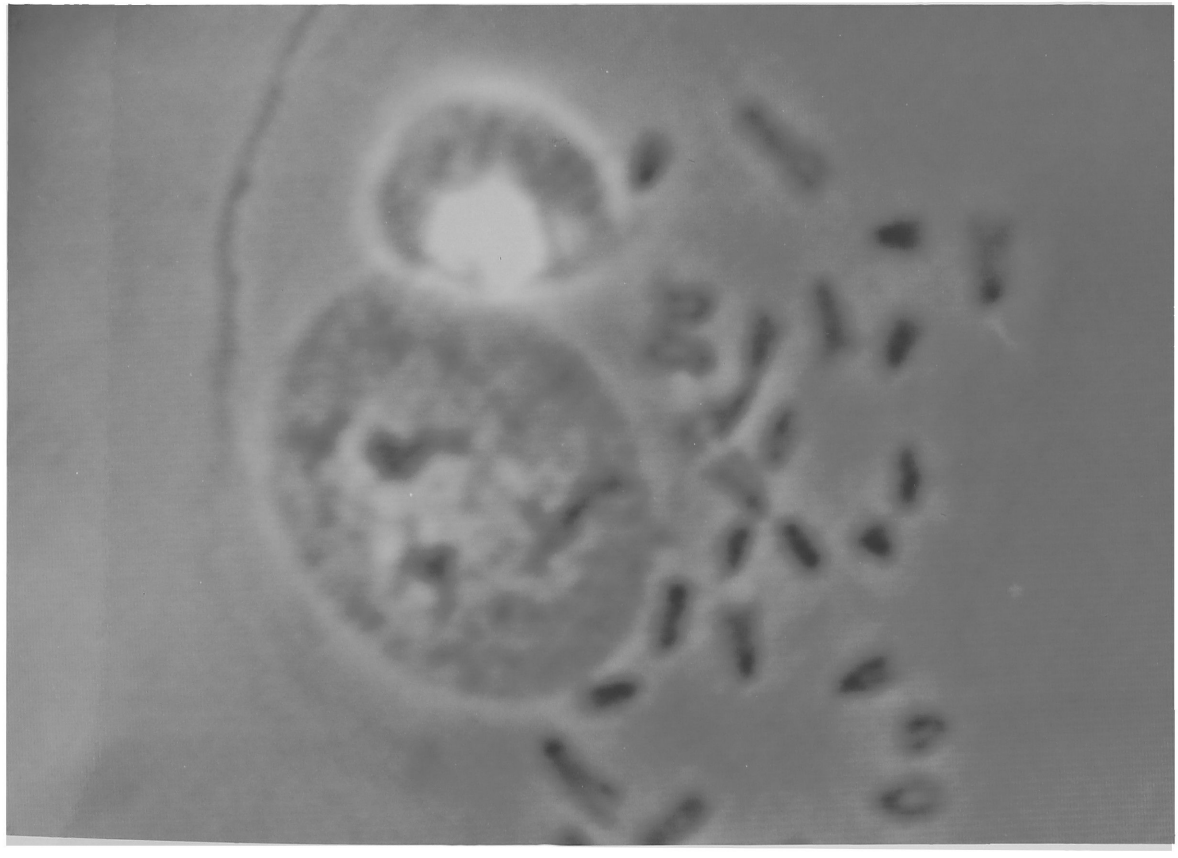

Microcloning and analysis of the chromosome 4 microclones:

After the microdissection and microcloning of the 73 unstained mid-chromosome 4 gene fragments, approximately 300 clones were obtained on plating of the λgt10 clone bank in the restrictive POP101 host. Each dissected gene fragment contained DNA from ~20% of mouse chromosome 4 and mouse chromosome 4 comprises approximately 6% of the total cellular DNA. Since the DNA content of a diploid cell is roughly 3pg, the dissected mass of DNA corresponds to about 2.6 pg of DNA.

The number of insert containing clones in the microdissected clone bank can be estimated since the clones were obtained from the input of ~1.3 ng of EcoRI digested λgt10 DNA as vector, the efficiency of packaging of the religated vector was previously demonstrated to be ~1.2×10^8 pfu/μg vector, and the religated vector had a clear plaque morphology background of < 1 pfu in the POP101 strain per 1250 pfu seen when plated with the non–restrictive C600 strain. Using these figures, approximately 170 of these clones would be expected to bear inserts.

Approximately 10% of these clones demonstrated dense radiographic signals when ^{32}P-random-primed radiolabeled total sonicated genomic mouse DNA was hybridized to them. Because random labeled total genomic mouse DNA consists primarily of repetitive sequences (since higher eukaryotic genomic DNA contains a predominance of repetitive elements) hybridizing clones contain highly repetitive elements and were excluded from further

analysis. Of the remaining 170 clones, the average insert size was approximately 180 bp [range: 50 – 1300 bp in length (Table 3.5)]. Individual microclones were then used to define RFLPs (restriction fragment length polymorphisms) between the C57BL/6J and *M. spretus* inbred mouse lines. Approximately 30% of these clones gave smears on hybridization to restriction digests of the C57BL/6J and *M. spretus* mouse DNA, although the intensity of the smear varied between clones. Presumably, these clones either contain low copy number repetitive sequences, or due to their small size, were missed in the original screening for highly repetitive DNA. These clones were also discarded. Fifteen microclones which detect single copy sequences by Southern hybridization to mouse DNA, did not reveal C57BL/6J X *M. spretus* polymorphisms with some or all of the following restriction endonucleases -- BamHI, BglII, EcoRV, HaeIII, HindIII, MspI, PvuI and RsaI — and were not analyzed further. The remaining C57BL/6J X *M. spretus* polymorphic clones consisted of apparently unique, or very low copy number sequences.

Number of dissected fragments	73
Total number of microclones recovered	~170
Size range of the recovered microclones	50bp - 1.3kb
Average size of the cloned fragments (102 analyzed)	180 bp
Percentage of sized microclones containing highly repetitive sequences	~10%
Percentage of sized microclones containing moderate copy number repeats	~30%
Total number of single/low copy number microclones	62
Number of single/low copy number microclones genetically mapped	47
Number of single/low copy number microclones without C57BL/6J x *M. spretus* RFLPs	15
Number of microclones unlinked to *db*	6

Table 3.5. Characteristics of the mid-4 chromosome microdissection.

Genetic resolution of the chromosome 4 microclones:

Moderate resolution genetic maps of the region surrounding the *db* mutation utilizing 48 offspring of the (C57BL/6J *db/db* X DBA/2J) F1 x (C57BL/6J *db/db* X *M. spretus*) F1 intercross (Figure 3.19), and of chromosome 4 employing 98 offspring of the (C57BL/6J X *M. spretus*) F1 X C57BL/6J backcross (Figures 3.3 and 3.12) have been described. In addition, 134 offspring of a (C57BL/6J *ob/ob* X DBA/2J) F1 x (C57BL/6J *ob/ob* X *M. spretus*) F1 [B6D2 *ob*/+ F1 X B6*spretus ob*/+ F1] intercross were haplotyped for the *M. spretus* allele of *Ifa* and *D4Rp1*. Fourteen of these animals demonstrated recombination events between *Ifa* and *D4Rp1* by RFLP analysis. Since C57BL/6J X DBA/2J polymorphisms were not detectable for the all the probes employed, the offspring of these three crosses represent 280 potential

C57BL/6J X *M. spretus* recombination events in the region of the *db* locus. By RFLP analysis, all 280 animals were haplotyped for *M. spretus* alleles at 8 previously mapped loci, demonstrating the order *b — Ifa — Jun — Odc–4 — db — C8B — D4Rp1 — Glut–1 — Lck* (Figure 3.31). An anonymous simple sequence repeat (SSR), *D4Mit205*, previously assigned to chromosome 4 (William Dietrich and Eric Lander, personal communication) was then mapped utilizing size variation of the SSR as detected by electrophoresis of the radiolabelled PCR product on denaturing sequencing gels, to the *Jun — Odc–4* interval. An anonymous human DNA segment, *D1S85*, was mapped by RFLP analysis to the *db — C8B* interval (Figures 3.30 and 3.31). Forty-seven single/low-copy number microclones which demonstrated C57BL/6J X *M. spretus* RFLPs were analyzed for their inheritance of the *M. spretus* allele among subsets of the recombinant animals (Figure 3.30). Six of the microclones, *D4Rck48, 64, 78, 116, 126*, and *153* were unlinked to any of the chromosome 4 markers. These probes were also not linked to *Gdc–1* which is located on mid-chromosome 15, but all six were linked to one another (data not shown).

Because of the large number of meiosis and probes involved in generating the genetic map, different subsets of the progeny were used to position different microclones. Consequently, precise positioning of each of the microclones relative to the other chromosome 4 markers was not always possible. Such ambiguity is indicated in Figure 3.31 by lines which delineate

the area in which the microclone resides. With the exception of *D4Rck23*, all of the microclones mapped to an approximately 21cM region, extending from 1cM proximal to *b* to approximately 2.6cM distal to *Lck*. The order of these 41 microclones (all of which mapped to chromosome 4) relative to the 8 previously mapped loci, the anonymous markers *D4Mit205* and *D1S85*, and *db* was obtained by minimizing the number of double crossovers and then confirmed by use of the MAPMAKER program which constructs RFLP linkage maps by multi-point linkage analysis (Figure 3.31) (Lander, et al., 1987). The MAPMAKER analysis demonstrated that the order between neighboring groups of markers presented is 166X more likely than any other possible order. If the order of the most proximal marker groups, [*D4Rck4, 32, 49A, 138, 196*] — [*D4Rck52,205*] is assigned to their most likely configuration, then the confidence of the order as presented is increased to 5370X more likely than any other possible order.

Although the microclones were not routinely searched for such, one of the microclones, *D4Rck41*, was found to have a C57BL/6J X DBA/2J Taq I RFLP. Pedigree analysis of this locus among the F2 progeny of the (C57BL/6J *db/db* X DBA/2J) F1 intercross (cross shown in Figure 2.4) demonstrated 20 recombination events among 40 of 48 (no data is available for 8 animals) *Lck* — *db* recombinants previously described (Figure 3.20). The genetic location of D4Rck41, approximately halfway between *Lck* and *db* among the

interspecific progeny used in the microclone analysis (Figure 3.31), is therefore quite similar to what is seen among the B X D intraspecific progeny.

Three of the microclones, *D4Rck49*, *60*, and *122*, demonstrated two independently segregating polymorphic *M. spretus* alleles. In Figures 3.30 and 3.31, the larger of the two *M. spretus* alleles, is denoted by the suffix 'A' (>8 kb BglII for *D4Rck49A*, ~2 kb TaqI for *D4Rck60A*) whereas the smaller *M. spretus* allele (~3 kb BglII for *D4Rck49B*, ~1kb TaqI for *D4Rck60B*) is denoted by the suffix 'B'. Both alleles of *D4Rck49* and *60* are located on chromosome 4, and there were recombination events between the 'A' and 'B' alleles for each probe. Thus, it is unlikely the 'A' and 'B' alleles of each probe represent single copy sequences which originated from the same locus. In the case of *D4Rck122*, the ~0.7 kb RsaI *M. spretus* allele (designated *D4Rck122A*) is located on chromosome 4 as shown in Figure 3.31, whereas the smaller ~0.4 kb RsaI *M. spretus* allele (*D4Rck122B*) is unlinked to all chromosome 4 markers (data not shown). Since *D4Rck49* and *D4Rck60* each define at least two separate loci located on chromosome 4, it is possible that these two microclones are part of a repetitive element which is specific to chromosome 4.

Figure 3.30. Pedigree analysis of the 41 microclones, 8 previously mapped loci, the anonymous markers *D4Mit205* and *D1S85*, and *db* utilizing the 1) 48 offspring (designated by the prefix 'db') of the (C57BL/6J *db/db* X DBA/2J) F1 x (C57BL/6J *db/db* X *M. spretus*) F1 intercross (Figure 2.5) (2) 16 offspring (designated by the prefix 'SC') of the (C57BL/6J X *M. spretus*) F1 X C57BL/6J backcross (Figure 2.1) with demonstrated recombination events between *b* and *Lck* (Figure 3.2) (from a total of 98 offspring examined for those loci by RFLP analysis), and (3) 16 offspring (designated by the prefix 'os') of a (C57BL/6J *ob/ob* X DBA/2J) F1 x (C57BL/6J *ob/ob* X *M. spretus*) F1 [B6D2 *ob*/+ F1 X B6*spretus ob*/+ F1] intercross which demonstrated recombination events between *Ifa* and *D4Rp1* (from a total of 134 offspring examined by RFLP analysis) (Friedman, et al., 1991). The mapped loci are listed at the top. Since C57BL/6J X DBA/2J polymorphisms were not detectable for the all the probes employed, the offspring of these three crosses represent 280 potential C57BL/6J X *M. spretus* recombination events in the region of the *db* locus. The open box represents the inheritance of the C57BL/6J allele, the filled box the *M. spretus* allele, the diagonally hatched box instances for which data is not available, and the horizontally striped box represents animals not segregating *db*.

D4Rck4
D4Rck196
D4Rck138
D4Rck32
D4Rck49A
D4Rck52
b
D4Rck140
D4Rck65
D4Rck151
D4Rck58
D4Rck83
D4Rck130
D4Rck137
D4Rck122A
D4Rck119
D4Rck143
D4Rck117
D4Rck28
D4Rck60A
D4Rck9
Ifa
D4Rck124
D4Rck173
D4Rck1
D4Rck111
D4Rck131
Jun
D4Mit205
Odc-4
db
D4Rck22
D4Rck69
D1S85
D4Rck12
C8B
D4Rck142
D4Rck41
D4RRp1
D4Rck13
D4Rck16
D4Rck57
Glut-1
D4Rck3
D4Rck53
D4Rck109
D4Rck103
D4Rck60B
D4Rck49B
Lck
D4Rck23
db303
db833
sc124
sc347
db331
os702
db314
os662
os619
sc200
sc368
sc101
os618
sc199
os645
sc209
os641
db324
db330
db305
sc366
os649
sc350
os624
os714
os712
os676
os684
os691
os715
os701
sc127
os637
db306
db313
db338
db339
db830
db309
db312A
sc122
sc201
sc341
sc365
sc367
sc373
db312
db315
db316
db318
db322
db328

Figure 3.31. The derived genetic linkage map of mouse chromosome 4 including the mid/distal chromosome 4 microdissection clones. The order of the 41 microclones relative to the 8 previously mapped loci, the anonymous markers *D4Mit205* and *D1S85*, and *db* was obtained by minimizing the number of double crossovers (Figure 3.30) and then confirmed by use of the MAPMAKER program which constructs RFLP linkage maps by multi-point linkage analysis (Lander, et al., 1987). The MAPMAKER analysis demonstrated that the order between neighboring groups of markers presented is 166X more likely than any other possible order. If the order of the most proximal marker groups, [*D4Rck4, 32, 49A, 138, 196*] — [*D4Rck52,205*] is assigned to their most likely configuration, then the confidence of the order as presented is increased to 5370X more likely than any other possible order. The distances between markers (in cM) are the recombination frequencies between successive markers [(# recombinant animals / total number of animals scored)] X 100 and were confirmed by the MAPMAKER analysis. The map spans an approximately 21 cM distance. Two microclones, *D4Rck22* and *D4Rck69*, are located just distal to *db*. The *db* locus is flanked by *Odc–4* and these two distal markers which lie within an ~1.5cM distance. No correlation between the centromere and the most proximal markers is intended.

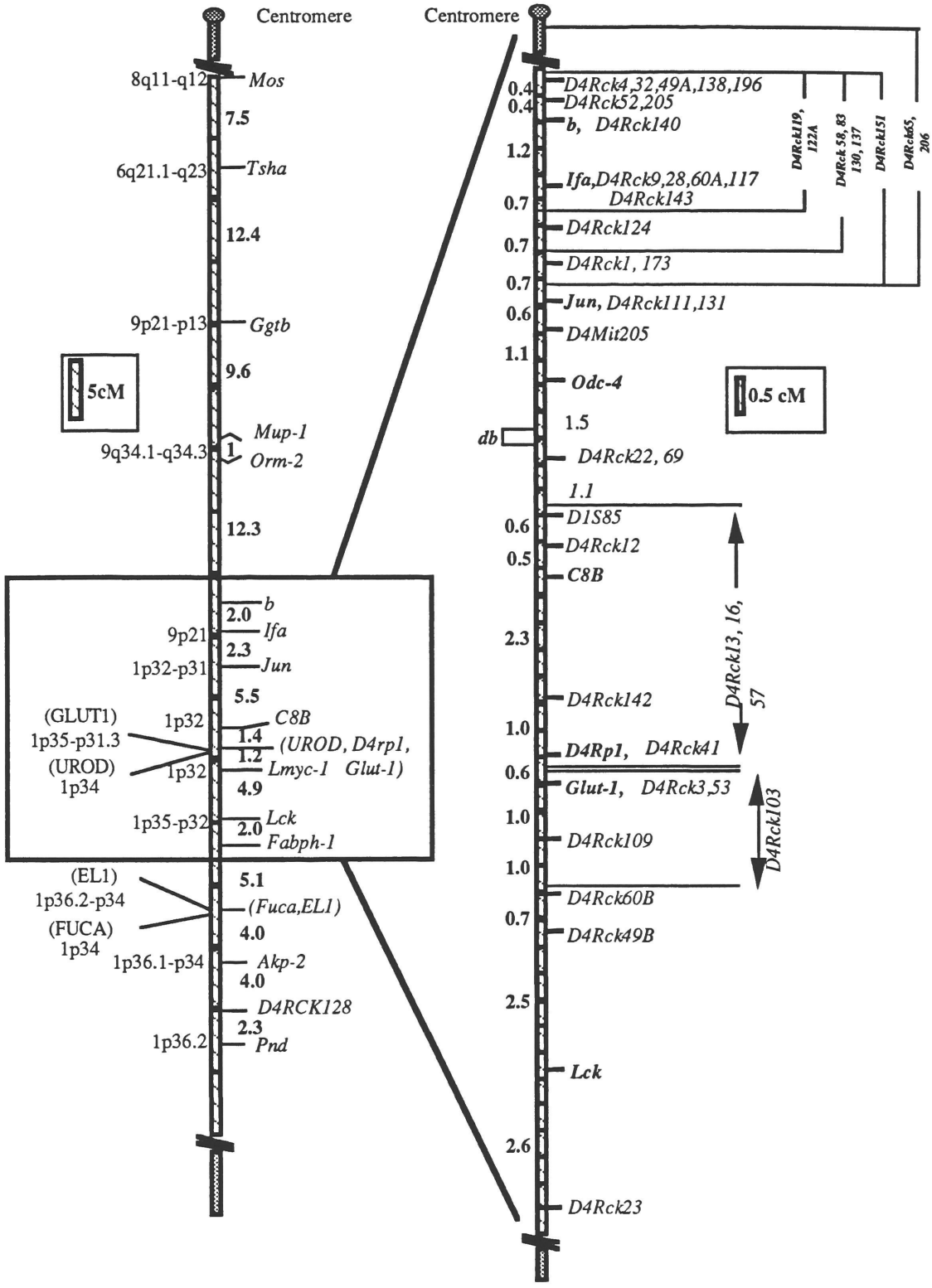

Molecular Genetic Map of Mouse Chromosome 4

Molecular Genetic Map of Mid/Distal Mouse Chromosome 4 Microdissection

Cloning and analysis of the mouse *Pgm-2* gene

Cloning of the *Pgm-2* gene by PCR:

Phosphoglucomutase is an enzyme involved in carbohydrate metabolism which catalyzes the conversion of glucose 1-phosphate to glucose 6-phosphate. Before the advent of modern molecular biological techniques, linkage analysis required the use of biochemical or phenotypical variants as markers. As early as 1964, gel electrophoretic techniques were developed for detecting the phosphoglucomutase gene product (Spencer, et al., 1964). Soon after detection of the enzyme was made possible, it became apparent that there were at least three distinct autosomal genes involved in the production of phosphoglucomutase in humans (Parrington, et al., 1968; Dawson and Jaeger, 1970; Hopkinson and Harris, 1965; Hopkinson and Harris, 1966; Hopkinson and Harris, 1968; van Cong, et al., 1971; McAlpine, et al., 1970; McAlpine, et al., 1975; Douglas, et al., 1973; Jongsma, et al., 1973). In the mouse, two electrophoretic variants, denoted *Pgm-1* and *Pgm-2* were quickly established (Shows, et al., 1969; Hutton and Roderick, 1970; Chapman, et al., 1971) and the third was eventually electrophoretically characterized as well (Johnson, et al., 1981). Because the alleles were named by their electrophoretic properties, a problem in nomenclature arose; *Pgm-1* in human corresponds to *Pgm-2* in mouse, *Pgm-2* in human to *Pgm-1* in mouse, and the *Pgm-3* locus is the same in both (Johnson, et al., 1981; Nadeau, 1989). In the current genetic

map (Doolittle, et al., 1991), *Pgm-1* is located on mouse chromosome 5, *Pgm-2* is located on mouse chromosome 4, and *Pgm-3* is located on mouse chromosome 9.

The location of *Pgm-2* on mouse chromosome 4, just proximal to *db* and its importance in carbohydrate metabolism, made it a candidate gene for *db*, or at least a close marker. Erythrocyte hemolysates and tissue extracts of kidney, muscle, liver, brain, spleen, heart and lung all express *Pgm-2* as demonstrated by electrophoresis in the mouse, and furthermore appeared to account for most of the activity in those tissues as well (Shows, et al., 1969). A review of the literature revealed that the phosphoglucomutase protein, as expressed in rabbit skeletal muscle, had been isolated and sequenced (Ray, 1983). Since *Pgm-2* had been previously shown to account for most phosphoglucomutase activity in skeletal muscle, the assumption was made that the sequenced rabbit skeletal muscle protein was homologous to the mouse *Pgm-2* protein. Reverse translation of the protein product revealed two areas which if conserved in the mouse, would provide low-degeneracy oligoprimers with an expected product size of 780bp.

Two oligoprimers of the sequence (1) 5'-AA(A/G) CA(A/G) CA(A/G) TT(T/C) GA(T/C) (T/C)T(A/G) GA(A/G) A and (2) 5'-GC(T/C) TC(T/C) A(A/G) (A/G) TC(T/C) TTC ATC AT(T/C) TT were synthesized and used to amplify an ~780bp product from a mouse liver cDNA library by 35 cycles of PCR with annealing at 55°C for 2 minutes. The product was isolated by electrophoresis into NA-45 paper and the ends were made blunt by addition of 1U klenow enzyme and dNTPs. The product was then subcloned into an EcoRV digested/phosphatased bluescript II +KS vector. Sequencing of 5 small-scale individual subclone plasmid-preparations revealed the same sequence in each independent isolate but with no noticeable homology to the predicted sequence of *Pgm-2*.

In order to test whether this initial PCR consisted of both the correct *Pgm-2* PCR product, and a contaminating sequence, a second set of oligos, 1) GC TCT AGA (C/T)AA (A/G)TT (T/C)AA (G/A)CC NTT (C/T)AC NGT NGA (N = all 4 dNTPs) and a copy of oligo (2) above with a PstI site added at the 5' end were synthesized [GC CTG CAG C(C/T)T C(C/T)T (A/G) (A/G)T C(C/T)T TCA TCA T(C/T)T T] and used to amplify a 780bp product, under the original conditions, using 1/100th of the initial PCR as template. To the amplified reaction, 10 µl of the appropriate restriction buffer was added with 3 µl (30U) each of XbaI and PstI. The digested product was electrophoresed through agarose, isolated with NA-45 paper and subclones into the appropriately prepared XbaI/PstI digested bluescript II +KS plasmid vector. After

electroporation into the bacterial strain DH5α, and plating on LB/ampicillin plates containing IPTG and X-Gal, 5 individual white colonies were picked and dideoxy sequenced. The sequence of the subcloned products is shown in Figure 3.32. The hypothetical translated protein of this sequence (Figure 3.33) demonstrated substitutions at position 438 (threonine) and position 417 (histidine) of the rabbit muscle *Pgm* by asparagine and glutamine respectively, in mouse. Although both asparagine and glutamine are uncharged at physiological pH, the amide side chain of asparagine is considerably more hydrophilic than the aliphatic side chain of threonine, and the ring sructure of histidine is bulkier than the amide side chain of glutamine. What physiologic role(s), if any, these substitutions cause awaits further study.

```
    *   10    *   20    *   30    *   40    *   50    *   60
gagattgtggactcagtggaggcctatgccacaatgctgagaaacatcttcgatttcaac
gcactgaaggagctactctctggtccaaacagactgaagatccgcatagacgccatgcac
ggagttgtgggaccgtacgtaaagaagatcctctgtgaagaacttggtgcccctgcaaac
tcagctgtgaactgtgtccccctggaggattttggaggccaccatcccgaccccaatctc
acctatgctgctgacctagtggagaccatgaagtcaggagagcatgatttcggggctgcc
tttgatggtgacggggatcgaaacatgattctgggcaagcacgggttctttgtgaatcct
tctgactctgtggctgtcatcgctgccaacatcttcagcattccgtacttccagcagacc
ggggtccgtggctttgcacgcagcatgcccacaagtggtgctctggaccgggtagcaaat
gccacaaagatcgctttgtatgagacccccactggctggaagtttttgggaatttgatg
gatgcaagcaagctgtccctctgtggagaggagagctttgggaccggttcggaccatatc
cgagagaaagatggactgtgggccgtcctggcctggctctccattctggccacccgcaaa
cagagcgtggaggacatcctcaaagaccactggcagaagtttggtcggaacttctttacc
aggtatgactacgaggaggtggaagctgagggtgcaaacaagatgatgaaagatctagaa
    *   10    *   20    *   30    *   40    *   50    *   60
```

Figure 3.32. The 780 bp of DNA sequence obtained from the mouse *Pgm–2* clone as determined by sequencing of the subcloned PCR fragments.

```
                                                  10        20        30
mouse                                          EIVDSVEAYATMLRNIFDFNALKELLSGPN
                                               X:::::::::::::::::::::::::::::
PGMR    YAICPDLKVDLGVLGKQQFDLENKFKPFTVEIVDSVEAYATMLRNIFDFNALKELLSGPN
          160       170       180       190       200       210

                 40        50        60        70        80        90
mouse   RLKIRIDAMHGVVGPYVKKILCEELGAPANSAVNCVPLEDFGGHHPDPNLTYAADLVETM
        ::::::::::::::::::::::::::::::::::::::::::::::::::::::::::::::
PGMR    RLKIRIDAMHGVVGPYVKKILCEELGAPANSAVNCVPLEDFGGHHPDPNLTYAADLVETM
          220       230       240       250       260       270

               100       110       120       130       140       150
mouse   KSGEHDFGAAFDGDGDRNMILGKHGFFVNPSDSVAVIAANIFSIPYFQQTGVRGFARSMP
        ::::::::::::::::::::::::::::::::::::::::::::::::::::::::::::::
PGMR    KSGEHDFGAAFDGDGDRNMILGKHGFFVNPSDSVAVIAANIFSIPYFQQTGVRGFARSMP
          280       290       300       310       320       330

               160       170       180       190       200       210
mouse   TSGALDRVANATKIALYETPTGWKFFGNLMDASKLSLCGEESFGTGSDHIREKDGLWAVL
        ::::::::::::::::::::::::::::::::::::::::::::::::::::::::::::::
PGMR    TSGALDRVANATKIALYETPTGWKFFGNLMDASKLSLCGEESFGTGSDHIREKDGLWAVL
          340       350       360       370       380       390

               220       230       240       250       260
mouse   AWLSILATRKQSVEDILKDHWQKFGRNFFTRYDYEEVEAEGANKMMKDLE
        ::::::::::::::::::::.:::::::::::::::::::::.::::::X
PGMR    AWLSILATRKQSVEDILKDHWHKFGRNFFTRYDYEEVEAEGATKMMKDLEALMFDRSFVG
          400       410       420       430       440       450
```

Figure 3.33. The protein sequence of the mouse *Pgm-2* derived by translation of the cloned cDNA compared to the sequence of rabbit skeletal muscle *Pgm*. The translated mouse *Pgm-2* sequence is shown on the top, the rabbit muscle *Pgm* (noted PGMR) at the bottom. Note the substitution (in mouse with respect to rabbit) of glutamine (Q) for histidine (H) at position 417, and asparagine (N) for a threonine (T) at position position 438 of the complete rabbit muscle *Pgm*.

RFLP mapping of the *Pgm-2* locus in the interspecific *laboratorius* X *spretus* crosses: Southern hybridization of the 780 bp partial cDNA described above demonstrated C57BL/6J X *M. spretus* polymorphisms (Figure 3.35) with the enzymes Taq I (3 *M. spretus* bands) and Bgl II (1 *M. spretus* band). RFLP analysis amongst the 48 offspring of the (C57BL/6J *db/db* X DBA/2J) F1 X (C57BL/6J *db/db* X *M. spretus*) F1 ('db*spretus*') interspecific intercross, demonstrated that two of the Taq I bands were linked to *db* on chromosome 4 (0/48 recombinants) and one band was not, while the polymorphic Bgl II band did not segregate with *db* but did segregate (0/48 recombinants) with the unlinked Taq I band.

As shown in Figure 3.31, the *db* locus is flanked by *Odc–4* proximally and *D4Rck22* and *D4Rck69* distally. *Odc–4* demonstrated 0/194 recombinants with *Pgm-2* amongst the progeny of the two interspecific C57BL/6J x *M. spretus* crosses not segregating *db* (Figure 3.30) which were used for positioning the mid-4 dissection microclones. In addition, 3/98 progeny (representing 196 meiosis) of the intersubspecific F2 intercross between (C57BL/6J *db/db* X *M. castaneus*)F1 *db/+* animals (Figure 2.6) which carried the *M. castaneus* RFLP allele for *Ifa* (Figure 3.21) also demonstrated the *M. castaneus* allele for *Pgm–2* . These data place *Odc–4* and *Pgm–2* approximately 1.5cM proximal to *db*.

The two bands which were unlinked to *db* probably represent the same locus, and since *Pgm* represents a family of at least three members,

segregation analysis was carried out in order to test whether these unlinked bands represented one of the other (*Pgm–1* or *Pgm–3*) alleles which are located on mouse chromosomes 5 and 9 respectively. In order to test this hypothesis, a Bgl II RFLP was defined for a probe which detects the *Kit* locus located approximately 3 cM distal to *Pgm–1* on mouse 5 (Doolittle, et al., 1991), and was then used to type the 48 'db*spretus*' offspring. Additionally, a pair of oligos which define an SSR for *Cypla–1* (Love, et al., 1990) located approximately 15 cM proximal to *Pgm–3* on mouse 9 (Doolittle, et al., 1991) were synthesized, one primer kinased, and the polymorphism detected by PCR amplification of each 'db*spretus*' offspring's DNA followed by acrylamide gel electrophoresis. Pedigree analysis of the *Pgm-2* Taq I/Bgl II bands which were unlinked to *db* revealed that *Kit* and *Cypla–1* were also unlinked to them. Therefore the unlinked bands cannot represent either of the other two known *Pgm* alleles.

Genomic screening of the λFixII library as described (see page #64), with the *Pgm-2* cDNA probe at a final wash stringency of 2X SSC, 0.1% SDS at room temperature, resulted in the isolation of 12 genomic clones. Direct PCR of the phage clones was performed with oligomers spaced approximately 200 bp apart (spanning the putative intron/exon boundary, Figure 3.34). Two of the clones demonstrated a PCR fragment of ~1300 bp which is believed to result from the presence of an intron, while two others manifested an ~200 bp PCR fragment. Sequencing of the 1300 bp PCR fragment, subcloned into a 'T-

tailed' EcoRV digested vector (Marchuk, et al., 1991), revealed the 5' 'GU' donor and 3' 'GA' splice acceptor sequences which are indicative of an intron/exon boundary (Figure 3.34). This intron was missing from the ~200bp PCR fragment and thus the Taq I/Bgl II bands which are unlinked to *db*, may represent a processed psuedogene which does not map to mouse chromosomes 4,5 or 9.

A

```
    *   10    *   20    *   30    *   40    *   50    *   60
gacacagttcacagctgagtttgcaggggcaccttgttcttcacagaggatcttctttac
gtacggtcccacaactgtaacaaattaaaggatgaagagccaaaccgtaaaacttattaa
aacatggaatggcttgaggg
```

B

```
    *   10    *   20    *   30    *   40    *   50    *   60
gagattgtggactcagtggaggcctatgccacaatgctgagaaacatcttcgatttcaac
gcactgaaggagctactctctggtccaaacagactgaagatccgcatagacgccatgcac
ggaggtacgcgctgggaggcctgcaaagacagggagctgatctctgctgtgtgcgccca
```

Figure 3.34. Sequence of intron/exon boundaries of a 1300 bp chromosome 4 specific *Pgm-2* probe generated by PCR. Both sequences are shown in the orientation they were sequenced. Intronic sequence is both underlined and italicized. A) The 3' end of the intron begins at base 75 as demonstrated by the 3'-GA RNA (CT in the DNA) consensus sequence at bases 1 and 2 of the 3' end of the putative intron. B) The 5' end of the intron begins at base 125 as demonstrated by the 5'-GU (GT in the DNA) consensus sequence in the first two bases of the putative 5' end of the intron.

Figure 3.35. Southern hybridization of the *Pgm-2* 780 bp partial cDNA clone demonstrating C57BL/6J X *M. spretus* RFLPs with the restriction endonucleases Taq I and Bgl II. The polymorphic Taq I band marked with an '*', as well as the polymorphic Bgl II band, did not segregate with *db* among the 48 offspring of the B6D2 *db*/+ X B6*spretus* *db*/+ interspecific intercross (Figure 2.4). The remaining two Taq I bands cosegregated with *db*. Since the unlinked polymorphic bands do not cosegregate with either *Kit* on chromosome 5, or *Cypla-1* on chromosome 9, these bands cannot represent either *Pgm-1* (chromosome 5) or *Pgm-3* (chromosome 9). Although it is likely that these bands represent a processed psuedogene, the presence of a fourth *Pgm* allele cannot be excluded.

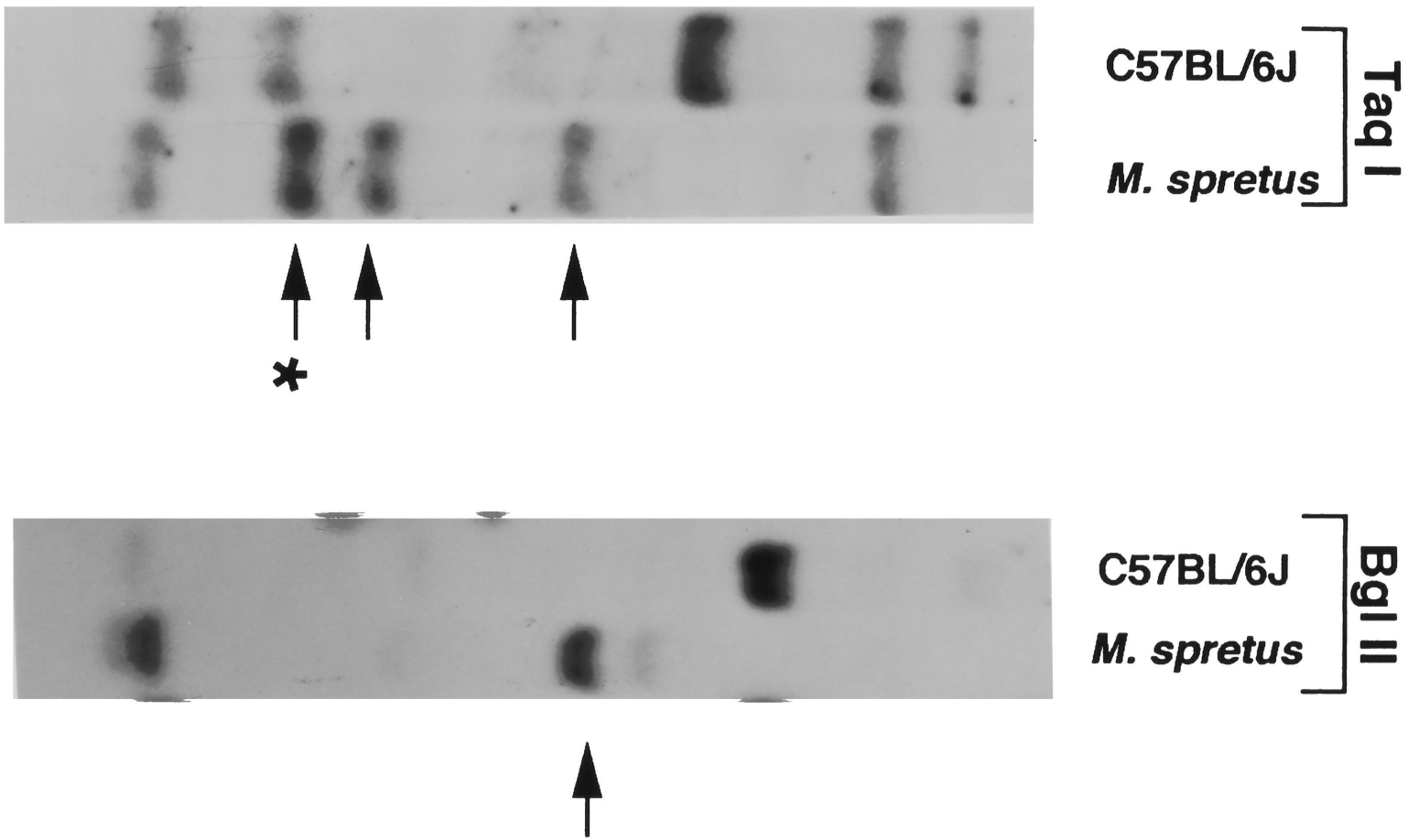
C57BL/6J
M. spretus
Taq I
*
C57BL/6J
M. spretus
Bgl II

Isolation of YACS containing the *C8B* and *D4Rck69* probes:

Hybridization screen for a *C8B* containing YAC: Before successful microdissection of the *db* region of chromosome 4, the closest flanking markers to *db* were *Jun* and *C8B* (Figure 3.3 and 3.19). Since the *Jun* — *db* interval is known to be ~3 cM, the likelihood of a YAC being able to significantly close the physical distance between them of up to 9 megabases (assuming a distance of 1 - 3 Mb/cM) is unlikely. The *db* — *C8B* interval however was not as clearly defined, and perhaps a significant gap could be closed by YAC walking. Additionally, having been unable to define a C57BL/6J X DBA/2J RFLP for any of the closest distal flanking markers (*C8B, D4Rp1, UroD*), the 564 B X D meiosis which comprised the intraspecific C57BL/6J *db/db* X DBA/2J backcross (Figure 2.3) and intercross (Figure 2.4) were unavailable as a mapping resource for these loci with respect to *db*. The only information available was from the *48* (C57BL/6J X DBA/2J) F1 X (C57BL/6J X *M. spretus*) F1 offspring (Figure 2.5) for which C57BL/6J X *M.spretus* RFLPs were readily identifiable (the intersubspecific C57BL/6J X *M. castaneus* intercross segregating *db* had not yet been begun). Since a YAC bearing *C8B* would almost certainly contain some sequence with an identifiable B X D polymorphism, it would be possible to access the intraspecific meiosis for positioning the distal markers with relation to *db*.

Hybridization screening of Dr. Lehrach's YAC library by Dr. Roger Cox using the *C8B* PCR probe described (Table 2.2) yielded three positive signals whose corresponding yeast, believed to bear YACs containing *C8B*, were sent to our laboratory for further analysis. Southern hybridization of a standard overnight pulse-field gel separation, demonstrated that the three YACS were approximately 300 kb, 450 kb and 1.2 Mb in size. Cloning of one the two ends of the YAC by 'inverse PCR' was accomplished by Dr. Donald Siegel, and hybridization of this YAC end to the somatic cell hybrid panels previously described (Table 3.4) demonstrated that the YAC end was located on chromosome 4. Efforts to clone the other YAC end by "bubble" and "inverse PCR" continue. Inter B2-PCR of the 1.2 Mb YAC yielded a product which was radiolabeled and hybridized under standard blocking conditions to a panel of restriction endonuclease digested DNAs. A polymorphism between C57BL/6J and either DBA/2J, *M. spretus* or *M castaneus*, was apparent with the enzyme TaqI (Figure 3.36). However, when the same probe was hybridized to a Southern blot of the (C57BL/6J *db/db* X DBA/2J) intraspecific N2 and F2 *Ifa — Lck* recombinants, although control C57BL/6J and DBA/2J animals on the blot manifested the identical polymorphism, no RFLP was visible between the C57BL/6J *db/db* and DBA/2J mice. Hybridization of the identical probe to Taq I digests of the B X D RI line DNA demonstrated the expected pattern of C57BL/6J and DBA/2J alleles, and positioned *C8B* near *Mtv-13* on

chromosome 4 (Table 3.6). As seen in Figures 3.17 and 3.19, *Mtv-13* is located approximately 6 cM distal to *db*.

The reason for the discrepancy of RFLP pattern between the C57BL/6J and C57BL/6J *db/db* mice is unclear. However it may be due to contamination of the C57BL/6J *db/db* strain by some amount of DBA/2J genome. The original *db/db* mutation arose on the C57BL/KsJ strain, which originated from the C57BL/6J mouse strain. Phenotypic and metabolic differences between homozygous *db/db* or *ob/ob* animals when bred on the two strains are readily apparent (Coleman and Hummel, 1975; Coleman, 1982; Leiter, 1981), however genetic polymorphisms between the two strains are not readily identifiable. In an unreported collection of these genomic differences by Dr. Douglas Coleman (Jackson Labs, personal communication), the majority of RFLP differences found between the two strains demonstrated a C57BL/KsJ allele identical in size to the corresponding DBA/2J allele, which differed in size from the C57BL/6J allele. It is possible that the C57BL/KsJ strain arose by contamination of the C57BL/6J strain with some amount of DBA/2J genome. Because the C57BL/6J *db/db* congenic strain had been carried for about 7 generations prior to its use in the described crosses, any contaminating DBA/2J DNA in the vicinity of the *db* locus may not have had a sufficient number of generations to be lost. If this were the case, then it may not be possible to demonstrate an RFLP between the C57BL/6J *db/db* and DBA/2J strains for loci located in the *db* — *C8B* interval, and the offspring of

the intraspecific crosses will not be informative for mapping markers in this region. No B X D polymorphism has been identified for either of the two closest proximal markers to *db*, *Pgm-2* and *Odc-4* (Figure 3.31), making it impossible to obtain confirmation of this hypothesis by a demonstrated extension of this process proximal to *db*. Additionally, the utility of the B X D intraspecific offspring for mapping in the region distal to *Ifa* and proximal to *db*, is not known since DBA/2J DNA may also be found in this region. Work to define the limits of this region will continue as closer flanking markers with B X D polymorphisms become available.

	1	2	5	6	8	9	11	12	13	14
C8B	D	B	D	O	B	D	B	D	B	D
Mtv-13	D	B	D	B	B	D	B	D	B	D
Pmv-19	D	B	D	B	B	D	B	D	B	D

	15	16	18	19	20	21	22	23	24	25
C8B	B	D	O	B	B	D	D	D	B	D
	X									
Mtv-13	D	D	D	B	B	D	D	D	B	D
		X								
Pmv-19	D	B	D	B	B	D	D	D	B	D

	27	28	29	30	31	32
C8B	D	B	D	D	B	D
		X				
Mtv-13	D	D	D	D	B	D
Pmv-19	D	D	D	D	B	D

Table 3.6. B X D RI line data for the inter-B2 repeat PCR *C8B* YAC probe. There are 2/24 recombinants with *Mtv-13*, located ~6 cM distal to *db* (Figure 3.19), and 3/24 recombinants with *Pmv-19*, suggesting the order cen — *Pmv–19* — *Mtv-13* — *C8B*. The letter 'B' denotes inheritance of the C57BL/6J allele, 'D' the DBA/2J allele, and 'O' denotes an RI strain for which the strain distribution pattern (SDP) is unknown for a specific marker.

Figure 3.36. Demonstration of *C8B* RFLPs between inbred mice using inter-B2 repeat PCR of a 1.2 Mb *C8B* YAC. DNA from C57BL/6J ('B'), DBA/2J ('D'), *M. spretus* ('S') and *M. castaneus* ('C') were digested with Taq I, and hybridized to the inter-B2 repeat probe after preannealing the probe to an excess of C57BL/6J sonicated mouse DNA to block any repetitive sequences. RFLPs with respect to C57BL/6J mice are apparent for all three counterstrains (DBA/2J, *M. spretus* and *M. castaneus*).

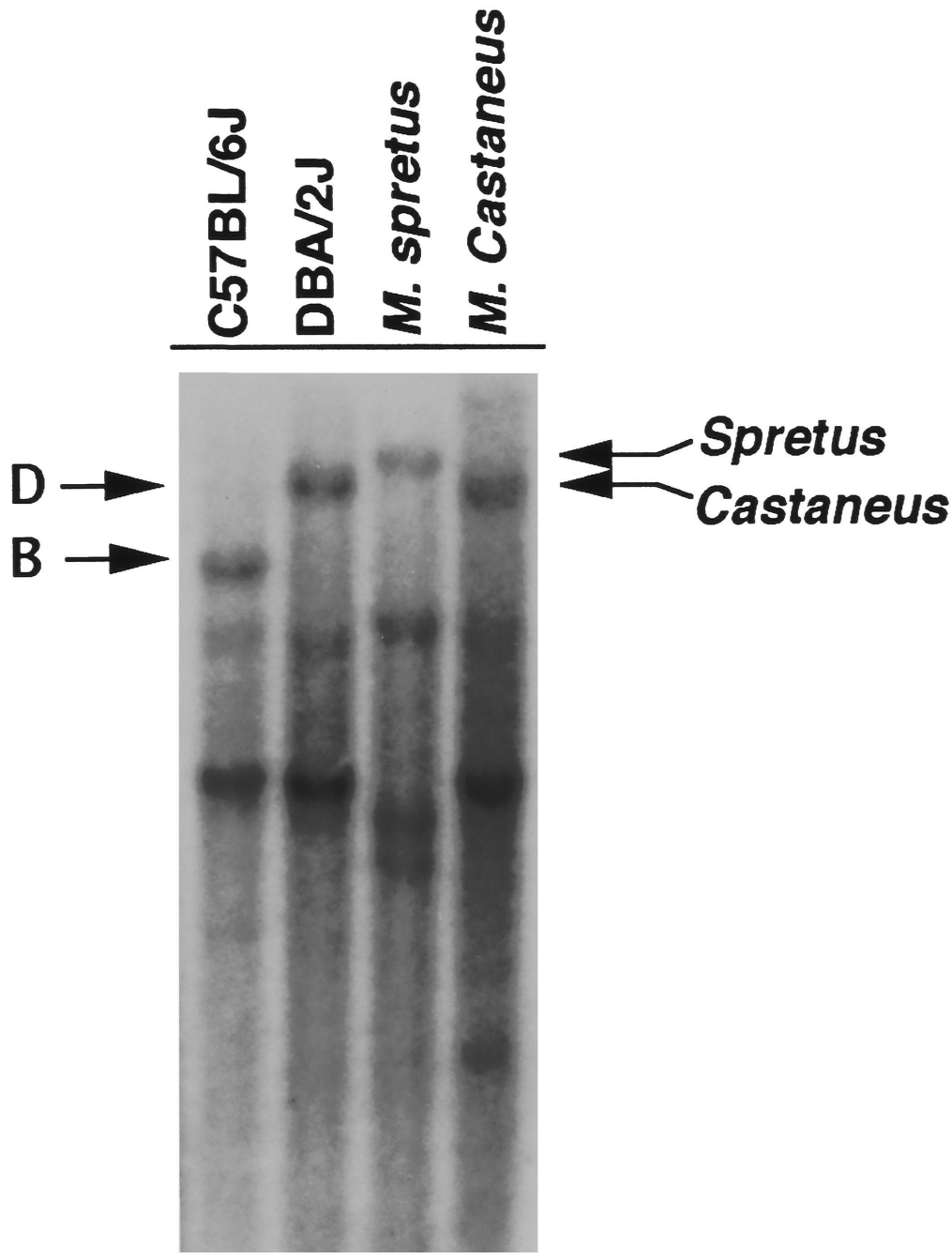
C57BL/6J
DBA/2J
M. spretus
M. Castaneus
D
B
Spretus
Castaneus

PCR screening for YACs containing the *Pgm-2, D4Rck22* and *D4Rck69* locus:

Three complex pool aliquots of the Princeton YAC library (Dr. Shirley Tilghman) were obtained. Oligos corresponding to the known sequences of the *Pgm-2, D4Rck22,* and *D4Rck69* loci were generated from the known sequences. For *D4Rck69,* 6 of the complex pools were positive by either PCR and Southern hybridization, or by using nested PCR. Simple pools corresponding to three of the complex pools were screened. One set of simple pools obtained by 'nested PCR' screening, was negative (i.e. the positive in the corresponding complex pool was a false positive), however two of the simple pool sets yielded positive results. Three other sets of simple pools remain to be screened. A positive was then obtained from screening the row/column pools corresponding to one of the two positive simple pools (row/column screening was performed by S. Chang), the other row/column pool set remains to be screened. The YAC corresponding to the positive row/column is being obtained.

Screening of the complex pools with nested oligos derived from the *D4Rck22* sequence yielded three positive complex pools. The simple pool sets which make up these three positive complex pools were obtained. Of these three complex pool sets, one has tested negative for the presence of *D4Rck22* (a false positive complex pool screen) and two sets demonstrated positive results. The corresponding row/column sets for these positives are being obtained.

Screening of the Princeton YAC library complex pools for YACs containing *Pgm-2* is currently underway.

Pulse-field analysis of the *Pgm–2, D4Rck22,* and *D4Rck69* loci: Hybridizations to pulse-field gels separating fragments ≤ ~2 Mb, of the *D4Rck22* and *D4Rck69* microclones and a 1.3 kb *Pgm-2* PCR fragment corresponding to a chromosome 4 specific (*Pgm-2* specific) intron/exon boundary fragment were completed. Bands of ~500kb (Asc I), <200kb (BssHII), 460kb (Ela I) and 460kb (Not I) were demonstrated for *D4Rck69*, of ~500kb (BssHII), 600kb (Cla I), and 200-245 kb (Nru I) for *D4Rck22*, and of ~300kb (BssHII and EagI), 1 Mb (Not I), and 580 kb (Nru I) for *Pgm-2*. Partial digestions of Not I and BssHII were attempted by serially diluting the enzyme (15 dilutions of 50% activity each) before addition to the agarose blocks. Separation of the fragments using pulse times of 15 minutes at 70 V for 5 days, were selected to separate fragments in the 500 kb - 3 Mb range. Hybridization of these probes to Southern blots of pulse-field gels failed to yield any interpretable hybridization pattern.

Chapter 4: Discussion

Physiological determinants of obesity

Obesity is the most prevalent nutritional disturbance in modern western societies. Depending upon the diagnostic criteria employed, it has been estimated that as many as 20% of children and 30% of adults in the United States are obese (Burton, et al., 1975).

In functional terms, obesity is a maladaptive increase in the size of the adipose organ relative to lean body mass. Optimal adipose tissue content is dependent upon a variety of factors which include age, health status, genotype and environment. There are clearly physiological and environmental states — such as early pregnancy and incipient famine — when it is advantageous for an individual to have extra calories stored as fat. In other circumstances, such as late gestation or in an environment of readily available food, this extra fat may actually constitute a health hazard. Thus, the definition of obesity is context dependent. A corollary of this argument is that this phenotype will be very sensitive to environmental and other non-genetic factors. This very sensitivity of body composition to phenotype to environment has confounded efforts to quantify the hereditability of obesity.

Body composition is determined by the balance between energy input and energy output. When input and output are of equal magnitude, body composition (degree of adiposity) remains constant. An imbalance between energy intake and expenditure results in a gain or loss of stored energy,

mainly as fat (since more energy is stored as fat than in protein or carbohydrate (Hirsch, et al., 1989)), until a new equilibrium position is achieved. The components of energy input (food intake) and energy output (resting metabolic rate, physical activity, thermic effects of feeding) are determined (Keesey, 1989). Pertaining to energy output, the *resting metabolic rate* represents the portion of energy (close to 60% of total expenditure) which is used in such processes as maintaining the body at constant temperature, in electrolyte and fluid balance, and providing for the nourishment of the organs at rest. The second component of energy output, *physical activity,* is the most variable. It is the determinant of total body expenditure most under conscious control, and represents the cost of activity above baseline. Feeding is an active process, and there is a cost in absorbing, metabolizing, and storing nutrition which is termed the *thermic effects of feeding*. Despite our knowledge as to the components of both energy intake and output, the cellular events which regulate both the input and output aspects of energy homeostasis are poorly understood. A major problem in the study of these systems is that their controls are interlocked in such a way as to make the experimental disarticulation of these processes extremely difficult.

In attempting to understand the regulation of the adipose tissue organ size, it is important to define which parameter is being regulated, either or both, intake or output. Studies examining the relationship of food intake to regulation of body weight have demonstrated no important contribution of

short-term (<24 hours) regulation of intake, but increasing concordance of intake with energy expenditure when longer (≥ 1 week) accounting of intake is considered (Martin, et al., 1991). Experiments in which intake is monitored after a period of either increased or decreased intake has established a new equilibrium weight, demonstrate that food intake diminishes if body weight rises above the 'normal' equilibrium weight , and rises if forced below the 'normal' equilibrium weight (Keesey, 1989). Studies in both rodents and man show similar findings (Leibel and Hirsch, 1984). From these studies, it appears as if intake can be adjusted to 'defend' a set body weight .

The factors that have been implicated as regulators of food intake are numerous. Food in the gastrointestinal system, particularly causing gastric distension, has a demonstrated effect in reducing food consumption. Sham feeding in rats, caused by surgical bypass of the stomach, leads to almost constant eating (Young, et al., 1974). In rats in whom an extra stomach had been transplanted (Koopsman, 1981), distension with pyloric clamping leads to decreased food intake, implying that innervation of the GI tract is not necessary to reduce food intake in cases of extreme distension. Additionally, distension of the duodenum also decreases food intake (Davis and Campbell, 1978). However, vagotomy did block satiation in response to large gastric distension, but not to smaller amounts (Morley, 1987). An interpretation of these data is that gastric distension may play a role in satiety, through both

neural and endocrinological means, although the distension must be large, such as during times of "overindulgence" (Morley, 1987).

A number of hormonal agents have been implicated as gut satients. Both gastrin and gastrin-releasing peptide have been shown to inhibit food intake. Somatostatin inhibits food intake in both rats and baboons (Lotter, et al., 1981). In a study described by the authors, humans with somatostatin producing tumors demonstrated weight loss. However, it is unclear if it is possible to separate the effect of the somatostatin from the cachexia of cancer (perhaps related to somatostatin or other hormones). Bombesin, which shares a similar C-terminal decapeptide with gastrin releasing factor, appears to reduce food intake by a non-vagally determined means, and perhaps by potentiating the effects of other peptides such as CCK (Morley, 1987).

Cholecystokinin (CCK) is a 33 amino acid peptide which acts in a paracrine and endocrine fashion in the GI tract, and as a neurotransmitter centrally. Peripherally administered CCK decreases food intake in rats of all ages (Gibbs, et al., 1973) and in humans (Weller, et al., 1990), and appears to cause satiety via the CCK-A (alimentary) receptor. Corticotropin-releasing hormone (CRF) can inhibit feeding when injected in the region of the ventromedial nucleus or third ventricle. Neuropeptide Y (NPY) is one of the most abundant neuropeptides in the CNS, and with wide-ranging effects including increasing feeding after central administration in rats, mice, squirrels, and pigs (Morley, 1987). This increase can also be seen after

administration of Peptide YY, galanin, growth-hormone releasing hormone and β-endorphin (Bray, 1989a).

The serotonin precursors, tryptophan and 5-hydroxytryptophan both decrease food intake. Drugs which cause release of serotonin from nerve endings (fenfluramine) and/or block the reuptake of serotonin (fenfluramine and fluoxetine, [fluoxetine brand name *Prozac*]) cause a decrease in food intake and when used in humans, cause a modest decrease in body weight (Levine, et al., 1987; Ferguson and Feighner, 1987). Infusion of norepinephrine into the ventromedial hypothalamus (VMH) increases food intake as well, whereas infusion into the paraventricular nucleus has no effect (Shimazu, et al., 1986).

These latter experiments, where neurotransmitters and hormones have been infused into discrete areas of the brain are especially interesting in light of information known from experiments where these same areas have been destroyed by either chemical, electrical or mechanical means. Infusion of low doses of monosodium glutamate to neonatal mice, damages the arcuate nucleus causing an increase in fat deposition despite hypophagia (Lorden and Caudale, 1986). Morley (Morley, 1987), notes that in view of the prominent tracts of NPY neurons from the arcuate nucleus to the hypothalamus, that the decrease in food intake secondary to monosodium glutamate administration, may be secondary to a loss of NPY. Gold thioglucose injections, which lead to hyperphagia and increased adiposity in

mice and rats, selectively destroys the ventromedial hypothalamus (VMH) (Marshall, et al., 1955). In general, the destruction of the ventromedial hypothalamus causes subsequent hyperphagia and obesity while lateral hypothalamic lesions produce a hypophagic syndrome with an associated loss of body fat (Bray and York, 1979; Mayer, et al., 1955; Coleman and Hummel, 1970; Coleman, 1978). These lesions however, effect both food intake as well as energy expenditures.

The data supporting mechanisms able to adjust energy expenditure in order to maintain body weight is also convincing. Kleiber (Kleiber, 1947) noted that the resting energy expenditure of many animals, ranging in size from rodents to cows could be expressed as a function of their body weight (Figure 4.1). The resulting equation, termed "the Kleiber function", states that the daily resting expenditure of animals is proportional to their body weight raised to the 0.75 power.

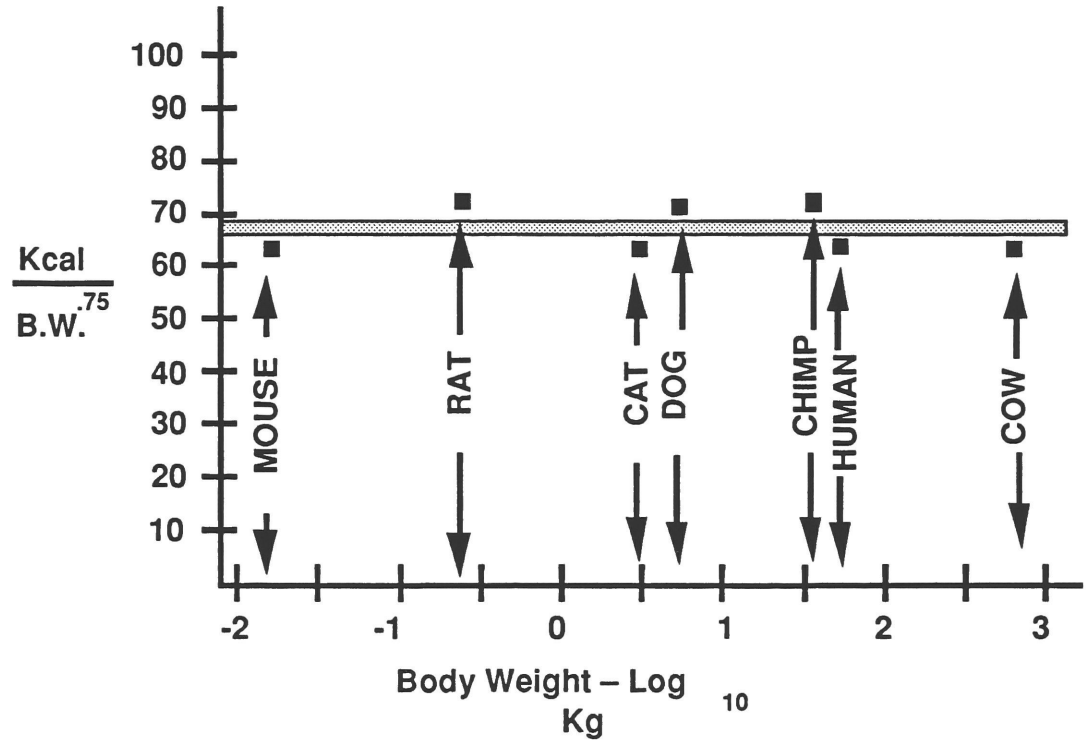

Figure 4.1. Relationship of energy expenditure to body weight, among different mammals, when expressed proportionally to (body weight)$^{.75}$, a relationship termed the "Kleiber function". Adapted from (Keesey, 1989) which was itself adapted with permission from the original (Kleiber, 1947).

Further preliminary unpublished evidence (Keesey, 1989), suggests that the metabolic mass as expressed by the Kleiber equation "may account for much of the variance in resting energy expenditure between different size members of the same species". Evidence is provided which demonstrates that the daily resting energy expenditure for rats is similar when body weight for each rat is raised to the 0.75 power. Furthermore when a rat's weight was reduced by 15%, the resting metabolic rate declined by 25% (Corbett, et al.,

1986). Not until the weight approached normal, did the metabolic rate return to the value predicted by the Kleiber equation. In human studies, declines in resting metabolic rate greater than that predicted by a defined weight loss, have also been noted (Leibel and Hirsch, 1984).

It appears then, that regulation of both food intake, and resting energy expenditure, is under metabolic control, and may play important roles in the regulation of body composition. Other determinants of total energy expenditure, the thermic effects of food and the energy associated with physical activity have not been as well examined. However, reduced total energy expenditure in one family study (Ravussin, et al., 1988), and reduced energy expenditure (particularly of physical activity) in a study of infants born to lean and overweight mothers (Roberts, et al., 1988), have suggested that reduced energy expenditure is an important factor in the development of obesity.

The effect of these controls seems to be in the maintenance of a set weight. Perturbation in the system which alters either the food intake or energy expenditure resulting in deviation from the 'set-point' weight, appears to be met with opposing metabolic changes. There is strong evidence, in the reviewed experiments, for the hypothalamus as being the point of integration of the afferent and efferent limbs of the energy system. However, the exact metabolic basis for this system remains unclear.

Continuing efforts to identify the defects responsible for obesity in humans has been impeded by experimental difficulties in precisely quantifying food intake and energy expenditure, as well as the apparent polygenic control of body composition in man. These considerations have stimulated interest in the simpler models of obesity occurring in certain inbred animals strains, particularly mice. Of the many mouse models of obesity that have been studied, the most intensely investigated have been the genetic obesity mutants, particularly *ob* and *db*. As noted, these animals are phenotypically indistinguishable when bred onto the same background strain. Parabiosis experiments have also suggested that the *ob* mutant may encode a circulating satiety factor for which the *db* mutant has a defective receptor.

Parabiosis

Parabiosis utilizing the A^{y} (Yellow) mouse

The first investigation of mice with a hereditary obesity defect, the yellow (A^{y}) mouse, was by Cuénot in 1905, although previous investigators had described the mice (Weitze, 1940). Initial parabiosis experiments, between yellow/obese non-inbred and 'normal' non-inbred mice, performed by Weitze (Weitze, 1940), suggested that a hormonal difference existed between 'normal' and A^{y} mice. Parabiotic union of the two types of mice caused the

yellow mouse to remain non-obese, thus she postulated that some hormonal type factor was responsible for the weight gain.

Wolfe, repeating the experiments (Wolfe, 1963), was unable to confirm these original findings. In his parabiotic unions, the growth of the yellow mice were unaffected by parabiosis to lean mice. Differences between the two experiments were substantial. The mice used by Weitze were not inbred, over 70% of her parabiotic pairs died within 72 days, and her final weight curves for the single mice were lower than that for non-parabiosed mice of the appropriate phenotype. The parabiotic operation performed by Wolfe was technically superior to that performed by Weitze. Whiskers and toe-nails on the sides of the animals to be joined were clipped, preventing eye/wound infections due to irritation. To prevent excessive stretching of the skin, strips were cut from the dorsal and opposing ventral surfaces, greatly reducing morbidity and mortality in the procedures. Evans blue dye was injected intraperitoneally into one pair member, and the remaining animal examined for presence of the dye, thereby insuring capillary anastomosis between the animals, and circulation connection. The superior technical nature of the parabiosis was evident in that there only eighteen parabiotic pairs (out of 106 prepared) died before 1 month of age, presumably of procedure related events and 2/60 isogenic pairs which died after 3 months. However, parabiotic unions between non-isogenic strains resulted in 12 deaths from 41 tested pairs during this same period. The lack of weight gain by the yellow partner of a

parabiotic union in Weitze's experiments, may have been the result of rejection (termed 'parabiosis intoxication'), rather than from a transferred hormonal agent.

Parabiosis of *db/db* and +/+ mice

}L/KsHu *db/db* with C57BL/KsJ +/+ mice, performed by Coleman and Hummel (Coleman and Hummel, 1969), demonstrated that the normal partner lost weight, became hypoglycemic and died of apparent starvation within 50 days of surgery. Four pairs of similarly parabiotically joined normal C57BL/KsHu and C57BL/KsJ mice, thrived until sacrifice 4 months after surgery, while one parabiotic pair of C57BL/KsHu *db/db* mice died at 24 days, one at 52 days and the other two survived past 60 days. Weights of the *db/db* partner in the *db/db* — +/+ pair were statistically significantly lower than single *db/db* animals, while the *db/db* — *db/db* individual weights were not provided. Additionally, at 3 weeks post-parabiosis, *db/db* animals in both the *db/db* — +/+ parabiotic pairs, and in the *db/db* — *db/db* pairs had lower [glucose] (162 ± 16.1 and 137 ± 19.6 mg/dl respectively) than single *db/db* animals (287 ± 40.7). Additionally, *db/db* animals in the *db/db* — +/+ parabiotic pairs demonstrated a lower insulin than single *db/db* mice (356 ± 26.5 vs. 888 ± 240 μu/ml), no insulins were reported for the *db/db* parabiotic pairs.

The initial interpretation of these data is that the *db/db* animals may have a large amount of a circulating satiety factor which caused the normal animals in parabiosis with them to starve themselves. Difficulties with the interpretation of these data occur since the differences in [glucose], [insulin] and weights between the single non-parabiosed *db/db*, *db/db — db/db* parabiosed, and *db/db* in the *db/db* — ++ parabiosis, support some effect of the parabiosis itself on the diabetic phenotype. *Db/db — db/db* parabionts should have been metabolically similar to the single *db/db* animals if no such effect were occurring. Although operational considerations may have contributed to the observed differences in glucose, insulin and weights, the *db/db* partner in the *db/db* — +/+ anastomosis would still be expected to have a similar metabolic profile to the *db/db — db/db* parabiotic pairs. Alleviation of diabetes in *db/db — db/db* parabionts may have resulted from their decreased weight, thereby improving their glucose tolerance. However, in Coleman's *ob/ob* parabiosis experiments (see next section), *ob/ob — ob/ob* parabionts manifested a less severe diabetic syndrome as compared to single *ob/ob* mice, despite gaining a similar amount of weight. The parabiotic normal control pairs however, appear to effectively rule out major histocompatibility as a cause for these differences or the starvation of the +/+ animals in parabiosis with *db/db* animals.

Parabiosis of *ob/ob* with *db/db* or +/+ mice

Three examples of parabiosis between *ob/ob* and +/+ mice (Hausberger, 1958; Chlouverakis, 1972; Coleman, 1973), one of which included *ob/ob* — *db/db* parabionts (Coleman, 1973), have been reported. Hausberger reported that parabiosis of lean mice with *ob/ob* mice suppressed weight gain in the obese animals and completely suppressed obesity in a few *ob/ob* animals. Chlouverakis found that lean parabiotic mice gained less weight when joined to another lean animal as compared to single lean mice and lost weight when parabiosed to *ob/ob* mice. Similarly, *ob/ob* animals in union with lean mice gained a relatively small amount of weight (2.5 ± 1.9 g) as compared to *ob/ob* animals joined with other *ob/ob* animals (11.7 ± 1.4 g) or single *ob/ob* animals (14.6 ± 2.5 g). A small, but statistically significant, drop in [glucose] in +/+ — +/+ parabionts compared to single lean animals was seen. *Ob/ob* animals had a lower blood glucose when joined to lean animals (203 ± 16.7 mg/dl) than when joined to obese animals (288.3 ± 46.7) or that seen in single obese animals (415 ± 50.4). No data were available from these studies concerning food intake. Animals were not weight reduced before parabiosis at ~4 weeks of age.

The parabiosis experiments described by Coleman were carried out in a technical fashion similar to the previously described *db/db* parabiosis (Coleman and Hummel, 1969). *Ob/ob* animals in parabiosis to lean animals demonstrated lower [glucose], [insulin], weight gains, and food intake as

compared to *ob/ob* animals parabiotically joined to other *ob/ob* animals. In addition, the *ob/ob* — *ob/ob* parabionts demonstrated lower [glucose] at three weeks, lower [insulin] at 60 days, but a similar weight gain, to single *ob/ob* animals. The lean partners of *ob/ob* animals did not differ significantly from single lean mice (data for the latter not reported). However, the weight gain, [glucose] and [insulin] associated with +/+ — +/+ parabionts were lower than single lean mice. These data do not differ significantly from those previously reported, except in the magnitude of the changes involved.

Analysis of the *ob* and *db* parabiosis experiments

The parabiotic union of the C57BL/6J-*db*^{2j} congenic to the C57BL/6J-*ob* congenic strain manifested results similar to those seen with the parabiosis of the C57BL/KsHu *db/db* with C57BL/KsJ +/+ mice. The *ob/ob* mouse exhibited anorexia, weight loss, hypoglycemia and eventual death. Together, these data were interpreted as evidence which supported the hypothesis that *ob/ob* animals have a genetic lesion in a circulating satiety factor to which *db/db* animals have a defective hypothalamic receptor for. Thus *db/db* animals overproduce this factor, causing anorexia and eventual death in any parabiotic union. *Ob/ob* animals would be expected to gain less weight, or fail to manifest obesity/diabetes, if able to obtain this factor through parabiosis.

The favored location for the putative satiety receptor which *db* is believed to encode, has been in a 'satiety center' in the hypothalamus. Much

of the speculation results from the similarity in phenotype, including in parabiosis, between hypothalamically lesioned animals and the genetically obese *ob* and *db* mutants. However, differences have been described between the obesity produced by the genetic obesities, and those that produce obesity by hypothalamic lesioning. For instance, the animals with a genetic obesity are hyperphagic, but unlike the hypothalamic obesities, this hyperphagia is not essential for the development of obesity (i.e. they demonstrate a decrease in energy expenditure), nor do they exhibit a diet dependence (high or low carbohydrates) in manifesting obesity (Bray, 1989b).

The hypothesis that *ob* encodes a 'satiety' factor to which *db* encodes the receptor, is substantiated to some degree by the parabiotic experiments and the fact that *ob/ob* and *db/db* animals are indistinguishable on the same genetic background. Strautz (Strautz, 1970), examining the development of obesity in *ob/ob* animals after transplantation of pancreatic islets in millipore filters, suggested that *ob/ob* animals are defective in producing a pancreatic factor(s). Within 14 days after implantation of non-obese islets into *ob/ob* animals, weight gain was stabilized, and glucose and insulin levels were reduced. Weight gain could be reestablished immediately after removal of these chambers, while hyperglycemia and hyperinsulinemia followed within 45 days. Gates et al. (Gates, et al., 1974) found that, in a similar paradigm, a non-β cell factor in islets could ameliorate the obese phenotype in the polygenic New Zealand obese (NZO) mouse. Since multiple genes are

involved in the pathogenesis of obesity in NZO mice, it is hard to conceptualize how the pancreatic "factor(s)" being replaced by these procedures could account for the primary lesions for all the genes which affect the pathogenesis of obesity in the NZO and *ob* mice. Because of this significant problem, these experiments should not be cited as evidence that the protein encoded for by the *ob* gene is expressed by the pancreas in such a manner that it was replaced during the pancreatic transplants. It may be that the amelioration seen in both the *ob/ob* and NZO mice after pancreatic transplantation is due to some secondary factor which ameliorates the symptoms but is not the central lesion, or may have been secondary to technical issues in the experiments.

These data, in conjunction with the hypothalamic studies described, are consistent with the presence of a circulating satiety factor produced peripherally (*ob*) to which a receptor (*db* — ? hypothalamic) exists. Possible difficulties in interpreting these results is that the functionality of the parabiotic anastomosis was not established (or at least not reported) in these studies, nor was mention made as to whether clipping of the nails and whiskers were affected (or not necessary), as in the case of Wolfe's *Ay* parabiosis. This latter technical consideration could cause delayed wound healing which affected the +/+ partner to a greater extent although the apparent survival of the +/+ — +/+ parabiotic pairs makes this latter possibility unlikely.

One possible confounding variable that was not addressed in the reported results is that in order to facilitate the operational procedure, the *db/db* animals (and although not specifically reported, it appears *ob/ob* animals as well) utilized were first reduced in weight by food restriction for 25 to 93 days until their weights were near normal. Reduced obese *db/db* animals may differ metabolically from *db/db* animals fed ad-libitum, as changes to retain the higher weight could be severe. Indeed, in these studies, reduced obese *db/db* animals never attained as severe hyperglycemia as *db/db* mice fed *ad libitum* throughout life. No mention is made in the *ob/ob* parabiosis experiments if the reduced *ob/ob* animals attained as severe hyperglycemia as *ob/ob* mice fed *ad libitum* throughout life. It is possible that products of metabolism, or an altered level of some neurochemical signal (such as CCK) resulting from the reduced–obese state, and not a physiologically functional satiety factor, could account for the anorexia in the normal and *ob/ob* partners of the *db/db* parabionts. Since *db/db* animals result from a different genetic lesion from *ob/ob* animals, it is conceivable that *db/db* animals cannot respond to this product as effectively as either *ob/ob* or normal mice. It is therefore possible to explain the death of both lean and *ob/ob* animals in parabiosis with *db/db* animals, if the latter had a high level of a factor which altered the metabolic homeostasis of non *db* animals, but did not necessarily cause satiety. Whether this state may have resulted from the reduction in weight that preceded the parabiosis of the

db/db animals or not, the result would be the starvation of the *db/db* animal's parabiotic partner.

Evidence for such a signal can be found in other parabiosis experiments (Harris and Martin, 1989; Martin, et al., 1991). In a parabiosis model which involved the union of two non-obese rats, one animal of each pair was tube fed until obese, during which time the 'lean' partner would lose weight. An *in-vitro* assay was developed that quantified fatty acid synthesis, and the assay used to screen blood drawn from the parabiotic rats for fatty acid synthesis inhibiting activity. A glycoprotein of M.W. > 30 kD, which inhibits fatty acid synthesis, appears to be released by the obese rat in response to significant weight gain. What role this, or other similar factors, may play in normal physiological maintenance of body weight in uncertain. Whether this is the factor, or a contributing factor, to the weight loss manifested by partners of *db/db* parabionts is also unclear. In interpreting the results any of these parabiosis experiments, the presence of such factors must be considered. Ideally, the parabiosis experiments involving the *db/db* mice could be repeated independently to confirm their results, and to take into consideration the questions that have been raised. However, the hypothesis of satiety factor/receptor is an important one, that needs serious consideration when analyzing the genetics, and implications of the possible cloning of the *ob* and *db* genes.

Alteration of the obesity/diabetes phenotype in genetically obese animals by steroids

Adrenal steroids have long been implicated in the development of diabetes and obesity. Cushing's disease, whose pathogenesis is varied, invariably leads to accumulation of body fat and the increased cortisol levels precipitating glucose intolerance. Obesity in rats induced by hypothalamic lesioning is alleviated to varying degrees by adrenalectomy (Bruce, et al., 1982). Food intake is reduced to near normal levels by adrenalectomy as well (Saito and Bray, 1984). Bray (Bray, 1989b; Bray, 1989a) notes that sympathetic activity is increased in genetically obese animals after adrenalectomy. CRF is increased after adrenalectomy owing to the loss of feedback inhibition by corticosterone, and CRF can inhibit feeding when injected in the region of the ventromedial nucleus or third ventricle (Morley, 1987). Bray has used these data to suggest that the defect in the *fa/fa* rat (and therefore in the *db/db* mouse as well) is in producing a modulator of the steroid-receptor complex with the promoter region of certain, yet undefined, steroid responsive genes. Increased levels of corticosteroids in *db/db* mice would decrease CRF production by feedback inhibition, causing an increase in weight and diabetogenesis. Although it is possible that the *db* gene product is a transcriptional repressor of certain steroid-responsive genes, it is no more probable than the steroid effect being secondary to another metabolic perturbation caused by loss of the *db* gene. However, these experiments do

clearly define that adrenal corticosteroids are permissive for the genetic obesities.

Sex steroid involvement in the pathogenesis of the obesity/diabetes of the genetically obese mice has been demonstrated as well. Estrogens tend to have a beneficial effect in alleviating the diabetes seen in homozygous C57BL/KsJ males (Prochazka, et al., 1986), whereas androgens exacerbate the diabetes (Paik, et al., 1982; Morrow, et al., 1980). Both estrone (Prochazka, et al., 1986), and dehydroepiandrosterone (DHEA) (Coleman, 1988) have demonstrated efficacy in alleviation of the diabetes component of the obese/diabetic syndrome evident in C57BL/KsJ db/*db* mice. DHEA had the additional benefit of reducing the rate of weight gain in C57BL/6J *db/db* and *ob/ob* mice, and in viable yellow (A^{vy}) mice it cause a marked decrease in weight gain and plasma [insulin] (Coleman, 1988). Differing levels of steroid sulfotransferase (ST) activity (which block the receptor - sex steroid interaction by sulfurylation of sex steroids) have been implicated in the diabetogenic pathogenicity of the background strain on which the *db* gene is engrafted (Erickson, et al., 1983; Leiter, et al., 1987). Increased activity of sulfurylation of estrone increases diabetogenesis, and the failure to sulfurylate DHEA (an androgen precursor) is associated with hyperglycemia amongst female C57BL/6J *db/db* mice (Leiter, et al., 1987). In general, failure to remove androgen prehormones (such as DHEA), to inactivate circulating androgens, or inactivation of estrogens (Leiter, et al., 1989), increases diabetogenicity of

the background strain on which *db* is engrafted. Conversely, increasing estrogen levels decrease the diabetogenicity of the background strain (Leiter, 1989). The steroid sulfohydrolase gene (STS), which is sex-linked and expressed on both the X and Y chromosomes, activates sulfated sex steroids by hydrolyzation of the sulfur group (Keitges, et al., 1987). Diabetogenicity of a particular strain towards *db*, may then be explained by the relative activity of cytosolic ST (inactivating sex steroids) and microsomal STS (activating sex steroids). However, the mechanism by which the sex steroids may alter diabetogenicity of the *db* gene is not known (Leiter, 1989). In these studies, the excess number of deaths seen among the males of the (C57BL/6J *db/db* X DBA/2J) F1 X C57BL/6J *db/db* intraspecific backcross is consistent with this pattern of attenuation of diabetogenesis by female sex hormones.

Discussion of experimental results

Generation of a moderate resolution genetic map of chromosomes 4 and 6

In order to localize the *db* and *ob* genes to chromosomal regions of mouse chromosomes 4 and 6 respectively, 10 probes on mouse chromosome 6 and 19 probes on chromosome 4 were mapped relative to one another using the offspring of an interspecific C57BL/6J X *M. spretus* backcross (Figures 2.1 and 3.3). Several new assignments were made, including *UROD*, *EL1*, and *C8B* on chromosome 4 as well as *Npy* and *NKNA* on chromosome 6. In addition, regional assignments for *Ggtb*, *Glut-1*, *Fuca*, and *Fabph-1* on chromosome 4, and *Rpl32* to distal chromosome 6, were made and refinements in the position of *Mup-1*, *Orm-2*, *b*, *Jun* and *Ifa* were established. Finally, *Cola-2* and *NKNA* were shown to be proximal to *Met*. The refinements in position can be seen in Figures 3.3 and 3.6, where the linkage maps generated by this study are compared to the composite mouse linkage maps of mouse chromosomes 4 and 6 respectively. These composite maps (personal communication) were compiled by M.T. Davisson, T.H. Roderick, A.L. Hillyard, and D. P. Doolittle at the Jackson Labs (Bar Harbor, Ma.) for June 1990.

The results of these studies generally agree well with the June 1990 Davisson -- Roderick map and other earlier reports (Ceci, et al., 1989), (Fletcher, et al., 1991) with a few exceptions. On chromosome 4, *Orm-2* was

positioned more proximally than has been previously reported. The prior positioning of *Orm-2* distal to brown was based on RI data from the AKxD RI lines in which the SDP of *Orm-1* was compared to *b* and *Ly-19*, (Baumann, et al., 1984) as well as the demonstration of tight linkage (0/58 backcrossed animals) between *Orm–1* and *Orm–2* (Baumann and Berger, 1985). Incorrect orders may be inferred from RI strain data because multiple recombination events can occur in generating each RI strain (Eicher and Lee, 1990; Nadeau, et al., 1991). Additional data from the (AKR/J x *M. spretus*) x AKR/J backcross identified 6/56 recombinants between *Orm–2* and *Mup–1* (Baumann and Berger, 1985). This study provided no information as to the placement of *Orm–2* with respect to *b* or *Ifa*. In a similar AKR/J x *M. spretus* backcross, 23 N2 progeny were typed for *Mup–1*, *Ifa* and *Orm–1* establishing the order cen -- *Mup–1* -- *Orm–1* -- *Ifa* (Nadeau, et al., 1986). These data are consistent with the positioning of *Orm-2* reported here. In support of the recombination frequencies demonstrated in this analysis, at least one other study (Ceci, et al., 1989) demonstrated a distance, in an N2 cross essentially identical to ours, between *Ifa* and *Mup-1* (of 15.6 cM). *Orm-2* has also been mapped to a similar location using a (NOD x C57BL/10) x NOD backcross. In this cross, 1/135 animals was recombinant between *Mup–1* and *Orm–2*, and *Orm–2* was positioned distal to *Mup–1* (John Todd, personal communication). Together these data strongly support the presented map order and distances for *Mup-1*, *Orm-2*, *b* and *Ifa*.

On chromosome 6, no linkage of *Pcn* or *Por* to any of the RFLPs was detected. Previous data mapping these genes (*Pcn, Por*) to chromosome 6 was based on the typing of somatic cell hybrids (Simmons, et al., 1985). The failure to detect linkage of these loci to other loci on chromosome 6 suggests that either the previous assignment was incorrect, or that there are differences in map position between *Mus laboratorious* and *Mus spretus*. Numerous studies employing interspecific *M. laboratorious* x *M. spretus* have been carried out, and to date only one rearrangement, a small inversion of mouse chromosome 17 associated with certain *t* haplotypes, has been detected between the laboratory *laboratorius* strains and *M. spretus* (Hammer, et al., 1989). This latter possibility can be examined by mapping *Pcn* and *Por* using intraspecific laboratory *laboratorius* crosses. If those studies generate similar results, then the previous mapping data may have been the result of rearrangement or the presence of another undetected chromosomal fragment in the interspecific somatic cell hybrids employed (Simmons, et al., 1985). Previous mapping efforts have demonstrated the sometimes erroneous results obtained when using interspecific somatic cell hybrids for gene mapping (Azen, et al., 1989).

A previous study assigned *Cola-2* to proximal chromosome 6, linked to *Met*. This study did not define the order of *Met* and *Cola-2* with respect to the centromere (Irving, et al., 1989). An order which positions *Cola–2* 7 cM distal to *Met* is apparent on the composite map (Jackson Labs) of mouse

chromosome 6 (Figure 3.6). The present study demonstrates that *Cola-2* is proximal to *Met*, and that the *NKNA* gene on human 7q is nonrecombinant with *Cola-2*, and is thus located proximal to *Met* as well. On distal mouse chromosome 6, the distance between *Prp* and *Kras–2* is calculated to be 7 (+/-2.7 (S.D.)) cM, while the composite map in Figure 3.6 has the same distance shown as 14 cM. A previous mapping study in this interval combined RI strain distribution patterns and data on *Kras–2* and *Prp* in three test crosses between laboratory strain mice, to demonstrate a weighted recombination frequency average of 0.168 +/- 0.038. (Azen, et al., 1989) The reasons for this discrepancy between the previous and present studies in the distance but not order of *Kras–2* and *Prp* are not apparent, but may be due, in part, to strain-specific differences in the crosses. As more probes are placed in this interval, and different crosses employed in mapping these probes, this discrepancy should be resolved.

The mapping data for chromosomes 4 and 6 extend previous observations concerning the synteny between distal mouse chromosome 4 and human 1p and between proximal mouse 6 and human chromosome 7p (Bucan, et al., 1986; Nadeau, 1989). On chromosome 6, two additional genes from human 7p, *NKNA* and *NPY*, have been mapped to the respective extreme proximal and distal ends of this syntenic group. The order of the genes between *NKNA* and *Npy* has been determined to be: *Cola-2* -- *Met* --

Cpa -- *Tcrb*. This interval defines an approximately 18 cM long conserved linkage group between mouse and man.

On chromosome 4, a group syntenic with human 1p extends from *Jun* proximally to *Pnd* distally. The breakpoint of this syntenic group in mouse appears to be in a 2 cM interval between *Jun* and *Ifa* on chromosome 4. In humans, the break appears to be distal to *ACADM* which was mapped to mouse chromosome 8 using the BxD RI lines. The gene order over this interval correlates extremely well between human and mouse (Figure 3.4). In the case of *UROD*, for which there is deviation in the order between human and mouse, the regional assignment in human was made on the basis of a single *in situ* hybridization experiment and has not been confirmed (Mattei, et al., 1985). *Jun* and *Lmyc-1*, which flank *UROD* in mouse (Figure 3.4), have been assigned to the 1p31- 32 bands in human by linkage studies (*Lmyc–1* --(Dracopoli, et al., 1988; Dracopoli, et al., 1989; Zelinski, et al., 1988; Rouleau, et al., 1990)), by analysis of somatic cell hybrids (*Jun* -- (Haluska, et al., 1988)) (*Lmyc–1* -- (Dracopoli, et al., 1989)), cell lines harboring translocations in this region (*Jun* -- (Hunt and Tereba, 199O)), and by *in-situ* hybridization (*Jun* -- (Hattori, et al., 1988; Haluska, et al., 1988)) (*Lmyc-1* -- (Nau, et al., 1985)). The order presented in Figures 3.3 and 3.4 of *Jun* — *UROD* — *Lmyc–1* — *Lck* is 300 times more likely than *Jun* — *Lmyc–1* – *UROD* – *Lck* and > 10^{15} times more likely than any other order in this region using the MAPMAKER program (Lander, et al., 1987). Considering the conservation of order between

the other 1p31-pter markers in human and mouse, the data suggest that order is conserved in the region of *Jun* — *Lmyc–1* as well, and that the previous assignment of *UROD* to 1p34 in human may be in error; its more likely location is 1p32. It will be of interest to compare the evolving genetic map of human 1p with the map reported here, and discern if the position of *UROD*, to 1p32 vs. 1p34, is correct.

As has been previously reported for mouse chromosomes 2 (Siracusa, et al., 1989), 4 (Ceci, et al., 1989; Fletcher, et al., 1991), 7 (Saunders and Seldin, 1990), 9 (Kinglsey, et al., 1989), and 12 (Seldin, et al., 1989; Blank, et al., 1988), evidence is presented for suppression of multiple recombination events on mouse 4 and 6. These studies fail to confirm the previous reports of segregation distortion on distal (Ceci, et al., 1989) and proximal (Shaper, et al., 1990) chromosome 4, but is similar to a report which failed to detect segregation distortion on chromosome 4 (Fletcher, et al., 1991). The reason for these discrepancies is unclear.

Use of a flow-sorted 4:6 library to increase saturation of the genetic maps

Detailed genetic and physical mapping of mammalian chromosomes is greatly facilitated when a source of DNA probes which is enriched for the chromosome of interest is available. Several methods are currently available for developing chromosome specific clone banks. These include: 1)

chromosomal microdissection and microcloning (Bates, et al., 1986; Tonjes, et al., 1991; Ludecke, et al., 1989) 2) the screening of libraries from somatic cell hybrids (including irradiation hybrids) with species specific repeat sequences (Glaser, et al., 1990)and 3) fluorescent-activated chromosome sorting.

The availability of a library prepared by fluorescent-activated sorting of individual chromosomes provides a source of probes that is of high complexity and which can be used directly for genetic mapping. This approach, which has been used successfully to prepare libraries from each of the human chromosomes, has greatly accelerated the genetic mapping of individual human chromosomes. The use of this technique for sorting human chromosomes has been facilitated by the fact that the human chromosomes are metacentric, of disparate sizes and are often found as the only human chromosome in mouse:hamster somatic cell hybrids. Chromosome sorting of mouse chromosomes has been limited by the fact that the mouse chromosomes are acrocentric and of generally similar size. In addition, very few mouse chromosomes are found in monochromosomal hybrids (Cram, et al., 1990; Bartholdi, et al., 1987; Gray and Cram, 1990).

Nevertheless, sorting of mouse chromosomes has proven possible when the source of the mouse chromosome was karyotypically abnormal. The most notable example has been the use of cells from mice carrying the T(X;7)1 Ct translocation as a source of active and inactive X chromosomes (Disteche, et al., 1981). Flow sort libraries enriched for the mouse X

chromosome have been derived using this cell line. The general approach suggested by these studies of using translocation chromosomes as the source of chromosomes for FACS has not been fully explored. The availability of a great number of translocation chromosomes in mouse including Robertsonian translocations (centromeric fusions between chromosome pairs) makes it possible in principle to enrich for DNAs from any of the mouse chromosomes or from specific chromosome pairs (Capanna, et al., 1976). Comprehensive lists of the available Robertsonian chromosomes have been compiled and document a wide range of available chromosome pairs.

In order to test the feasibility of using Robertsonian chromosomes for chromosome sorting in mice, a fluorescent chromosome sorting of a 4.6 Robertsonian translocation chromosome was accomplished. This chromosome is 61.9% larger than mouse chromosome 1 which is the largest single mouse chromosome (Disteche, et al., 1981). In addition it is the only metacentric chromosome in the cells which carry it. These features have made it it possible to sort a library which is ~72% pure for these chromosomes which correspond to an ~6-fold enrichment. This compares favorably with previous efforts to make chromosome specific libraries from the human genome or from the mouse X chromosome. DNA which is not from either of these chromosomes is likely the result of aggregation of chromosomal debris in larger complexes which sort along with the Robertsonian chromosome.

A total of 14 new loci from this library have been placed on the locus map of these chromosomes as reported here (Figures 3.12). In addition, eight microsatellite sequences from the library have also been mapped to chromosome 4 and 6 by Cornall et al. (Cornall, et al., 1991). While there is a somewhat higher density of loci on distal chromosome 6, it is unlikely that the library is enriched for sequences from a particular subchromosomal region since the sorting of the chromosome requires that it be intact. It is anticipated that the continued use of this resource as a source of anonymous DNA sequences should allow the rapid development of dense genetic maps of these chromosomes. The use of simple sequence repeats (SSRs or microsatellites) has particular appeal in this regard because these sequences define sequence tagged sets that can be used to type genetic crosses directly. Preliminary experiments to isolate these sequences from the library suggest that SSRs are present at the expected frequency and that they likewise map with the expected frequency to chromosome 4 or 6. The mapping of 278 such sequences should result in ~100 novel SSRs being placed on each of the genetic maps of chromosomes 4 and 6. The use of automated sequencing and robotics make the mapping of this number of loci feasible. In addition these data demonstrate the feasibility of using mouse Robertsonian chromosomes to generate libraries enriched for sequences from selected pairs of mouse chromosomes.

Segregation of the *db* gene in interspecific and intraspecific crosses

The initial steps in attempting to clone the *db* gene were directed at creating a complete genetic map of mouse chromosome 4, in essence creating the framework for further mapping efforts focusing on regional localization of *db*. Before consideration could be given towards microdissection of the region, and creation of the high density genetic map needed for initiation of the physical mapping, it was important to accurately determine where *db* is located on the chromosome, as well as create the genetic resource for determining where new loci are located relative to *db*. Previous experiments by others had determined that the *db* gene was located near the misty (*m*) coat color marker (Lane, 1968; Doolittle, et al., 1991). With the knowledge that *m* was near *db*, and also near *Ifa*, it was possible to select flanking markers from the previously described chromosome 4 mapping studies with which to initiate the genetic mapping of the *db* gene itself.

The position of *db* was obtained relative to a series of RFLPs by characterizing 132 N2 offspring of the intraspecific backcross between C57BL/6J *db/db* and B6D2 F1 *db/+* mice (Figure 2.3), and 48 obese progeny of the B6D2 F1 *db/+* X B6*spretus* F1 *db/+* intercross (Figure 2.5). Additional mapping data, and a suitable source of future meiotic information was obtained from the 216 F2 offspring of the intraspecific F2 intercross between(C57BL/6J *db/db* X DBA/2J) F1 mice (Figure 2.6), however in-depth analysis of the pedigree was not performed. Since the 396 offspring of the

B6*castaneus* F1 *db*/+ X B6*castaneus* F1 *db*/+ intercross (Figure 2.4) were used exclusively for mapping of the microclones, and generation of a dense genetic map for physical mapping, these animals are not included in the following discussion of the intraspecific B6D2 *db*/+ X B6 *db*/*db* (N2) backcross and interspecific B6D2 *db*/+ X B6*spretus* (F2) crosses.

A protocol using BMI (weight/length^2) and plasma [glucose] and [insulin] was used to assign genotype at the *db* locus. Inclusion of measurements of [glucose] and [insulin] in this analysis ensured correct assignment of genotype among the progeny of the intraspecific cross. Despite these precautions, analysis of the progeny of the interspecific B6D2 *db*/+ X B6*spretus db*/+ interspecific cross suggested either a phenotypic misassignment or a double crossover in one apparently obese (*db*/*db*) animal (#337). Mapping of additional RFLPs between the flanking markers *Jun* and *D4Rp1* will be necessary to distinguish these possibilities.

Data from the intraspecific backcross and interspecific *spretus* cross position *db* approximately 10 cM distal to *b* (the brown locus), 4.5 cM distal to *P*λ *Mm3*$_2$, 3 cM distal to *Ifa* and *Jun*, 5cM proximal to *D4Rp1* and *MTV–13*, 7 cM proximal to *Glut–1* and 12 cM proximal to *Lck*, (see Figure 3.19). This gene order is consistent with that previously reported. Specifically, the data position *MMTV* distal, and *Ifa* proximal, to *db*, as suggested by Huppi et al. (Huppi, et al., 1988). Because some probes could not be mapped on both

crosses, the order of *MMTV* relative to *Glut–1* and *D4Rp1* remains ambiguous.

These data demonstrate that *db* is flanked by a series of RFLPs which have been mapped to human chromosome 1p31-36 (see Figure 3.4), and suggest that if there is a human homologue of *db* it would probably map to chromosome 1p. This information may be useful in the analysis of the heritability of human obesity and type II diabetes. Humans with a defect in the human homologue of the *db* gene (if one exists) might be expected to cosegregate RFLPs from this chromosome with an obese and/or diabetic phenotype in human pedigrees.

The characterization of the progeny of the crosses described is an important first step in the genetic mapping of this region. However, the future utility of the B X D offspring (both N2 and F2 crosses) in defining the sub-centimorgan intervals surrounding *db* is uncertain. The lack of a C57BL/6J *db/db* X DBA/2J *C8B* RFLP, despite the presence of a C57BL/6J X DBA/2J RFLP suggests contamination of the region surrounding *db* by DBA/2J genome. YACS obtained from screening of the *Pgm-2, D4Rck22 and D4Rck69* loci will be used to define B X D polymorphisms, which will allow the question of the extent of this 'contamination' to be resolved. Any markers demonstrating a polymorphism of any type, SSR, DGG or RFLP, can access the combined 566 meiosis in the B X D N2 and F2 crosses. This will expedite the ultimately narrowing of the nonrecombinant around *db*.

Expansion of these crosses or other similar crosses according to the protocols suggested should allow even finer genetic mapping of this mutation to the sub-centimorgan level. (Freud, 1973).

As part of the phenotypic characterization of the N2 animals, plasma concentrations of glucose and insulin were measured. Analysis of these data reveals that there is a wide range of plasma [glucose] among the *db/db* progeny of the C57BL/6J *db/db* x B6D2 F1 *db/+* backcross, demonstrating a continuous rather than a bimodal distribution. In fact, frank diabetes is frequent in these animals, and in two cases in the intraspecific backcross would have resulted in a misassignment of genotype if only body weight or BMI had been scored. The wide range of [glucose] noted, and the lack of a bimodal distribution, of plasma [glucose] and [insulin] among *db/db* N2 animals support the hypothesis that variability in the development of diabetes among the N2 *db/db* animals results from polygenic influences for the background strain's effect on the development of diabetes accompanying the *db* mutation.

Previous investigators have demonstrated a potent effect of genetic background on the diabetes phenotype of *ob* and *db* animals (Leiter, 1981; Leiter, et al., 1981; Hummel, et al., 1972; Coleman and Hummel, 1975). The diabetes of *db/db* animals is reported to be severe in congenic DBA/2J *db/db* strains, and milder in *db/db* congenic C57BL/6J animals (Leiter, et al., 1981).

The genetic basis for this phenotypic difference between C57BL/6J and DBA/2J mice is unknown.

If the difference in the propensity for diabetes between the C57BL/6J and DBA/2J strains were inherited as a single allele, segregation of the N2 animals into two distinct groups with regard to [glucose] and/or [insulin] would be expected. The wide range of plasma [glucose] and [insulin] in the *db/db* N2, and the failure to detect a bimodal distribution in plasma [glucose] or [insulin] in these animals, (representing either the C57BL/6J or DBA/2J allele), indicate that more than one locus in combination with environmental differences are likely to be responsible for the differential strain susceptibility to the diabetogenic influence of *db*. The conclusion that polygenes can contribute to differences in the diabetogenicity of the *db/db* genotype amongst inbred strains is consistent with that reached by Kaku et al. in the context of an intercross between C3H/HeJ x C57BL/6J +/+ animals (Kaku, et al., 1988), and between *db*/+ C57BL/KsJ and 129/J mice (Kaku, et al., 1989).

One other interesting finding concerned the life span of the male *db/db* N2 animals. Previous studies have shown that congenic C57BL/6J *db/db* animals of either sex have a mildly reduced lifespan compared to the average of 22 months in wild-type (+/+) mice (Coleman, 1978). Studies of the congenic strain DBA/2J *db/db* have reported respective mortalities of 73% and 25% by five months of age in males and females (Leiter, et al., 1981). In

the present study, male progeny of the intraspecific cross appeared to show a markedly increased rate of death that apparently occurred prior to their weaning at 4 weeks of age. Premature death of males prior to weaning is surprising given results from earlier studies of DBA/2J and C57BL/KsJ *db/db* animals which report an increased mortality of males between three and five months of age. In addition, the F2 offspring did not demonstrate a premature loss of males. While differences in diabetes susceptibility and viability between male and female animals have been demonstrated in other circumstances, the reason for premature death among the male N2 animals remains unclear (Leiter, et al., 1987; Boucher, et al., 1974; Morrow, et al., 1980).

Microdissection and Microcloning of mid/distal chromosome 4

The potential to rapidly generate region-specific clone banks by the techniques of microdissection and microcloning has been well documented in other laboratories. The high degree of restriction fragment length polymorphism between interspecific *Mus Laboratorius* x *Mus Spretus* crosses greatly facilitates the mapping of such clones. These two established procedures have been combined in order to develop a high resolution genetic map encompassing the *db* mutation on mouse chromosome 4. The map positions the *db* locus, 7 known genes, 41 microclone markers, and 3 other anonymous probes to a 21cM region of mid/distal mouse chromosome 4, an

area compromising approximately 25% of the total length of this chromosome. In addition, efforts to map the additional ~110 single or low copy microclones continue, and should further saturate this region of chromosome 4 with molecular markers.

The density of markers shown in Figure 3.31 is high, with an average of one probe every 0.5 cM. However, the distribution of the 41 microclones is not even over the 21 cM region. Twenty-six microclones are located within an approximately 7cM region just proximal of *db*, which includes the *b*, *Ifa*, *Jun*, *Odc–4* loci, and the anonymous probe *D4Mit205*. An additional 14 microclones occupy an 11.5 cM region distal to *db* which includes the *C8B*, *D4Rp1*, *Glut–1* loci and the anonymous human probe D1S85. It is unclear whether this distribution is non-random and reflects diminished recombination in the regions around *Ifa* and *D4Rp1*.

The order of the markers as presented in Figure 3.31 is 166X more likely than any other using the MAPMAKER program, which utilizes multi-point linkage analysis to generate genetic maps (Lander, et al., 1987). In addition if the order of the most proximal marker groups, [*D4Rck4, 32, 49A, 138, 196*] — [*D4Rck52,205*] is fixed in their most likely configuration, then the diagramed order is increased to 5370X more likely than any other possible order. The density of markers located in these two regions, including groups of microclones which have not yet been separated genetically from one other, should be a good starting point for the physical mapping of a large portion of

mouse chromosome 4. Any microclone that cannot be physically linked up with its neighbor by Pulsed Field Electrophoresis (PFGE) might be incorporated into the burgeoning physical map by utilizing Yeast Artificial Chromosomes (YACs).

As shown in Fig. 3.31 the *db* locus is flanked by *Odc–4* proximally and *D4Rck22* and *D4Rck69* distally. The genetic distance between these two sets of markers is approximately 1.5 cM. Since, the majority of the meioses used to generate the map do not segregate the *db* mutation, the exact placement of *db* in relation to the flanking markers is not possible using the data presented. However, *Odc–4* demonstrated 0/194 recombinants in the two interspecific C57BL/6J x *M. spretus* crosses with the single-copy probe which detects the *Pgm–2* locus in mouse. In addition, 3/98 progeny (representing 196 meiosis) of the intersubspecific F2 intercross between (C57BL/6J *db/db* X *M. castaneus*) F1 *db/+* animals which carried the *M. castaneus* RFLP allele for *Ifa* (Figure 3. 21) also demonstrated the *M. castaneus* allele for *Pgm–2* (data not shown). These data place *Odc–4* and *Pgm–2* approximately 1.5cM proximal to *db*. Two recombinants have been detected between *db* and both *D4Rck22* and *D4Rck69* among the 48 offspring of the [B6D2 *db/+* F1 X B6*spretus db/+* F1] intercross (Figure 3.30), as well as one recombinant (from a total of 772 meiotic events) among the B6*castaneus db/+* F1 intercross animals (Figure 3.21). These three recombinant animals establish that *D4Rck22* and *D4Rck69* are distal to *db*. Together, these data support the placement of *Odc–4* and *Pgm–2* about 1.5 cM

proximal to *db* and position *D4Rck22* and *D4Rck69* distal and quite close to *db*. It may be that the two recombination breakpoints described between *D4Rck22/D4Rck69* and *db* amongst the B6D2 F1 X B6*spretus* F1 offspring (animals db324 and db330), as well as the recombination event noted in the intersubspecific *castaneus* intercross, are located within a very short physical distance of one another. Efforts to cross these three breakpoints using physical methods will be continued.

Many of the probes described in this report may also prove useful for high resolution genetic mapping of other mutations which reside in the interval between *b* and *Lck*. These mutations include: dominant ears reduced (*Dre*) (Kelly, 1968), depilated (*dep*) (Mayer, et al., 1976), pintail (*pt*) (Finlayson, et al., 1969; Hollander and Strong, 1951; Hollander, 1976; Lane, 1963; Collins and Hutton, 1970; Sweet, 1985); McFarland, personal communication), abnormal spermatozoan head (*azh*) (Mewistrich and Trostle-Weige, 1989), polysyndactyly (*Ps*) (Johnson, 1969; Johnson and Wallace, 1979; Hollander and Waggie, 1977; Phillips, 1974; Lane, 1973), head blebs (*heb*) (Varnum and Fox, 1981), dysgenetic lens (*dy̆l*) (Sanyal, et al., 1986), clasper (*cla*) (Sweet, 1985), meander tail (*mea*) (Fletcher, et al., 1991), hairpatches (*hpt*) (Lane, 1968; Phillips, 1974), achondroplasia (*cn*) (Lane, 1973), snubnnose (*sno*) (Hollander, 1976), B cell maturation factor 1 (*Bmfr–1*) (Sidman, et al., 1986) and lipopolysaccharide (endotoxin) response (*Lps*) (Coutinho and Meo, 1978; O'Brien, et al., 1980; Watson, et al., 1978b; Watson,

et al., 1978a). The approximate position of these loci relative to the microclones can be surmised by consulting the consensus report for chromosome 4 (Blank, et al., 1991).

The average size of the cloned inserts in this study is somewhat small (Table 3.5). It is believed that the recovery of small (<300bp) EcoRI clones in microdissection / microcloning is due to the loss of larger cloneable EcoRI fragments secondary to random hydrolysis of DNA caused by the acid fixation used to prepare the metaphase spreads for the microdissection (Brown and Greenfield, 1987) Use of methanol: acetic acid concentrations, in the fixation step of the metaphase spread preparation, of both 3:1 (as in the present study) and 9:1 have both been reported to yield small EcoRI fragments after microcloning. There are however, at least two reports of microdissection/microcloning which yielded a similar number of microclones with an average insert size of 3.3 kb (range 0.2 - 10 kb) (Tonjes, et al., 1991) or 3.2 kb. (range 0.6 - 8 kb) (Weber, et al., 1990). In those studies, a standard 3:1 methanol:acetic acid fixation step was employed in the preparation of the metaphase spreads, and fixation times were minimized to avoid depurination. In the present study, an average insert size of approximately 180bp was obtained employing a 3:1 methanol:acetic acid fixation step. This average insert size is slightly lower than the 150 - 300bp reported previously (Brown and Greenfield, 1987). Because it appears possible to obtain a large insert size using a standard methanol:acetic acid fixation in

the preparation of the metaphase spreads, the reason for the discrepancies in size distributions between laboratories in unclear. It is possible that small differences in the metaphase spread preparation procedures utilized influences the extent of acid hydrolysis of the metaphase DNA. In any case, the small size of the microclones in the present study did not compromise the ability to construct a dense genetic map.

Six of the single-copy microclones analyzed to date were unlinked to all of the chromosome 4 markers tested but were all tightly linked to one another It appears likely that these microclones were obtained as a result of some consistent error in the microdissection. Because of the much larger size of chromosome 4 in relation to chromosome 15, it seems unlikely that this error resulted from confusion as to which half of the 4:15 Robertsonian chromosome was chromosome 4. Consistent with this conclusion is the fact pedigree analysis of the 6 unlinked clones did not demonstrate linkage with a mid-chromosome 15 marker *Gdc–1* (data not shown). The possibility of a rearrangement in the cell line resulting in the transfer of another chromosome's DNA to mid-chromosome 4 cannot be ruled out, although no gross aberration was apparent on G-banding during previous passages of the cell line.

Three microclones, *D4Rck49*, *D4Rck60* and *D4Rck122* were found to be represented at least twice in the mouse genome. The microclones *D4Rck49* and *D4Rck60* each demonstrated two C57BL/6J x *M. spretus* RFLPs. Both

copies of *D4Rck49* and *D4Rck60* were assigned to separate locations on chromosome 4. The hybridization signals on Southern analysis were complex for these two microclones; distinct alleles of each microclone had variable intensity suggesting the possibility of variable number of copies at each location in the genome (data not shown). Because of the complex hybridization patterns, the total number of copies of *D4Rck49* and *D4Rck60* and the location of each possible cluster in the genome, remains unclear. *D4Rck122* demonstrated two distinct *M. spretus* bands on Southern hybridization to total mouse DNA digested with RsaI. These two RFLPs segregated independently. The larger ~0.7 kb *M. spretus* RFLP was located in the proximal portion of chromosome 4 covered by the microclones (Figure 3. 31), while the other ~0.4 kb *M. spretus* RFLP was unlinked to chromosome 4 markers which cover nearly the entire length of that chromosome (data not shown). Prior studies have described microclones which detect moderately repetitive sequences which behave as single loci, as well as microclones which detect loci on multiple chromosomes (Brockdorff, et al., 1987). It is possible that *D4Rck49* and *D4Rck60* detect unique chromosome 4 specific repetitive elements. Further characterization of these two microclones may provide further insight into the nature of the repetitive elements.

Despite the rapid increase in the number of markers mapped in the mouse genome, there are still large gaps in certain areas of the genetic map. The procedures of microdissection and microcloning provide a relatively

straightforward and reliable means of obtaining a large number of clones from a discrete area of a specific chromosome. Improvements in the technique, such as the recovery of clones from G-banded chromosomes, promise to greatly improve the accuracy and reproducibility of the dissection. In the present study, the microdissection steps were not performed in an oil chamber, making determination of the chromosomal region to be dissected significantly easier and more accurate. As a result, the microclones were tightly clustered in the region of the *db* locus, significantly increasing the likelihood of these, and other markers, being physically linked to one another.

Physical mapping and Summary

The closest flanking markers to *db* are *Odc-4* and *Pgm-2* proximally and *D4Rck22* and *D4Rck69* distally (Figure 4.3). Proximal to *db*, *Pgm-2* is superior to *Odc–4* for further analysis because single copy clones specific for *Pgm-2* are available, and single copy probes and sequences are a necessary prerequisite for efficient YAC screening. The two microclones *D4Rck22* and *D4Rck69* are located distally to *db*, however the exact genetic distance between the microclones and *db* is difficult to assess. Only 1/772 (C57BL/6J *db/db* X *M.castaneus*) F1 intercross offspring was recombinant with *db*, providing an estimated distance from *db* of <0.125 cM, however two recombinants were

demonstrated amongst the 48 obese progeny of the B6D2 F1 X B6*spretus* F1 intercross. The large discrepancy between these two results is unusual, but not inconceivable, as different mouse strains manifest different recombination frequencies. Indeed, because the counterstrains in these two crosses differed, the data for the two cannot be combined to provide an overall estimate of the *db* — *D4Rck22/69* genetic distance. Whether the *db* — *D4Rck22/69* interval is in an area which demonstrates increased recombination between C57BL/6J *db/db* and *M. spretus*, or recombination suppression between C57BL/6J *db/db* and *M. castaneus* will become apparent as the physical mapping progresses. Considering that the estimated distance from *Pgm-2* to *db* of 1.5 cM approximates the calculated distance from *Pgm-2* to *D4Rck22/69*, it is probable that the microclones are located close to *db*, and that the two recombination breakpoints in the *db* — *D4Rck22/69* interval defined by the interspecific animals, are located within a short physical distance. Support for this hypothesis comes from unpublished results in a C57BL/6J mea/mea X *M. castaneus* backcross (Colin Fletcher and Nathaniel Heintz, *personal communication*). In 400 meiosis, no recombinations were seen between *D4Rck22* and *D4Rck69*, and 6/445 animals were recombinant between *Pgm-2* and the microclones (Figure 4.3), which approximates the 1.3 cM distance just mentioned. These data support the placement of *D4Rck22* and *D4Rck69*, distal, but extremely close to *db*.

The apparent inability to physically link the *D4Rck22* and *D4Rck69* microclones to one another by pulse-field electrophoresis is surprising considering the close genetic distances between the two. However, the failure to detect such physical linkage is likely secondary to technical considerations. Indeed, PCR screening for a YAC containing *D4Rck69* has been completed and this YAC may also contain the *D4Rck22* locus. PCR and hybridization screening for YACs containing both the *Pgm-2* and *D4Rck22* loci are nearing completion as well. Access to these YACs will facilitate the creation of a YAC contig in the region of *db*, as well as provide the resources for a directed walk towards the gene by cloning the ends of the YACS, and using those ends to rescreen the YAC libraries. Although the figure of 1 cM = 2 X 10^6 bp of DNA in mouse is widely quoted, the actual physical distances in the *db* — *D4Rck22 /69* interval may differ significantly. Since YAC clones of up to 1.5 Mb have been described, it would not be surprising if a YAC containing one of these sequences, might also contain the *db* locus itself. Such a YAC would contain either or both the *D4Rck22* or *D4Rck69* loci and would cross over the *db* locus as demonstrated by it containing a *db* — *Pgm–2* recombination breakpoint.

If a single YAC could not be isolated which contained defined breakpoints on both sides of *db*, a single such YAC could be created from overlapping YACs by homologous recombination. Long-range restriction mapping using clones derived from the YAC may demonstrate an area which is deleted or otherwise rearranged in *db/db* mice as compared to wild-type

mice. This area would contain the putative *db* gene and could be directly cloned.

Once a YAC believed to carry the *db* gene has been obtained, the expressed sequences within it must be identified and characterized. Methods for cloning these expressed sequences include 1) using clones derived from a YAC, or the region containing *db*, to screen cDNA libraries (possibly of hypothalamic origin), 2) exon trapping, 3) the localization of the CpG islands which are usually located 5' upstream of genes, and which are often the digestion site of so-called "rare" cutter restriction endonucleases (e.g. NotI), and 4) the definition of areas whose sequence is conserved between different species.

Perhaps the most difficult aspect of cloning the *db* gene is determining whether a candidate gene based on position, encodes *db*, without knowing anything about the *db* protein. Although a large rearrangement or deletion may be apparent on a long-range restriction map surrounding the *db* locus, a smaller deletion or rearrangement may be detected by probing standard Southern blots of *db*/*db* and +/+ animals with a positional candidate gene. Obviously, the *db* gene must differ in sequence from its corresponding wild-type allele. If the molecular defect underlying the *db* mutation in a particular strain is a missense or nonsense mutation, then Northern blots of affected and non-affected animals may demonstrate a difference when probed with a positional candidate. Any difference between these animals in either

transcript abundance or size would support its being the *db* gene. Denaturing gradient gels, which can detect a single base pair difference between two DNA fragments, can be employed to detect as little as a single base pair difference between db/db and wild-type alleles, which does not alter mRNA size or abundance. Sequencing of the candidate gene from both *db/db* and +/+ animals would then be undertaken to demonstrate the mutation.

Cloning of the *db* gene is facilitated by the fact that multiple *db* mouse alleles as well as two *fa* rat mutations (*fa* in rat is homologous to *db* in mice) have been characterized. All the aforementioned methods will be used simultaneously on all the available mutations, increasing the likelihood one of the mutations may be more easily noticed. Additionally, the gene which underlies the *db* mutation would be expected to be mutated in all the different strains of mice and in rats. By combining these available resources, it is more likely that the genetic defect underlying the db gene will be uncovered.

The availability of a 5 - 10 cM level genetic map of the mouse genome will also permit the delineation of the number and approximate locations of alleles influencing continuous quantitative traits such as body composition and diabetes. The high degree of linkage and synteny homology between the mouse and human genomes (Nadeau, 1989) suggests that phenotype-linked sequences obtained from the mouse will be useful in analyzing human pedigrees segregating analogous phenotypes. Work in analyzing suitable

human pedigrees using the flanking markers described herein, as well as markers in proximity to the other mouse obesity mutants, has begun.

The similarity between the obesity syndromes produced as a result of mutations in the mouse and obesity in humans suggest that the normal human homologs of these mutant alleles may play an important physiological role in determining body composition and diabetes susceptibility in man. Further support for this derives from the fact that the *db* mutation appears to have arisen in another species (*fa* – rat) as well as in mouse. That the *fa* (rat) and *db* (mouse) genes are likely homologs provides a unique opportunity to combine the complementary advantages of mouse genetics and rat physiology in exploring the action of these genes.

The cloning and characterization of the entire family of mutant genes which cause obesity syndromes in rodents, and studies of inter-strain background modifiers in the metabolic parameters altered by the obese phenotype in the inbred mouse, will undoubtedly provide insights into the metabolic control of body composition and diabetes in man.

Figure 4.2. Summary map of the *Odc-4*, *Pgm-2*, *D4Rck22*, and *D4Rck69* loci flanking *db*. *Odc-4* and *Pgm-2* are located approximately 1.5 cM from both *db* and *D4Rck22/69*. *D4Rck22* and *D4Rck69* demonstrated 2 recombinants between themselves and *db* amongst the 48 progeny of the B6D2 *db*/+ F1 X B6*spretus db*/+ F1 interspecific intercross but only 1/772 recombinants amongst the offspring of the (B6*castaneus db*/+) intersubspecific intercross (positioning these loci distal to *db* as well). Combination of these data cannot be done because the counterstrains differ, however it is likely that these loci are located ~0.125 cM distal to *db*, and that the 2 interspecific intercross recombinants are located within a very short physical interval of one another. Abbreviations used to denote the offspring of the different crosses are:
a) '*dbspretus*': (C57BL/6J *db*/*db* X DBA/2J) F1 X (C57BL/6J *db*/*db* X *M. spretus*) F1 interspecific intercross (Figures 2.5 and 3.30).

b) '*dbcastaneus*': (C57BL/6J *db*/*db* X *M.castaneus*) F1 intersubspecific intercross (Figures 2.6 and 3.21).

c) '*obspretus*': (C57BL/6J *ob*/*ob* X DBA/2J) F1 X (C57BL/6J *ob*/*ob* X *M. spretus*) F1 interspecific intercross recombinants between *Ifa* and *D4Rp1* (Figure 3.30).

d) The B6*castaneus mea*/+ X B6 *mea*/*mea* N2 offspring were bred by, and the typing of those animals with the markers indicated were performed by, Colin Fletcher and Nathaniel Heintz (The Rockefeller University).

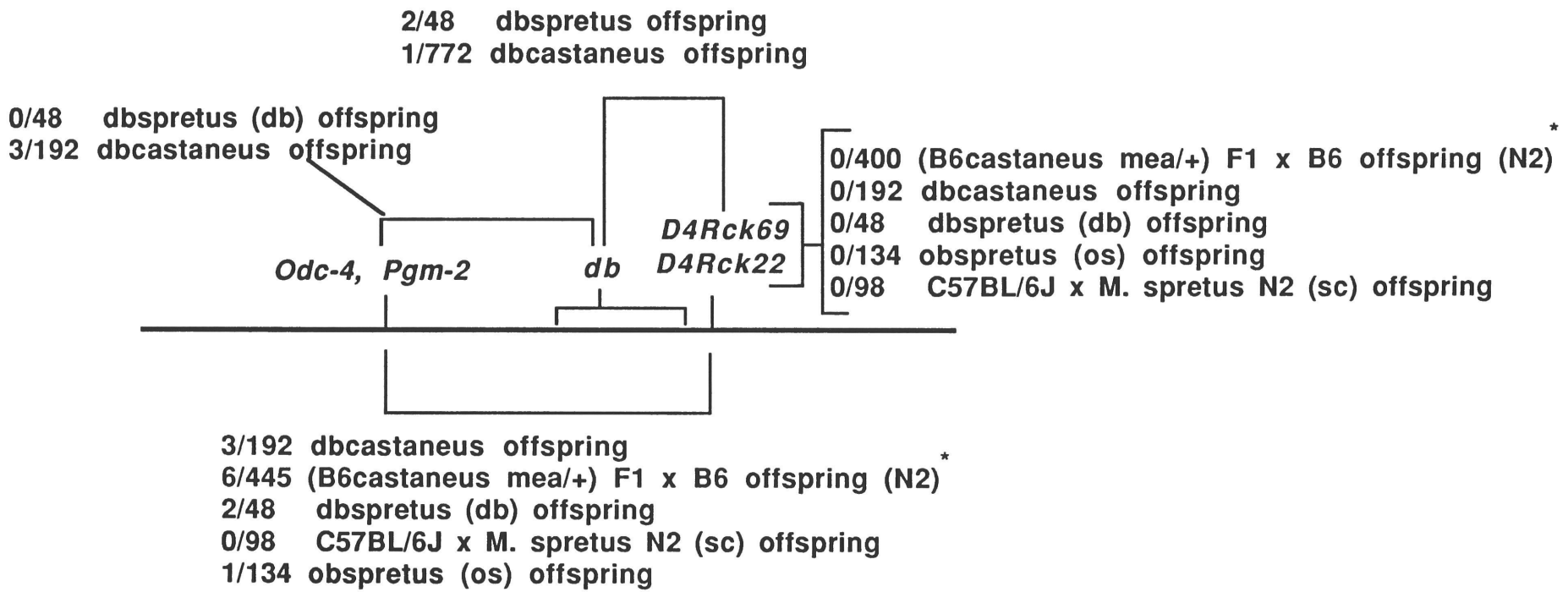
2/48 dbspretus offspring
1/772 dbcastaneus offspring
0/48 dbspretus (db) offspring
3/192 dbcastaneus offspring
0/400 (B6castaneus mea/+) F1 x B6 offspring (N2) *
0/192 dbcastaneus offspring
0/48 dbspretus (db) offspring
0/134 obspretus (os) offspring
0/98 C57BL/6J x M. spretus N2 (sc) offspring
D4Rck69
D4Rck22
Odc-4, Pgm-2
db
3/192 dbcastaneus offspring
6/445 (B6castaneus mea/+) F1 x B6 offspring (N2) *
2/48 dbspretus (db) offspring
0/98 C57BL/6J x M. spretus N2 (sc) offspring
1/134 obspretus (os) offspring

References

1. Allen J, Novotny J, Martin J and Heinrich G (1987) Molecular structure of mammalian neuropeptide Y: Analysis by molecular cloning and computer-aided comparison with crystal structure of avian homologue. *Proc. Natl. Acad. Sci. USA.* **84**: 2532-2536.

2. Allen TH, Peng MT, Chen KP, Huang TF, Chang C and Fang HS (1956) Prediction of total adiposity from skinfolds and the curvelinear relationship between external and internal adiposity. *Metabolism.* **5**: 346-352.

3. Alstrom CH, Hallgren B, Nilsson LB and Asander H (1959) Retinal degeneration combined with obesity, diabetes mellitus and neurogenous deafness: a specific syndrome (not hitherto described) distinct from the Laurence-Moon-Biedl syndrome. A clinical, endocrinological, and genetic examination based on a large pedigree. *Acta Psychiat. Neurol. Scand.* **34**(suppl. 129): 1-35.

4. Amar LC, Arnaud D, Cambrou J, Guenet JL and Avner PR (1985) Mapping of the mouse X chromosome using random genomic probes and an interspecific mouse cross. *EMBO J.* **4**: 3695-3700.

5. Angel L (1939) Constitution in female obesity. *Am. J. Phys. Antropol.*. **7**: 443-471.

6. Ann D, Smith MK and Carlson DM (1988) Molecular evolution of the mouse proline-rich protein mutigene family. *J. Biol. Chem.* **263**(22): 10887-10893.

7. Arlen Price R, Cadoret RJ, Stunkard AJ and Troughton E (1987) Genetic contribution to human fatness: an adoption study. *Am. J. Psychiatry.* **144**(8): 1003-1008.

8. Arlen Price R and Gottesman II (1991) Body fat in identical twins reared apart: roles for genes and environment. *Behav. Genet.* **21**(1): 1-7.

9. Arlen Price R, Ness R and Laskarzewski P (1990) Common major gene inheritance of extreme overweight. *Hum. Biol.* **62**(6): 747-765.

10. Arlen Price R and Stunkard AJ (1989) Commingling analysis of obesity in twins. *Hum. Hered.* **39**: 121-135.

11. Asayama K, Sharp RA and Burr IM (1985) Purification and radioimmunoassays for superoxide dismutase in the mouse: Tissue concentrations in different strains. *Int. J. Biochem.* **17**(11): 1171-1178.

12. Ashworth A, Williams BP, Buchberg AM, Goodfellow PN, Solomon E, Potter J and Willison KR (1989) Chromosomal localization of zinc finger protein genes in man and mouse. *Genomics.* **4**: 323--327.

13. Avner P, Amar L, Dandolo L and Guenet JL (1988) Genetic analysis of the mouse using interspecific crosses. *Trends Genet.* **4**: 18-23.

14. Azen EA, Davisson MT, Cherry M and Taylor BA (1989) *Prp* (proline-rich protein) genes linked to markers *Es-12* (esterase-12), *Ea-10* (erythrocyte alloantigen) and loci on distal mouse Chromosome 6. *Genomics.* (5): 415-22.

15. Bardet G (1920) *Sur un syndrome d'obesite infantile avec polydactylie et retinite pigmentaire.* Contribution a l'etude des formes cliniques de l'obesite hypophysaire. Paris, **479**.

16. Bartholdi MF, Meyne J, Albright K, Luedemann M, Campbell E, Chritton D, Deaven LL and Cram LS (1987) Chromosome Sorting by flow cytometry. *Molecular Genetics of Mammalian Cells.* Orlando, Fl., Academic Press.

17. Bates GP, Wainwright BJ, Willliamson R and Brown SDM (1986) Microdissection and Microcloning from the short arm of human chromosome 2. *Mol. Cell. Biol.* **6**(11): 3826-3830.

18. Batt RA (1983) Decreased food intake in response to cholecystokinin (pancreozymin) in widle-type and obese mice (genotype *ob/ob*). *Int. J. Obes.* **7**: 25-29.

19. Baumann H and Berger FG (1985) Genetics and evolution of the acute phase proteins in mice. *Mol. Gen. Genet.* **201**: 505-512.

20. Baumann H, Held WA and Berger FG (1984) The acute phase response of mouse liver. Genetic analysis of the major acute phase reactants. *J. Biol. Chem.* **259**: 566-73.

21. Berger FG, Syzmanski P, Read E and Watson G (1984) Androgen-regulated ornithine decarboxylase mRNAs of mouse kidney. *J Biol Chem.* **259**(12): 7941-7946.

22. Berglund O, Sehlin J and Taljedal IB (1980) Influence of the murine diabetes gene on rubidium ion efflux from perfused islets. *Diabetologia.* **19**: 45-49.

23. Biedl A (1922) Ein Geschwisterpaar mit adiposa-genitaler dystrophie. *Dtsch. Med. Wschr.* **48**: 1630 only.

24. Birnbaum MJ, Hapsel HC and Rosen OM (1986) Cloning and characterization of a cDNA encoding the rat brain glucose transporter protein. *Proc Nat Acad Sci USA.* **83**: 5784-5788.

25. Bjorntorp P (1990) Obesity and adipose tissue distribution as risk factors for the development of disease. A review. *Infusionstherapie.* **17**(1): 24-7.

26. Blank R, Eppig J, Fiedorek Jr. FT, Frankel WN, Friedman JM, Huppi K, Jackson I and Mock B (1991) Mouse chromosome 4. *Mammalian Genome.* **1**(suppl. 1): S51-S77.

27. Blank RD, Campbell GR, Calabro A and D'Eustachio P (1988) A linkage map of mouse chromosome 12: Localization of *Igh* and effects of sex and interference on recombination. *Genetics.* **120**(December): 1073-1083.

28. Botstein D, White R, Skolnick M and Davis R (1980) Construction of a genetic linkage map using restriction fragment length polymorphisms. *Am. J. Hum. Genet.* **32**: 314-333.

29. Bouchard C, Savard R, Despres J-P, Tremblay A and Leblanc C (1985) Body composition in adopted and biological siblings. *Hum. Biol.* **57**(1): 61-75.

30. Boucher BW, Hayashi K, Rosenthal J and Notkins AL (1974) Virus-induced diabetes mellitus. III. Influence of the sex and strain of the host. *J Infect Dis.* **131**: 462-466.

31. Bray GA (1989a) Genetic and hypothalamic mechanisms for obesity--finding the needle in the haystack. *Am. J. Clin. Nutr.* **50**: 891-902.

32. Bray GA (1989b) Nutrient balance and obeisty: An approach to control of food intake in humans. *Med. Clin. N. Amer.* **73**: 29-45.

33. Bray GA (1990a) Obesity and diabetes. *Acta Diab. Latina.* **27**(1): 81-88.

34. Bray GA (1990b) Obesity: Historical development of scientific and cutural ideas. *Int. J. Obes.* **14**(14): 909-926.

35. Bray GA and York DA (1979) Hypothalamic and genetic obesity in experimental animals: an autonomic and endocrine hypothesis. *Physiol. Rev.* **59**: 719-809.

36. Brockdorff N, Fisher EMC, Cavanna JS, Lyon MF and Brown SDM (1987) Construction of a detailed molecular map of the mouse X chromosome by microcloning and interspecific crosses. *EMBO J.* **6**(11): 3291-3297.

37. Brown SDM and Greenfield AJ (1987) A model to describe the size distribution of mammalian genomic fragments recovered by microcloning. *Gene*. **55**: 327-332.

38. Bruce BK, King BM and Phelps GR (1982) Effects of adrenalectomy and corticosterone administration on hypothalamic obesity in rats. *Am J Physiol.* **243**: E152-E157.

39. Bucan M, Yang-Feng T, Colberg-Poley AM, Wolgemuth DJ, Guenet J-L, Francke U and Lehrach H (1986) Genetic and cytogenetic localisation of the homeo box containing genes on mouse chromosome 6 and human chromosome 7. *EMBO J.* **5**: 2899-2905.

40. Buiting K, Neumann M, Ludecke H, Senger G, Claussen U, Antich J, Passarge E and Horsthemke B (1990) Microdissection of the Prader-Willi syndrome chromosome region and identification of potential gene sequences. *Genomics*. **6**: 521-527.

41. Burton BT, Foster WR, HIrsch J and Itallie TBV (1975) Health implications of obesity: NIH Consensus Development Conference. *Ann. Int. med*. **103**: 977-1077.

42. Butler MG (1990) Prader-Willi sydrome: current understanding of cause and diagnosis. *Am. J. Hum. Genet*. **35**: 319-332.

43. Caccia N, Kronenberg M, Saxe D, Haars R, Bruns GAP, Goverman J, Malissen M, WEillard H, Yoshikai Y, Simon M, Hood L and Mak TW (1984) The T cell receptor β chain genes are located on chromosome 6 in mice and chromosome 7 in humans. *Cell*. **37**: 1091-1099.

44. Capanna E, Gropp A, Winking H, Noack G and Civitelli M (1976) Robertsonian metacentrics in the mouse. *Chromosoma*. **58**: 341-353.

45. Carey JC and Hall BD (1978) Confirmation of the Cohen syndrome. *J. Pediat*. **93**: 239-244.

46. Ceci JD, Siracusa LD, Jenkins NA and Copeland NG (1989) A molecular genetic linkage map of mouse chromosome 4 including the localization of several proto-ongogenes. *Genomics*. **5**: 699-709.

47. Chapman VM, Ruddle FH and Roderick TH (1971) Linkage of isozyme loci in the mouse: *phosphoglucomutase-2* (*Pgm-2*), *mitochondrial NADP malate dehydrogenase* (*Mod-2*), and *dipeptidase-1* (*Dip-1*). *Biochem. Genet.* **5**: 101.

48. Charles SJ, Moore AT, Yates JRW, Green T and Clark P (1990) Alstrom's syndrome: further evidence for autosomal recessive inheritance and endocrinological dysfunction. *J. Med. Genet.* **27**: 590-592.

49. Chlouverakis C (1972) Insulin resistance of parabiotic obese-hyperglycemic mice (obob). *Horm Metab res.* **4**: 143-148.

50. Chudley AE, Lowry RB and Hoar DI (1988) Mental retardation, distinct facial changes, short stature, obesity, and hypogonadism: a new X-linked mental retardation syndrome. *Am. J. Hum. Genet.* **31**: 741-751.

51. Cohen Jr. MM, Hall BD, Smith DW, Graham CB and Lampert KJ (1973) A new syndrome with hypotonia, obesity, mental deficiency, and facial, oral, ocular, and limb abnormalities. *J. Pediat.* **83**: 280-284.

52. Coleman DL (1973) Effects of parabiosis of obese with diabetes and normal mice. *Diabetologia.* **9**: 294-298.

53. Coleman DL (1978) Obese and Diabetes: two mutant genes causing diabetes-obesity syndromes in mice. *Diabetologia.* **14**: 141-148.

54. Coleman DL (1979) Obesity genes: beneficial effects in heterozygous mice. *Science.* **203**: 663-665.

55. Coleman DL (1980) Acetone metabolism in mice: Increased activity in mice heterozygous for obesity genes. *Proc. Nat. Acad. Sci. USA.* **77**: 290-293.

56. Coleman DL (1982) Diabetes-obesity syndromes in mice. *Diabetes.* **31**(Suppl. 1): 1-6.

57. Coleman DL (1988) Therapeutic effects of dehydroepiandrosterone (DHEA) and its metabolites in obese-hyperglycemic mutant mice.

Pathogenesis and new approaches to the study of noninsulin-dependent diabetes mellitus. Alan R. Liss Inc.

58. Coleman DL and Eicher EM (1990) Fat (*fat*) and tubby (*tub*): Two autosomal recessive mutations causing obesity syndromes in the mouse. *J Hered*. **81**: 424-427.

59. Coleman DL and Hummel KP (1969) Effects of parabiosis of normal with genetically diabetic mice. *Am. J. Phys.* **217**(5): 1298-1304.

60. Coleman DL and Hummel KP (1970) The effects of hypothalamic lesions in genetically diabetic mice. *Diabetologia*. **6**: 263-267.

61. Coleman DL and Hummel KP (1975) Influence of genetic background on the expression of mutations at the diabetes locus in the mouse. II. Studies on background modifiers. *Isr. J. Med. Sci.* **11**: 708-713.

62. Collins FS, Drumm ML, Cole JL, Lockwood WK, Vande Woude GF and Iannuzzi M (1987) Construction of a general human chromosome jumping library, with application to cystic fibrosis. *Science*. **235**: 1046-1049.

63. Collins RL and Hutton JJ (1970) The position of autosomal glucose 6 phosphage dehydrogenase on linkage group VIII of the mose. *J. Hered.* **61**: 53-54.

64. Compton DA, Weil MM, Jones C, Riccardi VM, Strong LC and Saunders GF (1988) Long range physical map of the Wilms' tumor-aniridia region on human chromosome 11. *Cell.* **55**: 827-836.

65. Corbett SW, Stern JS and Keesey RE (1986) Energy expenditure in rats with diet-induced obesity. *Am J Clin Nutr.* **44**: 173-180.

66. Cornall RJ, M. FJ and Todd JA (1991) Mouse microsatellites from a flow-sorted 4:6 Robertsonian chromosome. *Genomics.* **submitted**:

67. Cornwall RJ, Prins J, Todd JA, Pressey A, DeLarto NH, Wicker LS and Peterson LB (1991) Type 1 diabetes in mice is linked to interleukin-1 receptor and *Lsh/Ity/Beg* genes on chromosome 1. *Nature.* **353**: 262-264.

68. Coutinho A and Meo T (1978) Genetic basis for unresponsiveness to lipopolysaccharide in C57BL/10Cr mice. **7**: 17-24.

69. Cram LS, Campbell M, Fawcett J and Deaven LL (1990) Polyamine buffer for bivariate human flow cytogenetic analysis and sorting. *Methods in Cell Biology*.

70. D'Hoostelaere LA and Gibson DM (1986) The organization of immunoglobulin variable kappa chain genes on mouse chromosome 6. *Immunogenetics*. **23**: 260-265.

71. Daly PA and Landsberg L (1991) Hypertension in obesity and NIDDM. Role of insulin and sympathetic nervous system. *Diabetes Care*. **14**(3): 240-248.

72. Darby JK, Willems PJ, Nakashima P, Johnsen J, Ferrell RE, Wijsman EM, Gerhard DS, Dracopoli NC, Housman D, Henke J, Fowler ML, Shows TB, O'Brien JS and Cavalli-Sforza LL (1988) Restriction analysis of the structural α-L- fucosidase gene and its linkage to fucosidosis. *Am. J. Hum. Genet.* **43**: 749-755.

73. Davenport CB (1923) *Body-build and its inheritance.* publication 329. Washington, D.C., Carnegie Institution.

74. Davis JD and Campbell CS (1978) Distension of the small intestines, satiety and the control of food intake. *Am J Clin Nutr.* **31**: S255.

75. Davisson MT, Roderick TH, Hillyard AL and Doolittle DP (1988) Linkage map of the mouse. *Mouse News Letter*. **81**: 12-19.

76. Dawson DM and Jaeger S (1970) Heterogeneity of phosphoglucomutase. *Biochem. Genet.* **4**: 1-9.

77. De Waard F, Cornelis JP, Aoki K and Yoshida M (1977) Breast cancer incidence according to weight and height in two cities of the Netherlands and in Aichi Perfecture, Japan. *Cancer*. **40**(3): 1269-1275.

78. Dean M, Kozak C, Robbins J, Callahan R, O'Brine S and Vande Woude GF (1987) Chromosomal localization of the *met* proto-oncogene in the mouse and cat genome. *Genomics*. **1**: 167-173.

79. Derman E, Krauter K, Walling L, Weinberger C, Ray M and Darnell JEJ (1981) Transcriptional control in the production of liver-specific mRNAs. *Cell*. **23**: 731-739.

80. Diesseroth A, Neinhaus A, Turner P, Valez R, Anderson WF, Ruddle F, Lawrence J, Creagen R and Kucherlapati R (1977) Localization of the human

alpha-globin structural gene to chromosome 16 in somatic cell hybrids by molecular hybridization assay. *Cell.* **12**: 205-218.

81. Dietrich W, Katz SE, Lincoln SE, Shin H, Friedman JM, Dracopoli N and Lander ES (1991) A genetic map of the mouse suitable for typing intraspecific crosses. **submitted**:

82. Disteche CM, Carrano AV, Ashworth LK, Burkhart-Schultz K and Latt SA (1981) Flow sorting of the mouse Cattanach X chromosome, *T(X;7) 1 Ct*, in an active or inactive state. *Cytogenet. Cell Genet.* **29**: 189-197.

83. Dixon WJ (1981) *BMDP Statistical Software.* University of California Press.

84. Dogget NA, Cheng J, Smith CL and Cantor CR (1989) The Huntington disease locus is most likely within 325 kilobases of the chromsome 4p telomere. *Proc. Nat. Acad. Sci. USA.* **86**: 10011-10014.

85. Donis-Keller H, Green P, Helms C, Cartinhour S, Weiffenbach B, Stephens K, Keith TP, Bowden DW, Smith DR, Lander ES, Botstein D, Akots G, Rediker KS, Gravious T, Brown VA, Rising MB, Parker C, Powers JA, Watt DE, Kauffman ER, Bricker A, Phipps P, Muller_Kahle H, Fulton TR, Ng S,

Schumm JW, Braman JC, Knowlton RG, Barker DF, Crooks SM, Lincoln SE, Daly MJ and Abrahamson J (1987) A genetic linkage map of the human genome. *Cell.* **51**: 319-337.

86. Doolittle DP, Hillyard AL, Guidi JN, Davisson MT and Roderick TH (1991) *GBASE - The genomic database of the mouse maintained at The Jackson Laboratory.*

87. Douglas AR, McAlpine PJ and Hamerton JL (1973) Regional localization of loci *PGM* and *6PGD* on human chromosome one by use of hybrids of chinese hamster-human somatic cells. *Proc. Nat. Acad. Sci. U.S.A.* **70**: 2737.

88. Dracopoli NC, Feltquate DM , Stanger BA, Rettig WJ and Housman DE (1989) Genetic map of chromosome 1p. *Cytog. and Cell Gen.* **51**(abstract): 993 only.

89. Dracopoli NC, Stanger BZ, Ito CY, Call KM, Lincoln SE, Lander ES and Housman DE (1988) A genetic linkage map of 27 loci from *PND* to *FY* on the short arm of human chromosome I. *Amer. J. Hum. Gen.* **43**: 462-70.

90. Ducimetiere P, Richard J and Cambien F (1986) The pattern of subcutaneous fat distribution in middle-aged men and the risk of coronary heart disease: The Paris Prospective Study. *Int. J. Obes.* **10**(1): 229-240.

91. Dudov KP and Perry RP (1984) The gene family encoding the mouse ribosomal protein *L32* contains a uniquely expressed intron-containing gene and an unmutated processed gene. *Cell.* **37**: 457-468.

92. Dustan HP (1991) Obesity and hypertension. *Diabetes Care.* **14**(6): 488-504.

93. Eicher EM and Lee BK (1990) The NXSM recombinant inbred strains of mice:genetic profile for 58 loci including the *Mtv* porviral loci. *Genetics.* **125**: 431-446.

94. Elliot EA, Matanoski GM, Rosenheim NB, Grumbine FC and Diamond EL (1990) Body fat patterning in women with endometrial cancer. *Gynec. Onc.* **39**(3): 253-258.

95. Erickson RP, Harper K and Kramer JM (1983) Identification of an autosomal loocus affecting steroid sulfatase activity among inbred strains of mice. *Genetics.* **105**: 181-189.

96. Feinberg AP and Vogelstein B (1983) A technique for radiolabeling DNA restriction endonuclease fragments to high specific acitivity. *Anal Biochem.* **132**: 6-13.

97. Feinberg AP and Vogelstein B (1984) Addendum: A technique for radiolabeling DNA restriction endonuclease fragments to high specific activity. *Anal Biochem.* **137**: 266-267.

98. Felson DT (1990) The epidemiology of knee osteoarthritis from the Framigham Osteoarthritis Study. *Sem. in Arthr. and Rheum.* **30**(3 Suppl 1): 42-50.

99. Ferguson JM and Feighner JP (1987) Fluoxetine-induced weight loss in overweight non-depressed humans. *Int J Obes.* **11**(suppl. 3): 163-70.

100. Festing MFW (1979) *Animal Models of Obesity.* New York, Oxford University Press.

101. Finlayson JS, Hudson DM and Armstrong BL (1969) Location of the Mup-a locus on mouse linkage groups VII. *Genet. Res.* **14**: 329-331.

102. 1. Fletcher C, Norman DJ and Heintz N (1991) Genetic mapping of meander tail, a mouse mutation affecting cerebellar development. Genomics. **9**: 647-655.

103. Fournier EK and Ruddle FH (1977) Stable association of the human transgene and host murine chromosomes demonstrated with trispecific microcell hybrids. *Proc. Nat. Acad. Sci.* **74**(9): 3937-3941.

104. Freud JE (1973) Modern Elementary Statistics. Prentice-Hall Inc.

105. Fried SK and Kral JG (1987) Sex differences in regional distribution of fat-cell size and lipoprotein lipase activity in morbidly obese patients. *Int. J. Obes.* **11**: 129-140.

106. Friedman JM, Leibel RL, Siegel DA, Walsh J and Bahary N (1991) Molecular mapping of the mouse ob gene. *Genomics.* **11**: 1054-1062.

107. Fryns J-P, Kleczkowska A, Smeets E, Thiry P, Geutjens J and Van den Berghe H (1990) Cohen syndrome and de novo reciprocal translocation t(5;7)(q33.1;p15.1). *Am. J. Med. Genet.* **37**: 546-547.

108. Fukushima H, De Wet JR and O' Brien JS (1985) Molecular cloning of a cDNA for human α-L-fucosidase. *Proc. Natl. Acad. Sci. USA.* **82**: 1262-1265.

109. Garn SM and Clark DC (1976) Trends in fatness and the origins of obesity. *Pediatrics.* **57**: 443-456.

110. Garn SM, Sullivan TV and Hawthorne VM (1989) Fatness and obesity of the parents of obese individuals. *Am. J. Clin. Nutr.* **50**: 1308-1313.

111. Gates RJ, Hunt MI and Lazarus NR (1974) Further studies on the amelioration of the characteristics of New Zealand obese (NZO) mice following transplantation of islets of Langerhans. *Diabetologia.* **10**: 401-406.

112. GDB (1990) *Genome Data Base [Machine-readable data file].*

113. Gessler M, Poustka A, Cavenee W, Neve RL, Orkin SH and Bruns GAP (1990) Homozygous deletion in Wilms tumours of a zinc-finger gene identified by chromosome jumping. *Nature.* **343**: 774-778.

114. Gibbs J, Young RC and Smith GP (1973) Cholecystokinin decreases food intake in rats. *J. Comp Physiol Psychol.* **84**: 488-95.

115. Glaser T, Rose E, Morse H, Housman D and Jones C (1990) A panel of irradiation-reduced hybrids selectively retaining human chromosome 11p13: Their structure and use to purify the WAGR gene complex. *Genomics*. **6**: 48-64.

116. Goff S, D' Eustachio P, Ruddle FH and Baltimore D (1982) Chromosomal assignment of the endogenous proto-oncogene *C-abl*. *Science*. **218**: 1317-1319.

117. Gray DS (1989) Diagnosis and prevalence of obesity. *The Medical Clinics of North America: Obesity*. Philadelphia, W. B. Saunders Co.

118. Gray JW and Cram LS (1990) Flow karyotyping and chromosome sorting. *Flow Cytometry and Sorting*. New York, N.Y., Wiley-Liss Inc.

119. Green JS, Parfey PS, Harnet JD, Farid NR, Cramer BC, Johnson G, Heath O, McManamon PJ, O'Leary E and Pryse-Phillips W (1989) The cardinal manifestations of Bardet-Biedl syndrome, a form of Laurence-Moon-Biedl syndrome. *New Eng. J. Med.* **321**: 1002-1009.

120. Greenstein MA (1990) Prader-Willi and Angelman sydromes in one kindred with expression consistent with genetic imprinting (Abstract). *Am. J. Hum. Genet.* **47**(suppl.): A59 only.

121. Haldane JBS (1919) The combination of linkage values, and the calculation of distances between the loci of linked factors. *J Genet.* **8**: 299-309.

122. Hall BD and Smith DW (1972) Prader-Willi syndrome: a resume of 32 cases including an instance of affected first cousins, one of whom is of normal stature and intelligence. *J Pediat.* **81**: 286-1293.

123. Haluska FG, Huebner K, Isobe M, Nishimura T, Croce CM and Vogt PK (1988) Localization of the human *Jun* protooncogene to chromosome region 1p31-32. *Proc. Nat. Acad. Sci. USA.* **85**: 2215-2218.

124. Hammer MF, Schimenti J and Silver LM (1989) Evolution of mouse chromosome 17 and the origin of inversions associated with *t* haplotypes. *Proc. Nat. Acad. Sci. USA.* **86**: 3261-3265.

125. Hanauer A, Cherry M, Fujita R, Driesel AJ, Gilgenkrantz S and Mandel JL (1990) The Friedrichs Ataxia gene is assigned to chromosome 9q13-q21 by

mapping of tightly linked markers and shows linkage disequilibrium with D9S15. *Am J Hum Genet.* **46**(1): 133-137.

126. Harris RBS (1990) Role of set-point theory in regulation of body weight. *FASEB J.* **4**: 3310-3318.

127. Harris RBS and Martin RJ (1989) Physiological and metabolic changes in parabiotic partners of obese rats. *Hormones, Thermogenesis and Obesity.* New York, Elsevier Science Publishing Co.

128. Hasstedt SJ, Ramirez ME, Kuida H and Williams RR (1989) Recessive inheritance of a relative fat pattern. *Am. J. Hum. Genet.* **45**: 917-925.

129. Hattori K, Angel P, Le Beau MM and Karin M (1988) Structure and chromosomal localization of the functional intronless human JUN protooncogene. *Proc. Nat. Acad. Sci. USA.* **85**: 9148-9152.

130. Hausberger FX (1958) Parabiosis and transplantation experiments in hereditary obese mice. *Anat Rec.* **130**: 313 (abstr).

131. Heller R, Garrison RJ, Havlik RJ, Feinlab M and Padgett S (1984) Family resemblances in height and relative weight in the Framingham heart study. *Int. J. Obes.* **8**: 309-405.

132. Henderson BE, Casagrande JT, Pike MC, Mack T, Rosario I and Duke A (1983) The epidemiology of endometrial cancer in young women. *Br. J. Cancer.* **47**: 749-756.

133. Herbert V, Lau KS, W. GC and Bleicher SJ (1965) Coated charcoal immunoasssay of insulin. *J. Clin. Endoc. Metab.* **25**: 1375-1384.

134. Heuckeroth RO, Birkenmeier EH and Levin MS (1987) Analysis of the tissue-specific expression, developmental regulation, and linkage relationships of a rodent gene encoding heart fatty acid binding protein. *The Journal of Biological Chemistry.* **262**(20): 9709-9717.

135. Heyden S and Schneider KA (1990) Obesity and hypertension: epidemiological aspects of the relationship. *J. Hum. Hyperten.* **4**(4): 431-435.

136. Hirsch J, Fried SK, Edens NK and Leibel RL (1989) The fat cell. *Med. Clin. North Am.* **73**(1): 83-96.

137. Hirsch J and Leibel RL (1988) New light on obesity. *New Eng. J. Med.* **318**(8): 509-510.

138. Hollander WF (1976) Genetic spina bifida occulta in the mouse. *Am. J. Anat.* **146**: 173-180.

139. Hollander WF and Strong LC (1951) Pintail, a dominant mutation linked with brown in the house mouse. *J. Hered.* **42**: 179-182.

140. Hollander WF and Waggie KS (1977) Meander tail: a recessive mutant located in chromosome 4 of the mouse. *J. Hered.* **68**: 403-406.

141. Honey NK, Sakaguchi AY, Lalley PA, Quinto C, Rutter WJ and Naylor SL (1986) Assignment of the gene for carboxypeptidase A to human chromosome 7q22-gter and to mouse chromosome 6. *Hum Genet.* **72**: 27-31.

142. Hopkinson DA and Harris H (1965) Evidence for a second "structural" locus determining human phosphoglucomutase. *Nature.* **208**: 410-412.

143. Hopkinson DA and Harris H (1966) Rare phophoglucomutase phenotypes. *Ann. Human Genet.* **30**: 167-181.

144. Hopkinson DA and Harris H (1968) A third phosphoglucomutase locus in man. *Ann. Human Genet.* **31**: 359-367.

145. Howard OMZ, Rao AG and Sodetz JM (1987) Complementary DNA and derived amino acid sequence of the beta subunit of human complement protein C8: Identification of a close structural and ancestral relationship to the alpha subunit C9. *Biochem.* **26**: 3565-3570.

146. Hubert HB, Feinlab M, McNamara PM and Castelli WP (1983) Obesity as an independent risk factor for cardiovascular disease: a 26 year follow-up of participants in the Framigham Heart Study. *Circulation.* **67**(5): 968-977.

147. Hummel KP, Coleman DL and Lane PW (1972) The influence of genetic background on expression of mutations at the diabetes locus in the mouse. I. C57BL/KsJ and C57BL/6J strains. *Biochem. Gen.* **7**: 1-3.

148. Hummel KP, Dickie MM and L. CD (1966) Diabetes, a new mutation in the mouse. *Science.* **153**: 1127-1128.

149. Hunt JD and Tereba A (199O) Molecular evaluation of chromosome 1p abnormalities in neuroblastoma. *Genes, Chrom. and Cancer.* **2**: 137-146.

150. Huppi KB, Mock A, Schricker P, D'Hoostelaere LA and Potter M (1988) Organization of the distal end of mouse chromosome 4. *Curr Topics in Microbiol Immunol.* **137**: 276-88.

151. Hutton JJ and Roderick TH (1970) Linkage analyses using biochemical variants in mice. III. Linkage relationships of eleven biochemical markers. *Genet. Res.* **37**: 123-131.

152. Huynh TV, Young RA and Davis RW (1985) *DNA cloning: a practical approach.* Oxford, IRL press.

153. Ingalls AM, Dickie MM and Snell GD (1950) Obese, a new mutation in the house mouse. *J. Hered.* **41**: 317-318.

154. Irving NG, Hardy JA, Bahary N, Friedman JM and Brown SDM (1989) The α2 chain of type 1 collagen does not map to mouse chromosome 16 but maps close to the met proto-oncogene on mouse chromosome 6. *Cytog. Cell Gen.* **50**: 121-122.

155. Jackson IJ (1987) The real reverse genetics: targeted mutagenesis in the mouse. *TIG.* **3**(5): 119-120.

156. Jackson IJ (1988) A cDNA encoding tyrosinase-related protein maps to the brown locus in mouse. *Proc. Natl. Acad. Sci. USA.* **85**: 4392-4396.

157. Jacob HJ, K. L, Lincoln SE, Kusumi K, Bunker RK, Mao Y, Ganten D, Dzau VJ and Lander ES (1991) Genetic mapping of a gene causing hypertension in the stroke-prone spontaneously hypertensive rat. *Cell.* **67**: 213-224.

158. Johnson DR (1969) Polysyndactyly, a new mutant gene in the mouse. *J. Embryol. Exp. Morphol.* **53**: 327-333.

159. Johnson DR and Wallace ME (1979) Crinkly-tail, a mild skeletal mutant in the mouse. *J. Embryol. Exp. Morphol.* **53**: 327-333.

160. Johnson FM, Hendren RW, Chasalow F, Barnett LB and Lewus SE (1981) A null mutation at the mouse phosphoglucomutase-1 locus and a new locus, *Pgm-3. Boochem. Genet.* **19**(5/6): 599-615.

161. Jongsma A, van Someron H, Westerveld A, Hagemeijer A and Perason P (1973) Localization of genes on human chromosomes by studies of human-Chinese hamster somatic cell hybrids. Assignment of PGM_3 to chromosome

C6 and regional mapping of the *PGD*, *PGM* and *Pep-C* genes on chromosome A1. *Humangenetik.* **20**: 195-202.

162. Kadish AH, Little RL and Steinberg JC (1968) A new and rapid method for the determination of glucose by measurement of rate of oxygen consumption. *Clin. Chem.* **14**: 116-131.

163. Kaku K, Fiedorek FT, Province M and Permutt MA (1988) Genetic analysis of glucose tolerance in inbred mouse strain. Evidence for polygenic control. *Diabetes.* **37**: 707-713.

164. Kaku K, Province M and Permutt MA (1989) Genetic analysis of obesity-induced diabetes associated with a limited capacity to synthesize insulin in C57BL/Ks mice: evidence for polygenic control. *Diabetologia.* **32**: 636-643.

165. Kannel WB, Cupples LA, Ramaswami R, Stoke 3rd J, Kreger BE and Higgins M (1991) Regional obesity and risk of cardiovascular disease; the Framigham Study. *J. Clin. Epid.* **44**(2): 183-190.

166. Keesey RE (1989) Physiological regulation of body weight and the issue of obesity. *Med. Clinics N. Amer.* **73**: 15-27.

167. Keitges EA, Schorderet DF and Gartler SM (1987) Linkage of the steroid sulfatase gene to the sex-reversed mutation in the mouse. *Genetics*. **116**: 465-468.

168. Kelley DP, Kim J-J, Billadello JJ, Hainline BE, Chu TW and Strauss AW (1987) Nucleotide sequence of medium-chain acyl-CoA dehydrogenase mRNA and its expression in enzyme-deficient human tissue. *Proc. Natl. Acad. Sci. USA*. **84**: 4068-4072.

169. Kelley KA and Pitha PM (1985) Characterization of a mouse interferon gene locus I. Isolation of a cluster of four a interferon genes. *Nucl. Acids Res.* **13**: 805-823.

170. Kelly EM (1968) Dominant reduced ear. *Mouse News Lett.* **38**: 31.

171. Kidd JR, Matsubara Y, Castiglione CM, Tanaka K and Kidd KK (1990) The locus for the medium-chain acyl-CoA dehydrogenase gene on chromosome 1 is highly polymorphic. *Genomics*. **6**: 89-93.

172. Kinglsey DM, Jenkins NA and Copeland NG (1989) A molecular genetic linkage map of mouse chromosome 9 with new localizations for the *Gsta*, *T3q*$_{\iota}$ *Ets-1* and *Ldlr* loci. **123**: 165-172.

173. Kirchgessner TG, LeBoeuf RC, Langner CA, Zollman S, Chang CH, Taylor BA, Schotz MC, Gordon JI and Lusis AJ (1989) Genetic and developmental regulation of the lipoprotein lipase gene: Loci both distal and proximal to the lipoprotein lipase structural gene control enzyme expression. *J. Biol. Chem.* **264**: 1473-1482.

174. Kirkilionis AJ, Gregory CA and Hamerton JL (1991) Long-range restriction mapping and linkage analysis of the Prader-Willi chromosome region (PWCR). *Genomics.* **9**: 524-535.

175. Kiss P and Osztovics M (1990) Familial translocation, t(2;5) (p23;q31) follow-up after 15 years. *Clin. Genet.* **38**(5): 397-8.

176. Kleiber M (1947) Body size and metabolic rate. *Physiol. Rev.* **15**: 511-541.

177. Knowler WC, Pettitt DJ, Saad MF, Charles MA, Nelson RG, Howard BV, Bogardus C and Bennett PH (1991) Obesity in the Pima Indians: its magnitude and relationship with diabetes. *Am . J. Clin. Nutr.* **53**(6 Suppl): 1543S-1551S.

178. Koopsman HS (1981) The role of the gastrointestinal tract in the satiation of hunger. *The Body Weight Regulatory System: Normal and Disturbed Mechanism*. New York, Raven Press.

179. Kourides IA, Barker PE, Gurr JA, Pravtcheva DD and Ruddle FH (1984) Assignment of the genes for the α and β subunits of thyrotropin to different mouse chromosomes. *Proc. Natl. Acad. Sci. USA.* **81**: 517-519.

180. Krause JE, Chirgwin JM, Carter MS, Xu ZS and Hershey AD (1987) Three rat preprotachykinin mRNAs encode the neuropeptides substance P and neurokinin A. *Proc. Natl. Acad. Sci. USA.* **84**: 881-885.

181. La Vecchia C, Negri E, D' Avanzo B, Franceschi S and Boyle P (1991) Risk factors for gallstones requiring surgery. *Int. J. Epid.* **20**(1): 209-215.

182. Laakso M and Pyorala K (1990) Adverse effects of obesity on lipid and lipoprotein levels in insulin-dependent and non-insulin-dependent diabetes. *Metab Clin & Exp.* **39**(2): 117-122.

183. Lander ES and Botstein D (1989) Mapping Mendelian factors underlying quantitative traits using RFLP linkage maps. *Genetics.* **121**: 185-199.

184. Lander ES, Green P, Abrahamson J, Barlow A, Daly MJ, Lincoln SE and Newburg L (1987) MAPMAKER: an interactive computer package for constructing primary genetic linkage maps of experimental and natural populations. *Genomics*. **1**(2): 174-181.

185. Lane PW (1963) Whirler mice, a recessive behavior mutation in linkage group VIII. *J. Hered*. **54**: 263-166.

186. Lane PW (1968) Mapping of the *db* locus. *Mouse News Lett*. **38**: 24.

187. Lane PW (1973) Achondroplasia (*cn*). *Mouse News Lett*. **49**: 33.

188. Lapidus L, Bengtsson C, Larsson B, Pennert K, Rubo E and Sjorstom L (1984) Distribution of adipose tissue and risk of cardiovascular disease and death: A 12-year follow-up of participants in the population study of women in Gothenburg, Sweden. *Br. Med. J*. **289**: 1257-1261.

189. Larsson B, Svardsudd K, Welin L, Wilhelmsen L, Bjorntorp P and Tibblin G (1984) Abdominal adipose tissue distribution, obesity, and risk of cardiovascular disease and death: A 13-year follow-up of participants in the study of men born in 1913. *Br. Med. J*. **288**: 1401-1404.

190. Laskarzewski PM, Khoury P, Morrison JA, Kelly K, Mellies MJ and Glueck CJ (1982) Familial Obesity and leanness. *Int. J. Obes.* **7**: 505-527.

191. Lauer MS, Anderson KM, Kannel WB and Levy D (1991) The impact of obesity on left ventricular mass and geometry. The Framingham Heart Study. *JAMA.* **266**(2): 231-236.

192. LaVecchia C, Franceschi S, Decarli A, Gallus G and Tognoni G (1984) Risk factors for endometrial cancer at different ages. *J Natl Cancer Inst.* **73**(5): 667-671.

193. Legoury E, Depinho R, Zimmerman K, Collum R, Yancopoulos G, Mitsock L, Kriz R and Alt FW (1987) Structure and expression of the murine Lmyc gene. *EMBO J.* **6**: 3359-3366.

194. Leibel RL (1990) Is obesity due to a heritable difference in "set point" for adiposity. *West. J. Med.* **153**: 429-431.

195. Leibel RL, Bahary N and Friedman JM (1990) Genetic variation and nutrition in obesity: Approaches to the molecular genetics of obesity. *Genetic Variation and Nutrition.* Karger Publishing.

196. Leibel RL and Hirsch J (1984) Diminished energy requirements in reduced-obese patients. *Metabolism*. **33**: 164-170.

197. Leibel RL and Hirsch J (1987) Site and sex-related differences in adenoreceptor status of human adipose tissue. *J. Clin. Endocrinol. Metab.* **78**: 1205-1210.

198. Leiter EH (1981) The influence of genetic background on expression of mutations at the diabetes locus in the mouse. IV. Male lethal syndrome in CBA/Lt mice. *Diabetes*. **30**: 1034-1044.

199. Leiter EH (1989) The genetics of diabetes susceptibility in mice. *FASEB J.* **3**: 2231-2241.

200. Leiter EH, Chapman HC and Coleman DL (1989) The influence of genetic background on the expression of mutations at the diabetes locus in the mouse. V. Interaction between the *db* gene and hepatic sex steroid sulfotransferases correlates with gender-dependent susceptibility to hyperglycemia. *Endocrinology*. **124**: 912-922.

201. Leiter EH, Coleman DL, Eisenstein AB and Strack I (1980) A new mutation (*db*^{3J}) at the diabetes locus in strain 129/J mice. *Diabetologia*. **19**: 58-65.

202. Leiter EH, Coleman DL and Hummel KP (1981) The influence of genetic background on the expression of mutations at the diabetes locus in the mouse. III. Effect of H-2 haplotype and sex. *Diabetes*. **30**: 1029-1035.

203. Leiter EH, Phuoc HL and Coleman DL (1987) Susceptibility to *db* gene and streptozotocin-induced diabetes in C57BL mice: control by gender-associated, MHC-unlinked traits. *Immunogenetics*. **26**: 6-13.

204. Levine LR, Rosenblatt S and Bosomworth J (1987) Use of a serotonin reuptake inhibitor, fluoxetine, in the treatment of obesity. *Int J Obes*. **11**(suppl 3): 185-190.

205. Lew EA and Garfinkel L (1979) Variations in mortality by weight among 750,000 men and women. *J Chronic Dis*. **32**(8): 563-576.

206. Liau G, Yamanda Y and de Crombrugghe B (1985) Coordinate regulation of the levels of type III and type I collagen mRNA in most but not all mouse fibroblasts. *J. Biol. Chem*. **260**(1): 531-536.

207. Licata G, Scaglione R, Barbagallo M, Parrinello G, Capuana G, Lipari R, Merlino G and Ganguzza A (1991) Effect of obesity on left ventricular function studied by radionuclide angiocargiography. *Int. J. Obes.* **15**(4): 295-302.

208. Lincoln AL, Daly M and Lander E (1991) PRIMER: A computer program for automatically selecting PCR primers. *Whitehead Institute Technical Report.*

209. Lindsey JR (1979) *The Laboratory Rat.* New York, Academic.

210. Lohman TG (1981) Skinfolds and body density and their relation to body fatness: A reveiw. *Hum. Biol.* **53**: 181-225.

211. Longini IM, Higgins MW, Hinton PC, Moll PP and Keller JB (1984) Genetic and environmental sources of familial aggregation of body mass in Tecumseh, Michigan. *Hum. Biol.* **56**(4): 733-757.

212. Lorden JF and Caudale A (1986) Behavioral and endocrinological effects of single injections of monosodium glutamate in the mouse. *Neurobehav Toxicol Teratology.* 8(5): 509-519.

213. Lotter EC, Krinsky R, M. MJ, Treener CM, Porte D and Woods SC (1981) Somatostatin decreases food intake in rats and baboons. *J Comp Physiol Psychol.* **95**(2): 278-287.

214. Love JM, Knight AM, McAleer MA and Todd JA (1990) Towards construction of a high-resolution map of the mouse genome using PCR analysed microsatellites. *Nucleic Acids Res.* **18**(14): 4123-4130.

215. Ludecke H, Senger G, Claussen U and Horsthemke B (1989) Cloning defined regions of the human genome by microdissection of banded chromosomes and enzymatic amplification. *Nature.* **338**: 348-350.

216. Lukaski HC (1987) Methods for the assessment of human body composition: Traditional and new. *Am. J. Clin. Nutr.* **46**: 537-556.

217. Mann W, Venkatrej VS and Auerbach AD (1989) Two hour DNA hybridizations using a new transfer membrane. *Nuc. Acids Res.* **17**(13): 5410 only.

218. Manson JE, Colditz GA, Stampfer MJ, Willet WC, Rosner B, Monson RR, Speizer FE and Hennekens CH (1990) A prospective study of obesity and risk of coronary heart disease in women. *New Eng. J. of Med.* **322**(13): 882-889.

219. Marchuk DA, Drumm M, Saulino A and Collins FS (1991) Construction of T-vectors, a rapid and general system for direct cloning of unmodified PCR products. *Nucl Acids Res.* **19**(5): 1154 only.

220. Marshall NB, Barrnett RS and Mayer J (1955) Hypothalamic lesions in goldthioglucose injected mice. *P.S.E.B.M.* **90**: 240-244.

221. Marth JD, Disteche C, Pravtcheva D, Ruddle F, Krebs EG and Perlmutter RM (1986) Localization of a lymphocyte-specific protein tyrosinase kinase gene (*lck*) at a site of frequent chromosomal abnormalities in human lymphomas. *Proc. Natl. Acad. Sci. USA.* **83**: 7400-7404.

222. Marth JD, Peet R, Krebs EG and Perlmutter RM (1985) A lymphocyte-specific protein-tyrosone kinase gene is rearranged and overexpressed in the murine T cell lymphoma LSTRA. *Cell.* **43**: 393-404.

223. Martin RJ, White BD and Hulsey MG (1991) The regulation of body weight. *Amer Scient.* **79**: 528-541.

224. Mattei MG, Dubart A, Beaupain D, Goossens M and Mattei JF (1985) Localization of the uroporphyrinogen decarboxylase gene to 1p34 band, by in situ hybridization. *Cytogenet. Cell Genet.* **40**: 692 only.

225. Mayer J, French RG, Zighera CF and Barrnett RJ (1955) Hypothalamic obesity in the mouse production, description and metabolic characteristics. *Am. J. Physiol.* **182**: 75-82.

226. Mayer TC, Kleiman NJ and Green MD (1976) Depilated (*dep*), a mutant gene that effects the coat of the mouse and acts in the epidermis. *Genetics.* **84**: 59-65.

227. McAlpine PJ, Hopkinson DA and Harris H (1970) The relative activities attributable to the three phosphoglucomutase loci (PGM_1, PGM_2, PGM_3) in human tissues. *Ann Hum Genet.* **34**: 169-175.

228. McAlpine PJ, Mohandas T and Hammerton JL (1975) Isozyme analysis of somatic cell hybrids: assignment of the phosphoglucomutase$_2$ (PGM_2) gene locus to chromosome 4 in man with data on the molecular structure and human chromosome assignment of six additional markers. *Isozymes, Vol. IV. Genetics and Evolution.* New York, Academic Press.

229. McCormick MK, Shero JH, Cheung MC, Kan YW, Hieter PA and Antonarakis SE (1989) Construction of human chromsome 21-specific yeast artificial chromsomes. *Proc. Nat. Acad. Sci. USA.* **86**: 9991-9995.

230. Mewistrich ML and Trostle-Weige PK (1989) Azh. *Mouse News Lett.* :

231. Moll PP, Burns TL and Lauer RM (1991) The genetic and environmental sources of body mass index variability: The muscatine poderosity family study. *Am J Hum Genet.* **49**: 1243-1255.

232. Monaco AP, Neve RL, Colletti-Feener C, Bertelson CJ, Kurnit DM and Kunkel LM (1985) Isolation of candidate cDNAs for portions of the Duchenne muscular dystrophy gene. *Nature.* **323**: 646-650.

233. Morley J (1987) Neuropeptide regulation of appetite and weight. *Endocrine Reviews.* **8**(3): 256-286.

234. Morris RD, Rimm DL, Hartz AJ, Kalkhoff RK and Rimm AA (1989) Obesity and heredity in the etiology of non-insulin-dependent diabetes mellitus in 32,662 adult white women. *Am. J. Epid.* **130**(1): 112-121.

235. Morrow PL, Freedman A and Craighead JE (1980) Testosterone effect on experimental diabetes mellitus in encephalomyocarditis (EMC) virus infected mice. *Diabetologia*. **18**: 247-249.

236. Mrosovsky N and Powley TL (1977) Set points for body weight and fat. *Behav. Biol*. **20**: 205-223.

237. Myers RM, Lumelsky N, Lermann LS and Maniatis T (1985) Detection of single base substitutions in total genomic DNA. *Nature*. **313**: 495-498.

238. Nadeau JH (1989) Maps of linkage and synteny homologies between mouse and man. *Trends Genet*. **5**(3): 82-86.

239. Nadeau JH, Berger FG, Kelley KA, Pitha PM, Sidman CL and Worrall N (1986) Rearrangement of genes located on homologous chromosomal segments in mouse and man: The location of genes for alpha- and beta-interferon, alpha-1 acid glycoprotein-1 and -2, and aminolevulinate dehydratase on mouse chromosome 4. *Genetics*. **104**: 1239-1255.

240. Nadeau JH, Herrmann B, Bucan M, Burkart D, Crosby JL, Erhart MA, Kosowsky M, Kraus JP, Michiels F, Schnattinger A, Tchetgen M-B, Varnum D, Willison K, Lehrach H and Barlow D (1991) Genetic maps of mouse

chromosome 17 including 12 new anonymous DNA loci and 25 anchor loci. *Genomics*. **9**: 78-89.

241. Nakamura Y, Leppert M, O'Connell P, Wolff R, Holm T, Culver M, Martin C, Fujimoto E, Hoff M, Kumlin E and White R (1987) Variable Number of Tandem Repeat (VNTR) Markers for Human Gene Mapping. *Science*. **235**: 1616-1622.

242. Nau MM, Brooks BJ, Battey J, Sausville E, Gazdar AF, Kirsch IR, McBride OW, Bertness V, Hollis GF and Minna JD (1985) *L-myc*, a new myc-related gene amplified and expressed in human small cell lung cancer. *Nature*. **318**: 69-73.

243. Neel JV (1962) Diabetes mellitus: A "thrifty" genotype rendered detrimental by "progress"? *Am. J. Hum. Genet*. **14**: 353-62.

244. Neuget AI, Lee WC, Garbowski GC, Waye JD, Forde KA, Treat MR and Fernoglio-Preiser C (1991) Obesity and colorectal adenomatous polyps. *J. Nat. Can. Inst*. **83**(5): 359-361.

245. Newman B, Selby JV, Quesenberry Jr. CP, King MC, Friedman GD and Fabsitz RR (1990) Nongenetic influences of obesity on other cardiovascular

disease risk factors: an analysis of identical twins. *Am. J. Pub. Health.* **80**(6): 675-678.

246. Noll WW and Collins M (1987) Detection of human DNA polymorphisms with a simplified denaturing gradient gel electrophoresis technique. *Proc Nat Acad Sci USA.* **84**: 3339-3343.

247. Nomura A, Heilbrun LK and Stemmerman GN (1985) Body-mass index as a predictor of cancer in men. *J. Nat. Cancer Inst.* **74**(2): 319-323.

248. O'Brien AD, Rosenstreich DL, Scher I, Campbell GH, MacDermott RP and Forman SB (1980) Genetic control of susceptibility to Salmonella typhimurium in mice: role of the *Lps* gene. *J. Immunol.* **124**: 20-24.

249. Ohlson LO, Larsson B, Svardsudd K, Welin L, Ericksson H, Wilhelmsen L, Bjorntorp P and Tibblin G (1985) The influence of body-fat distribution on the incidence of diabetes mellitus: 13.5 years of follow-up of the participants in the study of men born in 1913. *Diabetes.* **34**(10): 1055-1058.

250. Paik S–, Michelis MA, Kim YT and Shin S (1982) Induction of insulin dependent diabetes by streptozocin. Inhibition by estrogen and potentiation by androgens. *Diabetes.* **31**: 724-729.

251. Parrington JM, Craickshank G, Hopkinson DA, Robson EB and Harris H (1968) Linkage relationships between the three phosphoglucomutase loci PGM_1, PGM_2, and PGM_3. *Ann Hum Genet.* **32**: 27-34.

252. Paterson AH, Lander ES, Hewitt JD, Peterson S, Lincoln SE and Tanksley SD (1988) Resolution of quantitative traits into Mendelian factors by using a complete linkage map of restriction fragment length polymorphisms. *Nature.* **335**: 721-726.

253. Perel E and Killinger DW (1979) The interconversion and aromatization of androgens by human adipose tissue. *J Steroid Biochem.* **10**(6): 623-627.

254. Phillips RJS (1974) Location of *Och. Mouse News Lett.* **50**: 42 only.

255. Pi-Sunyer FX (1991) Health implications of obesity. *Am. J. Clin. Nut.* **53**(6 Suppl): 1595S-1603S.

256. Prikazska M and Beno I (1991) Pain and osteoarticular changes in obese persons. *Casopis Lekaru Ceskych.* **130**(2): 41-43.

257. Prochazka M, Premdas FH, Leiter EH and Lipson LG (1986) Estrone treatment dissociates primary versus secondary consequences of "diabetes" (*db*) gene expression in mice. *Diabetes.* **35**: 725-728.

258. Propst F, Rosenberg MP, Iyer A, Kaul K and Vande Woude GF (1987) *c-mos* proto-oncogene RNA transcripts in mouse tissues: Structural features, developmental regulation, and localization in specific cell types. *Mol. Cell. Biol.* **7**: 1629-1637.

259. Province MA and Rao DC (1985) Path analysis of family resemblance with temporal trends: Applications to height, weight, and quetelet index in Northeastern Brazil. *Am. J. Hum. Hered.* **37**: 178-192.

260. Quetelet A (1836) *Sur l'homme et le developpement de ses facultes, ou essai de physique sociale.* Bruxelles, L. Hauman & Cie.

261. Ravussin E, Lillioja S, Knowler WC, Dr. PH, Christin L, Freymond D, Abbott WGH, Boyce V, Howard B and Bogardus C (1988) Reduced rate of energy expenditure as a risk factor for body-weight gain. *N. Eng. J. Med.* **318**(8): 467-472.

262. Ray (1983) The complete amino acid sequence of rabbit muscle phosphoglucomutase. *J Biol Chem.* **258**(15): 9166-9174.

263. Rebuffe-Scrive M, Eldh J, Hafstrom LO and Bjorntorp P (1986) Metabolism of mammary, abdominal, and femoral adipocytes in women before and after menopause. *Metabolism.* **35**(9): 792-797.

264. Remmers JE (1990) Sleep apnea. *Proceedings, Annual Meeting of the Medical Section of the American Council of Life Insurance.* : 75-81.

265. Riordan JR, Rommens JM, Kerem B, Alon N, Rozmahel R, Grzelczak Z, Zielenski J, Lok S, Plavsic N, Chou J, Drumm ML, Iannuzzi MC, Collins FS and Tsui L (1989) Identification of the Cystic fibrosis gene: cloning and characterization of complementary DNA. *Science.* **245**: 1066-1073.

266. Roberts SB, Savage J, Coward WA, Chew B and Lucas A (1988) Energy expenditure and intake in infants born to lean and overweight mothers. *N. Eng. J. Med.* **318**(8): 461-466.

267. Robertson EJ (1986) Pluripotent stem cell lines as a route into the mouse germ line. *TIG.* (January): 9-13.

268. Romano M, Boulch PL and Romeo P-H (1987) Rat uroporphyrinogen decarboxylase cDNA: nucleotide sequence and comparison to human uroporphyrinogen decarboxylase. *Nuc. Acids Res.* **15**(17): 7211.

269. Rouleau GA, Bazanowski A, Gusella JF and Haines JL (1990) A genetic map of chromosome 1: comparison of different data sets and linkage programs. *Genomics.* **7**: 313-318.

270. Ruddle NH, Conta BS, Leinwand L, Kozak C, Ruddle F, Besmer P and Baltimore D (1978) Assignment of the receptor for ecotropic murine leukemia virus to mouse chromosome 5. *J. Exp. med.* : 451-465.

271. Ryan J, Barker PE and Ruddle FH (1986) An EcoRI restriction fragment length polymorphism at the *KRAS2* locus on mouse chromosome 6. *Nucl. Acids Res.* **14**: 9222 only.

272. Ryder K and Nathans D (1988) Induction of protooncogene c-jun by serum growth factors. *Proc. Natl. Acad. Sci. USA.* **85**: 8464-8467.

273. Saito M and Bray GA (1984) Adrenalectomy and food restriction in the genetically obese (*ob/ob*) mouse. *Am J Physiol.* **246**: R20-R25.

274. Sanyal S, Nie RV, Moes JD and Hawkins RK (1986) Map position of dysgenetic lens (*dyl*) locus on Chromosome 4 in the mouse. *Genet. Res.* **48**: 199-200.

275. Saunders AM and Seldin MF (1990) A molecular genetic linkage map of mouse chromosome 7. *Genomics.* **8**: 525-535.

276. Schapira DV (1991) Diet, obesity, fat distribution and cancer in women. *J. Am. Med. Wom. Assoc.* **46**(4): 126-130.

277. Schapira DV, Kumar NB, Lyman GH, Cavanagh D, Roberts WS and LaPolla J (1991) Upper-body fat distribution and endometrial cancer risk. *JAMA.* **266**(13): 1808-11.

278. Schinzel A and Bernasconi S (1990) Short-stature, brachydactyly, small ears, and a pattern of minor anomalies in brother and sister born to consanguineous parents: a hitherto unreported syndrome? *Am. J. Med. Genet.* **36**: 243-246.

279. Schlundt DG, Hill JO, Sbrocco T, Pope-Cordle J and Kasser T (1990) Obesity: A biogenetic or biobehavioral problem. *Int. J. Obes.* **14**: 815-828.

280. Selby JV, Newman B, Quesenberry Jr. CP, Fabsitz RR, King M-C and John Meany F (1989) Evidence of genetic influence on central body fat in middle age twins. *Hum. Biol.* **61**(2): 179-193.

281. Seldin MF, Howard TA and D' Eustachio P (1989) Comparison of linkage maps of mouse chromosome 12 derived for laboratory strain intraspecific and *Mus Spretus* interspecific backcrosses. *Genomics.* **5**: 24-28.

282. Shaper NL, Shaper JH, Bertness V, Chang H, L. KI and Hollis GF (1986) The human galactosyltransferase gene is on chromosome 9 at band p13. *Somat. Cell. Mol. Genet.* **12**: 633-636.

283. Shaper NL, Shaper JH, Hollis GF, Chang H, Kirsch IL and Kozak CA (1987) The gene for galactosyltransferase maps to mouse chromosome 4. *Cytogenet. Cell Genet.* **44**: 18-21.

284. Shaper NL, Shaper JH, Meuth JL, Fox L, Chang H, Kirsch IR and Hollis GF (1986) Bovine galactosyltransferase: Identification of a clone by direct immunological screening of a cDNA expression library. *Proc. Natl. Acad. Sci. USA.* **83**: 1573-1577.

285. Shaper NL, Shaper JH, Peyser M and Kozak CA (1990) Localization of the gene for β–1,4-galactosyltransferase to a position in the centromeric region of mouse chromosome 4. *Cytogenet and Cell Genet.* **54**: 172-174.

286. Shibahara S, Tomita Y, Sakakura T, Nager C, Chaudhuri B and Muller R (1986) Cloning and expression of cDNA encoding mouse tyrosinase. *Nucl. Acids Res.* **14**(6): 2413-2427.

287. Shimazu T, Noma M and Saito M (1986) Chronic infusion of norepinephrine into the ventromedial hypothalamus induced obesity in rats. *Brain Res.* **369**: 215-23.

288. Shinton R, Shipley M and Rose G (1991) Overweight and stroke in the Whitehall Study. *J. Epid. & Comm. Health - London.* **45**(2): 138-142.

289. Shows TB, Ruddle FH and Roderick TH (1969) Phosphoglucomutase electrophoretic variants in the mouse. *Biochem. genet.* **3**: 25-35.

290. Sidman CL, Marshall JD, Beamer WG, Nadeau JH and Unanue ER (1986) Two loci affecting B cell responses to B cell maturation factors. *J. Exp. Med.* **163**: 116-128.

291. Simmons DL, Lalley PA and Kasper CB (1985) Chromosomal assignments of genes coding for components of the mixed-function oxidase system in mice. *J. Biol. Chem.* **260**: 515-521.

292. Siracusa LD, Buchberg AM, Copeland NG and Jenkins NA (1989) Recombinant inbred strain and interspecific backcross analyses of molecular markers flanking the agouti color locus. *Genetics.* **122**: 669-679.

293. Sokal RR and Rohlf FJ (1981) Analysis of frequencies. *Biometry*. New York, Freeman.

294. Sorensen TIA, Arlen Price R, Stunkard AJ and Schulsinger F (1989) Genetics of obesity in adult adoptees and their biological siblings. *Brit. Med. J.* **298**: 87-90.

295. Southern E (1975) Detection of specific sequences among DNA fragments separated by gel electrophoresis. *J. Mol. BIo.* **98**: 503-517.

296. Spencer N, Hopkinson DA and Harris H (1964) Phosphoglucomutase polymorhism in man. *Nature.* **204**: 742-745.

297. Spiegel AM (1989) Pseudohyperparathyroidism. *The Metabolic Basis of Inherited Disease*. New York, McGraw HIll.

298. Strautz RL (1970) Studies of Hereditary-obese Mice (*ob/ob*) after implantation of pancreatic islets in millipore filter capsules. *Diabetologia*. **6**: 306-312.

299. Stunkard AJ, Foch TT and Hrubec Z (1986) A twin study of obesity. *JAMA*. **256**(1): 51-54.

300. Stunkard AJ, Harris JR, Pedersen NL and McClearn GE (1990) The body-mass index of twins who have been reared apart. *N. Engl. J. Med*. **322**: 1483-1487.

301. Stunkard AJ, Sorensen TIA, Hanis C, Teasdale TW, Chakraborty R, Schull WJ and Schulsinger F (1986) An adoption study of human obesity. *New Eng. J. Med*. **314**(4): 193-198.

302. Sweet HO (1985) Clasper (cla). *Mouse News Lett*. **73**: 18 only.

303. Taskinen MR and Nikkila EA (1981) Lipoprotein lipase of adipose tissue and skeletal muscle in human obesity: Response to glucose and semi-starvation. *Metabolism*. **30**: 810-.

304. Terao M and Mintz B (1987) Cloning and characterization of a cDNA coding for mouse placental alkaline phosphatase. *Proc. Nat. Acad. Sci. USA*. **84**: 7051-7055.

305. Todaro GJ and Green H (1963) Quantitative studies of the growth of mouse embryonal cells in culture and their development into established lines. *J. Cell Bio*. **17**: 299-313.

306. Tomita T, Doull V, Kimmel JR and Pollock HG (1984) Pancreatic polypeptide and other hormones in pancreas of obese (*ob/ob*) mice. *Diabetologia*. **27**: 454-459.

307. Tonjes RR, Weith A, Rinchik EM, Winking H, Carnwath JW, Kaliner B and Dieter P (1991) Microclones derived from the mouse chromosome 7 D-E bands map within the proximal region of the c^{14CoS} deletion in albino mutant mice. *Proc. Nat. Acad. Sci. USA*. : in press.

303. Taskinen MR and Nikkila EA (1981) Lipoprotein lipase of adipose tissue and skeletal muscle in human obesity: Response to glucose and semi-starvation. *Metabolism*. **30**: 810-.

304. Terao M and Mintz B (1987) Cloning and characterization of a cDNA coding for mouse placental alkaline phosphatase. *Proc. Nat. Acad. Sci. USA*. **84**: 7051-7055.

305. Todaro GJ and Green H (1963) Quantitative studies of the growth of mouse embryonal cells in culture and their development into established lines. *J. Cell Bio*. **17**: 299-313.

306. Tomita T, Doull V, Kimmel JR and Pollock HG (1984) Pancreatic polypeptide and other hormones in pancreas of obese (*ob/ob*) mice. *Diabetologia*. **27**: 454-459.

307. Tonjes RR, Weith A, Rinchik EM, Winking H, Carnwath JW, Kaliner B and Dieter P (1991) Microclones derived from the mouse chromosome 7 D-E bands map within the proximal region of the c^{14CoS} deletion in albino mutant mice. *Proc. Nat. Acad. Sci. USA*. : in press.

308. Trayhurn P and James WPT (1978) Thermoregulation and non-shivering thermogenesis in the genetically obese (*ob/ob*) mouse. *Pflugers Arch.* **373**: 189-193.

309. van Cong N, Billardon C, Picard JY, Feingold J and Frezal J (1971) Liason probable (linkage) entre les locus PGM_1 et *peptidase C* chez l'homme. *C. R. Acad. Sci.* **272**: 485.

310. Varnum DS and Fox SC (1981) Head blebs: a new mutation on Chromosome 4 of the mouse. *J. Hered.* **72**: 293 only.

311. Wallace MR, Marchuk DA, Andersen LB, Letcher R, Odeh HM, Saulino AM, Fountain JW, Brereton A, Nicholson J, Mitchell AL, Brownstein BH and Collins FS (1990) Type I neurofibromatosis gene: Identification of a large transcript disrupted in three NF1 patients. *Science.* **249**: 181-186.

312. Wallis J, Williamson R and Chamberlain S (1990) Identification of a hypervariable microsatellite polymorphism within D9S15 is tightly linked to Friedrichs Ataxia. *Hum Genet.* **85**(1): 98-100.

313. Watson J, Kelley K, Largen M and Taylor BA (1978a) The genetic mapping of a defective *LPS* response gene in C3H/HeJ mice. *J. Immunol.* **120**: 422-424.

314. Watson J, Largen M and McAdam KPW (1978b) Genetic control of endotoxic response in mice. *J. Exp. Med.* **147**: 39-49.

315. Weber J, Weith A, Kaiser R, K.-H. G and Olek K (1990) Microdissection and microcloning of human 7q22-32 region. *Som. Cell and Mol. Gen.* **16**(2): 123 - 128.

316. Weitze M (1940) *Hereditary Adiposity in MIce and the Cause of this Anomaly*. København, Store Nordiske Videnskabsboghandel.

317. Weller A, Smith GP and Gibbs J (1990) Endogenous cholecystokinin reduces feeding in young rats. *Science.* **247**: 1589-1591.

318. Welsh JJ, Narbaitz R and Begin-Heick N (1985) Metabolic effects of dietary manganese supplementation in *ob/ob* mice. *J. Nutr.* **115**(7): 919-928.

319. West KM (1978) *Epidemiology of diabetes and its vascular complications*. New York, Elsevier.

320. Williams SA and Birnbaum MJ (1988) *J. Biol. Chem.* **263**: 19513-18.

321. Wilson M, Mulley J, Gedeon A, Robinson H and Turner G (1991) New X-linked syndrome of mental retardation, gynecomastia, and obesity is linked to DXS255. *Am. J. Hum. Genet.* **40**: 406-413.

322. Wolfe GL (1963) Growth of inbred yellow mice (A*y*a) and non-yellow (*aa*) mice in parabiosis. *Genetics*. **48**: 1041-1058.

323. Wood TG, McGeady ML, Blair DG and Vande Woude GF (1983) Long terminal repeat enhancement of v-mos transforming activity: identification of essential regions. *J. Virol.* **46**(3): 726-736.

324. Yang-Feng TL, Floyd-Smith G, Nemer M, Drouin J and Francke U (1985) The pronatriodilantin gene is located on the distal short arm of human chromosome 1 and on mouse chromosome 4. *Am. J. Hum. Genet.* **37**: 1117-1128.

325. Young RC, Gibbs J, Antin J, Holt J and Smith GP (1974) Absence of satiety during sham feeding of the rat. *J Comp Physiol Behav.* **87**(5): 795-800.

326. Zelinski T, Verville G, White L, Hamerton JL, McAlpine PJ and Lewis M (1988) Confirmation of the assignment of *MYCL* to chromosome 1 in humans and its position relative to *RH*, *UMPK*, and *PGM1*. *Genomics*. **2**: 154-6.

327. Zucker LM (1960) Two way selection for body size in rats, with observations on simultaneous changes in coat color pattern and hood size. *Genetics*. **45**: 467-483.

End